232
Topics in Current Chemistry

New Aspects
in Phosphorus Chemistry IV

Volume Editor: Jean-Pierre Majoral

With contributions by
G. Balazs · W. Dabkowski · J.-P. Dutasta · D. Gudat
Y. Ikeda · B.P. Johnson · J. Le Bideau · D. Leclercq
J. Michalski · P.H. Mutin · M. Scheer · K. Taira
Y. Takagi · M. Tanaka · A. Vioux

Springer

The series *Topics in Current Chemistry* presents critical reviews of the present and future trends in modern chemical research. The scope of coverage includes all areas of chemical science including the interfaces with related disciplines such as biology, medicine and materials science. The goal of each thematic volume is to give the nonspecialist reader, whether at the university or in industry, a comprehensive overview of an area where new insights are emerging that are of interest to a larger scientific audience.

As a rule, contributions are specially commissioned. The editors and publishers will, however, always be pleased to receive suggestions and supplementary information. Papers are accepted for *Topics in Current Chemistry* in English.

In references *Topics in Current Chemistry* is abbreviated Top Curr Chem and is cited as a journal.

Visit the TCC home page at http://www.springerlink.com

The use of general descriptive names, registered names, trademarks, etc. in this publication does not imply, even in the absence of a specific statement, that such names are exempt from the relevant protective laws and regulations and therefore free for general use.

Topics in Current Chemistry
is also Available Electronically

For all customers who have a subscription to Topics in Current Chemistry, we offer the electronic version via SpringerLink free of charge. Please contact your librarian who can receive a password for free access to the full articles by registering at:

http://www.springerlink.com

If you do not have a subscription, you can still view the tables of contents of the volumes and the abstract of each article by going to the SpringerLink Homepage, clicking on "Browse by Online Libraries", then "Chemical Sciences", and finally choose Topics in Current Chemistry.

You will find information about the

– Editorial Board
– Aims and Scope
– Instructions for Authors
– Sample Contribution

at http://www.springeronline.com using the search function.

Preface

Volumes 1-3 concerning "New Aspects in Phosphorus Chemistry" have already appeared in print. This mini-series now continues with volume 4 which will be followed by a fifth volume in a few months.

In the present volume, our intention was to cover several modern approaches to phosphorus chemistry which were not, or at least not completely, covered in the previous volumes. The selected topics are expected to have broader relevance and to be interesting to a more general readership, since key aspects of phosphorus chemistry are pointed out. Indeed, several fields are investigated: coordination chemistry, catalysis, supramolecular chemistry, biochemistry, hybrid organic-inorganic materials, new ambiphilic ligands, and biology.

The preparation of stable complexes with transition metal-phosphorus triple bonds is of fundamental importance and constitutes a novel field of coordination chemistry. The contribution of B.P. Johnson, G. Balazs, and M. Scheer reports the synthesis and isolation of such complexes for transition metals in high oxidation states; in contrast, the corresponding complexes with transition metals in low oxidation states were found to exist only as highly reactive intermediates. A synthetic concept to generate directly such intermediates is documented. The present knowledge of the reactivity pattern of all these types of compounds is summarized in chapter 1.

In chapter 2, M. Tanaka summarizes the current state of the art of the homogeneous catalysis of H-P bond addition reactions, thus showing that as hydrosilylation and hydroboration, the H-P addition reactions are among the indispensable modern synthetic reactions needed by researchers in organic and main group element chemistry.

Supramolecular chemistry is concerned with many aspects of molecular architecture, organization, and self-assembly. The development of such a field around new phosphorylated hosts such as cavitands, hemicryptophanes provides an interesting new area of investigations in the design of host-guest systems. The contribution of J.P. Dutasta (chapter 3) points out the extremely important role played by phosphorus groups in producing assemblies of high stability; special attention has been given to the presentation and the structural aspect of this original class of phosphorus hosts and their complexes.

In a well documented chapter 4, J. Michalski and W. Dabkowski describe the preparation and applications of tricoordinated phosphorus compounds in synthesis of biophosphates and their structural analogues and illustrate the recent trends with a series of selected examples.

Metal phosphonates form a fascinating class of hybrid organic-inorganic solids with intermingled architectures in which the nature of the organic moiety plays a determining role. In chapter 5, A. Vioux, J. LeBideau, P.H. Mutin, and D. Leclercq show that grafting of organophosphorus reagents opens up the possibility of functionalizing practically any metal oxide support with the desired physical and chemical properties. Indeed organophosphorus coupling agents are quite complementary to organosilane coupling agents, the first being more suitable for the preparation of hybrid materials based on metals, metal oxides and carbonates, the others being more efficient with silicon containing inorganic supports.

Chapter 6, written by D. Gudat, is concerned with zwitterionic phospholide derivatives which can be considered as useful ambiphilic ligands. This review gives an account of the current knowledge on the synthesis, physical properties, and - in particular - chemical behavior of phosphino-substituted phospholide derivatives.

The last chapter, by Y. Takagi Y. Ikeda, and K. Taira is focused on ribozyme (RNA molecules) mechanisms. The biological functions of RNA molecules depend on their adoption of given three-dimensional structures, the presence of charged phosphodiester bonds playing an important role. Some ribozymes utilize metal ions as catalysts while others use the metal ions to maintain appropriate three-dimensional structures. All the examples reported in this chapter demonstrate that the mechanisms exploited by naturally existing ribozymes appear to be more diverse than originally expected.

In conclusion I do hope that the variety and the quality of the scientific contents will attract the interest of all the readers who should find some inspiration and profit.

Toulouse, September 2003   Jean-Pierre Majoral

Contents

Contents of Volume 220
New Aspects in Phosphorus Chemistry I

Volume Editor: Jean-Pierre Majoral
ISBN 3-540-42246-3

Contents of Volume 223
New Aspects in Phosphorus Chemistry II

Volume Editor: Jean-Pierre Majoral
ISBN 3-540-44086-0

Contents of Volume 229
New Aspects in Phosphorus Chemistry III

Volume Editor: Jean-Pierre Majoral
ISBN 3-540-00714-8

Complexes with a Metal-Phosphorus Triple Bond

Brian P. Johnson · Gabor Balazs · Manfred Scheer

Institute of Inorganic Chemistry, University of Karlsruhe, 76128 Karlsruhe, Germany
E-mail: mascheer@chemie.uni-karlsruhe.de

Abstract A survey of the existing complexes containing a transition metal-phosphorus triple bond is presented. Based on the different types of these complexes—terminal and asymmetrically bridged complexes with a phosphido ligand as well as the linearly coordinated phosphinidene complexes—their characteristic structural and bonding features as well as trends in their NMR data are discussed and compared. The present knowledge of the reactivity pattern of these types of compounds is summarized, which represents a field with tremendous perspectives.

Keywords Phosphorus ligand · ^{31}P NMR spectroscopy · Metathesis · Multiple bonds · Transition metal complexes

List of Abbreviations

Ad	1-Adamantyl
Ad$'$	2-Adamantyl
CN	Coordination number
Cp$''$	1,3-Bis(*tert*-butyl)cyclopentadienyl, 1,3-C$_5$(C(CH$_3$)$_3$)$_2$
Cp*	Pentamethylcyclopentadienyl, C$_5$(CH$_3$)$_5$
Cy$'$	1-Methylcyclohexyl, 1-C$_6$H$_{10}$(CH$_3$)
Et	Ethyl, CH$_2$CH$_3$
HOMO	Highest Occupied Molecular Orbital
i-Pr	iso-Propyl, CH(CH$_3$)$_2$
LUMO	Lowest Unoccupied Molecular Orbital
Me	Methyl, CH$_3$
Mes	Mesityl, 2,4,6-Trimethylphenyl, 2,4,6-C$_6$H$_2$(CH$_3$)$_3$
N$_3$N, TREN	Tris(2-(trimethylsilylamido)ethyl)amine, ((CH$_3$)$_3$SiNCH$_2$CH$_2$)$_3$N
Np	Neopentyl, CH$_2$C(CH$_3$)$_3$
OTf	Triflate, [CF$_3$SO$_3$]$^-$
Ph	Phenyl, C$_6$H$_5$
Ph*	2,4,6-Tris(*tert*-butyl)phenyl, 2,4,6-C$_6$H$_2${C(CH$_3$)$_3$}$_3$
Ph$'$	2,6-Dimethylphenyl, 2,6-C$_6$H$_3$(CH$_3$)$_2$
Ph$''$	3,5-Dimethylphenyl, 3,5-C$_6$H$_3$(CH$_3$)$_2$
t-Bu	*tert*-Butyl, C(CH$_3$)$_3$
t-Bu$'$	*tert*-Butyl, C(CD$_3$)$_2$CH$_3$
THF, thf	Tetrahydrofuran

1
Introduction

For a long time complexes with a triple bond between a transition metal and a main group 15 element were known exclusively for nitrogen [1, 2]. Examples for this include complexes of the type [Cl$_4$MN]$^-$ (M=Mo, W, Re, Ru, Os) [3] possessing very short metal nitrogen bond distances. Furthermore they are characterized by a high nucleophilicity towards Lewis-acids like BF$_3$ and a high tendency of intermolecular aggregation [1, 4].

Up until 1995 for phosphorus the situation can be characterized as follows: from the possible two principle coordination modes of phosphido ligands [5] containing a metal-phosphorus triple bond, the terminal type A and the asymmetrically bridging type B, there were no stable and fully spectroscopically characterized compounds known (the situation for the heavier homologues was the same). However, since the interest for such compounds possessing a highly reactive potential was substantial, a large amount of speculation about the possible existence of such intermediates was published. In [6] the stage of existing speculations has been summarized.

$$L_nM \equiv P \qquad L_nM \equiv P \rightarrow M'L_m \qquad L_nM \equiv P - R \qquad L_nM = P$$
$$\quad\ \ \textbf{A} \qquad\qquad\qquad \textbf{B} \qquad\qquad\qquad\qquad \textbf{C} \qquad\qquad\qquad \textbf{D} \quad R$$
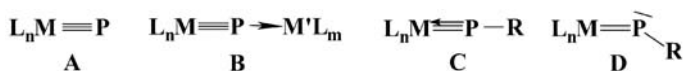
In 1995 a breakthrough occurred in this field: in February we were able to show the synthesis and the spectroscopic properties of the first complexes of type B [7], and in August the first isolated and structurally characterized complexes containing terminal metal-phosphorus triple bonds (type A) were independently obtained and published in back-to-back articles by the groups of Cummins [8] and Schrock [9]. Since then, a rapid development has occurred in the synthesis and particularly in the study of the reactivity pattern of complexes with phosphorus-transition metal triple bonds. This review chapter will highlight the development in this field by giving an overview from 1995 until the current stage of research.

By writing about complexes containing triple bonds between phosphorus and transition metals, one has to take into account the triple-bond character of phosphinidene complexes which are in a nearly linear coordination mode (type C) in contrast to the usual bent coordination mode D possessing typical double-bond features. Due to the additional π-donation bonding ability of the PR moiety to the metal atom in type C and the observed bond lengths, this type of complexes has to be included into the classes of metal-phosphorus triple bond compounds. Thus, at the end of this review will appear a chapter highlighting the appropriate compounds of type C.

2
Terminal Phosphido Ligand Complexes

2.1
Synthesis of Terminal Phosphido Ligand Complexes

One of the first isolated and structurally characterized phosphido complexes [$(t$-Bu$'$Ph$''$N)$_3$Mo$\equiv$P] (**1a**) was obtained from the reaction of a molybdenum(III) complex with P_4 in 79% yield (Eq. 1) [8]. The molybdenum starting material [$(t$-Bu$'$Ph$''$N)$_3$Mo] is planar, and the three unpaired electrons are localized on the Mo atom [10], engendering an ideal environment for the reduction of white phosphorus and formation of the triple bond. **1a** can transfer the phosphido ligand to another complex [$(t$-BuPhN)$_3$Mo] via a heterocumulene intermediate to give [$(t$-BuPhN)$_3$Mo$\equiv$P] (**1b**) [11] (Eq. 2).

Mo(NPh*t*-Bu)₃   Mo(NRPh″)₃

1a   **1b**

R = *t*-Bu'

2a   **2b**   **1c**

R = *i*-Pr, M = Na(thf)
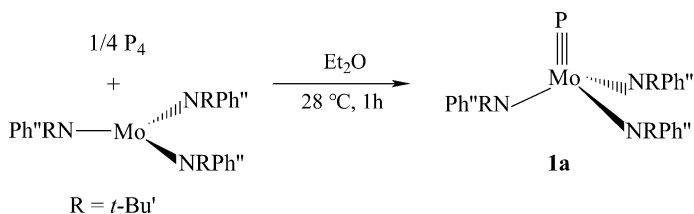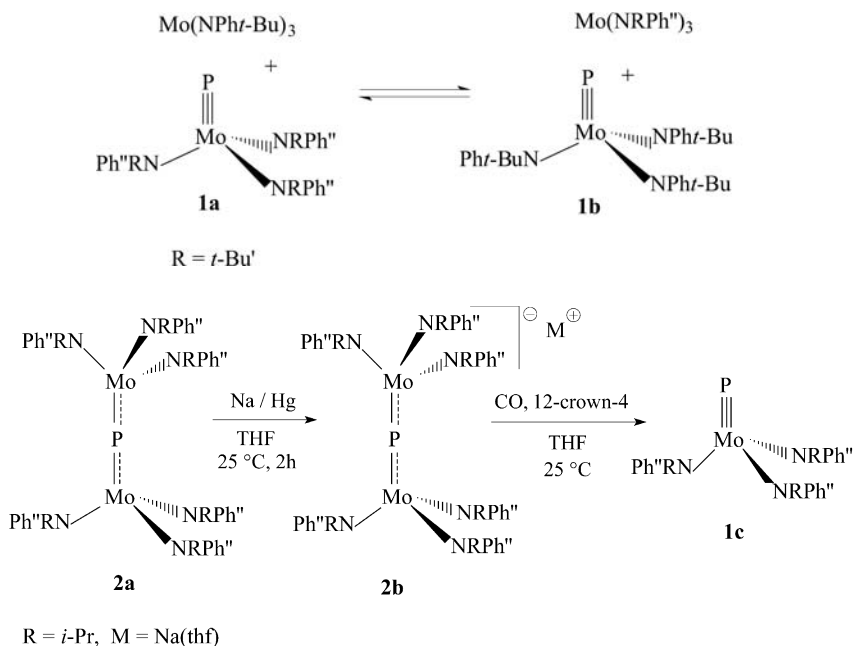
Amide ligands with sterically less demanding *i*-Pr group were also intro-
duced in the synthesis of [(*i*-PrPh″N)₃Mo≡P] (**1c**), which was obtained by
reducing the heterocumulene **2a** to the anion **2b** (Eq. 3) [12] and subsequent
reaction with CO. **1c** was obtained in an 83% overall yield. Recently, the re-
action of **1c** with alcohols was reported to lead to the exchange of the amido
ligands with alkoxy ligands. In the particular case of 1-methylcyclohexanol,
alcoholysis of **1c** provided the kinetically stable terminal phosphido complex
[(Cy'O)₃Mo≡P] (**3a**) (Eq. 4) [13] in 57% yield as a yellow crystalline solid.
Use of less bulky alcohols led to slow dimerization of the formed alkoxide-
supported terminal phosphido complex [13]. A long-lived (t$_{1/2}$ = ca. 6 h at
20 °C) terminal phosphido complex [(AdO)₃Mo≡P] (**3b**) is formed when **1c**
is treated with 3 equiv. of 1-adamantol in *n*-pentane. Over a period of about
one day **3b** dimerizes in toluene solution to [(AdO)₃MoP]₂.

$$(Ph″RN)_3Mo\!\equiv\!P \xrightarrow[\text{- 3 HNRPh″}]{\text{+ 3 HOR'}} (R'O)_3Mo\!\equiv\!P$$

R = *i*-Pr

3a: R = Cy'
3b: R = Ad
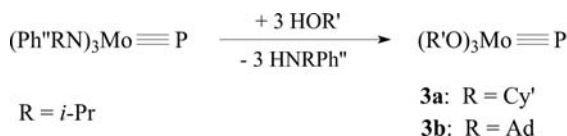
Trialkoxy complexes of tungsten with terminal phosphido ligands could
not yet be isolated. They were postulated to be very reactive intermediates
in different transformation reactions, e.g., during the metathesis reaction of
[W₂(OR)₆] with phosphaalkynes [6, 14]. However, we were able to character-
ize the complex [(*t*-BuO)₃W≡P] (**3c**) by ^{31}P-NMR spectroscopy by monitor-
ing the metathesis reaction of [W₂(O*t*-Bu)₆] with MesC≡P in the tempera-

ture range from −70 to 25 °C (Eq. 5) [15]. Complex **3c** is formed at about 215 °K and at 263 °K it reacts further with phosphaalkyne to form four-membered-ring derivatives.
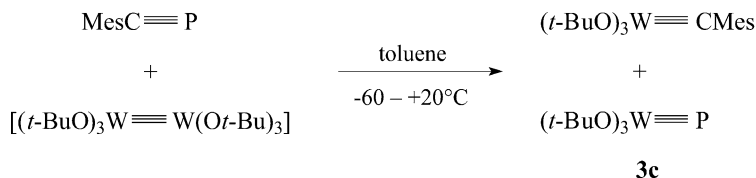
Simultaneously with the published synthesis of **1a** [8] Schrock et al. reported on the use of the N_3N ligand for the synthesis of the phosphido complexes $[(N_3N)M{\equiv}P]$ (**4**) (M = Mo (**4a**), M = W (**4b**)) [9]. This ligand smoothly promotes the formation of a multiple bond between the transition metal and the ligand *trans* to the intramolecular N donor. Thus, the reaction of two equivalents of LiP(H)Ph with $[(N_3N)MCl]$ (M = Mo, W) (Eq. 6) gives the terminal phosphido complexes **4a,b** [16].
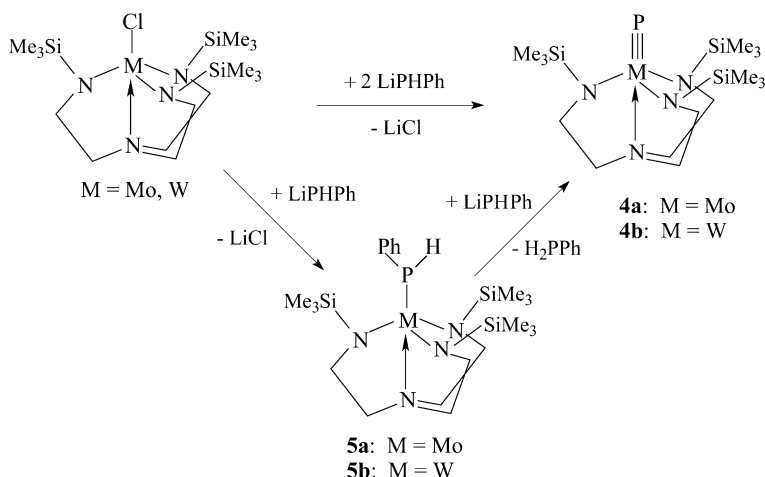
As intermediates the phenylphosphanido complexes $[(N_3N)M(PPhH)]$ (**5**) are formed. It was speculated that deprotonation by an excess of LiP(H)Ph gives $PhPH_2$ and a lithiated derivative of **5** which decomposes to give the terminal phosphido complexes **4** and LiPh. Alternatively, it was shown that LiPh can also be used as a base to convert complexes **5** into **4**. **4b** was obtained as yellow cubes in 50% yield, when the reactants were heated at 80 °C for 48 h in a mixture of toluene and THF (4:1). A higher yield (88%) was achieved by using a 1:1.3 stoichiometric ratio and a temperature of 110 °C over a period of 48 h in toluene. Reducing the amount of LiP(H)Ph to a 1:1 ratio, $[(N_3N)W{\equiv}P]$ (**4b**) and traces of $[(N_3N)W(PPhH)]$ (**5b**) were obtained, but in this reaction **5b** could not be separated from **4b** readily. **4b** can also be obtained starting from $[(N_3N)WCl]$ and Li_2PPh or $LiPH_2$, whereas **4a** is

not obtained in any significant yield by the same routes. **4a** was obtained in good yield via the reaction in Eq. (6) as a yellow diamagnetic solid by heating the reactants at 70 °C for 12 h in a 1:2 ratio in a mixture of toluene and THF. Using a 1:1 ratio of the reactants, [(N₃N)Mo(PPhH)] (**5a**) was isolated in good yield. Heating **5a** in toluene at 120 °C for three days did not give **4a**. However, reacting **5a** with PhLi in toluene-d_8 at 110 °C for four days gives **4a** in 90% yield [16].
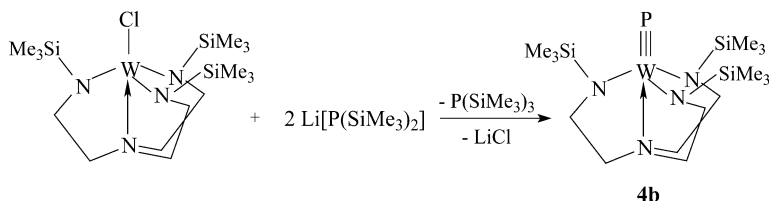
Alternatively, we introduced the use of lithium-bis(trimethylsilyl)phosphanide Li[P(SiMe₃)₂] in the reaction with [(N₃N)WCl] to give the phosphido complex **4b** [17]. By this route **4b** was obtained in 65% yield by heating the reactants in toluene at 80 °C for two days. No Me₃Si substituted phosphanido derivative could be detected by following reaction (**7**) by ³¹P-NMR spectroscopy. However, the growing amounts of **4b** is accompanied by an increase in the amount of P(SiMe₃)₃ indicating that the formation of the phosphanido complex [(N₃N)W-P(SiMe₃)₂] of the reaction in Eq. (7) is the rate-determining step and that the phosphanido intermediate is rapidly metallated by a second equivalent of LiP(SiMe₃)₂ and transformed into the product **4b**. The use of [E(SiMe₃)₂]⁻ (E = P, As) helped to open up the synthetic approach to the heavier triple bond homologues as, e.g., the synthesis of [(N₃N)W≡As] [17]. Interestingly, whereas the phosphido complexes **4** were successfully synthesized for molybdenum and tungsten, efforts to obtain analogous TREN complexes of chromium according to reaction at Eq. (7) failed [18]. Obviously, the low stability of the Cr⁶⁺ oxidation state renders the formation of such a triple bond complex unfavorable.

2.2
Structure and Bonding of Terminal Phosphido Ligand Complexes

The M≡P triple bonds in complexes **1**, **3** and **4** are kinetically stabilized by sterically encumbering amido and alkoxy ligands, which offer a well-defined protective pocket. The crystal structures of complexes **1a** and **4b** are shown in Fig. 1. The threefold symmetric auxiliary ligand sets create a situation favorable to metal-phosphorus triple bonding in that the degenerate d_{xz} and d_{yz} metal orbitals are mostly unoccupied and available for π-bonding to the phosphorus atom. In the case of the TREN ligands of complexes **4**, this C₃ symmetry is essentially forced by the rigid nature of the ligand backbone [19], and these complexes achieve added stabilization through donation of the axial amino group to the metal. The local geometry about the metal atom
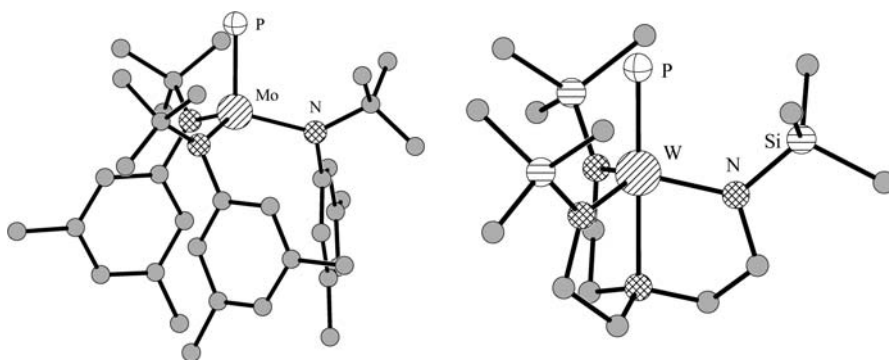
Fig. 1 Molecular structures of [(t-Bu′Ph″N)₃Mo≡P] (**1a**, *left*) [8] and [(N₃N)W≡P] (**4b**, *right*) [9]. H-atoms are omitted for clarity

in each structurally characterized complex **1–3** is nearly tetrahedral, while in the TREN complexes **4** the geometry about the metal approaches trigonal bipyramidal with the TREN ligand bent slightly away from the phosphido ligand.

All terminal phosphido complexes are characterized by extremely short M≡P bond lengths, as listed in Table 1. The ³¹P-NMR spectra of the terminal phosphido complexes reveal signals at extremely low field, which has become a signature property in identifying new metal phosphides. Low-field ¹³C-NMR shifts are also characteristic of the related family of transition-metal alkylidyne complexes, whose ¹³C signals are observed between 200 and 400 ppm [20]. The extreme deshielding of the phosphorus atom in M≡P complexes is in stark contrast to the related phosphaalkynes [21] and iminophosphenium cations [22], whose ³¹P-NMR signals are found upfield from the associated phosphaalkenes and iminophosphines. However, the low-field ³¹P shifts of terminal phosphido complexes are fully consistent with the dramatic low-field ¹³C-NMR shift of the anionic terminal molybdenum-carbido complex K(2,2,2-crypt)⁺[(t-Bu′Ph″N)₃Mo≡¹³C]⁻ (δ(¹³C) =

Table 1 M≡P bond lengths and ³¹P-NMR data of terminal phosphido complexes of type A

	d(M≡P) [Å]	δ(³¹P) [ppm]	¹J_{W,P} [Hz]	Ref.
[(t-Bu′Ph″N)₃Mo≡P] **1a**	2.119(4)	1216		[8]
[(t-BuPhN)₃Mo≡P] **1b**		1226		[11]
[(i-PrPh″N)₃Mo≡P] **1c**	2.116(3)	1256		[12]
[(Ad′Ph″N)₃Mo≡P] **1d**	2.107(3)	1215		[28]
[(Cy′O)₃Mo≡P] **3a**	2.114(2)	1130		[13]
[(AdO)₃Mo≡P] **3b**		1124		[13]
[(t-BuO)₃W≡P] **3c**		845	176	[15]
[(N₃N)Mo≡P] **4a**		1346		[9]
[(N₃N)W≡P] **4b**	2.162(4)	1080	138	[9]

501 ppm) [23, 24], which is isolobal with **1a**, as well as consistent with the low-field ^{15}N-NMR shift in the terminal nitrido complex [(t-Bu$'$Ph$''$N)$_3$Mo$\equiv$ ^{15}N] ($\delta(^{15}N)$ = 840 ppm) [25]. From a comparison of complexes **3a,b** with **3c** and of **4a** with **4b**, it is becoming apparent that terminal molybdenum phosphides generally display ^{31}P-NMR shifts at roughly 260 ppm downfield of the corresponding terminal tungsten phosphido complexes. ^{31}P-MAS-NMR data and ^{31}P chemical shielding tensors were reported for complexes **1a,b** and **4a,b** and showed extreme ^{31}P deshielding and large chemical shift anisotropy (CSA) values; the CSA of 2393 ppm in complex **4a** remains the highest value yet to be observed [26]. These effects were explained in terms of considerable paramagnetic shielding at directions perpendicular to the M$\equiv$P triple bond. Based on calculations using the B3LYP density functional method of a model complex, [(H$_2$N)$_3$Mo$\equiv$P], the perpendicular shielding was attributed to field-induced mixing between the σ(M-P) and π^*(M-P) molecular orbitals and the small energy gap between these orbitals. Additionally, for the W$\equiv$P phosphido complexes, the $^1J_{W,P}$ coupling constants are surprisingly small (**3c**: 176 Hz; **4b**: 138 Hz). This has been interpreted as a low degree of s-character in the σ-portion of the M$\equiv$P triple bond, a characteristic also presumed for [(t-Bu$'$Ph$''$N)$_3$Mo$\equiv$$^{13}C$]$^-$ based on the observation of small $^1J_{Mo,C}$ coupling constants in solid state ^{13}C-CP/MAS-NMR measurements [24]. This view has been supported for the phosphido complex **4b** by calculations using the PESHO method [27], which show low contributions of the tungsten 6s and phosphorus 3s orbitals to the W-P σ-bond [17].

Computational analysis by Frenking et al. [29] showed the M$\equiv$P bond to be a true triple bond, whose σ and π components are rather unpolarized according to B3LYP/II calculations using the NBO method. Polarization is increased toward the phosphorus ligand by addition of an axial amino donor, as in the TREN complexes **4a,b**, creating a higher basicity in the phosphorus atom. The NBO partitioning also showed the s contribution at phosphorus in the M$\equiv$P σ bond to be low (ca. 20%), whereas that at the metal was significantly higher (35–40%). This is in slight contrast to the PESHO calculations [17], which showed low s contributions in the σ bond at both atoms and mostly d character at the metal.

Stretching frequencies and force constants for the M$\equiv$P bond have been derived from Raman spectroscopic data for compounds [(N$_3$N)Mo$\equiv$P] (**4a**) and [(N$_3$N)W$\equiv$P] (**4b**), as well as for related nitrido and arsenido complexes [30]. For W$\equiv$E (E = N, P, As), force constants were shown to decrease with increasing M$\equiv$E bond length, while for each respective pnicogenido ligand E, the force constant for the W complex was greater than that of the Mo complex, a trend also reflected in literature data for transition metal nitrido and oxo complexes [20].

2.3
Reactivity of Terminal Phosphido Ligand Complexes

2.3.1
General

In the first structurally characterized complexes of type A the metal-phosphorus triple bonds are kinetically stabilized by bulky substituents at the amido ligands. Therefore, these compounds reveal exclusively 'end-on' reactivity via the phosphorus lone pair. This reactivity pattern seems also valid for the solution stable alkoxide derivative $[(Cy'O)_3Mo\equiv P]$, for which the reaction potential is under investigation [13]. In contrast, due to their lesser degree of kinetic stabilization by bulky substituents the short-lived alkoxide containing complexes $[(R'O)_3W\equiv P]$ ($R'=t$-Bu (**3c**), Ph' (**3d**)), generated by the metathesis reaction between the alkoxide-dimer and the phosphaalkyne (cf. Eq. 8), show additionally a high 'side-on' reactivity towards the phosphaalkynes of the reaction mixture. Thus, there occurs a formal cycloaddition reaction with the phosphaalkynes, and a subsequent 1,3-OR' shift yields the formation of four-membered diphospha-metallo-cyclobutane derivatives **6** (Eq. 8) [15, 31, 37].

In addition to the formation of the four-membered ring derivatives **6** for the reaction of t-BuC≡P with $[(Ph'O)_6W_2]$ another reaction pathway is observed under formation of product **7** indicating that two of the intermediates **3d** undergo a dimerization reaction in which a phosphaalkyne was added, transferring two alkoxide ligands from W to P to allow the formation of a W-W bond (Eq. 9) [31]. The reductive W-W bond formation is a general reaction pattern of alkoxide containing complexes of tungsten [15, 32]. In general the reactivity pattern of complexes of type A can be subdivided into three classes as discussed below.

2.3.2
Addition Reactions

The trisamido molybdenum complex **1a** was oxidized by dimethyldioxirane at −78 °C to give the terminal PO ligand complex **8** in 73% yield [33]. Sulfurization by elemental sulfur, cyclohexensulfide (7-thiabicyclo[4.1.0]heptan) [8] or ethylene sulfide [34] results in the terminal PS complex **9**, while reaction with the 'Staudinger reagent' MesN$_3$ yields the imido addition product **10** with a novel monophosphadiazonium ligand (PNR$^+$) (Eq. 10) [8]. For **9** the bonding was analyzed by Frenking et al. [29] resulting in a bonding scheme with a M≡P triple bond and P-S single bond, as in [L$_n$M≡P-S], according to NBO calculations. This description was in accordance with [L$_n$M≡P-S] having a more satisfying Lewis structure, which the NBO method is programmed to seek out, about the metal center than the [L$_n$M=P=S] form. However calculation of the Wiberg bond indices pointed to the [L$_n$M=P=S] form. It was emphasized that both bonding descriptions remain plausible until more experimental data and more suited theoretical treatment become available for this special type of complex. From the available experimental data, it is interesting to note that the Mo-P bond distances for **8–10** are each slightly shorter than in the parent Mo phosphido complex **1a**, thus lending support to the preservation of the Mo≡P triple bond, although reactivity studies on the PO complex **8** suggest that the PO ligand behaves as [L$_n$M=P=O] [33, 34].

The addition of electrophiles like Me$^+$ [30] to the complexes **4** results in the formation of **11a,b** corresponding to the reaction in Eq. (11). Whereas complex **11a** is not stable at room temperature and must be prepared and

isolated at −35 °C, the W derivative **11b** is formed quantitatively by methylation at room temperature. For a corresponding As derivative of **11a** an X-ray diffraction analysis reveals an almost linear coordination mode of the AsMe ligand (173.3(6)°), indicating together with the W-As bond length (2.249(1) Å) the triple bond character of this bond and therefore the existence of complexes of type C.

4a: M = Mo
4b: M = W

11: R = Me; M = Mo(**a**), W(**b**)

2.3.3
Coordination to Lewis Acids

Complex **4b** reacts with $[M(CO)_5(thf)]$ (M=Cr, W) to form initially complexes **12**, which could be characterized by their NMR data, although a second substitution in the *trans*-position is preferred leading to the linear complexes **13a,b** [17]. The driving force of the *trans* substitution was calculated via the corresponding isodesmic reaction and was found to be the formation of $[M(CO)_6]$ [17].

4b

12a: M = Cr
12b: M = W

13a: M = Cr
13b: M = W

Furthermore the complexes **4** were reacted towards cationic Rh complexes (generated from $[Rh(CO)_2Cl]_2$ and $TlPF_6$) to form twofold *trans* substituted products **14a,b** (Eq. 13) [16]. Both the reaction with $[M(CO)_5(thf)]$ (M=Cr, W) as well as with $[Rh(CO)_2L_2]^+$ reveal the tendency of the $[(N_3N)M\equiv P]$

ligand to favor a second substitution in the *trans* position due to their large steric influence.

4a,b

L = Me₃CN

14a: M = Mo
14b: M = W

Furthermore, the formation of linear complexes with pure σ acceptors of main group element moieties is possible. By reacting **4b** with GaCl₃ complex **15** is formed [35]. Interestingly, attempts to add BH₃ (starting from the adduct BH₃·SEt₂) to the phosphido complex **4b** yields insoluble products. Apparently, Me₃SiH elimination occurs, which leads to subsequent polymerization reactions. This result is in line with the decomposition reaction of **15** in CH₂Cl₂ over a longer period of time where the 'dimer' **16** is obtained indicating the developing 'side-on' reactivity, if the kinetically stabilizing Me₃Si groups are removed. However, if solutions of **4b** are treated with BF₃·OEt₂ a short lived addition product could be recorded by ^{31}P-NMR studies (δ 607 ppm, $^1J_{W,P}$ 478 Hz) [35].

15 **16**

The bonding situations of the products presented in this section are discussed below as bridging phosphido triple-bond systems.

2.3.4
Miscellaneous

Cummins et al. were able to show that a transfer of a terminal phosphido ligand in complex **1a** occurs by reacting it with the unsaturated trivalent Mo complex possessing a different set of auxiliary amido ligands (cf. Eq. 2). It was possible to isolate the intermediate [{(t-Bu^{l}PhN)₃Mo}₂(μ-P)] (**2c**) with a linearly bridging phosphido ligand in a heterocumulene bonding situation. This paramagnetic complex (($1\pi_u)^4(1\pi_g)^3$ electron configuration) is an example of a growing family of such heterocumulenes [36].

Furthermore, Cummins et al. were able to show that the amido ligands of complex **1c** can be exchanged by more strongly acidic alcohols. Depending on their steric influence either monomeric complexes with terminal phosphido ligands were obtained (c.f. Eq. 4) or phosphido bridged dimers were isolated [13]. Starting from Ph′OH the latter type of reaction results in the formation of **17**. Although in solution **17** was shown to exist as the two expected isomers (*cis/trans*) only the *cis* isomer crystallizes from these solutions and was structurally characterized by X-ray diffraction methods.

3
Asymmetrically Bridged Phosphido Ligand Complexes

3.1
Synthesis of Asymmetrically Bridged Phosphido Ligand Complexes

The metathesis reaction of $[W_2(Ot\text{-}Bu)_6]$ with $t\text{-}BuC{\equiv}P$ leads to the phosphido complex $[(t\text{-}BuO)_3W{\equiv}P]$ (**3c**) as a highly reactive intermediate [14, 15]. The concept we followed in this particular area was the stabilization of this species by blocking the lone pair at the phosphido atom. Thus, this reaction was carried out in the presence of Lewis-acidic carbonyl complexes of the type $[M(CO)_5(thf)]$ (M = Cr, W) or $[Cp''Mn(CO)_2(thf)]$ at low reaction temperatures. By this method it is possible to stabilize the product as $[(t\text{-}BuO)_3W{\equiv}P{\rightarrow}M(CO)_5]$ (M = Cr (**18a**), W (**18b**)) [7, 15] and $[(t\text{-}BuO)_3W{\equiv}P{\rightarrow}MnCp''(CO)_2]$ (**18c**) [37], but the subsequent reactivity of the phosphido complexes could not be completely hindered in that a part of the metathesis products **18** and especially $[(t\text{-}BuO)_3W{\equiv}Ct\text{-}Bu]$ react further with $t\text{-}BuC{\equiv}P$ to form four-membered ring derivatives which are transformed after subsequent 1,3-Ot-Bu shift to the metallo-phospha-cyclobutadiene derivatives **19** and **20** (Scheme 1). In contrast to complexes of type A (complexes **1** and **4**) complexes **18** possess a high 'side-on' reactivity due to the flexibility of the alkoxide ligands, and the overall complex is stabilized by fixation of the P lone pair to Lewis acidic metal carbonyls. This feature, however, was a disadvantage in the synthesis of these compounds via the metathesis reaction. The reaction led to inseparable mixtures, which contained the desired phosphido compounds **18** and the corresponding alkylidyne complex as well as the four-membered ring derivatives **20** and **19**. Through fractionated crystallization it was possible to enrich complexes **18** in solution and characterize them spectroscopically [7, 15, 37].

$(t\text{-BuO})_3W \equiv\!\!\!\equiv W(Ot\text{-Bu})_3 \quad + \quad RC \equiv P \,/\, ML_n$

$ML_n = Cp''Mn(CO)_2$
$M(CO)_5$
$M = Cr, W$
$R = t\text{-Bu, Ad}$

$-21°C, THF$

$(t\text{-BuO})_3W \equiv\!\!\!\equiv CR \qquad + \qquad (t\text{-BuO})_3W \equiv\!\!\!\equiv P \longrightarrow ML_n$

18a: $ML_n = Cr(CO)_5$
18b: $ML_n = W(CO)_5$
18c: $ML_n = Cp''Mn(CO)_2$

$+ \, RC \equiv P$ $+ \, RC \equiv P$

1,3-Ot-Bu shift   1,3-Ot-Bu shift

$(t\text{-BuO})_2W$ ... POt-Bu (with C–R, C–R ring) **20**

$R = t\text{-Bu, Ad}$

$(t\text{-BuO})_2W$ ... POt-Bu (with ML$_n$, P, C–R ring)

19a: $ML_n = Cr(CO)_5$
19b: $ML_n = W(CO)_5$
19c: $ML_n = Cp''Mn(CO)_2$

Scheme 1 Three-component reaction for the synthesis of **18**

To prevent the latter mentioned subsequent reactions, the bulky phosphaalkyne Ph*C≡P as well as tungsten alkoxides of reduced size as, e.g., [W$_2$(ONp)$_6$] were employed in these three-component reactions with no significant success [15]. The crucial steps for the side-product free synthesis of the phosphido complexes **18** are the introduction of a phosphaalkyne possessing a moderate steric bulkiness, which lies between those of t-BuC≡P and Ph*C≡P, and resulting from the ^{31}P-NMR studies (cf. Eq. 5), a reaction temperature mode allowing the complete metathesis reaction to take place at very low temperatures over a long period of time until all the phosphaalkyne has been converted into the metathesis products (about 12 h); only then is the reaction mixture allowed to reach room temperature. We found that MesC≡P meets these steric requirements, and the three-component-reaction between MesC≡P, [W$_2$(Ot-Bu)$_6$] and [M(CO)$_5$(thf)] (M = Cr, W), carried out at −78 °C and warmed up to ambient temperature within 15 h, succeeded in the synthesis and isolation of the phosphido complex **18a,b** (Scheme 2) [15]. Furthermore, if t-BuC≡P is incorporated into these reactions, the steric requirements of the alkoxide dimer has to be slightly increased. Thus, t-BuC≡P reacts with [W$_2$(OPh′)$_6$] and [M(CO)$_5$(thf)] (M=Cr, W) under the

described conditions to form the novel phosphido complexes **21a,b** in good yields (Scheme 2) [32]. MesC≡P was also successfully used in the latter reaction.

$$(t\text{BuO})_3\text{W}\!\!=\!\!\!=\!\!\text{W}(\text{O}t\text{Bu})_3 \qquad\qquad (\text{Ph'O})_3\text{W}\!\!=\!\!\!=\!\!\text{W}(\text{OPh'})_3$$
$$+ \qquad\qquad\qquad\qquad\qquad +$$
$$\text{MesC}\!\!\equiv\!\!\text{P}/[\text{thfM(CO)}_5] \qquad\qquad \text{RC}\!\!\equiv\!\!\text{P}/[\text{thfM(CO)}_5]$$

$$\downarrow \text{-78°C, THF} \qquad\qquad\qquad \downarrow \text{-78°C, THF}$$

$$(t\text{BuO})_3\text{W}\!\!\equiv\!\!\text{CMes} \qquad\qquad (\text{Ph'O})_3\text{W}\!\!\equiv\!\!\text{CR}$$
$$+ \qquad\qquad\qquad\qquad +$$

$$\boxed{(t\text{BuO})_3\text{W}\!\!\equiv\!\!\text{P}\!\longrightarrow\!\text{M(CO)}_5} \qquad \boxed{(\text{Ph'O})_3\text{W}\!\!\equiv\!\!\text{P}\!\longrightarrow\!\text{M(CO)}_5}$$

18a,b   M = Cr, W   **21a**: M = Cr
                  R = *t*-Bu, Mes   **21b**: M = W
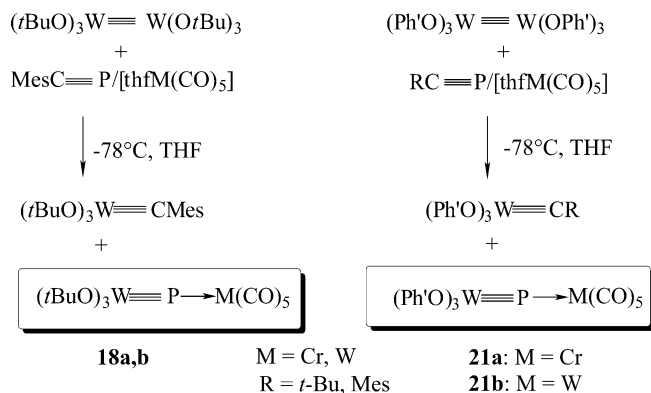
Scheme 2 Synthesis of the phosphido complexes **18a,b** and **21a,b**

Complexes **21** can only be isolated as their THF adducts. Attempts to synthesize **21** by using no THF as solvent failed. The Lewis basicity of the Ph′O ligands appears to be insufficient to compensate for the electron deficiency at the tungsten atom, and coordination of an additional THF molecule becomes necessary. The high stability of the THF adducts was furthermore confirmed by DFT studies of these compounds.

3.2
Structure and Bonding of Asymmetrically Bridged Phosphido Ligand Complexes

The phosphido complexes which are coordinated by a Lewis-acid are listed in Table 2. In comparison to their uncoordinated analogues they reveal a trend of slightly longer W-P bond lengths, large upfield shifts in the ^{31}P-NMR spectra, and a dramatic increase in the $^1J_{\text{W,P}}$ coupling constants for the appropriate W complexes. The M≡P bond length has been theoretically predicted to be slightly shortened by coordination to a pure σ-acceptor like BH$_3$ [17], but through coordination to a σ-acceptor/π-donor group like [M(CO)$_n$], electron density is donated into the antibonding orbitals of P, thus lengthening the M≡P bond. According to structural data, coordination of **4b** to the σ-acceptor GaCl$_3$ retains a more or less unchanged W≡P bond length, consistent with the absence of π back bonding from GaCl$_3$. In contrast, the structural data of **13b** and **14b** reveal a lengthening of the W≡P bond due to the π-backbonding from the coordinated transition metal. For complexes **13** the [(N$_3$N)W≡P] ligand was analyzed and found to possess similar, but less pronounced ligating properties than CO [17].

From a comparison of the data in Table 1 and Table 2, coordination of the phosphido complexes **3c** and **4a,b** to a Lewis acidic fragment generally leads

Table 2 M≡E bond lengths and ^{31}P-NMR data of asymmetric coordinated phosphido ligand complexes

	d(M≡E) [Å]	δ(^{31}P) [ppm]	^{1}J$_{W,P}$ [Hz]	Ref.
[(N₃N)W≡P→Cr(CO)₅] **12a**		708.1	442	[17]
[(N₃N)W≡P→W(CO)₅] **12b**		662.6	450, 135	[17]
[(N₃N)W≡P→Cr(CO)₄←P≡W(N₃N)] **13a**		728.1	413	[17]
[(N₃N)W≡P→W(CO)₄←P≡W(N₃N)] **13b**	2.202(2)	679.8	426, 151	[17]
trans-[Rh{(N₃N)Mo≡P}₂(CO)(CH₃CN)]PF₆ **14a**		791.1 (d, J$_{Rh,P}$=67 Hz)		[16]
trans-[Rh{(N₃N)W≡P}₂(CO)(CH₃CN)]PF₆ **14b**	2.177(5), 2.173(5)	642.6 (d, J$_{Rh,P}$=79 Hz)	a	[16]
[(N₃N)W≡P→GaCl₃] **15**	2.168(4)	366	712	[35]
[(*t*-BuO)₃W≡P→Cr(CO)₅] **18a**		595.4	536	[7, 15]
[(*t*-BuO)₃W≡P→W(CO)₅] **18b**	2.132(4)	546.0	554, 163	[7, 15]
[(*t*-BuO)₃W≡P→MnCp″(CO)₂] **18c**		614.0	566	[37]
[thf(Ph′O)₃W≡P→Cr(CO)₅] **21a**		773.4	549	[32]
[thf(Ph′O)₃W≡P→W(CO)₅] **21b**	2.127(2)	718.5	562, 170	[32]

[a] Not given in the literature cited

to a pronounced ^{31}P upfield shift, corresponding to less deshielding at the phosphorus atom, and concomitant increase in the ^{1}J$_{W,P}$ coupling constants. The latter effect is based on an increase in the s character of the W≡P σ-bond due to the linear coordination of a substituent on the phosphorus lone pair, which possessed a large s character in the terminal coordination mode [17, 29]. Both these effects are especially pronounced for coordination of [(N₃N)W≡P] to a pure σ-acceptor like GaCl₃ (**4b**: 1080 ppm, 138 Hz; **15**: 366 ppm, 712 Hz). Large ^{1}J$_{W,C}$ coupling constants are also observed in the ^{13}C-NMR spectra of the related tungsten alkylidyne complexes, whose ^{13}C signals reveal ^{1}J$_{W,C}$ coupling constants on the order of 200–300 Hz [38].

   Coordination of the alkoxide-supported phosphido complexes to [M(CO)ₙ] in complexes **18** reveal similar spectroscopic trends, while no structural data is available for complex **3c** for comparison, as it undergoes subsequent reactions. With 2.127(2) Å **21b** reveals the shortest W≡P triple bond distance reported so far (Fig. 2). Theoretical calculations employing BP86 density functional methods on the model compounds [(HO)₃W≡P] (**3e**), [(HO)₃W≡P→W(CO)₅] (**21c**), and [thf(HO)₃W≡P→W(CO)₅] (**21d**) show a slight shortening of the W≡P bond due to coordination of the phosphido phosphorus lone pair in **3e** to a [W(CO)₅] fragment [32], in accordance with an increase in the s-character in the W≡P bond. This coordination of the phosphido ligand is accompanied by rehybridization of the lone pair on the P atom from sp$^{0.14}$ to sp$^{0.98}$ in **21c**. The coordination of the Lewis base THF via the low-lying LUMO+1 σ* type orbital of **21c** leads to an elongation of this triple bond in **21d** but stabilizes the overall complex. The bonding energy for THF in **21d** was calculated to be 54 kJ/mol, and this co-ordination was shown to increase the energy of the HOMO-LUMO gap sig-
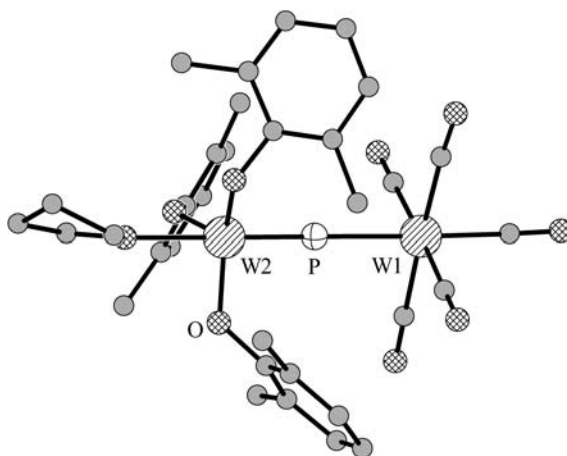
Fig. 2 Molecular structure of [thf(Ph′O)₃W≡P→W(CO)₅] (**21b**) [32]. H-atoms are omitted for clarity

nificantly in **21d** in comparison to **21c** while leading to an increased polarization of the W≡P bond [32].

In Fig. 3 the MO schemes and the structural parameters of **3e** and **21c** are compared using B-P86/SVP density functional theory and RI-J approximations [39]. In general the phosphido ligand complexes of types A and B
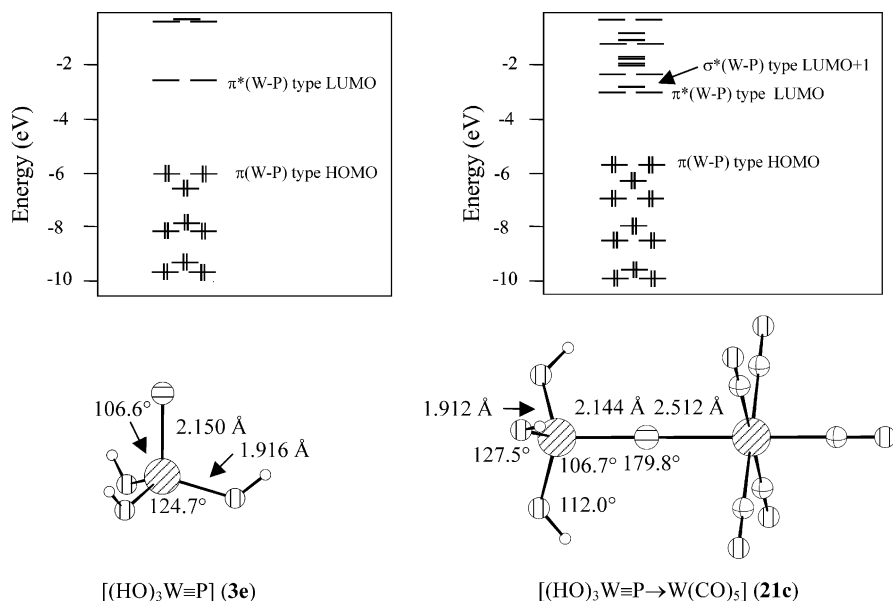
Fig. 3 Comparison of the MO schemes and structural parameters of complexes **3e** and **21c** using the B-P86/SVP density functional theory and RI-J approximations [39]

(Fig. 3) show π orbitals to be the HOMO orbitals. Thus, the primary reactivity pattern should be the 'side-on' reactivity. However, this reactivity is generally not allowed in the phosphido complexes with tris-amido ligand sets due to their kinetic stabilization by bulky substituents. Therefore, experimentally, only the less crowded and more flexible alkoxide complexes **18** and **21** show the anticipated 'side-on' access to the triple bond.

3.3
Reactivity of Asymmetrically Bridged Phosphido Ligand Complexes

The alkoxide complexes **18** and **21** are stable compounds at room temperature in the solid state as well as in solutions of nonpolar solvents like, e.g., *n*-pentane. Due to the high flexibility of the alkoxide ligands in complexes **18** and **21** in solution and additionally the relatively weak THF donation in **21**, the triple bond of these compounds remains accessible and makes them highly 'side-on' reactive. Thus, toluene solutions of **18b** and **21b** react at ambient temperature over a longer period of time under formal reductive dimerization combined with the loss of two RO ligands to give dark-green crystals of **22** and **23** (Eq. 15), which contain a planar W_4P_2 core.
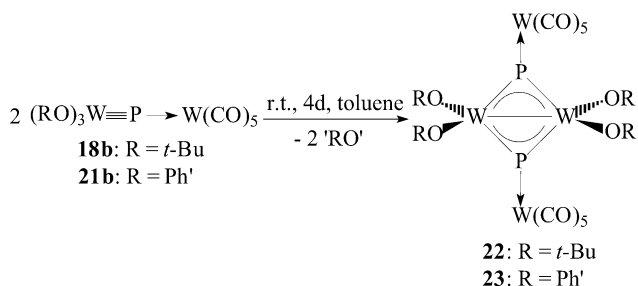
Some selected reactions of **21b** were investigated [32]. In the reaction with [(Ph'O)$_4$W=O] the dinuclear compound **24** is formed (Eq. 16) containing an almost planar W_2OP four-membered ring system. The structure of **24** reveals that after the formal cycloaddition reaction a reductive W-W bond formation occurs under loss of OPh' moieties.
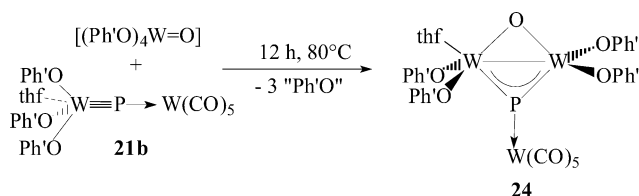
Furthermore, the phosphido complex **21b** reacts with [(PPh$_3$)$_2$Pt (η^2-C$_2$H$_4$)] to give the dinuclear complex [(Ph'O)$_2$WPt(PPh$_3$)(μ-PPh$_2$) {(μ-PPh)W(CO)$_5$}] (**25**) which also possesses a planar WP$_2$Pt four-mem-

bered ring unit [32]. The first step of the reaction is presumably a displacement of ethylene by the W≡P triple bond, so that an intermediate as indicated in Eq. (17) might be formed. Subsequently, an unusual 1,3-shift of one of the phenyl groups of the PPh$_3$ ligands to the phosphido phosphorus occurs to give a bridging PPh$_2$ and a bridging [PhPW(CO)$_5$] group in this novel phosphinidene derivative **25**. Transition-metal mediated P-C bond cleavages, important processes in homogeneous catalysis [40], occur usually at higher temperatures, while the reaction in Eq. (17) proceeds at temperatures as low as −10 °C. Density functional calculations on the simplified model compound [(HO)$_3$W(μ-PH$_2$)(μ-PH{W(CO)$_5$})Pt(PH$_3$)] (**25a**) were applied to gain insight into the bonding situation of the central WP$_2$Pt core [32]. Population analysis reveals significant W-Pt overlap population for **25a** in contrast to other phosphanido-bridged complexes like, e.g., [W(CO)$_4$(μ-PPh$_2$)$_2$Pt(PPh$_3$)] [41].
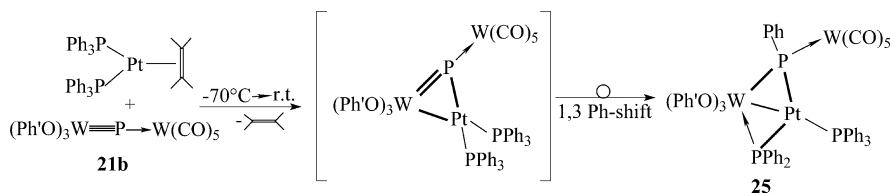
4
Linear Coordinated Phosphinidene Complexes

Though phosphinidene complexes were first isolated in 1987 and have thus existed significantly longer than phosphido complexes, stable examples still remain relatively rare [42]. Two types of terminal phosphinidene complexes [L$_n$MPR] exist: the linear complexes of type C and bent ones of type D. Representative examples of both types are summarized in Table 3. Metal-phosphorus triple bonding is present in phosphinidene complexes with an almost linear MPR arrangement of type C, as the filled p orbital of phosphorus can form an additional π bond to an empty d orbital on the metal. Complexes **8–10** exhibit the linear MPQ arrangement in type C but display a more complex bonding situation, as addressed above, than the linear phosphinidene complexes with organic substituents on phosphorus. No X-ray structural data has been published for compounds [(N$_3$N)M≡PMe]$^+$OTf$^-$ (**11a,b**), but the large upfield shift of the ^{31}P-NMR resonances (**11a:** 282.7 ppm, **11b:** 338.6 ppm) and large increase in ^{1}J$_{W,P}$ coupling constant (**11b:** 748 Hz) in comparison to the parent compounds [(N$_3$N)M≡P] (**7a,b**) indicate a bonding situation similar to that in [(N$_3$N)W≡P→GaCl$_3$] (**15**), such that [(N$_3$N)M≡P] is coordinated to the pure σ-acceptor CH$_3^+$. A crystallographic study of the related complex [(N$_3$N)W≡AsMe]$^+$OTf$^-$ [16] revealed a slight shortening of the W≡As bond length (2.249(1) Å) from its parent compound [(N$_3$N)W≡As] (2.290(1) Å) [17] as well as a nearly linear W-As-C bond angle (173.3(6)°), although it is not known to what degree this

Table 3 ^{31}P-NMR data, M-P bond lengths, and M-P-Q bond angles of representative phosphinidene complexes

	$\delta(^{31}\text{P})$ [ppm]	$^1J_{W,P}$ [Hz]	d(M-P) [Å]	<M-P-Q [°]	Ref.
Complexes of Type C					
[(Ph″RN)$_3$Mo(PO)] **8**	269.8		2.079(5)	177.6(8)	[33]
[(Ph″RN)$_3$Mo(PS)] **9**	383		2.100(2)	a	[8, 34]
[(Ph″RN)$_3$Mo(PNMes)] **10**	159		2.085(5)	178.1(9)	[8]
[(N$_3$N)Mo≡PMe]$^+$OTf$^-$ **11a**	282.7				[16]
[(N$_3$N)W≡PMe]$^+$OTf$^-$ **11b**	338.6	748			[16, 30]
[(Ph$_2$MeP)Cl$_2$(CO)W≡PPh*] **26**	193.0	649	2.169(1)	168.2(2)	[43]
[(N$_3$N)Ta≡PCy] **27**	209.8		2.145(7)	a	[44]
Complexes of Type D					
[Cp*$_2$(Me$_3$PO)U=PPh*] **28**	71.1		2.562(3)	143.7(3)	[45]
[Cp$_2$(Me$_3$P)Zr=PPh*] **29**	729.4		2.505(4)	116.1(4)	[46]
[Cp$_2$Mo=PPh*] **30a**	799.5		2.370(2)	115.8(2)	[47]
[Cp$_2$W=PPh*] **30b**	661.1	153.5	2.349(5)	114.8(5)	[48]
[(t-Bu$_3$SiO)$_3$Ta=PPh] **31**	334.6				[49]
[Cp*(CO)$_3$W=PN(i-Pr)$_2$]$^+$AlCl$_4^-$ **32**	939	a	2.450(1)	118.7(1)	[50]

^{a} Not given in the literature cited

linearity is owed to the steric crowding of the N$_3$N ligand, thus lending indirect support to the classification of phosphinidene complexes **11a,b** as complexes of type C.

The differentiation between types C and D is substantiated, in part, by the generally shorter M-P bond lengths for type C. Direct comparison of the bond lengths of the tungsten complexes **26** (2.169(1) Å) and **30b** (2.349(5) Å) reveals a difference of almost 0.2 Å, while complex **26** has a W≡P bond length nearly identical to that of the terminal phosphido complex **4b** (2.162(4) Å). The $^1J_{W,P}$ coupling constants of complexes **11b** and **26** are quite similar and in the range of the Lewis-acid coordinated phosphido complexes of CN 2. The ^{31}P-NMR shifts for the linear phosphinidenes of type C are also found in the range of the coordinated phosphido complexes, whereas the phosphinidene complexes of type D (with the exception of **28**, whose NMR spectra demonstrate paramagnetic shifting due to U(IV)) generally show ^{31}P shifts at lower field.

5
Outlook

The synthesis of stable complexes with transition metal-phosphorus triple bonds is of fundamental importance and opens a novel chapter of a special field of coordination chemistry. The synthesis of analogous complexes with ligands of the heavier homologues like arsenic has partially been carried out [6], while for antimony and bismuth, the elusive M≡Sb and M≡Bi systems have now moved within reach. Moreover, the experimental and theoretical

evidence is now answering many fundamental questions on the properties of P_1 ligands. In general, the major challenges in this field now include the comprehensive study of the various reactivity patterns of these compounds. Thus, it opens up the synthetic pathway to novel ligands like terminally coordinated EO, ES, ESe, ETe as well as ENR ligands (E=P, As, Sb). Furthermore, the high 'side-on' reactivity of the alkoxide-substituted complexes **3**, **18**, **21** will lead to a larger scope of subsequent reactions including cycloaddition reactions, formation of novel metallo heterocycles, and cage compounds. The synthesis and isolation of complexes with metal-phosphorus triple bonds have been achieved for transition metals in high oxidation states. In contrast, for transition metals in low oxidation states it seems that such complexes exist only as highly reactive intermediates. Therefore we were highly interested in and finally succeeded in the development of a synthetic concept to generate such intermediates directly. For this purpose we used the Cp* migration of phosphinidene complexes of the formulae $[Cp*P\{M(CO)_5\}_2]$ (M=Cr, Mo, W) to form after thermal or photolytic activation intermediates of the type $[Cp*(CO)_2M \equiv P \rightarrow M(CO)_5]$ [51]. In trapping reactions with reactive substrates a large potential for extended reactivity studies [52] is opened up.

References

1. Dehnicke K, Strähle J (1981) Angew Chem 93:451; Angew Chem Int Ed Engl 20:413; (1992) Angew Chem 104:978; Angew Chem Int Ed Engl 31:955; Dehnicke K, Weller F, Strähle J (2001) Chem Soc Rev 30:125
2. Herrmann WA (1986) Angew Chem 98:57; Angew Chem Int Ed Engl 25:56
3. Knopp B, Lörcher K-P, Strähle (1977) Z Naturforsch B 32:1361; Liese W, Dehnicke K, Rogers RD, Shakir R, Atwood JL (1988) J Chem Soc Dalton Trans 1061; Phillips FL, Skapski AC (1975) Acta Cryst Sect B 31:2667; Liese W, Dehnicke K, Walker I, Strähle J (1979) Z Naturforsch B 35:693
4. C.f. about cyclotrimerization: Herrmann WA, Bogdanovic S, Priermeier T, Poli R, Fettinger JC (1995) Angew Chem 107:63; Angew Chem Int Ed Engl 34:112; Chisholm MH, Folting-Streib K, Tidtke DB, Lemoigno F, Eisenstein O (1995) Angew Chem 107:61; Angew Chem Int Ed Engl 34:110
5. The term phosphido ligand for the P^{3-} ligand corresponds to the IUPAC guidelines. Hitherto this name has often been used incorrectly for R_2P^- ligands
6. Scheer M (1997) Coord Chem Rev 163:271
7. Scheer M, Schuster K, Budzichowski TA, Chisholm MH, Streib WE (1995) Chem Commun 1671
8. Laplaza CE, Davis WM, Cummins CC (1995) Angew Chem 107:2181; Angew Chem Int Ed Engl 34:2042
9. Schrock RR, Zanetti NC, Davis WN (1995) Angew Chem 107:2184; Angew Chem Int Ed Engl 34:2044
10. Laplaza CE, Odom AL, Davis WM, Cummins CC (1995) J Am Chem Soc 117:4999
11. Johnson MJA, Lee PM, Odom AL, Davis WM, Cummins CC (1997) Angew Chem 109:110; Angew Chem Int Ed Engl 36:87

12. Cherry J-PF, Stephens FH, Johnson MJA, Diaconescu PL, Cummins CC (2001) Inorg Chem 40:6860
13. Stephens FH, Figueroa JS, Diaconescu PL, Cummins CC (2003) J Am Chem Soc 125:9264
14. Becker G, Becker W, Knebl R, Schmidt H, Hildenbrand U, Westerhausen M (1987) Phosphorus Sulphur 30:349; Becker G, Becker W, Knebl R, Schmidt H, Weber U, Westerhausen M (1985) Nova Acta Leopaldina 59:55; Binger P (1990) In: Regitz M, Scherer OJ (eds) Multiple bonds and low coordination in phosphorus chemistry. Thieme, Stuttgart, p 100
15. Scheer M, Kramkowski P, Schuster K (1999) Organometallics 18:2874
16. Mösch-Zanetti NC, Schrock RR, Davis WM, Wanninger K, Seidel SW, O'Donoghue MB (1997) J Am Chem Soc 119:11037
17. Scheer M, Müller J, Häser M (1996) Angew Chem 108:2637; Angew Chem Int Ed Engl 35:2492
18. Schneider S (2003) PhD thesis. Humboldt-University, Berlin, Germany
19. Schrock RR (1997) Acc Chem Res 30:9
20. Nugent WA, Meyer JM (1998) Metal-ligand multiple bonds. Wiley, New York
21. Becker G, Gresser G, Uhl W (1981) Z Naturforsh B 36:16
22. Niecke E, Nieger M, Reichert F (1988) Angew Chem 100:1781; Angew Chem Int Ed Engl 27:1715
23. Peters JC, Odom AL, Cummins CC (1997) Chem Commun 1995
24. Greco JB, Peters JC, Baker TA, Davis WM, Cummins CC, Wu G (2001) J Am Chem Soc 123:5003
25. Laplaza CE, Johnson MJA, Peters JC, Odom AL, Kim E, Cummins CC, George GN, Pickering IJ (1996) J Am Chem Soc 118:8623
26. Wu G, Rovnyak D, Johnson MJA, Zanetti NC, Musaev DG, Morokuma K, Schrock RR, Griffin RG, Cummins CC (1996) J Am Chem Soc 118:10654
27. Häser M (1996) J Am Chem Soc 118:7311
28. Cherry J-PF, Johnson AR, Baraldo LM, Tsai Y-C, Cummins CC, Kryatov SV, Rybak-Akimova EV, Capps KB, Hoff CD, Haar CM, Nolan S P (2001) J Am Chem Soc 123:7271
29. Wagener T, Frenking G (1998) Inorg Chem 37:1805; Wagener T, Frenking G (1998) Inorg Chem 37:6402
30. Johnson-Carr JA, Zanetti NC, Schrock RR, Hopkins MD (1996) J Am Chem Soc 118:11,305
31. Kramkowski P, Scheer M (2000) Angew Chem 112:959; Angew Chem Int Ed Engl 39:928
32. Kramkowski P, Baum G, Radius U, Kaupp M, Scheer M (1999) Chem Eur J 5:2890
33. Johnson MJA, Odom AL, Cummins CC (1997) Chem Commun 1523
34. Cummins CC (1998) Chem Commun 1777
35. Scheer M, Müller J, Baum G, Häser M (1998) Chem Commun 1051
36. Scheer M, Müller J, Baum G, Häser M (1998) Chem Commun 2505; Scheer M, Müller J, Schiffer M, Baum G, Winter R (2000) Chem Eur J 6:1252
37. Schuster K (1995) PhD thesis, University of Karlsruhe, Germany
38. Schrock RR (1986) Acc Chem Res 19:342
39. Ahlrichs R, von Arnim M (1995) TURBOMOLE, parallel implementation of SCF, density functional, and chemical shift modules. In: Clementi E, Corongiu G (eds) Methods and techniques in computational chemistry. STEF, Cagliary; Eichkorn K, Treutler O, Öhm H, Häser M, Ahlrichs R (1995) Chem Phys Lett 242:652; Becke AD (1988) Phys Rev A 38:3098; Perdew JP (1986) Phys Rev B 33:8822
40. Garrou PE (1985) Chem Rev 85:171 and references cited therein
41. Morrison ED, Harley AD, Marcelli MA, Geuffroy GL, Rheingold AL, Fultz WC (1984) Organometallics 3:1407
42. Cowley AH (1997) Acc Chem Res 30:445
43. Cowley AH, Pellerin B, Atwood JL, Bott SG (1990) J Am Chem Soc 112:6734
44. Cummins CC, Schrock RR, Davis WD (1993) Angew Chem 105:758; Angew Chem Int Ed Engl 32:756

45. Arney SJ, Schnabel C, Scott BC, Burns CJ (1996) J Am Chem Soc 118:6780
46. Hou Z, Breen TC, Stephan DW (1993) Organometallics 12:3158
47. Hitchcock PB, Lappert MF, Leung WP (1987) Chem Commun 1282
48. Bohra P, Hitchcock PB, Lappert MF, Leung WP (1989) Polyhedron 8:1884
49. Bonauno JB, Wolczanski PT, Lobkovsky EB (1994) J Am Chem Soc 116:11,159
50. Sterenberg BT, Udachin KA, Carty AJ (2001) Organometallics 20:2657
51. Scheer M, Leiner E, Kramkowski P, Schiffer M, Baum G (1998) Chem Eur J 4:1917; Schiffer M, Leiner E, Scheer M (2001) Eur J Inorg Chem 1661
52. Schiffer M, Scheer M (2001) Chem Eur J 7:1855

Homogeneous Catalysis for H-P Bond Addition Reactions

Masato Tanaka

Chemical Resources Laboratory, Tokyo Institute of Technology, 4259 Nagatsuta, Midori-ku, Yokohama 226-8503, Japan
E-mail: m.tanaka@res.titech.ac.jp

Abstract Although patents disclosed transition metal-catalyzed addition of PH$_3$ to formaldehyde and acrylonitrile more than four decades ago, exploration into the synthetic scope of and the mechanistic study on the metal complex-catalyzed addition of P-H bonds have been made only within the last ten years. Not only PH$_3$ but also a variety of P-H bonds have been found to add in the presence of metal complex catalysts. As for the substrate, recently reported new procedures are applicable to a wide range of alkenes, dienes, and alkynes. Control and even reversal of regioselectivity are also possible by tuning the ligand nature and by the use of an appropriate additive. Optically active compounds with chirality on phosphorus are also readily synthesized. This chapter summarizes the current state of the art in this emerging area of homogeneous catalysis, which provides a powerful tool to synthesize organophosphorus compounds.

Keywords H-P addition · Unsaturated carbon linkage · Transition metal complex · Homogeneous catalysis

1
Introduction

Organophosphorus compounds, useful in diverse applications, are still produced by classic methods such as Grignard and Arbuzov reactions. The drawback of these methods lies in that they are substitution reactions, which result in the formation of undesired co-products. In addition, these reactions are not always very selective. Although radical addition of the P-H bond is known, control of the selectivity is not easy either. Over the last two decades, the metal complex-catalyzed addition of P-H bonds to carbon-carbon unsaturated linkages has provided powerful alternative routes to organophosphorus compounds [1]. The selectivity of the reaction can be tuned by the modification of the electronic and steric nature of the catalysts. This chapter summarizes the state of the art in this emerging field of homogeneous catalytic transformation. Addition to carbonyl functionality is not described, but the addition of PH_3 to formaldehyde is also briefly mentioned since its mechanistic study is useful in mechanistic consideration of the processes within the coverage of this chapter.

2
Metal Complex-Catalyzed Addition of the P(III)-H Bond
to Unsaturated Compounds

2.1
## Transition Metal-Catalyzed Addition of PH_3 to Formaldehyde

Acid-catalyzed addition of PH_3 to formaldehyde is an industrial process producing $P(CH_2OH)_4{}^+$, useful as a flame retardant. As for the metal complex-catalyzed addition, platinum salts such as $PtCl_2$, $PtCl_4$, K_2PtCl_4, and K_2PtCl_6 or nickel and cobalt salts in conjunction with primary and secondary amines have been known since 1958 to catalyze the addition of PH_3 at $-3\sim5$ °C to formaldehyde (Scheme 1) [2, 3]. What is surprising is that the process, forming the phosphine, which is envisioned to suppress the catalysis due to its coordination, in practice, accelerates as the reaction proceeds.

$$PH_3 + HCHO \longrightarrow PH_2(CH_2OH) + PH(CH_2OH)_2 + P(CH_2OH)_3$$
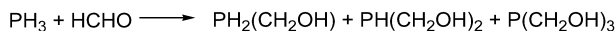
Scheme 1

Pringle and coworkers revisited this interesting process from synthetic and mechanistic viewpoints. The catalytic transformation using aqueous

HCHO and PH_3 proceeds in the presence of K_2PtCl_4 at room temperature and affords the crystalline product in an essentially quantitative yield in 2.5 h [4]. Palladium compounds are also active in the catalysis [5]. In these reactions the active species is believed to be zero valent. Two mechanistic possibilities have been proposed as illustrated in Scheme 2. The first elemental process involved in the catalytic cycle is oxidative addition of a P-H bond, which is well precedented [6]. In one of the mechanistic possibilities the processes that follow the oxidative addition are the insertion of the C=O bond into H-M species and P-C reductive elimination, the latter of which is also precedented [7]. In the other, the coordinating phosphide ligand makes a nucleophilic attack [8] at the formaldehyde carbon forming zwitterionic species.
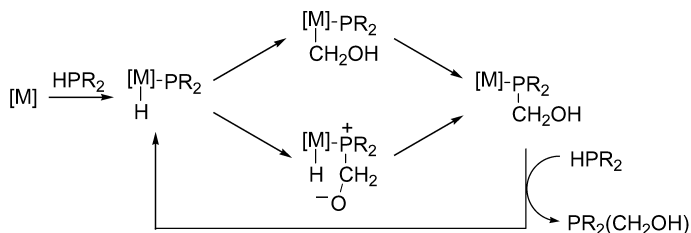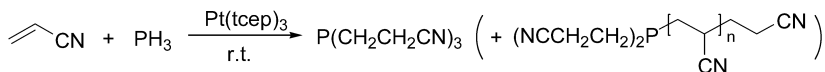

Scheme 2

In the research aiming at the application of the addition reaction, Pringle and co-workers found that bifunctional phosphine starting materials like $H_2PCH_2CH_2PH_2$ spontaneously react with formaldehyde in the absence of the catalyst, forming water-soluble chelating phosphines [9].

2.2
Transition Metal-Catalyzed Addition of PH_3 to Alkenes

Besides formaldehyde, Michael acceptors such as acrylonitrile and ethyl acrylate also serve as substrate to undergo the addition in the presence of various metal complexes [10–14]. Acrylonitrile affords $P(CH_2CH_2CN)_3$ tcep (Scheme 3). The order of catalytic activity is reported to be $Pt[P(CH_2CH_2CN)_3]_3 > Pd[P(CH_2CH_2CN)_3]_3 \approx IrCl[P(CH_2CH_2CN)_3]_3 > Ni[P(CH_2CH_2CN)_3]_3$. The solvent effect on the rate is not significant. In acetonitrile, however, a small amount of a telomer is formed.
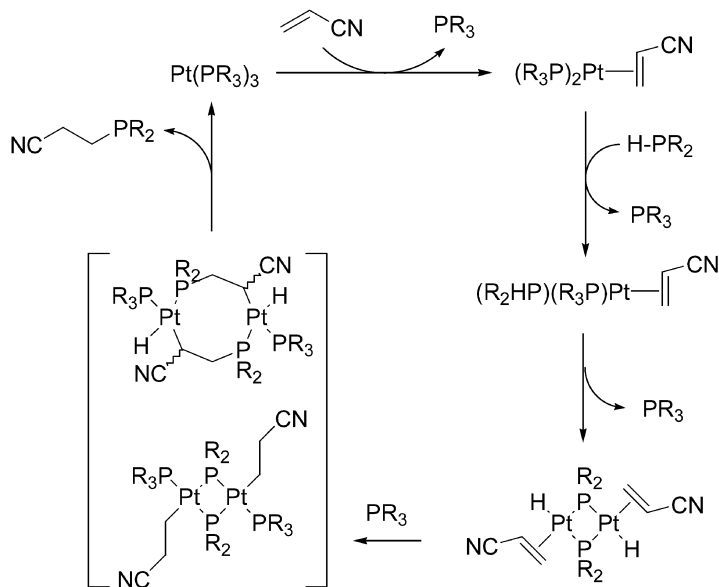

Scheme 3

In view of excess phosphine being inhibitory in many catalytic reactions, it is surprising that the hydrophosphination reaction is not suppressed by the phosphines formed. In agreement with this, the product phosphine $P(CH_2CH_2CN)_3$ is reluctant to form tetrakis(phosphine)platinum species, allowing the metal complex to be coordinatively unsaturated. Likewise, the

bis(phosphine)(acrylonitrile)platinum complex does not undergo displacement of the acrylonitrile ligand with $P(CH_2CH_2CN)_3$ even in the presence of 50 equivalents of the phosphine.
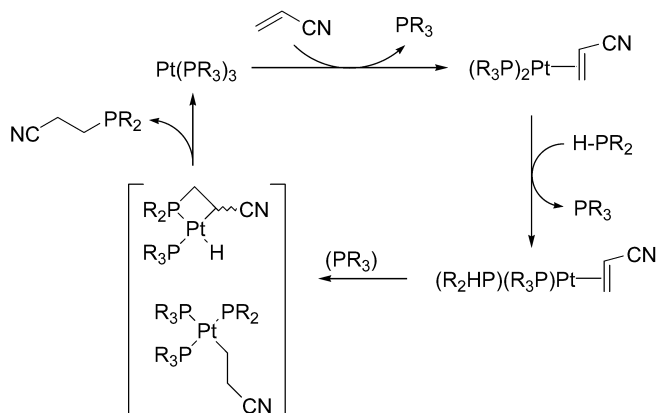
Scheme 4

The following two mechanistic possibilities have been proposed on the basis of kinetic studies. When the concentration of $P(CH_2CH_2CN)_3$ is high, the mononuclear mechanism has been proposed as shown in Scheme 4 [11,
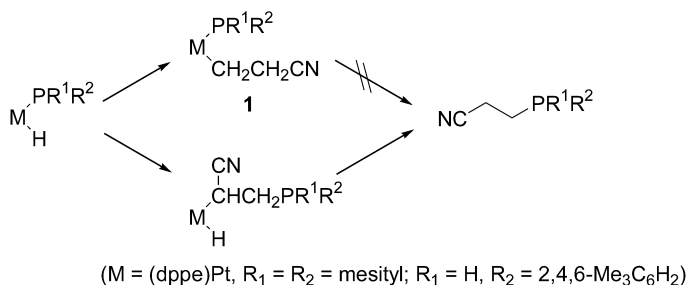

Scheme 5

12]. The elemental processes involved such as P-H oxidative addition and P-C reductive elimination are precedented (see above). The telomer formation may stem from the four-membered intermediate, which can relieve the ring strain upon further insertion of acrylonitrile into the Pt-C bond.

However, the other mechanism of catalysis involving dinuclear species was considered at low concentrations of $P(CH_2CH_2CN)_3$ (Scheme 5) [12].

Detailed mechanistic study by Glueck has revealed that the P-C bond forming process that follows the P-H oxidative addition comprises insertion of the C=C linkage into the P-M bond and C-H reductive elimination, not insertion into H-M and P-C reductive elimination, as far as platinum is concerned (Scheme 6) [13]. Thus, the phosphido hydrido complex $Pt(dppe)(PR^1R^2)H$ [dppe=1,2-bis(diphenylphosphino)ethane], upon treatment with 2 equivalents of acrylonitrile, affords $R^1R^2PCH_2CH_2CN$ ($R^1=R^2$=mesityl; R^1=H, R^2=2,4,6-$Me_3C_6H_2$). However, the possible intermediate 1 ($R^1=R^2$=mesityl; R^1=H, R^2=2,4,6-$Me_3C_6H_2$), readily prepared separately and isolated, is stable in solution even on heating. Furthermore, these complexes 1 are inactive in the catalytic hydrophosphination. Although insertion into the P-Pt bond was not directly observed when the supporting ligand was dppe, the methyl analogue, $Pt(dppe)(PR^1R^2)Me$ ($R^1=R^2$=mesityl; R^1=H, R^2=2,4,6-$Me_3C_6H_2$), and the dcpe [dcpe=1,2-bis(dicyclohexylphosphino)ethane] analogue, $Pt(dcpe)[PH(2,4,6-Me_3C_6H_2)]H$, do undergo insertion regioselectively, forming the (1-cyano-2-phosphinoethyl)platinum species. On the other hand, the analogous palladium complex $Pd(dppe)[PH(2,4,6-Me_3C_6H_2)]Me$ can be generated only at −78 °C and reductive elimination leading to $PHMe[PH(2,4,6-Me_3C_6H_2)]$ readily takes place at room temperature. In the hydrophosphination of unsaturated substrates using palladium catalysts, the reaction may proceed through insertion into the H-Pd bond followed by P-C reductive elimination.

(M = (dppe)Pt, $R_1 = R_2$ = mesityl; R_1 = H, R_2 = 2,4,6-$Me_3C_6H_2$)

Scheme 6

Pringle reported that ethyl acrylate also reacts similarly [14]. The radical addition at 70 °C forms a mixture of primary PH_2 (CH_2CH_2COOEt), secondary $PH(CH_2CH_2COOEt)_2$ and tertiary phosphines. The tertiary phosphine component is not pure $P(CH_2CH_2COOEt)_3$, but a mixture with telomers. However, Pt complex-catalyzed addition is very clean; when PH_3 is bubbled through a warmed solution of ethyl acrylate in the presence of 0.002 equiva-

lents of Pt(0) species, $P(CH_2CH_2COOEt)_3$ and the telomer are formed, the selectivity for $P(CH_2CH_2COOEt)_3$ being higher than 90% (Scheme 7). The formation of the primary and the secondary phosphines is negligible, suggesting that the reactivity of P-H bonds increases in the order $PH_3 < PH_2(CH_2CH_2COOEt) < PH(CH_2CH_2COOEt)_2$.
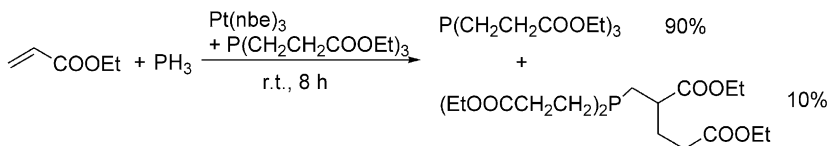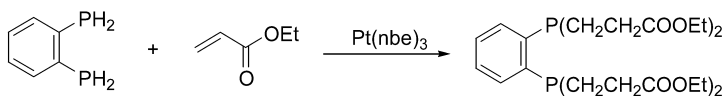

Scheme 7

The addition of $PH(CH_2CH_2COOEt)_2$ to the acrylate was separately studied to reveal that the reaction was complete in less than 90 min with the selectivity higher than 95%.

As was observed in the addition to acrylonitrile, the product phosphine does not inhibit the catalytic addition to the acrylate seriously. This is consistent with the observation that $P(CH_2CH_2COOEt)_3$ does not form $Pt[P(CH_2CH_2COOEt)_3]_4$ upon addition of extra $P(CH_2CH_2COOEt)_3$ to $Pt[P(CH_2CH_2COOEt)_3]_3$. Furthermore, addition of ethyl acrylate to $Pt[P(CH_2CH_2COOEt)_3]_3$ induces the phosphine displacement to afford $Pt(CH_2=CHCOOEt)[P(CH_2CH_2COOEt)_3]_2$.

Bifunctional phosphines also react forming chelating di-tertiary phosphines (Scheme 8). Serious catalysis inhibition by the product is not found.

Scheme 8

The mechanistic study on the hydrophosphination of activated olefins, in conjunction with rapid inversion of the configuration at the phosphorus center, was elaborated to develop asymmetric hydrophosphination catalyzed by a chiral phosphine platinum complex although the % ee is not excitingly high yet (Scheme 9) [15].
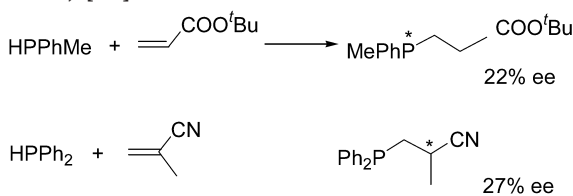
Scheme 9

Encouraged by the high reactivity of acrylonitrile and ethyl acrylate, the reaction of $CH_2=CHCF_3$ with PH_3 was attempted to reveal that it was totally unreactive [14]. However, styrene hydrophosphination with $HPPh_2$ was found by Beletskaya to be catalyzed by $Ni[P(OEt)_3]_4$ (Scheme 10) [16]. When divalent nickel complexes such as $Ni(PPh_3)_2Br_2$ are used, the reaction does not form the corresponding adduct, but oxidative dimerization of $HPPh_2$ forming Ph_2P-PPh_2 proceeds exclusively. The oxidative dimerization was also observed as a side reaction in the Ni(0)-catalyzed addition reaction. However, one equivalent of NEt_3 added to the reaction system completely suppresses the side reaction. A catalytic cycle comprising oxidative addition of a P-H bond, insertion of the C=C linkage into the resulting Ni-H bond and reductive elimination has been proposed, although mechanistic evidence has not been provided. $Pd(MeCN)_2Cl_2$ was also claimed to be active and β-selective in the addition reaction even at a lower temperature (90 °C). The oxidative dimerization does not appear to be a serious side reaction in the palladium catalysis.
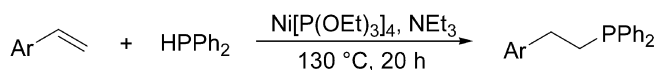
Ar (yield based on ^{31}P NMR): C_6H_6 (> 99), p-MeOC$_6$H$_4$ (> 99), o-MeOC$_6$H$_4$ (> 99), p-C$_5$H$_4$N (> 99), p-Me-o-C$_5$H$_3$N (> 95), o-C$_5$H$_4$N (> 99)

Scheme 10

2.3
Transition Metal-Catalyzed Addition of the P(III)-H Bond to Alkynes

Addition of the H-P bond to alkynes was also reported by Lin and Beletskaya [17]. $Pd(PPh_3)_4$, $Pd(dba)_2$ [dba=dibenzylideneacetone], $Pd(OAc)_2$, $Ni[P(OEt)_3]_4$, $Ni(acac)_2$ [acac=acetylacetonate], and $NiBr_2$ are all active al-

Table 1 Hydrophosphination of phenylacetylene

Catalyst	Conditions	Yield % (Product ratio)
Pd(PPh$_3$)$_4$	CH$_3$CN, 130 °C, 18 h	95 (0 : 14 : 86)
Pd(PPh$_3$)$_4$	C$_6$H$_6$, 130 °C, 18 h	95 (7 : 28 : 65)
Pd(OAc)$_2$	C$_6$H$_6$, 130 °C, 20 h	90 (64 : 10 : 26)
Pd(OAc)$_2$	CH$_3$CN, 130 °C, 7 h	89 (87 : 7 : 6)
Ni[P(OEt)$_3$]$_4$	C$_6$H$_6$, 80 °C, 10 h	> 93 (10 : 45 : 45)
Ni(acac)$_2$	C$_6$H$_6$, 80 °C, 60 h	> 82 (27 : 49 : 24)
NiBr$_2$	C$_6$H$_6$, 80 °C, 10 h	85 (86 : 14 : 0)
Pd(PPh$_3$)$_4$ + MeCOOH	CH$_3$CN, 80 °C, 12 h	> 92 (92 : 4 : 4)
Ni(acac)$_2$ + HP(O)(OEt)$_2$	C$_6$H$_6$, 80 °C, 10 h	90 (95 : 5 : 0)

though the selectivity is very much dependent on the catalyst. Selected examples are summarized in Table 1. As in the hydrophosphorylation that we found (see below), addition of acidic compounds reverses the regioselectivity.

The regiochemical reversal induced by the acidic compounds led them to propose the mechanisms illustrated in Scheme 11. In both catalytic cycles, the alkyne linkage inserts into the H-Pd bond; the left cycle (no acidic additive) forms linear alkenylpalladium complex, while the right cycle (with HX additive) generates branched alkenyl species. The provenance of the difference in the insertion regioselectivity has not been clearly addressed.
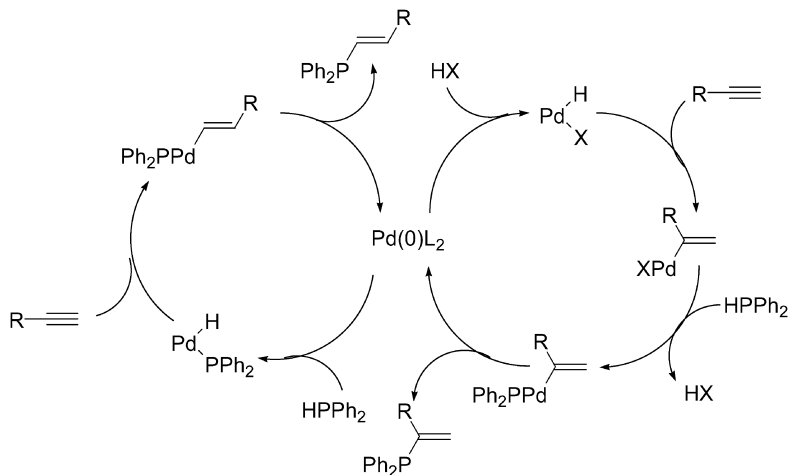
Scheme 11

Aliphatic alkynes are also reactive in the addition with HPPh$_2$, but the selectivity is low as compared with phenylacetylene unless a sterically demanding substituent is bound to the triple bond (Table 2).

Diphenylacetylene also reacted in the presence of Ni(acac)$_2$ at 80 °C to give *cis*-adduct selectively in 98% yield.

Table 2 Hydrophosphination of aliphatic alkynes

R	Conditions	Yield % (Product ratio)
Pr	C$_6$H$_6$, 1.5 h	88 (32 : 58 : 10)
^{t}Bu	C$_6$H$_6$, 2 h	90 (0 : 100 : 0)
MeOCH$_2$	CH$_3$CN, 3 h	87 (88 : 10 : 2)
Me$_2$NCH$_2$	CH$_3$CN, 60 h	83 (43 : 28 : 28)

Very recently, Dixneuf and coworkers have found that propargylic alcohols also undergo addition of Ph_2PH catalyzed by a ruthenium complex (Scheme 12) [18].

	Yield (%)	Z : E
$R^1 + R^2 =$ -$(CH_2)_5$-	70	95 : 5
$R^1 = R^2 =$ Me	81	75 : 25
$R^1 = R^2 =$ Et	55	75 : 25
$R^1 = R^2 = {}^i$Bu	50	80 : 20
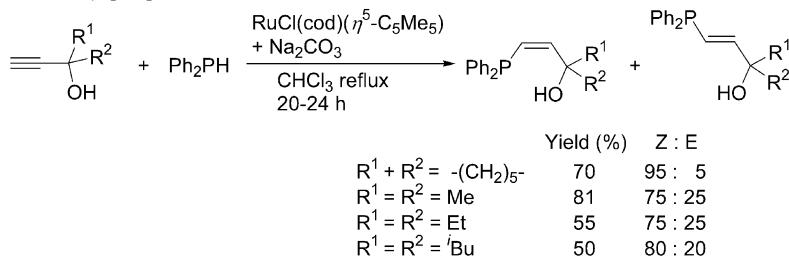
Scheme 12

This reaction is quite different from the other P-H addition reactions in that it involves external nucleophilic attack of $HPPh_2$ on the vinylidene ligand as shown in Scheme 13. The Z/E ratio depends on the structures of the substrate and the catalyst. Ru-Cp* (Cp*=η ^{5}-C_5Me_5) species selectively forms the Z isomer while Ru-Cp (Cp=η ^{5}-C_5H_5) favors the E isomer. Since the key intermediate is the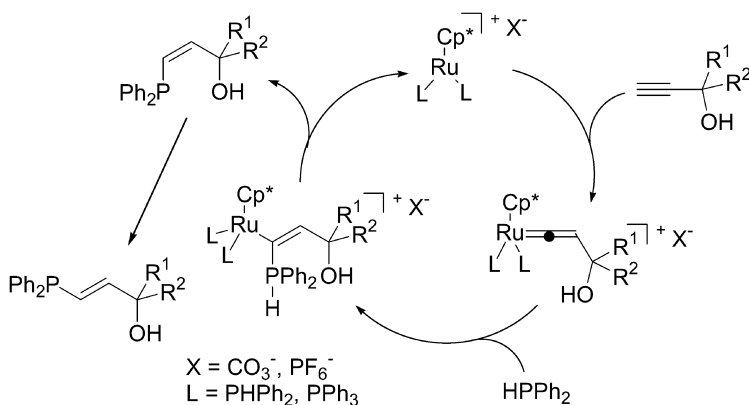 vinylidene species that has an electrophilic carbon, the reaction is applicable to other alkynes that are vinylidene precursors. Thus, phenylacetylene also reacts similarly to give $Ph_2PCH=CHPh$ (Z/E=93/7), while internal alkynes are totally unreactive.

Scheme 13

2.4
Lanthanide Metal-Catalyzed Addition

Lanthanide metals catalyze intramolecular hydrophosphination-cyclization of alkenyl- and alkynylphosphines rapidly at room temperature [19]. As summarized in Table 3, the reaction is quite general.

Table 3 Intramolecular hydrophosphination with Cp*$_2$YCH(SiMe$_3$)$_2$ precatalyst

H_2P⌒⌒⟍ (alkene)	cyclopentyl-P(H)-CH$_3$	TOF = 50.1 h^{-1} (25 °C)
H_2P⌒⟍⟍ (branched alkene)	2,5-dimethyl-pyrrolidinyl-P(H)	TOF = 340 h^{-1} (25 °C)
H_2P⌒⌒⌒⟍ (alkene)	cyclohexyl-P(H)-CH$_3$	TOF = 91.3 h^{-1} (25 °C)
H_2P⌒⌒⌒≡Ph (alkyne)	=CHPh substituted P(H) ring, Ph	TOF = 4.4 h^{-1} (22 °C)^a

^{a} Cp*$_2$LaCH(SiMe$_3$)$_2$ precatalyst was used.

Thermochemical consideration of the proposed catalytic cycle (Scheme 14) shows that insertion of an unsaturated carbon-carbon bond into the Ln-P bond is exothermic (−33 kcal/mol for an alkyne) or thermoneutral (for an alkene) and that the subsequent protonolysis of the resulting Ln-C bond with P–H is also exothermic (−7 kcal/mol for alkynes and −17 kcal/mol for alkenes). Kinetic and mechanistic studies have revealed that the turnover-limiting step is the insertion of the unsaturated linkage into the Ln-P bond (step i), which is followed by rapid protonolysis of the resulting Ln-C species (step ii). The catalyst resting state is presumed to be lanthanocene phosphine-phosphide species like Cp*$_2$Ln(PHR)(PH$_2$R) (R=alkenyl group), a model complex of which, dimeric [Cp*$_2$YPHPh]$_2$, was isolated.
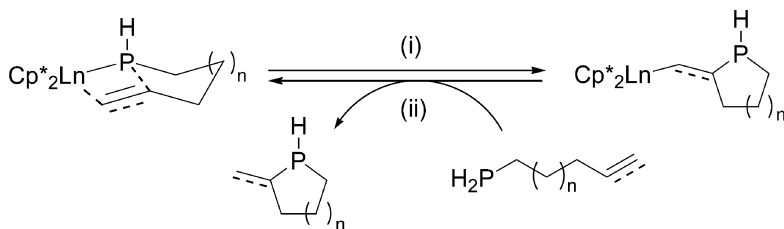
Scheme 14

Recently, intermolecular hydrophosphination of alkynes was also reported with ytterbium-imine complex catalyst precursors [20]. Aromatic alkynes react at room temperature to afford (*E*)-isomers, while aliphatic ones require heating at 80 °C and, quite surprisingly, (*Z*)-isomers (*trans*-addition products) are formed preferentially (Table 4). In this respect the ytterbium-catalyzed reactions are different from the radical process, in which the (*E*)-isomer formed initially isomerizes to the (*Z*)-isomer.

Table 4 Ytterbium-catalyzed intermolecular hydrophosphination of alkynes

R^1 = Ph, R^2 = Ph	r.t., 5 min	Quant (E/Z = 100/0)	-
R^1 = Ph, R^2 = Me	r.t., 5 min	Quant (E/Z = 80/20)	0%
R^1 = Ph, R^2 = H	r.t., 5 min	Quant (E/Z = 76/24)	0%
R^1 = ^{n}Pr, R^2 = ^{n}Pr	80 °C, 6 h	95% (E/Z = 0/100)	-
R^1 = ^{n}Hex, R^2 = H	r.t., 5 min	52% (E/Z = 27/73)	34%
R^1 = ^{t}Bu, R^2 = H	r.t., 3 h	62% (E/Z = 0/100)	10%

A mechanism that involves ytterbium phosphide species has been proposed, similarly to the foregoing intramolecular hydrophosphination. Generation of the phosphide species is supported by the formation of $Ph_2CDNHPh$ (after aqueous quench) upon treatment of the imine complex with Ph_2PD (Scheme 15). Lanthanide phosphide is known to react with THF, forming a 4-diphenylphosphino-1-butoxyl species [21], which was indeed found as a side product in the catalytic hydrophosphination of disubstituted aliphatic alkynes run in THF, supporting further the ytterbium-phosphide intermediate (Scheme 16).
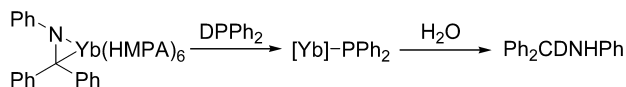
Scheme 15

The ytterbium-catalyzed reaction can be applied to other unsaturated compounds as summarized in Scheme 17.
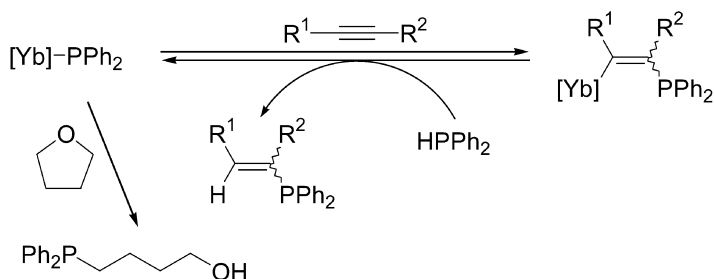
Scheme 16
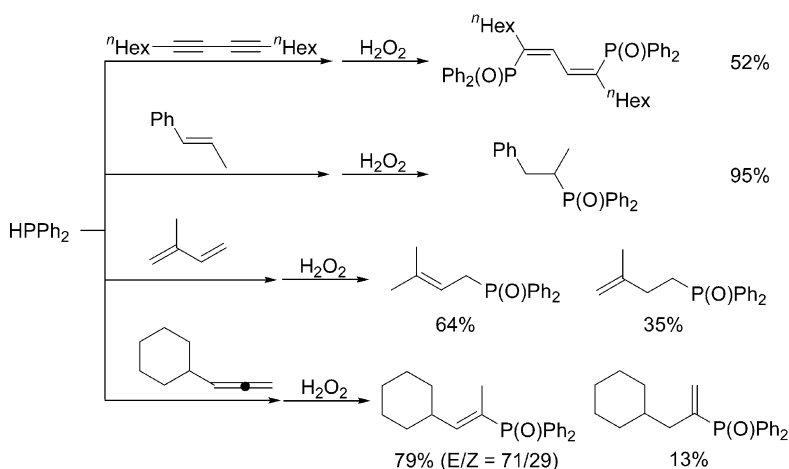
Scheme 17

3
Transition Metal-Catalyzed Addition of Hydrogen Phosphonate

Hydrogen phosphonates $[(RO)_2P(O)H]$ and secondary phosphine oxides $R_2P(O)H$ exist in equilibrium with their P(III) tautomers, $(RO)_2P(OH)$ and $R_2P(OH)$, respectively, the P(V) tautomers being more favored under ambient conditions. As ligands, they coordinate, like tertiary phosphines, to transition metals to form complexes, which have been used as catalysts for organic reactions. However, catalytic addition reactions of P(V)-H bonds have not been scrutinized until recently.

3.1
Addition to Alkynes

The H-P bond in hydrogen phosphonates readily adds across a C≡C bond [22]. Upon treatment of 1-octyne with dimethyl phosphonate in the presence of a palladium complex in refluxing tetrahydrofuran, the addition reaction proceeds smoothly to afford dimethyl 1-octen-2-ylphosphonate (2) regio- and stereo-selectively (Scheme 18).
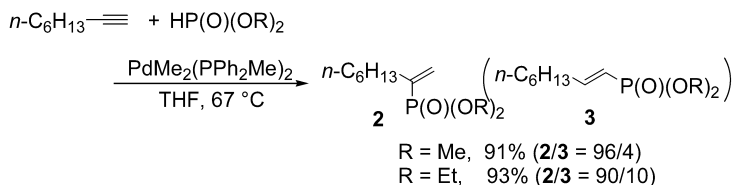
Scheme 18

Palladium(0) or readily reducible palladium(II) species that have less basic ligands display high activity in the addition reaction. Thus, *cis*-PdMe$_2$(PPh$_3$)$_2$, Pd(CH$_2$=CH$_2$)(PPh$_3$)$_2$, Pd(PPh$_3$)$_4$, and the combination of Pd(OAc)$_2$ and PPh$_3$ efficiently catalyze the reaction, while Pd(II) complexes such as PdCl$_2$, PdCl$_2$(PPh$_3$)$_2$, PdCl$_2$(PhCN)$_2$, Pd(OAc)$_2$ are totally inactive.

The palladium-catalyzed hydrophosphorylation is applicable to a wide range of alkynes, both aliphatic and aromatic, affording the corresponding adducts in high yields with high regioselectivities (Scheme 19). Alkene linkages are inert under the conditions. Accordingly, 1-ethynylcyclohexene reacts exclusively at the triple bond.
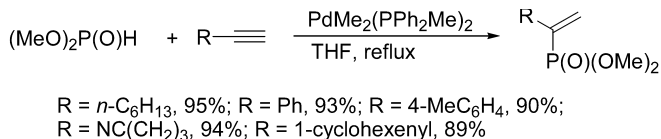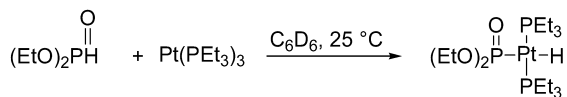
$$(MeO)_2P(O)H \quad + \quad R\!\!-\!\!\equiv \quad \xrightarrow[\text{THF, reflux}]{PdMe_2(PPh_2Me)_2} \quad \overset{R}{\underset{P(O)(OMe)_2}{\diagup\!\!\diagdown}}$$

R = *n*-C$_6$H$_{13}$, 95%; R = Ph, 93%; R = 4-MeC$_6$H$_4$, 90%;
R = NC(CH$_2$)$_3$, 94%; R = 1-cyclohexenyl, 89%
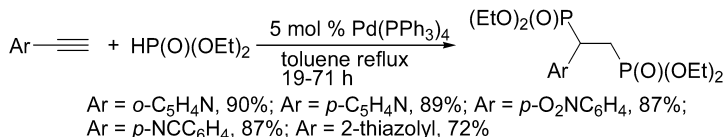
Scheme 19

The hydrophosphorylation of internal alkynes is somewhat slow. For instance, the reaction of 4-octyne with diethyl phosphonate resulted in 82% yield only after heating for 65 h. Only *cis*-isomer was observed in ^{1}H NMR spectroscopy.

Treatment of (EtO)$_2$P(O)H with Pt(PEt$_3$)$_3$ cleanly forms HPt[P(O)(OEt)$_2$](PEt$_3$)$_2$ via oxidative addition of the H-P bond (Scheme 20), which we believe is the initiation process of the catalysis. Mechanistic detail of the hydrophosphorylation reaction will be described for the reaction with alkene compounds.

$$\overset{O}{\underset{}{\|}} \atop (EtO)_2PH \quad + \quad Pt(PEt_3)_3 \quad \xrightarrow{C_6D_6,\ 25\ °C} \quad (EtO)_2\overset{O}{\overset{\|}{P}}\!-\!\overset{PEt_3}{\underset{PEt_3}{Pt}}\!-\!H$$

Scheme 20

When the reaction is run using excess hydrogen phosphonate (3 equivalents), sequential addition of two molecules of the phosphonate takes place to form 1,2-bisphosphonate as shown in Scheme 21 [23]. As described above, the first addition affords the branched isomer with a trace of the linear byproduct. Only the former is reactive to undergo the second addition forming the bisphosphonate as illustrated in Scheme 22.

$$Ar\!\!-\!\!\equiv \quad + \quad HP(O)(OEt)_2 \quad \xrightarrow[\substack{\text{toluene reflux}\\ \text{19-71 h}}]{5\ mol\ \%\ Pd(PPh_3)_4} \quad \underset{Ar \qquad P(O)(OEt)_2}{\overset{(EtO)_2(O)P}{\diagdown\!\!\diagup}}$$

Ar = *o*-C$_5$H$_4$N, 90%; Ar = *p*-C$_5$H$_4$N, 89%; Ar = *p*-O$_2$NC$_6$H$_4$, 87%;
Ar = *p*-NCC$_6$H$_4$, 87%; Ar = 2-thiazolyl, 72%
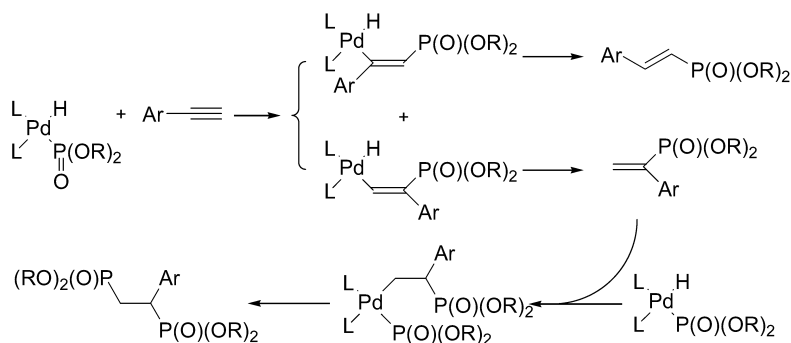
Scheme 21

Scheme 22

Rhodium complexes are not active in the addition reaction of acyclic hydrogen phosphonates such as dimethyl phosphonate. However, $RhCl(PPh_3)_3$ has proved to catalyze the reaction efficiently when the five-membered one **4a** was used [24].

The nature of the solvent significantly affects the progress of the reaction (Table 5). Thus, the reaction in toluene proceeds smoothly in the beginning, but 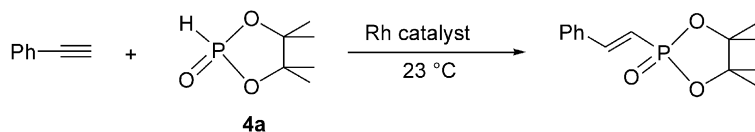the activity diminishes gradually and eventually the reaction stops while there still remain both starting materials. In contrast, the activity is sustained when the solvent is acetone (or other polar solvents) and the reaction

Table 5 Rhodium-catalyzed hydrophosphorylation of phenylacetylene[a]

Catalyst	Solvent	Reaction time (h)	Yield (%)[b]
$RhCl(PPh_3)_3$	Toluene	2	31
		24	43
		48	48
		1[c]	100
	Acetone	2	85
		4	100
$RhBr(PPh_3)_3$	Acetone	0.5	76
		2	90
		5	100
$RhI(PPh_3)_3$	Acetone	0.5	80
		2	95
		5	100

[a] 3 mol % Rh catalyst, equimolar phenylacetylene and **4a** (0.81 M solution).
[b] Determined by ^{1}H NMR.
[c] At 80 °C.

Table 6 Rhodium-catalyzed hydrophosphorylation of alkynes

81%

95 (93)%

79 (92)%

92 (81)%

93 (91)%

97 (87)%

76 (98)%

46 (75)%

89 (96)%

95 (91)%

82 (86)%

Conditions: RhBr(PPh$_3$)$_3$ (1~2 mol %), acetone, 25 °C, 20 h. Yield data given in parentheses were obtained under following conditions: RhCl(PPh$_3$)$_3$ (1~2 mol %), toluene, 100~110 °C, 2~6 h Selectivity > 98% (^{31}P NMR) in each reaction. (OR)$_2$ stands for OCMe$_2$CMe$_2$O.

proceeds to completion in 4 h. Bromo- and iodo-analogues of RhCl(PPh$_3$)$_3$ are even more active. Synthesis of a series of alkenylphosphonates using RhBr(PPh$_3$)$_3$ at room temperature or RhCl(PPh$_3$)$_3$ at 100 °C is summarized in Table 6.

The favorable performance of polar solvents is associated with the concentration of the active species. At least five species (**5–9**) are generated in the mixture upon treatment of RhCl(PPh$_3$)$_3$ with the five-membered hydrogen phosphonate **4a** (Scheme 23). Species **8** and **9**, which are not ligated by triphenylphosphine, have proved to be inactive, while **5–7** are all able to catalyze the reaction.
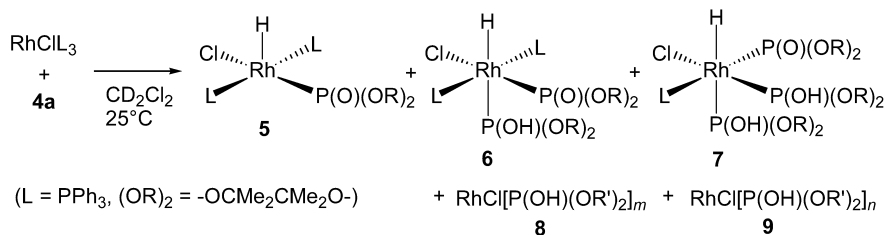

(L = PPh$_3$, (OR)$_2$ = -OCMe$_2$CMe$_2$O-)

Scheme 23

Table 7 Solvent effect on the generation of rhodium species

$$\textbf{4a} + RhCl(PPh_3)_3 \xrightarrow[\text{rt, 24 h}]{} \textbf{5} + \textbf{6} + \textbf{7} + \textbf{8} + \textbf{9}$$

4a : RhCl(PPh$_3$)$_3$	Solvent	**5** : **6** : **7** : **8** : **9**
3 : 1	Acetone	10 : 57 : 16 : 17 : 0
17 : 1	Acetone	0 : 0 : 40 : 60 : 0
3 : 1	Toluene	15 : 28 : 47 : 10 : 0
17 : 1	Toluene	0 : 0 : 7 : 36 : 57

As the data summarized in Table 7 indicate, less polar toluene is prone to promote transformation among the species 5→6→7→8, 9, i.e., from a species of a higher coordination number of triphenylphosphine to a lower number. In acetone on the other hand, the quantity of species **5–7** is more sustained even at higher ratios of **4a** to Rh (i.e., more similar to the catalytic reaction).
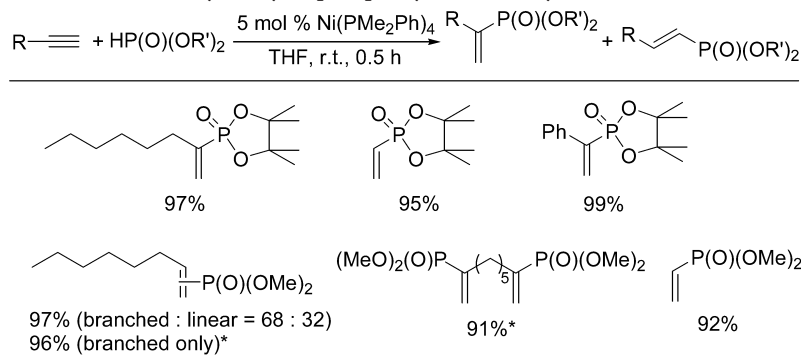
A second factor from which the solvent effect stems is associated with the insertion process. The reaction of species **6** with phenylacetylene revealed that the insertion took place into the H-Rh bond (Scheme 24). Although isolation of species **10** was not possible due to its high reactivity, 2D NMR techniques confirmed the structure. In CD$_2$Cl$_2$, a polar solvent, the process took place smoothly even at room temperature to generate **10** (and **11β** through reductive elimination from **10**). However, the process was sluggish in toluene and more than 93% of **6** remained unchanged even after 24 h.
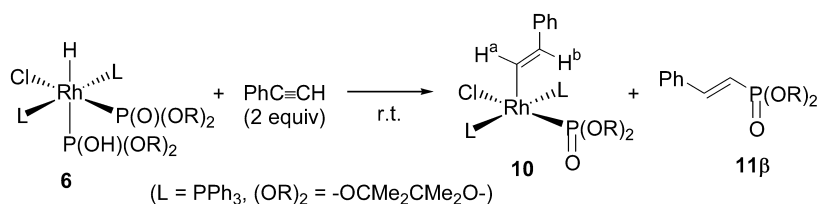
Solvent	Time (h)	**10** (%)	**11β** (%)
CD$_2$Cl$_2$	20	34	66
	4 (50 °C)	0	quant
Toluene	24	> 93% of **6** remained	

Scheme 24

Nickel complexes have proved to be active for hydrophosphorylation of alkynes [17a, 25]. Not only the five-membered phosphonate but also commercially available dialkyl phosphonates readily react in the presence of

**Table 8** Nickel-catalyzed hydrophosphorylation of alkynes

$$R\text{---}\!\!\equiv + HP(O)(OR')_2 \xrightarrow[\text{THF, r.t., 0.5 h}]{5 \text{ mol \% Ni(PMe}_2\text{Ph)}_4} \quad \substack{R \\ \text{||}}P(O)(OR')_2 \quad + \quad R\diagup\!\!\diagdown P(O)(OR')_2$$

97%   95%   99%

97% (branched : linear = 68 : 32)
96% (branched only)*

$(MeO)_2(O)P\diagdown\!\!\diagup_5 P(O)(OMe)_2$

91%*

$P(O)(OMe)_2$

92%

* Ph$_2$P(O)OH (10 mol % relative to the substrate) was added.

Ni(PMe$_2$Ph)$_4$, as exemplified in Table 8. However, the use of dimethyl phosphonate usually results in the formation of a mixture of branched and linear isomers. Addition of diphenylphosphinic acid to the reaction system significantly improves the selectivity for the branched isomer (see below).
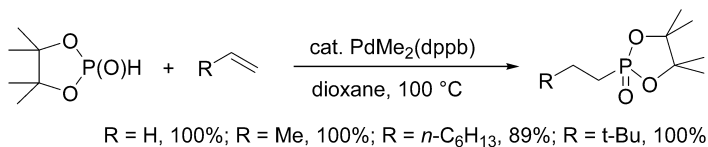
3.2
Addition to Alkenes and Dienes

Alkenes are much less reactive in the H-P bond addition reactions than alkynes. However, 1,3,2-dioxaphospholane 2-oxide (**4a**), a five-membered hydrogen phosphonate of pinacol, is exceptionally reactive with alkenes although dialkyl and diaryl phosphonates such as **4b–d** are totally unreactive (Scheme 25) [26]. Very interestingly, six-membered hydrogen phosphonates **4e,f** are also unreactive under identical conditions.

4a   (MeO)$_2$P(O)H **4b**   **4e**   **4f**
                 (i-PrO)$_2$P(O)H **4c**
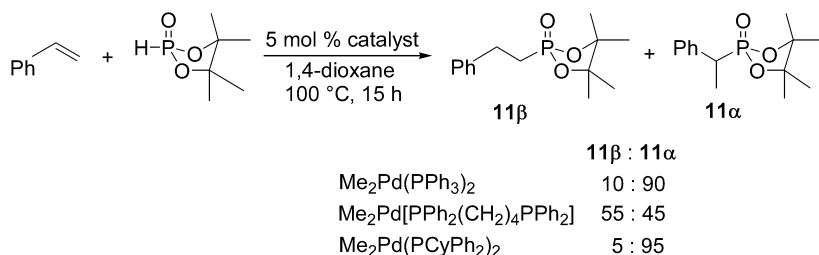   (PhO)$_2$P(O)H **4d**
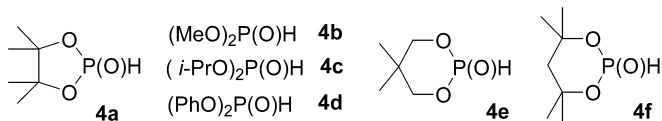
Scheme 25

As Scheme 26 demonstrates, the terminal alkene reactions using palladium-dppb [dppb=1,4-bis(diphenylphosphino)butane] catalyst systems usual-

$$\text{pinacol-P(O)H} + R\diagup\!\!\diagdown \xrightarrow[\text{dioxane, 100 °C}]{\text{cat. PdMe}_2(\text{dppb})} R\diagdown\!\!\diagup P(O)\text{-pinacol}$$

R = H, 100%; R = Me, 100%; R = n-C$_6$H$_{13}$, 89%; R = t-Bu, 100%
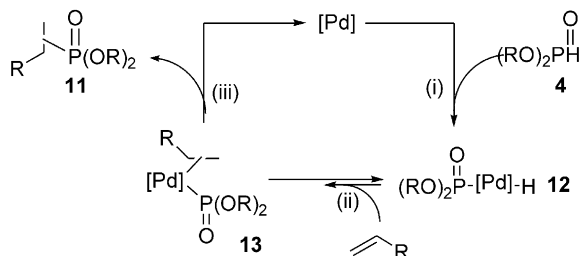
Scheme 26

ly form linear phosphonates with high regioselectivities. Internal alkenes are less reactive (cyclohexene, 37%), but strained cyclic ones can undergo the reaction smoothly (norbornene, 83%; cyclopentene, 87%).

The reaction of styrene required tuning of the ligand nature to achieve acceptable selectivities; the use of PPh$_2$Cy (Cy=cyclohexyl) proved to be the right choice for the selective synthesis of the branched isomer **11α** (Scheme 27)
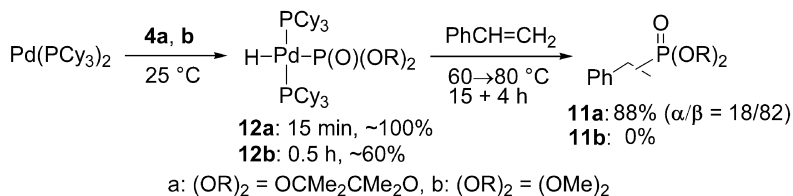

	11β : 11α
Me$_2$Pd(PPh$_3$)$_2$	10 : 90
Me$_2$Pd[PPh$_2$(CH$_2$)$_4$PPh$_2$]	55 : 45
Me$_2$Pd(PCyPh$_2$)$_2$	5 : 95

Scheme 27

The hydrophosphorylation of alkenes appears to proceed via the sequence of events illustrated in Scheme 28.

Scheme 28

As for the oxidative addition (step i), both cyclic and acyclic hydrogen phosphonates, **4a** and **4b**, react with Pd(0) to generate the corresponding adducts **12a** and **12b** (Scheme 29). Although five-membered **4a** is somewhat more reactive, this small difference in reactivity does not account for the lack of catalytic addition of **4b**.


12a: 15 min, ~100%
12b: 0.5 h, ~60%

11a: 88% (α/β = 18/82)
11b: 0%

a: (OR)$_2$ = OCMe$_2$CMe$_2$O, b: (OR)$_2$ = (OMe)$_2$

Scheme 29

However, the reactivity of **12a** and **12b** with an olefin is very much dependent on the structure of the alcohol moiety in the phosphoryl ligand. Complex **12a**, having a pinacolate moiety, reacts smoothly with styrene to afford the addition product (**11a**), while **12b**, generated starting with dimethyl phosphonate, does not furnish the corresponding product (**11b**) at all. Accordingly, the rate-determining step appears to be either the insertion (step ii) or the reductive elimination process (step iii). Deuterium labeling experiments furnished further details of the mechanism (Scheme 30). When **12a-*d*** was treated with styrene at room temperature, **12a** and deuterated styrene were formed, suggesting the following; (1) the C=C linkage inserts into the H-Pd bond (hydropalladation), (2) the insertion process is reversible, and (3) the process is rapid at room temperature and cannot be rate-determining.
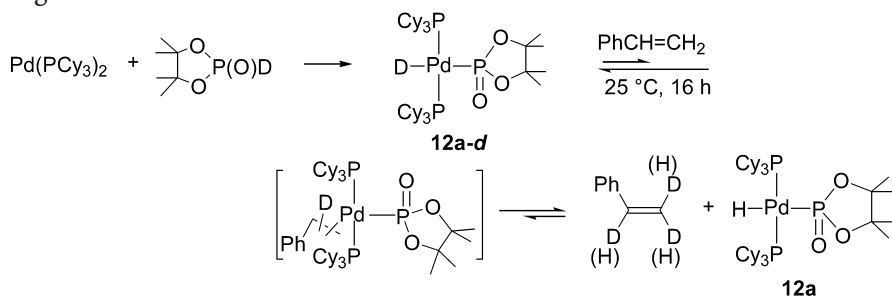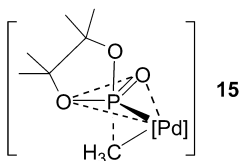

Scheme 30

Experiments to compare the reactivity difference in reductive elimination, a remaining candidate for the rate-determining process, were carried out using methyl(phosphoryl)palladium complexes **13a,b**, which cannot undergo β-hydrogen elimination (Scheme 31). Reductive elimination from complex **13a** proceeded readily affording methylphosphonate **14a** while **13b** was totally unreactive. On the basis of these results, it can be safely concluded that the rate-determining step is the reductive elimination process, which is the provenance of the significant reactivity difference depending on the structure of the alcohol moiety. Stockland and coworkers also studied the C-P(O) reductive elimination from (bipy)PdMe[P(O)(OPh)$_2$] and related complexes to reconfirm the lack of the reactivity. However, when PPh$_3$ was added, the complexes did reductively eliminate MeP(O)(OPh)$_2$ [27].
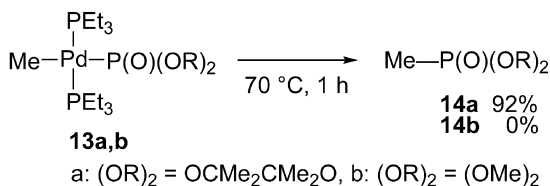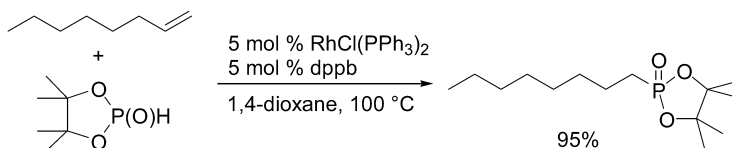

Scheme 31

The reason for the high reactivity of **13a** is ambiguous. The reductive elimination may proceed through a transition state like **15** (Scheme 32), where the ring oxygens occupy apical and equatorial positions, which allows relief of the ring strain of the five-membered ring.
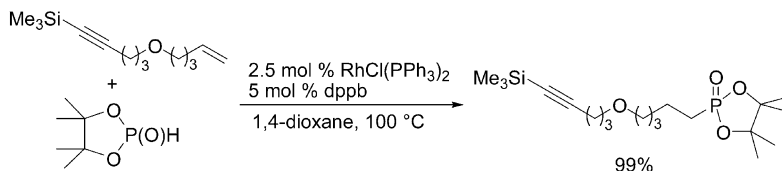

Scheme 32

The discovery of high reactivity of the five-membered hydrogen phosphonate **4a** has led to the development of RhCl(PPh$_3$)$_3$-catalyzed addition to alkenes in the presence of dppb as an additive (Scheme 33) [28]. The dppb additive is speculated to work as a reductant to re-activate catalytically inactive oxidized rhodium species, which can be formed during the catalysis, as suggested by gradual change in color from yellow to orange/brown. The formation of dppb oxide was indeed observed. Addition of dppb to a stalled reaction due to catalyst deactivation resumed the catalysis, where the yellow color of the mixture returned and the reaction proceeded to completion.
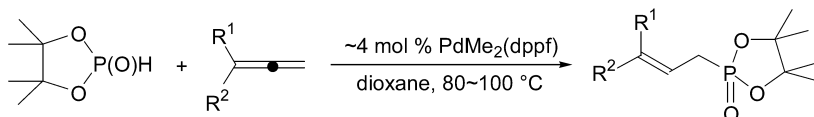

Scheme 33

Although various substrates that have two alkene linkages or both alkene and alkyne linkages conform to the catalysis, the chemoselectivity is rather low and mixtures of products are formed. However, when bulky Me$_3$Si is bound to the alkynyl bond in an en-yne substrate, the alkene moiety is selectively hydrophosphorylated (Scheme 34).

Scheme 34

More than two decades age, Hirao and coworkers briefly described a rather unsuccessful attempt of hydrophosphorylation of a diene; isoprene underwent Pd-catalyzed addition of diethyl phosphonate forming diethyl 3-methyl-2-buten-1-ylphosphonate in only 10% yield even under forcing conditions (150 °C, 20 h) [29]. By using the exceptionally reactive five-mem-

bered hydrogen phosphonate **4a**, the scope of the addition reaction can be extended to 1,2- and 1,3-dienes, as summarized in Scheme 35 and Table 9, respectively [30, 31]. The new procedures furnish allylic phosphonates of stereochemical integrity, and hence, the products are envisioned to allow numerous synthetic elaborations using Horner-Emmons olefination reactions.

R^1 = H, R^2 = *n*-Bu, 87%; R^1 = H, R^2 = *c*-hexyl, 61%; R^1 = H, R^2 = *t*-Bu, 81%; R^1 = H, R^2 = Ph, 87%; R^1 = R^2 = Me, 66%; R^1 + R^2 = -CH$_2$)$_5$-, 89%; R^1 = R^2 = Ph, 92%

Scheme 35

Table 9 Hydrophosphorylation of 1,3-dienes[a]

1,3-Diene	Conditions	Adduct[b]	% GC yield
	cat. PdMe$_2$(dppb) 100 °C, 12 h		97 (76)[c]
	cat. PdMe$_2$(dppb) 100 °C, 12 h		87 (80)[c]
	cat. PdMe$_2$(binap) 100 °C, 12 h		98 (*E/Z* = 83/17)
	cat. PdMe$_2$(dppf) 80 °C, 16 h		89 93(*E/Z* = 93/7)
	cat. PdMe$_2$(dppf) 60 °C, 12 h		80

[a] HP(O)(OCMe$_2$CMe$_2$O), diene (2~10 equiv), palladium catalyst (5 mol %), 1,4-dioxane (1 M).
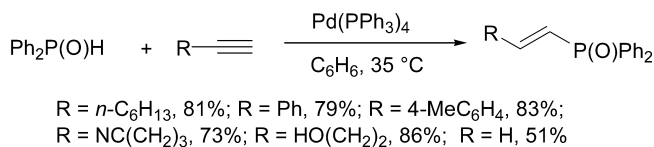[b] (OR)$_2$ = OCMe$_2$CMe$_2$O. [c] Isolated yield.

4
Transition Metal-Catalyzed Addition of Secondary Phosphine Oxides

4.1
Addition to Alkynes

Addition of the H-P bond in secondary phosphine oxides (hydrophosphinylation) also proceeds in the presence of palladium complexes (Scheme 36) [32]. Secondary phosphine oxides appear more reactive than hydrogen

phosphonates and the reaction proceeds even at room temperature. The striking difference from the reaction of hydrogen phosphonates lies in the regiochemistry; the major products are those with terminal attachment of phosphorus. The reaction is applicable to various alkynes. It is also interesting from a synthetic viewpoint to note that a starting material having a hydroxy substituent can be used as such without protection.

$$Ph_2P(O)H \quad + \quad R \equiv \quad \xrightarrow[\text{C}_6\text{H}_6, 35\,°\text{C}]{\text{Pd(PPh}_3)_4} \quad R \diagup\!\!\!\diagdown P(O)Ph_2$$

R = n-C$_6$H$_{13}$, 81%; R = Ph, 79%; R = 4-MeC$_6$H$_4$, 83%;
R = NC(CH$_2$)$_3$, 73%; R = HO(CH$_2$)$_2$, 86%; R = H, 51%
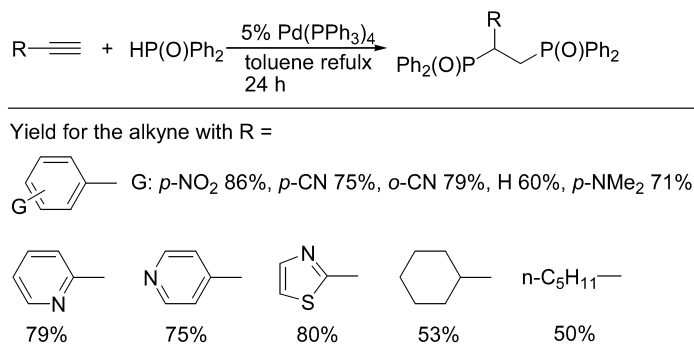
Scheme 36

The hydrophosphinylation is somewhat different in mechanistic detail from the hydrophosphorylation. Thus, the treatment of HP(O)Ph$_2$ **16** with Pt(PEt$_3$)$_3$ or Pd(PEt$_3$)$_3$ affords species **17a** or **17b** ligated by two units of HP(O)Ph$_2$, one that have experienced oxidative addition and the other that simply coordinates to the metal center as its P(III) tautomeric form, PPh$_2$(OH) (Scheme 37). The two units of phosphoryl ligands are mutually interacting through hydrogen bonding. When the palladium complex **17b** was treated with 1-octyne at room temperature, the signals due to the complex diminished while new signals assignable to olefinic protons and palladium-bound P(O)Ph$_2$ emerged, supporting the formation of intermediates **18α** and **18β** through insertion of 1-octyne into the H-Pd bond. The reaction did not proceed further at room temperature, but upon heating to 70 °C, the intermediate species were transformed to the corresponding alkenylphosphine oxides **19α** and **19β**. These results suggest that the catalysis involves oxidative addition of the H-P bond, hydropalladation with the triple bond, and C-P reductive elimination.
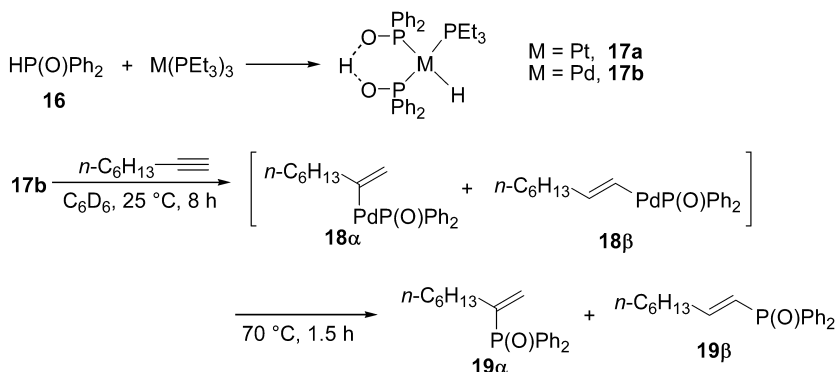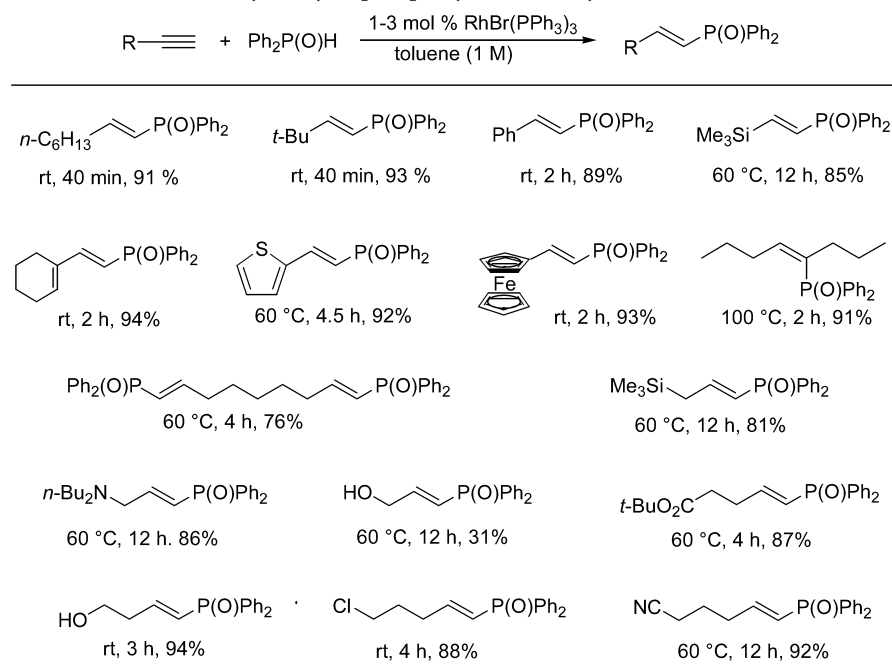

Scheme 37

By using three equivalents of diphenylphosphine oxide (relative to alkyne), the palladium-catalyzed reaction affords bisphosphine oxides in high

yields [33]. The reaction works with various aliphatic and aromatic terminal alkynes having electronegative, -neutral, and -positive functionalities as summarized in Scheme 38. It was confirmed that initially formed alkenylphosphine oxide undergoes the second hydrophosphinylation. The bisphosphine oxides were reduced with triethoxysilane catalyzed by Ti(O^{i}Pr)$_4$ to corresponding bisphosphines.

$$R\!\!=\!\!= \quad + \quad HP(O)Ph_2 \xrightarrow[\substack{\text{toluene refulx} \\ 24\ h}]{5\%\ Pd(PPh_3)_4} \quad Ph_2(O)P\overset{R}{\diagup}\!\!\diagdown P(O)Ph_2$$

Yield for the alkyne with R =

G: *p*-NO$_2$ 86%, *p*-CN 75%, *o*-CN 79%, H 60%, *p*-NMe$_2$ 71%

79%	75%	80%	53%	50%

Scheme 38

Table 10 Rhodium-catalyzed hydrophosphinylation of alkynes with Ph$_2$P(O)H

$$R\!\!=\!\!= \quad + \quad Ph_2P(O)H \xrightarrow[\text{toluene (1 M)}]{1\text{-}3\ mol\ \%\ RhBr(PPh_3)_3} \quad R\diagup\!\!\diagdown P(O)Ph_2$$

n-C$_6$H$_{13}$ ⌒ P(O)Ph$_2$	*t*-Bu ⌒ P(O)Ph$_2$	Ph ⌒ P(O)Ph$_2$	Me$_3$Si ⌒ P(O)Ph$_2$
rt, 40 min, 91 %	rt, 40 min, 93 %	rt, 2 h, 89%	60 °C, 12 h, 85%

⌒ P(O)Ph$_2$	S ⌒ P(O)Ph$_2$	Fe ⌒ P(O)Ph$_2$	⌒ P(O)Ph$_2$
rt, 2 h, 94%	60 °C, 4.5 h, 92%	rt, 2 h, 93%	100 °C, 2 h, 91%

Ph$_2$(O)P ⌒⌒⌒ P(O)Ph$_2$		Me$_3$Si ⌒ P(O)Ph$_2$
60 °C, 4 h, 76%		60 °C, 12 h, 81%

n-Bu$_2$N ⌒ P(O)Ph$_2$	HO ⌒ P(O)Ph$_2$	*t*-BuO$_2$C ⌒ P(O)Ph$_2$
60 °C, 12 h. 86%	60 °C, 12 h, 31%	60 °C, 4 h, 87%

HO ⌒ P(O)Ph$_2$	Cl ⌒ P(O)Ph$_2$	NC ⌒ P(O)Ph$_2$
rt, 3 h, 94%	rt, 4 h, 88%	60 °C, 12 h, 92%

Hydrophosphinylation of alkynes with $Ph_2P(O)H$ is also efficiently catalyzed by rhodium complexes as summarized in Table 10 [34]. In many cases, the reaction proceeds at room temperature and functional groups, inclusive of OH, tolerate the reaction conditions. Although Rh-PPh_3 precatalysts such as $RhCl(PPh_3)_3$, $RhBr(PPh_3)_3$, $RhI(PPh_3)_3$, $RhCl(CO)(PPh_3)_2$, and $RhH(CO)(PPh_3)_3$ are conveniently employed, NMR spectroscopy has suggested that PPh_3-free $PPh_2(OH)$-ligated rhodium species appear to carry out the catalysis.

4.2
Phosphinic Acid-Induced Reversal of Regioselectivity

Very interestingly, the regioselectivity of the palladium-catalyzed hydrophosphinylation can be switched by addition of a tiny quantity of diphenylphosphinic acid or other acidic compounds (Scheme 39) [35]. Thus, the linear product (**19β**), which is the major product under normal conditions (i.e., without the phosphinic acid), becomes the minor regioisomer, and instead, the branched isomer (**19α**) is formed as the prevailing product. Furthermore, the addition of the phosphinic acid enhances the catalytic activity. Note that the quantity of the palladium catalyst is 5 mol% relative to the reactant, and that the addition of only 1 mol% (relative to the reactant) of the phosphinic acid results in a substantial change in the regioselectivity. New palladium species, which are much more active in the catalysis, appear to be generated upon addition of the phosphinic acid or other acidic additives.

| $Ph_2P(O)OH$ (mol %)	Yield of **19** (α/β) (%)
0	75 (12/88)
1	92 (79/21)
5	99 (95/5)
10	96 (96/4)
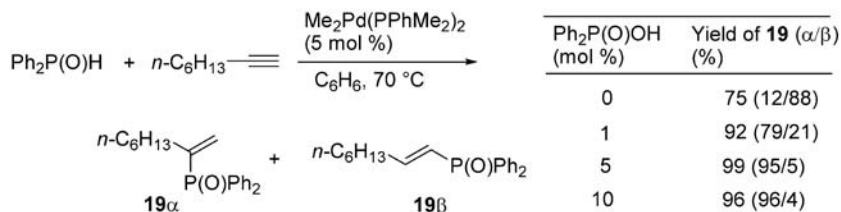
Scheme 39

The following experiments to identify the active species substantiate the mechanistic detail. Diphenylphosphinic acid was found to protonate the C-
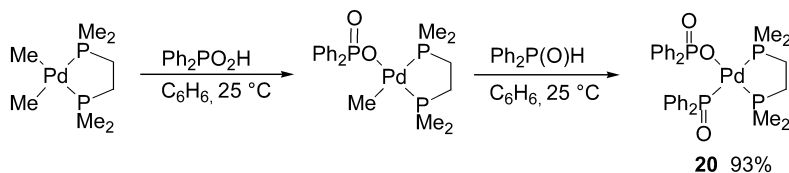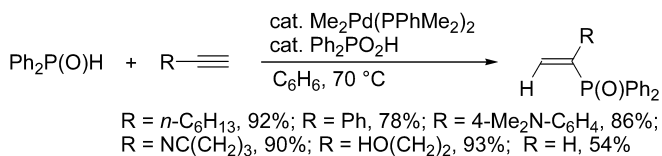

Scheme 40

Pd bond in Me$_2$Pd(dmpe) [dmpe=1,2-bis(dimethylphosphino)ethane] to generate phosphinate-palladium species with extrusion of a methane molecule (Scheme 40). Upon treatment the resulting palladium species with diphenylphosphine oxides, the remaining methyl-palladium bond was protonated and a phosphinyl(phosphinato)palladium complex (**20**) was isolated.

Complex **20** displayed exactly the same activity and regioselectivity as the species that was in situ generated by using the Me$_2$Pd(dmpe) and diphenylphosphinic acid mixture. Note that no reaction takes place under identical conditions when the reaction is run in the presence of Me$_2$Pd(dmpe) alone, due presumably to the too tight chelation of the dmpe ligand. However, the reaction has been made possible by the addition of the activity-enhancing phosphinic acid. On the basis of these experiments, we can safely conclude the mechanism as illustrated in Scheme 41, which involves insertion of alkyne into the P-Pd bond and protonation of the resulting alkenylpalladium intermediate.
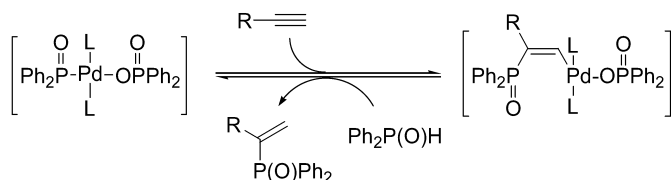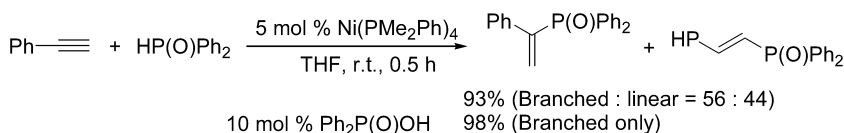

Scheme 41

The new procedure works well with various alkynes as summarized in Scheme 42.

R = n-C$_6$H$_{13}$, 92%; R = Ph, 78%; R = 4-Me$_2$N-C$_6$H$_4$, 86%;
R = NC(CH$_2$)$_3$, 90%; R = HO(CH$_2$)$_2$, 93%; R = H, 54%

Scheme 42

Although detailed studies have not been finished, our recent patent discloses that nickel complexes are also able to catalyze the hydrophosphinylation of alkynes under exceptionally mild conditions [25]. This reaction,
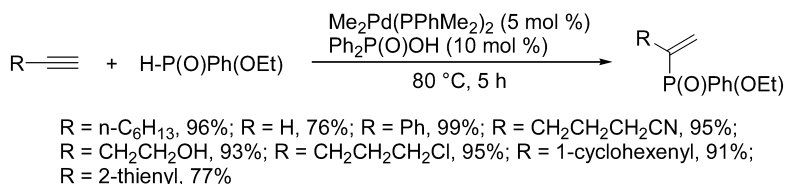

Scheme 43

shown in Scheme 43, as well as nickel-catalyzed hydrophosphorylation of al-
kynes (see above; see Table 8), also display similar phosphinic acid-induced
enhancement of the branched isomer formation.

5
Addition of Hydrogen Phosphinates and Extension to Synthesis of P-Chiral Phosphinates

As expected, hydrogen phosphinate, which is a hybrid structure of hydrogen
phosphonate and secondary phosphine oxide, adds to alkynes in the pres-
ence of the Pd-diphenylphosphinic acid catalyst system (Scheme 44) [36].
Normally, branched isomers are the major products, while trimethylsily-
lacetylene exceptionally affords the corresponding terminally phosphinylat-
ed product. Diphenylacetylene also reacts to afford the corresponding ad-
duct in 99% yield.

R = n-C$_6$H$_{13}$, 96%; R = H, 76%; R = Ph, 99%; R = CH$_2$CH$_2$CH$_2$CN, 95%;
R = CH$_2$CH$_2$OH, 93%; R = CH$_2$CH$_2$CH$_2$Cl, 95%; R = 1-cyclohexenyl, 91%;
R = 2-thienyl, 77%

Scheme 44

Nickel complexes also catalyze the reaction much more efficiently as
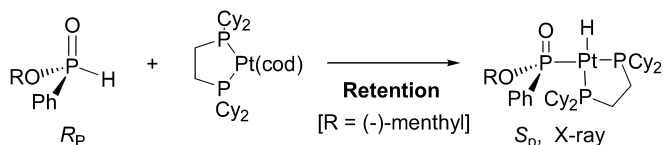shown in Scheme 45 [25].
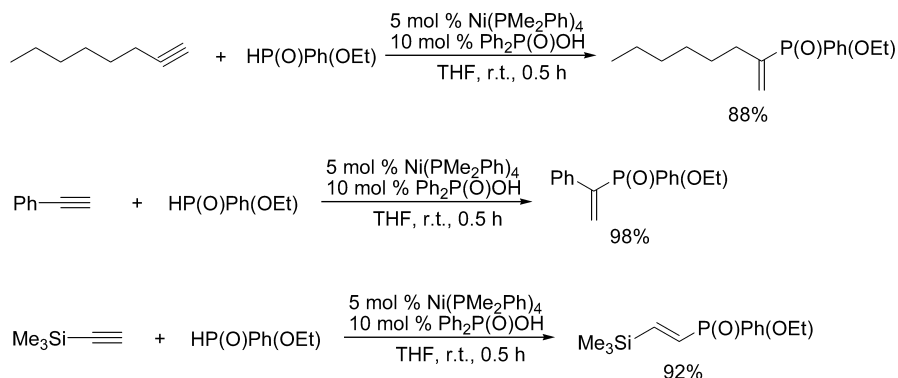
Scheme 45

P-Chiral organophosphorus compounds are of great importance in bio-
logical chemistry, organic synthesis and asymmetric catalysis. However,
their preparations usually require tedious steps. (−)-Menthyl phenylphos-

Table 11 Synthesis of optically active alkenylphosphinates via palladium-catalyzed H-P addition of (−)-menthyl phenylphosphinate
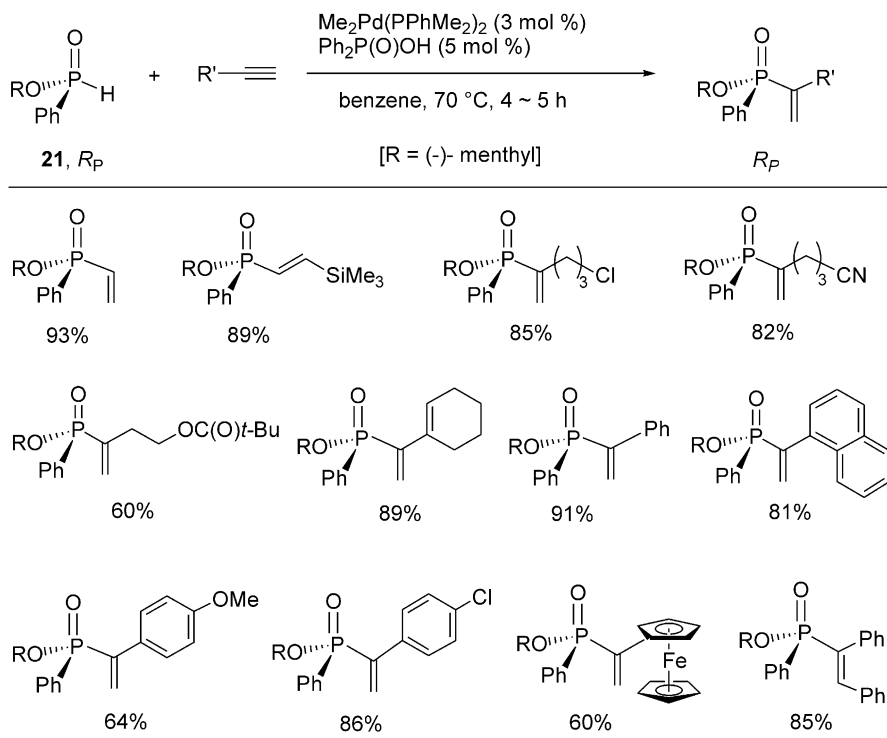
phinate **21**, a white solid easy to prepare and handle, has been known for more than 30 years. With this in mind, it is interesting to note that the addition of hydrogen phosphinates proceeds in a stereospecific manner. In practice, (−)-menthyl phenylphosphinate **21** reacts smoothly with a variety of alkynes to furnish a series of optically pure (−)-menthyl alkenylphosphinates (Table 11) [37]. The transformation retains the configuration at the phosphorus center with complete stereospecificity.

The oxidative addition of the phosphinate to Pd(0) species also proceeds with retention of configuration (Scheme 46), suggesting that the resulting H-Pd undergoes retentive insertion.
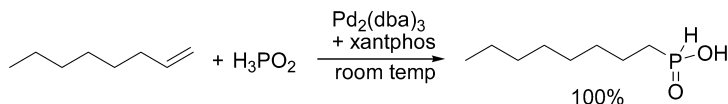

Scheme 46

6
Addition of Hypophosphite to Unsaturated Compounds

Hypophosphites also readily add across double or triple bonds as shown in Scheme 47, where xantphos=9,9-dimethyl-4,5-bis(diphenylphosphino)xan-
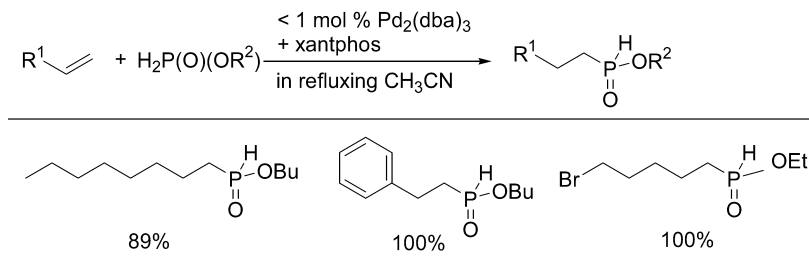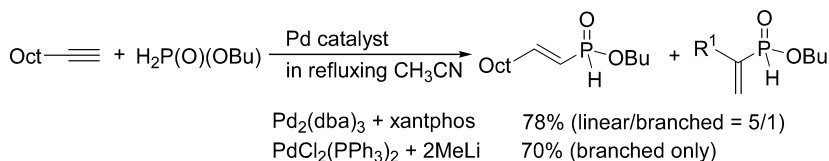

Scheme 47

thene [38]. Both mono- and bi-dentate phosphines display high performance as the ligand. The reaction of olefins affords only the linear product. Even aqueous H_3PO_2 can be used directly to afford the corresponding product in high yields (Scheme 48). The reaction complements the radical process; while the radical process works quite well for di- and trisubstituted olefins, the palladium catalyzed reaction works reluctantly with cyclohexene. On the other hand, styrene and 5-bromopent-1-ene, which are poor substrates in the radical process, are efficiently hydrophosphinylated in the palladium-catalyzed reaction.

Scheme 48

Interestingly, the regioselectivity is very much dependent on the structure of the ligand, as shown in Scheme 49.

Scheme 49

The H-P bond in hypophosphites appears much more reactive than that in the phosphinate products; the reactions of alkynes do not form symmetrically dialkenyl-substituted phosphinate $R_2P(O)(OR')$ (R=alkenyl group).

7
Conclusion

The author hopes that this chapter has convinced the readers of the value of homogeneous catalysis for the synthesis of organophosphorus compounds and for organo-heteroatom compounds in a broader sense. Hydrosilylation and hydroboration are indispensable modern synthetic reactions in this category. The H-P addition reactions herein described joins them as a third member. Although this chapter does not cover, the addition reactions of the S-P and Se-P bonds in thiophosphates [39] and selenophosphates [40] to alkynes also proceed in the presence of transition metal catalysts. In view of the wide use of phosphorus compounds, the new procedures will find practical applications.

References

1. Wicht DK, Glueck DS K (2001) In: Togni A, Grutzmacher H (eds) Catalytic hetero-functionalization. Wiley-VCH, Weinheim, p 143
2. Reuter M, Orthner L (1958) German Pat 1035135; (1960) Chem Abstr 54:14,124i
3. (a) Khardin AP, Tuzhikov OI, Grekow LI, Valetdinov RK, Pankov VI, Matveeva EV, Nazorova GV, Popov BN, Korolev AV (1985) Otkrytiya Izobret 79. Chem Abstr 103:71510; (b) Dorfman YA, Levina LV, Grekow LI, Korolev AV (1990) Kinet Catal 30:662; (1990) Chem Abstr 112:56,107
4. Ellis JW, Harrison KN, Hoye PAT, Orpen AG, Pringle PG, Smith MB (1992) Inorg Chem 31:3026
5. Hoye PAT, Pringle PG, Smith MB, Worboys K (1993) J Chem Soc Dalton Trans 269
6. Schunn RA (1973) Inorg Chem 12:1573; Ebsworth EAV, Gould RO, Mayo RA, Walkinshaw M (1987) J Chem Soc Dalton Trans 2831; Ebsworth EAV, Gould RO, Mayo RA, (1988) J Chem Soc Dalton Trans 477
7. Geoffroy GL, Rosenberg S, Shulman PM, Whittle RR (1984) J Am Chem Soc 106:1519; Fryzuk MD, Joshi K, Chadha RK, Rettig SJ (1991) J Am Chem Soc 113:8724
8. Bohle DS, Clark GR, Rickard CEF, Roper WR (1988) J Organomet Chem 353:355
9. Pringle PG, Brewin D, Smith MB, Worboys K (1995) In: Horvath IT, Joó F (eds) Aqueous organometallic chemistry and catalysis. Kluwer, Dordrecht, p 111
10. Reuter M, Wolf E (1960) Ger 1078574 (1961) Chem Abstr 55:16,427c
11. Pringle PG, Smith MB (1990) J Chem Soc Chem Commun 1701
12. Costa E, Pringle PG, Smith MB, Worboys K (1997) J Chem Soc Dalton Trans 4277
13. Wicht DK, Kourkine IV, Lew BM, Nthenge JM, Glueck DS (1997) J Am Chem Soc 119:5039; Wicht DK, Kourkine IV, Kovacik I, Glueck DS, Concolino TE, Yap GPA, Incarvito CD, Rheingold AL (1999) Organometallics 18:5381
14. Costa E, Pringle PG, Worboys K (1998) J Chem Soc Chem Commun 49
15. Wicht DK, Kovacik I, Glueck DS, Liable-Sands LM, Incarvito CD, Rheingold AL (1999) Organometallics 18:5141; Kovacik I, Wicht DK, Grewal NS, Glueck DS, Incarvito CD, Guzei IA, Rheingold AL (2000) Organometallics 19:950
16. Shulyupin MO, Kazankova MA, Beletskaya IP (2002) Org Lett 4:761
17. (a) Lin KC (1972) US Pat 3673285; (b) Kazankova MA, Efimova IV, Kochetkov AN, Afanas'ev VV, Beletskaya IP, Dixneuf PH (2001) Synlett 497

18. Jérôme F, Monnier F, Lawicka H, Dérien S, Dixneu PH (2003) Chem Commun 696
19. Douglass MR, Marks TJ (2000) J Am Chem Soc 122:1824; Douglass MR, Stern CL, Marks
    TJ (2002) J Am Chem Soc 123:10,221
20. Takaki K, Takeda M, Koshoji G, Shishido T, Takehira K (2001) Tetrahedron Lett 42:6357
21. Schumann H, Palamidis E, Loebel J (1990) J Organomet Chem 384:C49
22. Han L-B, Tanaka M (1996) J Am Chem Soc 118:1571
23. Allen A Jr, Manke DR, Lin W (2000) Tetrahedron Lett 41:151
24. Zhao C-Q, Han L-B, Goto M, Tanaka M (2001) Angew Chem Int Ed 40:1929
25. (a) Henkelmann J, Klass K, Arndt J-D (2000) Ger Pat 10054218.2; (b) Han L-B, Zhang C,
    Tanaka M (2002) Jpn Patent Application 2002-142,955
26. Han L-B, Mirzaei F, Zhao C-Q, Tanaka M (2000) J Am Chem Soc 122:5407
27. Levine AM, Stockland RA Jr, Clark R, Guzei I (2002) Organometallics 21:3278
28. Reichwein JF, Patel MC, Pagenkopf BL (2001) Org Lett 3:4303
29. Hirao T, Masunaga T, Yamada N, Ohshiro Y, Agawa T (1982) Bull Chem Soc Jpn 55:909
30. Zhao C-Q, Han L-B, Tanaka M (2000) Organometallics 19:4196
31. Mirzaei F, Han L-B, Tanaka M (2001) Tetrahedron Lett 42:297
32. Han L-B, Choi N, Tanaka M (1996) Organometallics 15:3259
33. Allen A Jr, Ma L, Lin W (2002) Tetrahedron Lett 43:3707
34. Han L-B, Zhao C-Q, Tanaka M (2001) J Org Chem 66:5929
35. Han L-B, Hua R, Tanaka M (1998) Angew Chem Int Ed Engl 37:94
36. Han L-B, Tanaka M (2002) Jpn Patent Kokai 2002-332,290
37. Han L-B, Zhao C-Q, Onozawa S-Y, Goto M, Tanaka M (2002) J Am Chem Soc 124:3842
38. Deprele S, Montchamp J-L (2002) J Am Chem Soc 124:9386
39. Han L-B, Tanaka M (1999) Chem Lett 863
40. Han L-B, Choi N, Tanaka M (1996) J Am Chem Soc 118:7000

New Phosphorylated Hosts for the Design of New Supramolecular Assemblies

Jean-Pierre Dutasta

Laboratoire de Chimie, École Normale Supérieure de Lyon, UMR CNRS no. 5182,
46 Allée d'Italie, 69364 Lyon 07, France
E-mail: dutasta@ens-lyon.fr

Abstract Development of chemistry around new phosphorylated hosts provides an interesting new area of investigations in the design of host-guest systems. Complex molecular architectures were obtained starting from hosts and cationic guests, exploiting the binding properties of elaborated phosphorylated cavitands and hemicryptophanes. The stereoselectivity of the phosphorylation reaction of cavitand based compounds, has been developed. Subsequently, a simple synthetic methodology was utilized for the synthesis of novel macrocyclic molecular structures. The cooperative effects of an aromatic cavity and the hard or soft donor phosphoryl groups are used to form highly stable assemblies. The outcome of this approach allows the formation of original supramolecular assemblies, featuring the elaboration of new materials. The potential of the phosphorylated cavitands and hemicryptophanes as precursors in the preparation of large supramolecular systems is examined. The role of the phosphorus groups is of prime importance to produce assemblies of high stability. Throughout this chapter, special attention has been given to the preparation and the structural aspect of this new class of phosphorus hosts and their complexes.

Keywords Phosphorylated hosts · Cavitands · Hemicryptophanes · Complexation · Host-guest systems · Supramolecular chemistry

1
# Introduction

1.1
Supramolecular Assemblies

Supramolecular chemistry is concerned with many aspects of molecular architecture, organization and (self-)assembly. Coordination chemistry and intermolecular interactions are the support for a wide variety of supramolecular systems, controlling the association of interacting entities and particularly host-guest complexes. Several principles improved the design of novel architectures for selective guest binding, among them, preorganization and complementarity of interacting groups leading to the design of highly sophisticated assemblies [1, 2]. The recognition of neutral or ionic guests and the organization of these new assemblies in supramolecular systems are expected to open new strategies for the preparation of new materials with specific properties (catalysis, magnetic material, optical or electronic devices, bio-sensors). The host-guest approach consists in organizing molecules, or self-assembling entities that lead to systems made of two or more interacting molecules or ions. In this sense, the design of cage and container molecules has been considerably investigated, and involved different strategies favoring weak intermolecular forces that stabilize the association of host and guest entities.

1.2
Phosphorylated Hosts

In the field of molecular recognition, the phosphorus hosts occupy a particular place probably because of the peculiar reactivity (and toxicity) of the phosphorus reagents. However phosphorus hosts are attractive because of their interesting outcomes in terms of oxidation state or valence state, and moreover in terms of molecular structure. The strong donating power of phosphane derivatives towards transition metals has been widely explored and is still unabated, especially for catalytic applications [3]. The phosphorylated PO compounds are also particularly attractive for hard cation recognition, and pioneering work in this field has been reported on alkaline metal ion coordination [4, 5]. This has given birth to the development of new phosphorylated ligands [6, 7]. For instance, the carbamoylphosphine oxide (CMPO)-substituted calixarenes [8] or cavitands [9, 10] are very efficient extractants for lanthanides and actinides. On the other hand, the sulfur atom of the PS thiophosphoryl group has more affinity for soft cations. Such functional groups have been introduced in elaborated and preorganized structures to increase the stability and selectivity of the so formed complexes [11]. Hardness and softness, structure and chirality, oxidation state and coordination state, all together make phosphorus groups very attractive for developing a new area of host-guest systems, where they are both building blocks and binding sites.

It is the purpose of this chapter to underline the fascinating possibilities of the phosphorus hosts to bind various species to get either two components complexes or multi components systems whose stoichiometry and structure will depend on the hosts and guests organization and affinities. A number of well-done reviews described the state of the art in matter of macrocyclic and macropolycyclic phosphorus ligands. The most widely investigated phosphorus-containing hosts are macrocycles with (thio)phosphorylated groups [20–22], phosphorus cryptands [14, 15, 23, 24], and phosphahemispherands [18, 25] (Scheme 1). Much attention is currently devoted to the cone shaped cavitands derived from the resorc[4]arenes which opened the route to promising preorganized hosts [26–31], and their phosphorus derivatives have received an intensive study to date [32–34]. This review focuses on the recent developments of the cavitand and cage hosts, where phosphorus is an essential element of the molecular architecture, with a particular attention for the PO or PS compounds. We will not consider the phosphorylated hosts where phosphorus is part of a pendant arm substituent. It is our choice not to describe the phosphorylated calixarene derivatives, which represents an important family of well known ligands for which several reviews appeared recently [32–34]. The aim of this chapter is to enlighten the possibilities of these phosphorylated hosts to create supramolecular systems in a wide general meaning, e.g., inclusion complexes and self-assembling systems, via metal-coordination or complexation of cationic species.
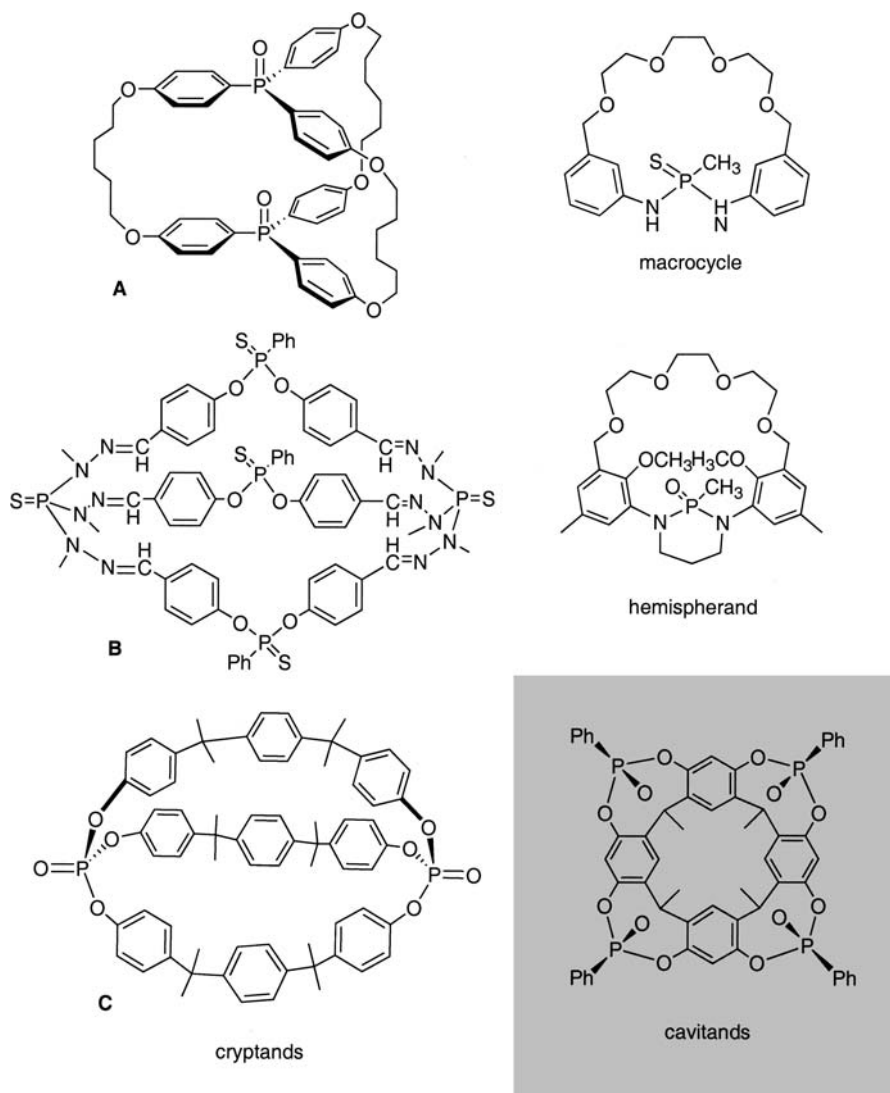
Scheme 1 Typical examples of phosphorylated cryptands **A** [12, 13], **B** [14, 15], **C** [16], macrocycle [17], hemispherand [18], and cavitand [19]

2
# Phosphorylated Cavitands

2.1
Stereochemistry

Cavitands are originally host compounds based on the resorc[4]arene [35] platform obtained from the condensation of resorcinol with aldehyde [36,

37]. The flexibility and the different conformations adopted by the re-
sorc[4]arene can be rigidified in the cone shape configuration by bridging
the phenol functions with different substituents [38]. We will report here on
the tetra-bridged phosphorus cavitands (phosphocavitand), whose general
structure is presented in Scheme 2 [39].
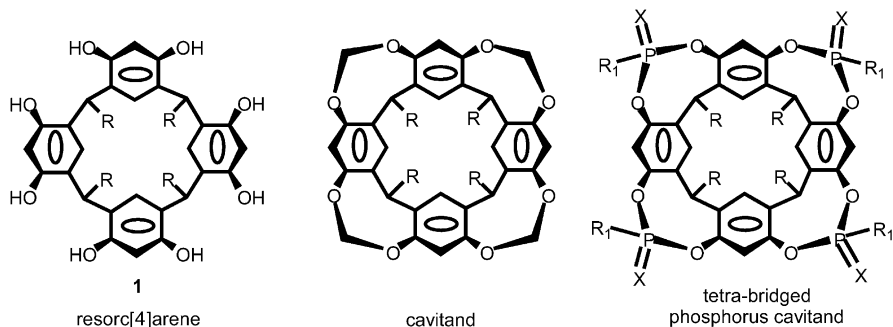
Scheme 2

In the tetra-bridged phosphocavitands, the preorganized structure is im-
posed by the fixed boat-chair conformation of the four fused eight-mem-
bered rings. Inwards (*i*) and outwards (*o*) configurations are defined rela-
tively to the *endo* and *exo* orientations of the P=X bonds (X=O, S, electron
pair), and six different stereoisomers arise from the equatorial or axial ori-
entation of the substituents on the phosphorus atoms (Scheme 3).
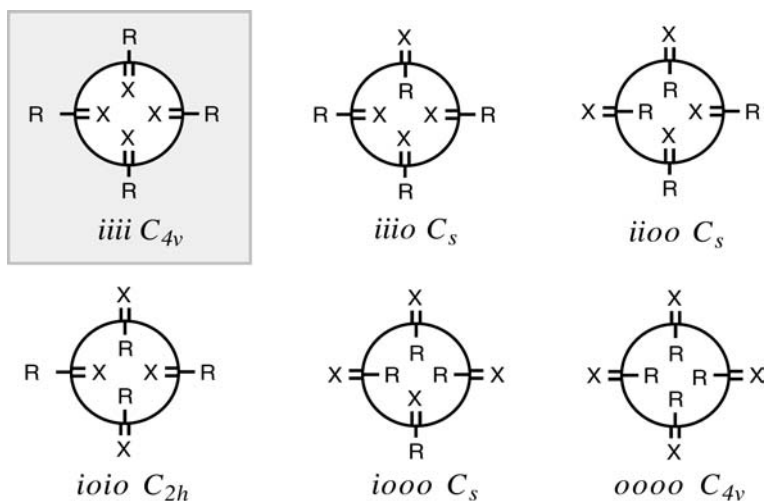
Scheme 3

The exclusive formation of one stereoisomer is rather unpredictable and
is often a difficult task. Thus to ensure optimized complexation properties,

it is interesting to benefit from the cooperative effects of the aromatic cavity and the P=X donating groups, and the *iiii* stereoisomer appears to be a prerequisite.

2.2
Synthesis Strategy

The cavitands are essentially synthesized from their resorc[4]arene precursors which are readily obtained by resorcinol condensation with aldehydes. The main feature comes from the different configurations that are expected for this tetrameric species and the relative thermodynamical stability of each isomer, which has been widely investigated by several authors. In addition, the conformational mobility of the resorc[4]arene molecules will depend on substitution at the upper and lower rims [28, 36, 40, 41]. The first attempt to synthesize a phosphorus bridged cavitand was to treat resorc[4]arene **1a** (**1**, R=CH$_3$) with phenylphosphonic dichloride or phenylphosphonothioic dichloride. Only inseparable isomer mixtures were obtained and isolation of the desired cavitands was not possible [42]. The first isolated phosphorylated resorcinol-based cavitand was described in 1992 by Markovsky et al., who prepared compound **D** from **1a** and four equivalents of *o*-phenylenechlorophosphate in the presence of triethylamine [43, 44]. For this compound, a tautomeric temperature and solvent dependent equilibrium exists between the spirophosphorane structure and the cyclic phosphate form (Scheme 4).

X = H, SiMe$_3$
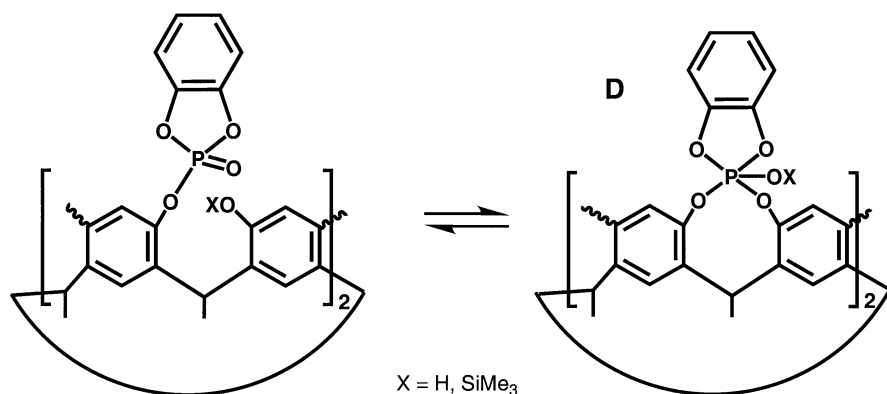
Scheme 4

The general synthetic route for the preparation of bridged phosphorus cavitand is outlined in Scheme 5. From the resorc[4]arene, bearing various substituents at the lower rim, the cyclization step, which leads to the formation of the four fused eight-membered rings, was performed with three-coordinated and four-coordinated phosphorus reagent to give respectively: tetra-phosphite, tetra-phosphonite, and tetra-phosphate or tetra-phosphonate derivatives.
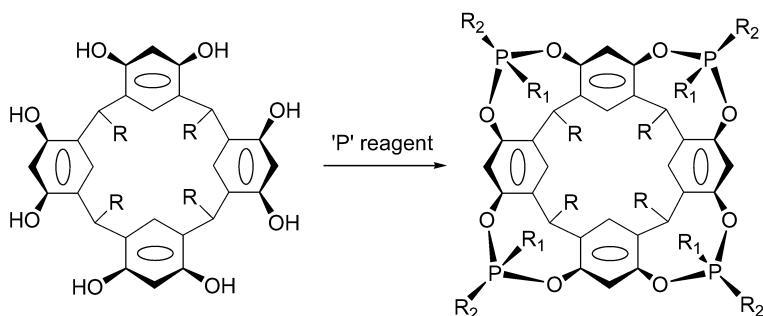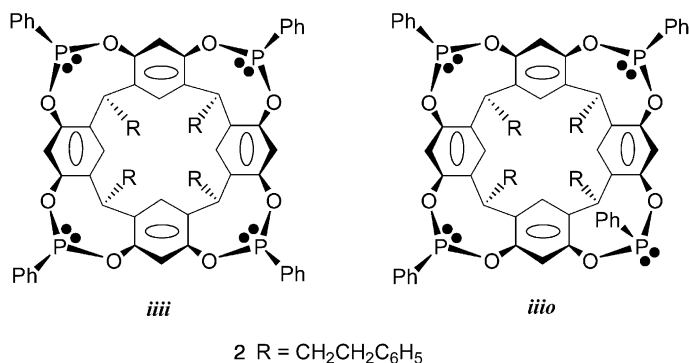
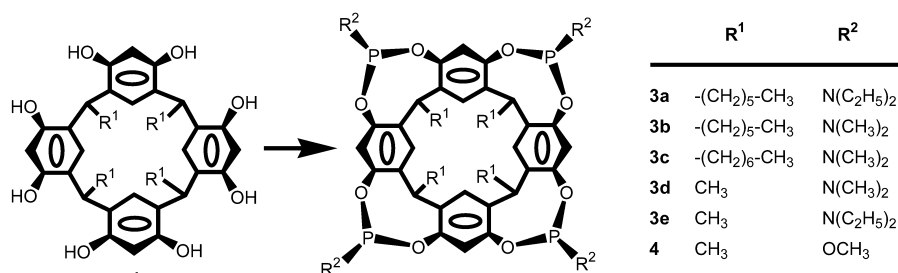**Scheme 5**

2.2.1
Phosphorus(III) Bridged Cavitands

In the approach of Puddephatt et al., the P-phenyl-phosphonitocavitand **2** was obtained by the reaction of phenylphosphonous chloride on resorc[4]arene **1b** (**1**, R=CH$_2$CH$_2$C$_6$H$_5$) in presence of pyridine as base. The reaction is stereoselective and yielded the bowl-shaped molecule **2** with the four P-phenyl groups directed outwards and the four lone pairs directed inwards (*iiii* configuration) [45–49] (Scheme 6). Molecular mechanics calculations performed on the six possible isomers of **2**, showed that the *iiii* isomer is preferred and the orientation of one phenyl group toward the macrocyclic cavity is probable (*iiio* isomer), but two or more phenyl groups oriented inwards are highly unlikely [48].

iiii   *iiio*

2 R = CH$_2$CH$_2$C$_6$H$_5$

Scheme 6

Alternative routes were used to prepare a series of tetra-bridged phosphorus(III) cavitands with PNR$_2$ (R=alkyl) or POMe groups and with various substituents at the lower rim of the cavity (Scheme 7). For instance, compounds **3a–3e** were synthesized from P(NR$_2$)$_3$ and the corresponding resorc[4]arene in benzene at room temperature [50], or in hot dioxane [51,

52]. Only the *iiii* configuration of **3e** was ascertained from the structure analysis of the sulfurized P=S derivative. From $CH_3OP(NR_2)_2$ the tetraphosphitocavitand **4** was obtained but its stereochemistry was not established [51, 52].
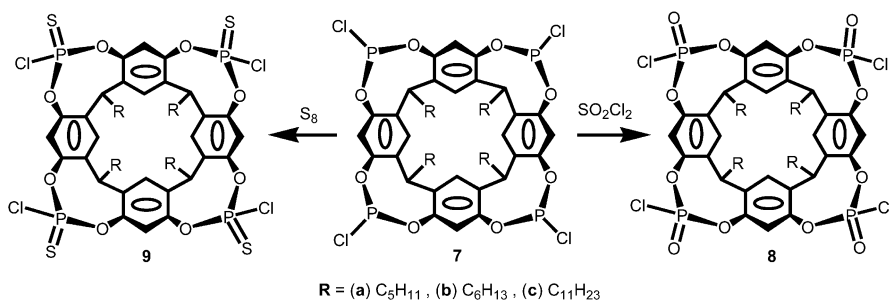

	R^1	R^2
3a	$-(CH_2)_5-CH_3$	$N(C_2H_5)_2$
3b	$-(CH_2)_5-CH_3$	$N(CH_3)_2$
3c	$-(CH_2)_6-CH_3$	$N(CH_3)_2$
3d	CH_3	$N(CH_3)_2$
3e	CH_3	$N(C_2H_5)_2$
4	CH_3	OCH_3

Scheme 7

In another approach using PCl_3 as phosphorylating agent, Schmutzler et al. synthesized the functionalized phosphocavitand **5** bearing four PCl groups. The solid state structure of the host revealed the *oooo* configuration with the four P-Cl bonds orientated inside the molecular cavity and the four lone pairs directed outwards [53] (Scheme 8). This new functionalized cavitand allowed the preparation of a large variety of new cavitand hosts bearing amino or alkyl groups on phosphorus by reaction with silylated amines to yield the tetra-amidophosphite derivatives, or with Grignard reagents to afford the tetra-alkyl phosphonite cavitands. In the latter case, the reaction of **5** with CH_3MgI only produced the *iiii* stereoisomer **6**, which was characterized by an X-ray crystal structure determination [53, 54]. Similarly, cavitands **7a–7c** with four phosphorus(III) P-Cl moieties and bearing longer alkyl substituents at the lower rim (R=C_5H_{11}, C_6H_{13}, $C_{11}H_{23}$), were produced in high yields (Scheme 9) [55].

	R^1	R^2	R^3
5	Cl	lone pair	CH_3
6	lone pair	CH_3	CH_3

Scheme 8

R = (a) C_5H_{11} , (b) C_6H_{13} , (c) $C_{11}H_{23}$
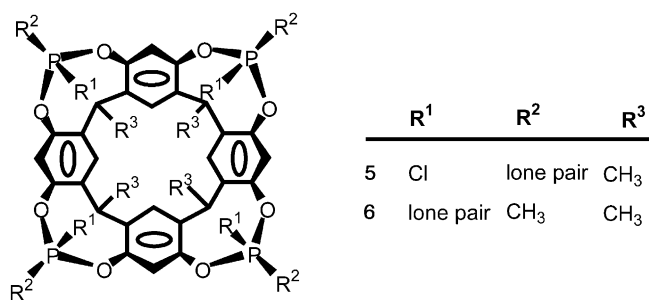
Scheme 9

2.2.2
Phosphorus(IV) Bridged Cavitands

In this section we will deal with the 4-coordinate phosphorylated cavitands (P=O or P=S), which are formally pentavalent (tetrahedral) $\lambda^5\sigma^4$ phosphorus species. We will use the phosphorus(IV) terminology to designate these compounds. Two families of phosphorus(IV) bridged cavitands have been considered depending on the P=O or P=S bridging groups that were used to create the new hosts. There are two main routes to synthesize these compounds. One is the direct cyclization with a phosphonic chloride or phosphonothioic chloride reagent, the second consists in the preparation of the phosphorus(III) parent compound which is subsequently oxidized to give P=O or P=S derivatives. In the case of the reaction with phosphorus(IV) reagent, the stereoselectivity of the reaction is of prime importance, and the possible formation of multiple isomers will depend on the reaction conditions. In the two steps procedure, it is necessary to consider the different stereoselectivities of the ring closure reaction with a phosphorus(III) reagent and the subsequent oxidation step. Furthermore, the lower reactivity of the P(IV) reagents compared to the P(III) species can play an important role. For instance, attempts to prepare P=O and P=S chlorophosphate cavitands have failed when resorc[4]arene was allowed to react with $OPCl_3$ or $SPCl_3$. Compounds **8** and **9** were only obtained using a two steps procedure starting from PCl_3. The 3-coordinate P-Cl derivative **7** was first obtained and subsequently oxidized with different oxidizing agents (DMSO, O_2, H_2O_2, SO_2Cl_2), but only SO_2Cl_2 gave unequivocally the 4-coordinated compound **8** in high yields. Similarly the addition of sulfur to **7** afforded the P=S compound **9** [55] (Scheme 9).

Indeed, it is well established that the direct oxidation of phosphorus(III) compounds with specific oxidizing agent or sulfur is a simple way to form P=O or P=S derivatives, and this strategy has been widely used in the chemistry of phosphorus cavitand. The P=O derivative of the tetra-amidophosphite cavitand **3d** was prepared stereoselectively by using the $(H_2N)_2CO/H_2O_2$ 1:1 adduct as oxidizing agent [53]. The addition of sulfur to **3d** and **3e** gave the tetraamido tetrasulfide derivatives **14d** and **14e** in 90–95% yields

[51, 52]. Following the same route compound **15** was obtained in 56% yield [56] (Scheme 10). Meanwhile, Nifanteev et al. reported the first X-ray structure of a phosphorus(IV) derivative, by describing the solid state structure of **14e**, which exhibited the *iiii* configuration with the four P=S bonds directed toward the molecular cavity [51].

	R	R'
14d	CH_3	CH_3
14e	C_2H_5	CH_3
15	C_2H_5	C_6H_5
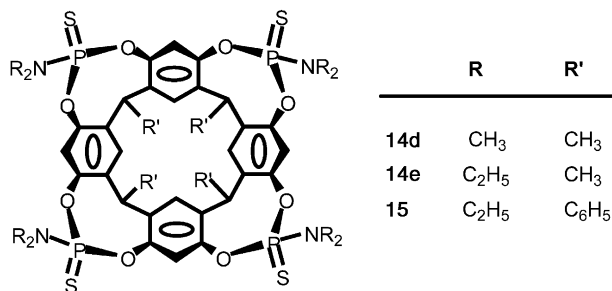
Scheme 10

Interestingly, to circumvent the lack of stereoselectivity in the synthesis of some substituted P=O cavitands, a 3-steps procedure was used. This was successfully applied to tetra-bridged phosphonatocavitand to get the tetra-oxide compound with the *iiii* configuration in high yields, when other route led only to a mixture of isomers. The 3-coordinate compound was first prepared and allowed to react with sulfur. The reaction proceeded with retention of configuration to give almost quantitatively the 4-coordinate P=S cavitand. The treatment with H_2O_2 in acetone solution resulted in the sulfur-oxygen exchange to give the tetra-oxide derivative with the same stereochemistry [57].

We will focus now on two series of tetra-bridged phosphorylated cavitands, which are of importance in regards to their potential host-guest properties and therefore as elements for the design of supramolecular systems. These are the phosphate derivatives, and the P-phenyl phosphonate or thiophosphonate compounds, which have been particularly investigated in our group.

2.2.2.1
Phosphatocavitands

The tetra-bridged phosphatocavitands **10a–j** (Scheme 11) were obtained by reaction of the corresponding resorc[4]arene with $ROP(O)Cl_2$ (R=aromatic or alkyl group) in acetone in presence of triethylamine as base. In most cases, several isomers due to the different orientation of the P=O bonds were formed in variable amounts, whereas the *iiii* and *oooo* stereoisomers were not, or only in trace amounts [58–62]. Usually, the *iiio* isomer is the most abundant compound and the strereoselectivity of the reaction was essentially attributed to the preference of the host molecule to fill the cavity with at

least one R^1 group, independently of the substitution on the aromatic rings of the cavity [58, 59].

	R^1	R^2
10a	ethoxy	H
10b	4-methylphenoxy	H
10c	4-*tert*-butylphenoxy	H
10d	4-chlorophenoxy	H
10e	2-phenylphenoxy	H
10f	2,6-diisopropylphenoxy	H
10g	2,4,6-trimethylphenoxy	H
10h	4-methylphenoxy	Br
10i	4-*tert*-butylphenoxy	Br
10j	4-chlorophenoxy	Br
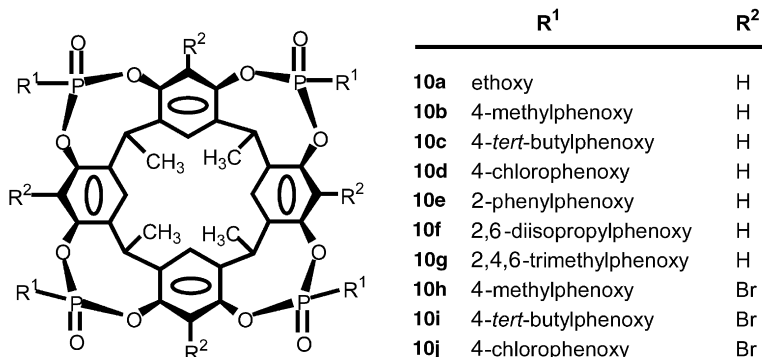
Scheme 11

This situation is different from that observed with the P(III)-phenyl phosphonite **2**, where the *iiii* isomer was the major compound formed. This is however predictable if we consider the highest mobility and thence the lower steric hindrance of the phosphate substituent as compared to the phenyl group in the phosphonite derivative. The P-OR group can be oriented outwards through rotation around the P-O bond. This has been exemplified by solving the solid state structure of the *ioio* isomer of **10b** where the two P-O-p-tolyl groups oriented inwards are clearly directed above the molecular cavity [60]. This trend to orientate at least one P-OR phosphate group inside the cavity is also observed in mixed-bridged phosphate cavitands where two or three phosphate bridges are replaced by -(CH$_2$)$_n$- bridges (n=1, 2). This is even more obvious for the mono-phosphate cavitand **11** with three CH$_2$ bridges, where the ratio i/o=4, indicates a clear preference for the PO$_{in}$ orientation [60] (Scheme 12).

PO$_{in}$ (*i*)   **PO$_{out}$ (*o*)**

11 Ar = O-C$_6$H$_4$-*p*-CH$_3$
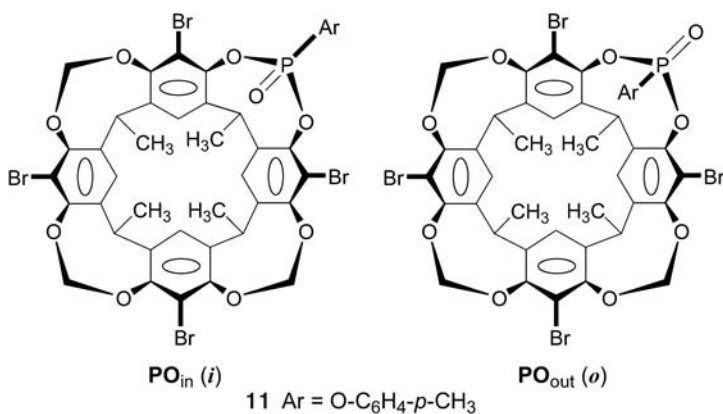
Scheme 12

2.2.2.2
Phenyl-phosphonatocavitands

The synthesis of tetra-bridged P-phenyl phosphonatocavitands **12** is particularly interesting. Indeed, the more hindering P-phenyl group should favor the outwards orientation of the aromatic ring and thus favor the formation of the *iiii* isomer with four converging phosphoryl oxygen atoms towards the host cavity. However, the issue of the reaction is highly dependent on the experimental conditions. Performed in acetone or THF solution in presence of triethylamine as base, the ring closure reaction of the corresponding resorc[4]arene with dichlorophenylphosphine oxide PhPOCl$_2$ led to isomeric mixtures in which the *iioo*, *ioio* and *iooo* were the major isomers formed, and neither *iiii* nor *iiio* isomers were observed [61]. The same reaction performed in toluene in presence of base showed the exact inverted tendency with mainly the formation of the *iiii* isomer, often associated with trace quantities of the *iiio* derivative (Scheme 13). The use of *N*-methylpyrrolidine as base dramatically increased the yield of the *iiii* isomer [63].

1a R = CH$_3$
1b R = CH$_2$CH$_2$C$_6$H$_5$

12a R = CH$_3$
12b R = CH$_2$CH$_2$C$_6$H$_5$
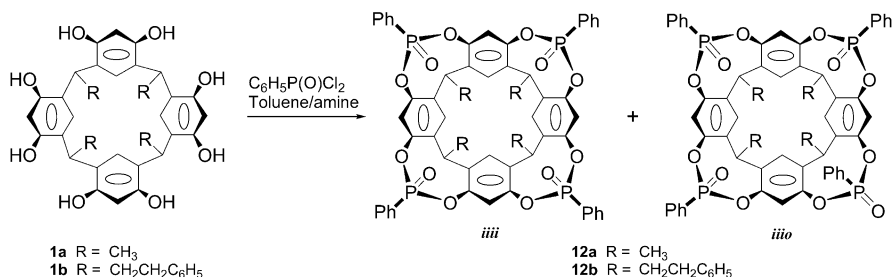
Scheme 13

Because of the different experimental conditions, the solvent/amine pair plays a crucial role in the formation of the *iiii* stereoisomer. Systematic study of the influence of the nature of the base, the reagent/base ratio, and the nature of the solvent (donating power), was performed with the phosphonatocavitands **12a** and **12b** (Table 1). The procedure is highly solvent dependent: the *iiii* stereoisomer is the major product obtained in toluene, associated with minor amount of *iiio* isomer. When the reaction is run in acetone other isomers are predominant (*ioio*, *iioo*, *oooi*) and the *iiii* stereoisomer is not observed. The use of catalytic amount of this amine (0.2 equiv) [64] did not lead to any extractable compounds, and using eight equivalents of amine to trap all the HCl formed, did not change dramatically the yield and the isomer ratio (entries 5 and 6, Table 1). In the presence of triethylamine the *iiii* and *iiio* isomers were formed in 28.5% and 7% yields respectively.

To explain these experimental data, we suggested that the *N*-methylpyrrolidinium salt which is formed during the reaction act as an efficient templating agent. A host-guest complex is formed between the ammonium salt and the resorc[4]arene cavity, which therefore spontaneously direct the strong donor phosphoryl groups toward the cavity favoring the formation of the *iiii*

Table 1 Isolated yields of *iiii* and *oooi* isomers of **12a** and **12b**[a]

Entry	Reagent	Amine	Amine equiv.	Solvent	% *iiii*	% *iiio*
1	**1a**	*N*-Methylpyrrolidine	1	Toluene	25	0
2[b]	**1a**	Triethylamine	10	Acetone	0	0
3	**1a**	*N*-Methylpyrrolidine	10	Acetone	0	0
4	**1b**	*N*-Methylpyrrolidine	0.2	Toluene	0	0
5	**1b**	*N*-Methylpyrrolidine	1	Toluene	51	5
6	**1b**	*N*-Methylpyrrolidine	8	Toluene	53	9
7	**1b**	Triethylamine	8	Toluene	28.5	7

[a] From [63]
[b] From [61]

stereoisomer (Scheme 14). In acetone the ammonium cation is more easily solvated, resulting in a significant inhibition of the complexation process, and ruling out any templating effect. The different effects observed between *N*-methylpyrrolidine and triethylamine as base, are attributed to the most efficient complexation of *N*-methylpyrrolidinium cation compared to triethylammonium. The N-CH$_3$ group of the *N*-methylpyrrolidinium can be deeply encapsulated in the host cavity leading to a better stability of the complex than that obtained with triethylammonium as guest (see below) [63, 65].

12a R = CH$_3$ 25%
12b R = CH$_2$CH$_2$C$_6$H$_5$ 46%
12c R = (CH$_2$)$_{10}$CH$_3$ 55%
12d R = (CH$_2$)$_7$OC$_6$H$_4$-*o*-NO$_2$ 40%
12e R = (CH$_2$)$_3$-OC$_6$H$_4$-*p*-NO$_2$ 31%
12f R = (CH$_2$)$_8$CH=CH$_2$ 51%
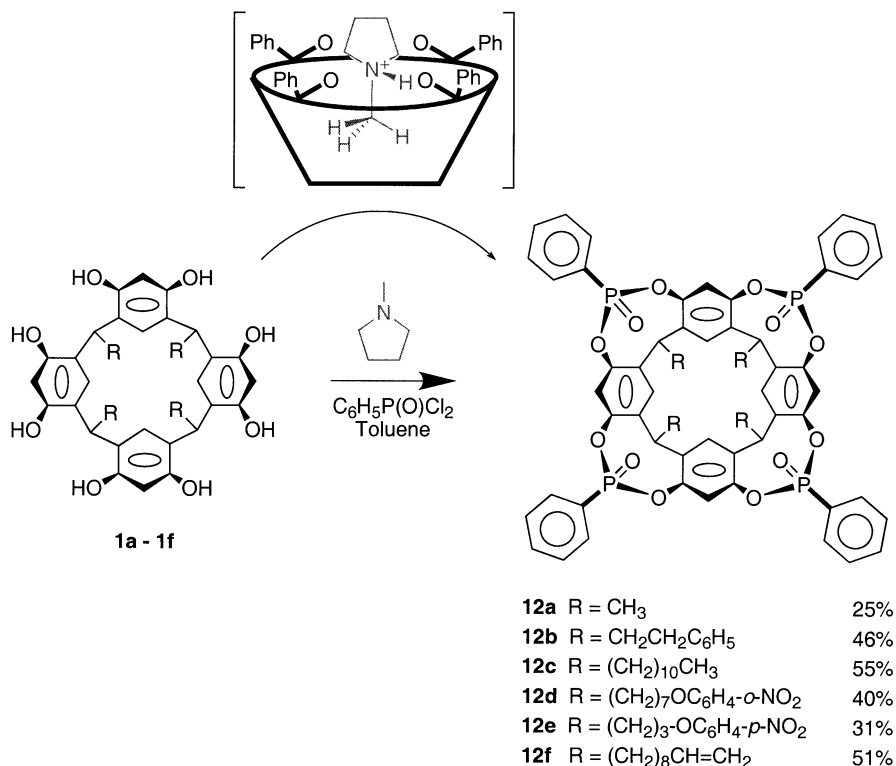
Scheme 14

Following this strategy, the stereoselective synthesis of the *iiii* stereoisomer of novel tetra-phosphonatocavitands having lower rim functionality has been reported [66, 67]. Cavitands **12c–12f** were respectively synthesized from functionalized resorc[4]arenes **1c–1f**. The addition of 1-decanethiol to **12f** in the presence of 9-borabicyclo[3.3.1]nonane (9-BBN) in THF afforded cavitand **12g** in 80 % yield (Scheme 15).

1f R = -(CH$_2$)$_8$-CH=CH$_2$

(i)

(ii)

12f R = -(CH$_2$)$_8$-CH=CH$_2$ 51%

12g R = -(CH$_2$)$_{10}$-S-(CH$_2$)$_9$-CH$_3$ 80%

(i) NMP (1 eq.), PhP(O)Cl$_2$ (4 eq.), toluene; (ii) 9-BBN, HS(CH$_2$)$_9$CH$_3$, THF
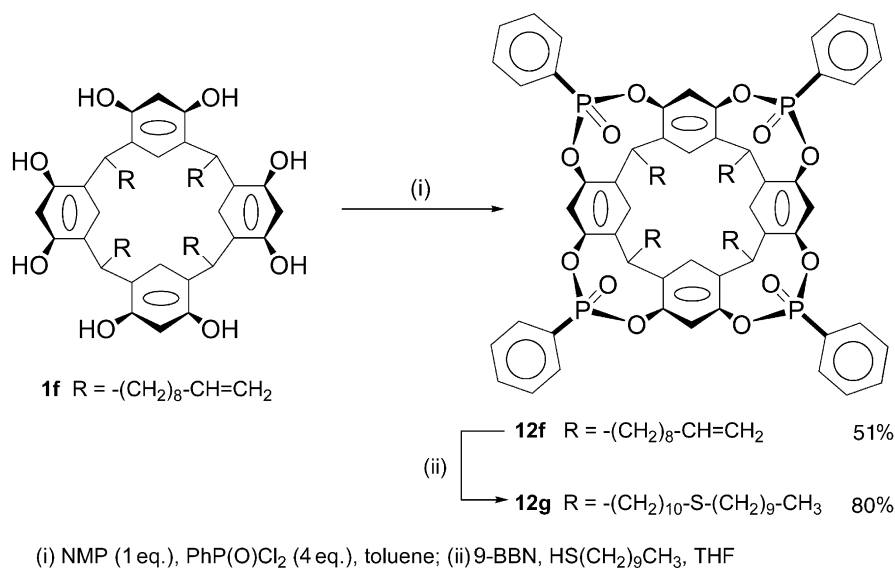
Scheme 15

The solid state structure determination of **12d** undoubtedly proved the *iiii* configuration of the molecule, which presents a pseudo-C_4 symmetry with the P=O bonds directed inward (Fig. 1) [66]. The crystal contains six solvent molecules per host. One acetonitrile molecule was found as a guest in the aromatic cavity. At the lower rim, a second molecule of acetonitrile occupied the position between the four long chain substituents.

To underline the effect of the P-phenyl group in the *iiio* isomer, the X-ray structure of the *iiio* isomer of cavitand **12c** was solved from single crystal X-ray analysis (Fig. 2). It is noteworthy that the inner space is almost entirely occupied by the inward oriented P-phenyl group, precluding less efficient complexation properties [68].

2.2.2.3
Phenyl-thiophosphonatocavitands

The use of thiophosphonic chloride reagent did not give clear results and more importantly, the stereoselectivity of the reaction is difficult to control. For instance, the reaction of C$_6$H$_5$P(S)Cl$_2$ with the resorc[4]arene **1c** afforded a mixture of isomers of **13**, which have been only partially purified by col-
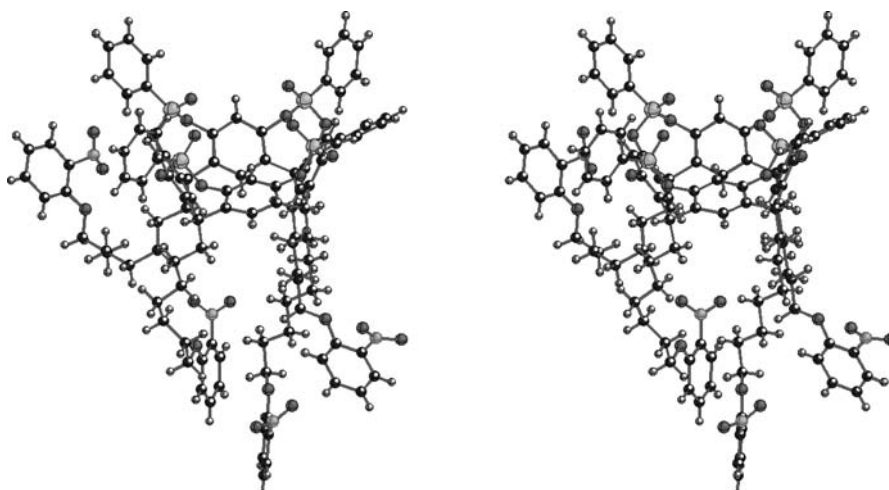
Fig. 1 Stereoview of the X-ray crystal structure of the tetra-phosphonatocavitand **12d**

umn chromatography. The *iiii* isomer was isolated in 21% yield, and the pure *iiio* isomer was hardly obtained, both being often still contaminated with other isomers [69]. The tetra-bridged P-phenyl thiophosphonatocavitand **13** was more conveniently prepared by the oxidation of the parent phosphorus(III) compound with sulfur, as outlined in Scheme 16. The first step is known to afford exclusively the *iiii* isomer [48] and the sulfurization step proceeded with retention of configuration, leading to the *iiii* stereoisomer **13** in 52% yield [70].
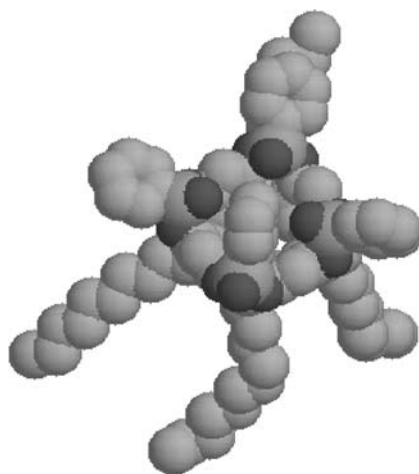
Fig. 2 Molecular structure of the *iiio* isomer of the tetra-phosphonatocavitand **12c** (hydrogen atoms have been omitted for clarity)
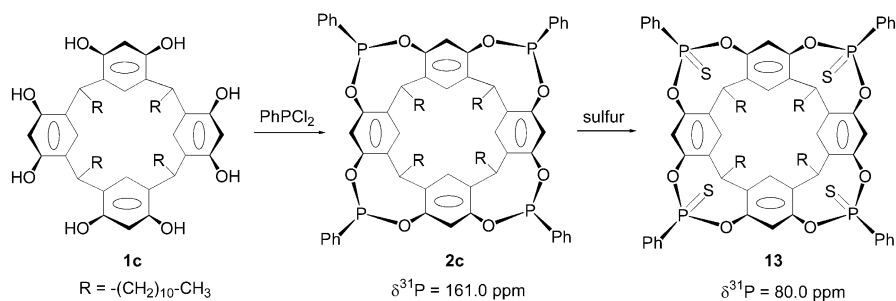
Scheme 16

The solid state structure of the thiophosphorylated host depicted in Fig. 3 shows unambiguously the all inward orientation of the four P=S bonds [71]. As in the oxidized parent compound **12c**, a solvent molecule (acetonitrile) is entrapped in the cavity of the host, and another one is embedded at the lower rim between the four long alkyl chain substituents.

The two-steps synthesis of thiophosphorylated cavitands is by far the best method to control the stereoselectivity of the resultant products. As for the P=O partners, it is important to obtain the all-inward oriented P=S donating groups in high yields to benefit from cooperative effects of the P=S donor groups and the aromatic cavity in the formation of host-guest complexes.
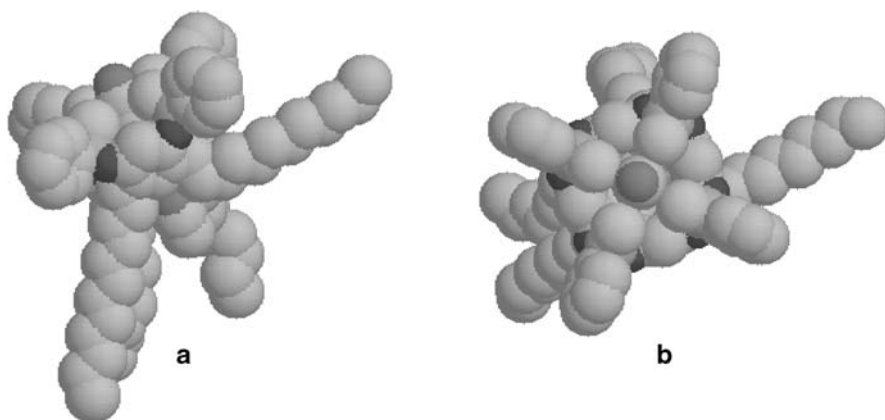
Fig. 3a,b Molecular structure of tetra-thiophosphonatocavitand **13**: **a** side view; **b** top view (hydrogen atoms have been omitted for clarity)

3
Host-Guest Complexes of Phosphorylated Cavitands

3.1
Metal Coordination with Phosphorus(III) Hosts

The phosphorus(III) species are particularly attractive for the transition metal ion coordination, e.g., for catalysis application. In **2** the free electron pairs of the four phosphorus atoms are oriented toward the macrocyclic cavity (*iiii* stereoisomer), allowing complexation of four transition metal cations [45–49]. The phosphorus atoms in **2** have been shown to interact with Au, Ag and Cu halides to form tetra-nuclear complexes. The **2**·(AuCl)$_4$ complex was formed by treatment of **2** with [AuCl(SMe$_2$)] and characterized by X-ray structure analysis. The AuCl units are bound to phosphorus through the gold atom and orientated inside the cavity. Complexes **2**·(AuX)$_4$ (X=Br, I) were also prepared by reaction of **2**·(AuCl)$_4$ with NaBr or KI respectively. The tetra-Pt complex **2**·[PtCl$_2$(SMe$_2$)]$_4$ was similarly formed when **2** was subjected to react with [PtCl$_2$(SMe$_2$)$_2$] [48].

A different behavior was observed when **2** was treated with [(MCCPh)$_n$] (M=Cu, Ag) in presence of pyridinium chloride to give the **2**·(M$_4$Cl$_5$) pyridinium salt complexes. The new species have the structure [C$_5$H$_5$NH]$^+$[**2**·Cu$_4$(μ-Cl)$_4$(μ_3-Cl)]$^-$ and [C$_5$H$_5$NH]$^+$[**2**·Ag$_4$(μ-Cl)$_4$(μ_4-Cl)]$^-$, respectively. In these cases, the anionic metal halide-cavitand complexes act as size-selective hosts for the inclusion of halide anions. Different [**2**·(M$_4$Cl$_4$Y)]$^-$ (Y=Cl, Br, I) structures are formed with the Y ion encapsulated in the center of the cavity (Scheme 17) (see below) [45–47]. The reaction of tetra-amidophosphitocavitand **3d** with CuCl yielded the anionic tetranuclear **3d**·Cu$_4$Cl$_5$ complex [54] (Scheme 18). The structure was confirmed by X-ray analysis, and showed central Cu$_4$Cl$_5$ unit with tetrahedral coordinated copper, analog to that described above with the tetra-P-phenyl compound **2** [47]. On the other hand, when **3d** was allowed to react with (tht)AuCl (tht=tetrahydrothiophene), the neutral tetra-gold complex was formed, also analog to the previously described gold complex of **2** [48].

$$R = CH_2CH_2C_6H_5$$
$$M = AuX\ (X = Cl, Br, I)$$
$$M = PtCl_2(SMe_2)$$

R = CH$_2$CH$_2$C$_6$H$_5$
M = Cu, X = Y = Br
M = Cu, X = Y = I
M = Cu, X = Cl, Y = I
M = Ag, X = Y = Cl
M = Ag, X = Y = Br
M = Ag, X = Y = I
M = Ag, X = Cl = I
M = Ag, X = Y = Cl
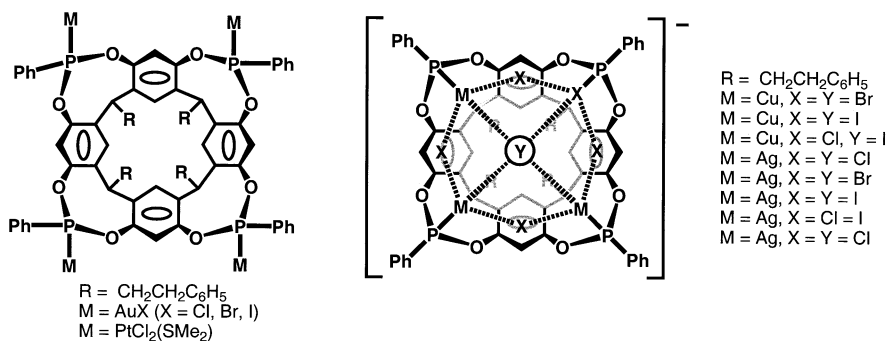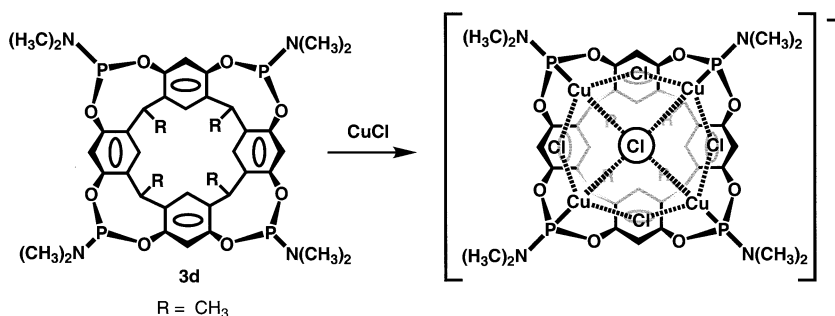
Scheme 17

Scheme 18

The reaction of amidophosphito cavitands with Cr, Mo, and W hexacarbonyl, and $C_5H_5Mn(CO)_3$ resulted in the formation of the binuclear complexes. The structure was elucidated by ^1H and ^{31}P NMR and X-ray diffraction analysis, and showed that the distal bi-nuclear structure was formed. The tetra-nuclear complex was only obtained with tetra-phosphitocavitand **14** and Cr or Mo hexacarbonyl (Scheme 19) [72].

R = CH_3 , $CH_2CH_2CH_3$
R' = CH_3 , C_2H_5
M = Cr, Mo, W

14•$[M(CO)_5]_4$

R = CH_3
M = Cr, Mo
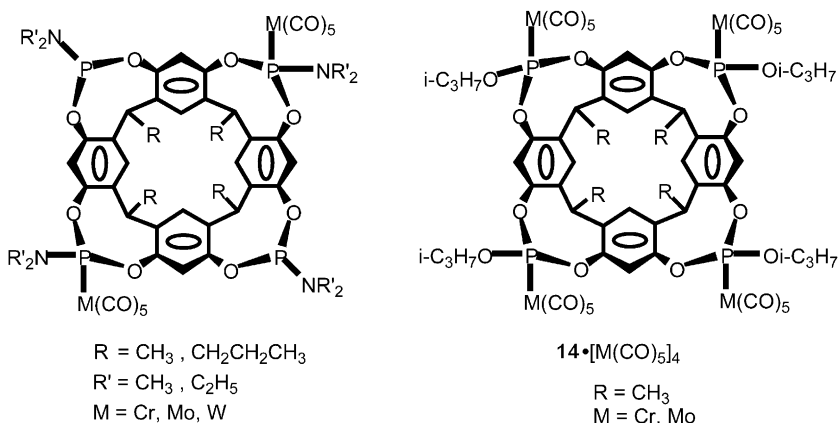
Scheme 19

3.2
Complexation of Neutral Guests

The complexation of neutral guests by tetra-bridged phosphorylated cavitands has been quite seldom investigated, although some specific host-guest interactions should favor the encapsulation of neutral species (H-bonding, van der Waals forces, hydrophobic effects or specific π-interaction). With the tetra-nuclear complexes of **2** described in the previous section, evidence for the encapsulation of alkyl-amine was reported. Only amine guest can in-

teract strongly with the gold atom in the $2 \cdot (AuCl)_4$ complex to give $[2 \cdot (AuCl)_4] \cdot RNH_2$ supramolecular assemblies as evidenced by NMR spectroscopy. To achieve the stability of the host-guest system the nitrogen interact with gold atom through its lone pair to form partially charged species together with the inclusion of the alkyl chain in the hydrophobic cavity of the host [48].

The binding properties of the *iiio, iioo, ioio, iooo,* and *oooo* isomers of tetra-bridged phosphatocavitands have been investigated in the gas phase by mass spectrometry. The formation of amine guest inclusion complex in the MS probe was strongly dependent on the stereochemistry of the cavitands: the more P=O bonds are oriented toward the inside of the cavity, the stronger the binding of the guest species [62]. Complementary studies were performed by LSIMS technique (Liquid Secondary Ion Mass Spectrometry) that confirmed the present results in regards with the number of interacting P=O groups and the rigidity of the cavity [73].

Interesting and important investigations were pursued by the Dalcanale's group to explore the potential of mono-phosphorylated cavitands (see Scheme 20) as supramolecular sensors for the detection of alcohols by using mass sensitive transducers [74]. Thin layers of cavitands were deposited on the sensitive surface of a quartz-crystal microbalance (QCM) piezoelectric sensor system, which in presence of analytes gave highly reproducible responses. The responses to C_1–C_5 linear alcohols with the different sensors coated with cavitands **15–17** were studied. The inward or outward orientation of the P=O bond is crucial and in favor of the *i* (PO$_{in}$) isomer. The cooperativity between hydrogen bonding with the P=O group and CH...π interactions with the aromatic cavity is enlightened by the different behavior of hosts **15(*i*)** and **17(*i*)** compared to the non-phosphorylated cavitands **18** and **19** respectively.

15(*i*) X = Br; Ar = Ph
16(*i*) X = Br; Ar = OPh
17(*i*) X = CH$_3$; Ar = Ph

R = -(CH$_2$)$_{10}$-CH$_3$

15(*o*) X = Br; Ar = Ph
16(*o*) X = Br; Ar = OPh

18 X = Br
19 X = CH$_3$
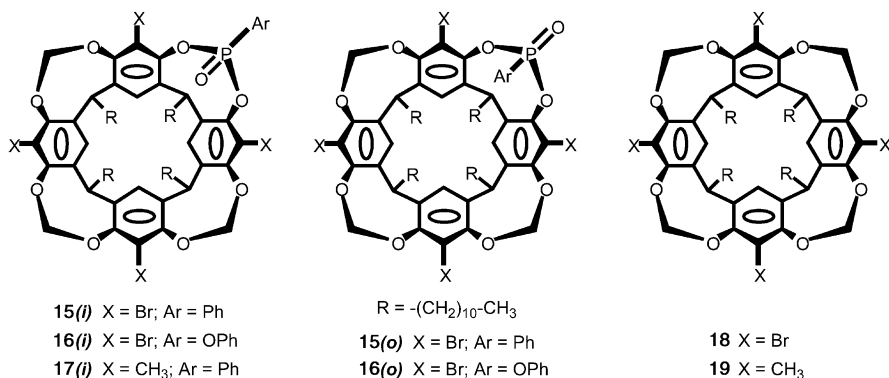
Scheme 20

The two-point interaction between PO$_{in}$ cavitands and alcohol guest was exemplified by the solid state structure of the **16(*i*)**·C$_2$H$_5$OH complex showing hydrogen bond to the P=O group and CH···π interactions between the

alkyl moiety and the aromatic rings of the cavity [74]. These data are among the few ones that explore the capabilities of the bridged-phosphorylated cavitands as sensor and demonstrate that they can be used as highly selective supramolecular mass sensors. The capabilities of phosphorus cavitands to form such host-guest complexes emphasize the real possibilities of these new hosts in the design of new molecular devices.

3.3
Anion Complexation

The complexation of anionic species by tetra-bridged phosphorylated cavitands concerns mainly the work of Puddephatt et al. who described the selective complexation of halides by the tetra-copper and tetra-silver complexes of **2** (see Scheme 17). The complexes are size selective hosts for halide anions and it was demonstrated that in the copper complex, iodide is preferred over chloride. Iodide is large enough to bridge the four copper atoms but chloride is too small and can coordinate only to three of them to form the $[2 \cdot Cu_4(\mu\text{-}Cl)_4(\mu_3\text{-}Cl)]^-$ complex so that in a mixed iodide-chloride complex, iodide is preferentially encapsulated inside the cavity. In the $[2 \cdot Ag_4(\mu\text{-}Cl)_4(\mu_4\text{-}Cl)]^-$ silver complex, the larger size of the Ag(I) atom allowed the inner chloride atom to bind with the four silver atoms. The X-ray crystal structure of the complexes revealed that one Y halide ion is encapsulated in the center of the cavity and bound to 3 copper atoms in $[2 \cdot Cu_4(\mu\text{-}Cl)_4(\mu_3\text{-}Cl)]^-$ (Y=Cl) [45] or to 4 copper atoms in $[2 \cdot Cu_4(\mu\text{-}Cl)_4(\mu_4\text{-}I)]^-$ (Y=I) and to 4 silver atoms in $[2 \cdot Ag_4(\mu\text{-}Cl)_4(\mu_4\text{-}Cl)]^-$ [47]. NMR studies in solution of the inclusion process showed that multiple coordination types take place in the supramolecular complexes.

The nucleophilic property of the encapsulated anion was dramatically changed compared to the free anion. Thus, $[2 \cdot Ag_4(\mu\text{-}Cl)_4(\mu_4\text{-}Cl)]^-$ acts as a nucleophile to convert alkyl-iodide to alkyl-chloride in high yield. Puddephatt proposed a mechanism where the $[2 \cdot Ag_4(\mu\text{-}Cl)_4(\mu_4\text{-}Cl)]^-$ anion reacts with alkyl-iodide to give $[2 \cdot Ag_4(\mu\text{-}Cl)_4(\mu_4\text{-}I)]^-$ and alkyl-chloride. The reaction occurs in high yield with the reactivity sequence tertiary>secondary>primary alkyl.

3.4
Complexation of Metal Cations

The main feature for cation recognition by tetra-bridged phosphorylated cavitands arises from the cooperative effect of the four phosphorus groups and the aromatic molecular cavity. In the phosphorus(IV) cavitands guest binding will be achieved through O (P=O) or S (P=S) coordination with different affinity for hard or soft metal ions. On the other hand, transition metal rim complexes described above can act as host for metal cation.

3.4.1
Binding to P→M Cavitand Complexes

The **2**·(AuCl)$_4$ and **2**·(PtCl$_2$SMe$_2$)$_4$ complexes (see above), show extractability properties vs. alkali metal ions, with a greater affinity for K$^+$ than for other alkali metal ions [48]. No structural data were available and the nature of the binding in the formation of these complexes was not investigated. Similarly, the anionic complexes [**2**·Cu$_4$(μ-Cl)$_4$(μ_3-Cl)]$^-$ and [**2**·Ag$_4$(μ-Cl)$_4$(μ_4-Cl)]$^-$ have been shown to act as host for the selective binding of alkali metal cations and divalent metal ions like Zn^{2+}, Cd^{2+}, Hg^{2+}, or Pb^{2+}. Both complexes extracts efficiently metal cations from aqueous solution into CH$_2$Cl$_2$ solution with selectivities, which are either unusual or not explainable without further investigations. Different binding mode are reported for the {[**2**-Cu$_4$(μ-Cl)$_4$(μ_3-Cl)]$^-$·Cs$^+$}$_2$ and [**2**·Ag$_4$(μ-Cl)$_4$(μ_4-Cl)]$_2^-$·Hg^{2+} complexes, and NMR studies in solution showed that anion and cation guests underwent rearrangement to give a fourfold symmetry of the assemblies. The solid state structure determination of both systems showed a dimeric supramolecular architecture where two cavitand complexes are bound through the included metal ion. The cation interacts strongly with the μ-Cl donors and in the case of the cesium complex, there exists specific stabilizing π-interactions with the P-phenyl groups of the host [49]. It is noteworthy that the transition metal rim complexes behave as host for mono- and divalent cationic guests. They are forming a new type of supramolecular assembly through original binding mode involving neutral cavitand host-upper rim metal halide coordination-metal cation complexation.

3.4.2
Binding to P=O Cavitands

In the tetra-bridged phosphocavitands containing four donor P(O)R groups, the P=O bonds can adopt the inward (*i*) or outward (*o*) orientations relatively to the molecular cavity. Only the *iiii* isomer with the four P=O groups oriented inwards can benefit from both cooperativity of P=O binding and π-interactions with the aromatic cavity of the resorc[4]arene framework [19, 63]. The complexation properties of new *iiii* tetra-phosphonatocavitands **12b–12d** and **12g** towards metal ions were characterized by extraction of the metal picrate from water to chloroform solution containing the host compound (Fig. 4).

The general trend is similar for the four hosts, although some discrepancy appears along these data. In spite of some systematic errors arising from the extraction method, it must be underlined for example the discrepancy of data for Ag$^+$. The silver(I) cation is much better extracted by the thioether-substituted host **12g** probably because Ag$^+$ can interact not only with the phosphorylated binding sites of the cavitand, but also with the thioether functionality of the lower rim. Furthermore, it must be pointed out that the lipophilicity of the host can interfere in the extraction process. For both alkaline and alkaline-earth picrate salts, the extractability increases with the
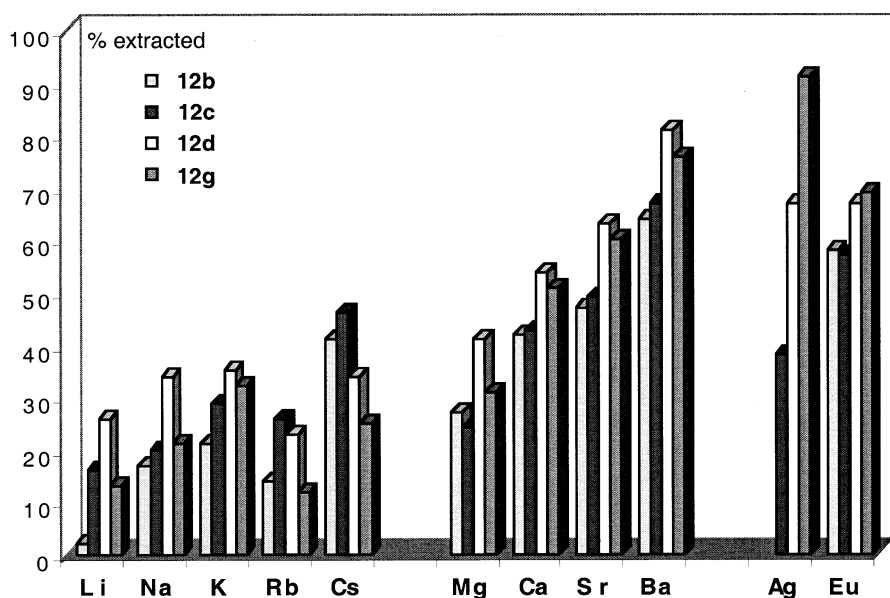
Fig. 4 % Extraction of metal picrates by phosphorylated cavitands **12b**, **12c**, **12d**, and **12g** (extraction of Ag(I) with **12b** was not measured)

ionic radius and the charge of the cation. One can also notice that the hosts are better extractants of alkaline-earth cations, which are much more hydrated than alkaline ones [75]. For instance, Ba^{2+} is two times more extracted than K^+ even so they have about the same ionic radius (1.33 and 1.35 Å, respectively). This strong ability to desolvate was attributed to both the tetra-phosphonate preorganized upper rim and the hydrophobicity of the molecular cavity. The stability constants K_a and free energies of complexation for **12b** vs alkali metal ions corroborate the extraction data and show a stronger affinity for cesium (Table 2).

The single crystal X-ray structure determination of the **12a**·Cs^+ complex gives a realistic view of the encapsulation of the guest cation inside the molecular cavity of the host. The cesium ion is deeply embedded into the cavity and lies 0.57 Å below the plane defined by the four P=O oxygen atoms. The guest interacts strongly with the four P=O oxygen atoms and has weak Cs^+-arene bonding with the aromatic rings of the cavity (Fig. 5) [63].

Table 2 Binding constants (K_a, L mol^{-1}) and free energies of complexation ($-\Delta G°$, kJ mol^{-1}) for complexes of **12b** with alkali metal cations[a]

	Li$^+$	Na$^+$	K$^+$	Rb$^+$	Cs$^+$
K$_a$	5.0×10^7	7.8×10^7	2.9×10^8	1.2×10^8	5.4×10^8
$-\Delta G°$	43.3±0.5	44.4±0.1	47.6±0.3	45.4±0.8	49.2±0.2

[a] From [63]
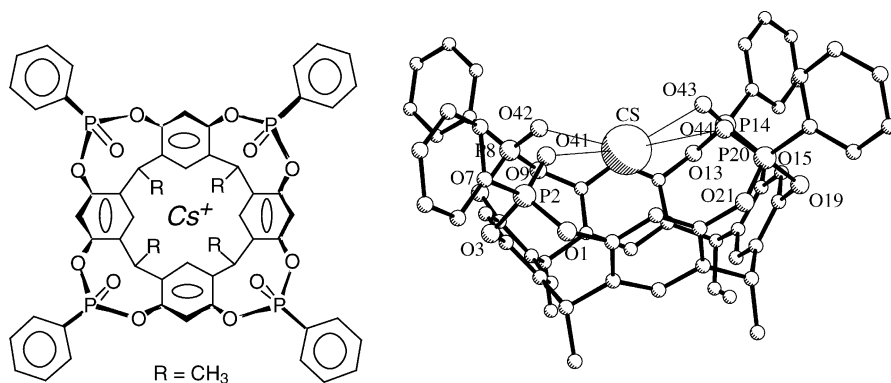
Fig. 5 Molecular structure of the **12a**·Cs$^+$Pic$^-$ complex (hydrogen atoms and picrate anion have been omitted for clarity)

3.4.3
Binding to P=S Cavitands

The ionophoric properties of **13** toward soft metal cations were evaluated by using the picrate extraction method. Metal ions like Ag$^+$ (91%), Tl$^+$ (38%) and Hg^{2+} (16%) were extracted efficiently with a maximum for Ag$^+$. Cu^{2+}, Ni^{2+}, Co^{2+}, Zn^{2+}, and Cd^{2+}, and Pb^{2+} ions were not extracted. The better extractability of **13** toward silver(I) cation was attributed to the latter's high affinity for sulfur. A fast exchange process, on the NMR time scale, was observed by ^{31}P NMR between free and complexed **13**. In presence of a twofold excess of Ag(I) salt, a 2:4 complex **13**$_2$·(AgPic)$_4$ was formed (see below) [70]. With this type of complex, the ionic radius of the metal ion is not concerned and the softness of the metal ion should be considered relatively to the soft
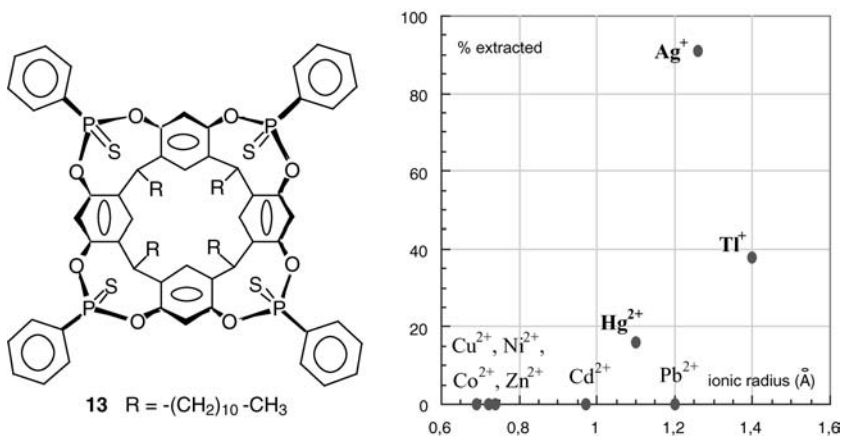
Fig. 6 % Extraction of metal ion by **13** vs the ionic radius of the guest

sulfur binding sites in **13** (Fig. 6). Although the structures of the Tl$^+$ and Hg^{2+} complexes are not known, NMR titration experiments showed that 1:1 complexes were formed.

3.5
Complexation of Ammonium Guests

The hard donor P=O groups of tetra-bridged phosphorylated cavitands are particularly attractive for ammonium cations complexation. Strong dipolar interactions between P=O and ammonium guest, together with efficient H-bonding with NH$^+$ entities, are indeed expected. Previous work by Dalcanale et al. allowed a clear characterization by LSIMS experiments of the complexation of alkyl- and arylammonium ions by phosphate-bridged cavitands [73]. This remarkable property was demonstrated with the tetra-phosphonate host **12b**, which forms in solution complexes with ammonium cations. Stability constants values of 52.4±0.1 kJ mol^{-1} (CH$_3$NH$_3^+$), 50.2±0.4 kJ mol^{-1} (*t*-C$_4$H$_9$NH$^+_3$) and 48.9±0.4 kJ mol^{-1} (NH$_4^+$) were measured in CHCl$_3$ solution. The structure of the **12a**·CH$_3$NH$_3^+$ complex shows the participation of H-bonds between NH$_3^+$ and the phosphoryl P=O groups, and stabilization through Van der Waals interactions between the NCH$_3$ methyl group and the cavity. Strong H-bonds between the NH$_3^+$ ammonium guest and two water molecules insure the stability of the assembly, as depicted in Fig. 7 [63].

More interestingly is the behavior of the extractability of host **12c** towards a series of methyl-ammonium guests (Fig. 8). Selectivity depends on both the number of methyl groups and hydrogen atoms present on the ammonium guests. The balance between the lipophilicity of the guest and the possibility for H-bonding can explain this selectivity curve. By decreasing the number of NH hydrogens the possibility of multiple H-bonding is lowered, but the lipophilicity increased. So the optimal guest appears to be (CH$_3$)$_2$NH$_2^+$. It is interesting to note that acetylcholine (AcCh), a biologically relevant cation, was efficiently extracted by **12c** (61 %) [76].
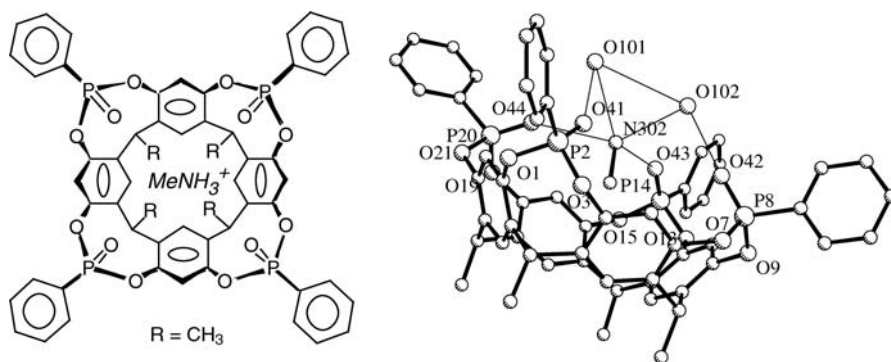
Fig. 7 Molecular structure of the **12a**·CH$_3$NH$_3^+$Pic$^-$ complex (hydrogen atoms and picrate anion have been omitted for clarity)
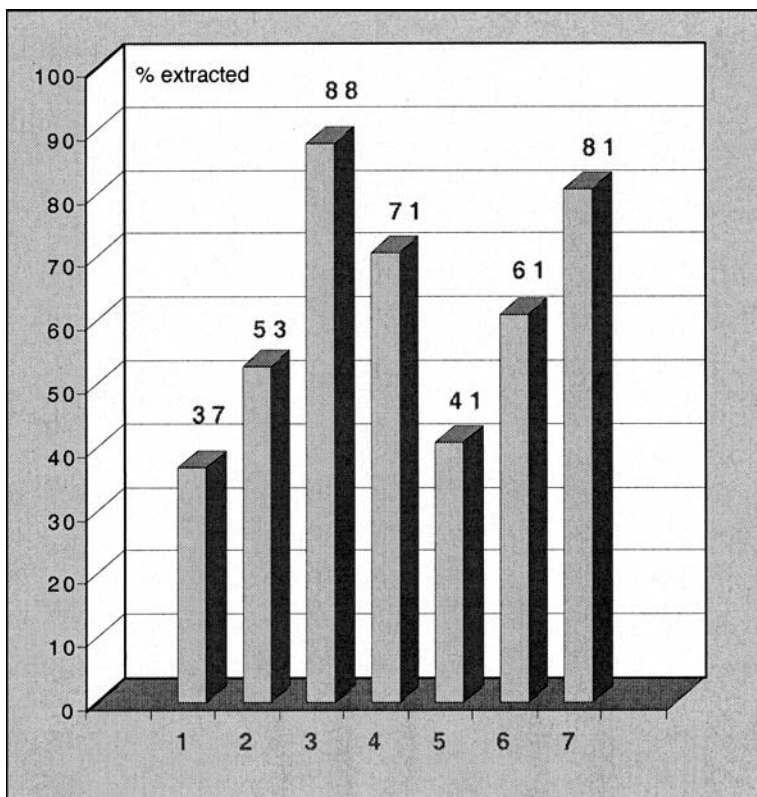
Fig. 8 Percentage extraction of ammonium cations by cavitand **12c**: **1**=NH$_4^+$, **2**=MeNH$_3^+$, **3**=Me$_2$NH$_2^+$, **4**=Me$_3$NH$^+$, **5**=Me$_4$N$^+$, **6**=AcCh, **7**=Et$_3$NH$^+$ [69]

The *iiii* stereochemistry of the host is of prime importance for the stability of the ammonium complexes. As an example weak association was measured between *c*-hexylammonium cation and the *iiio* isomer of phosphato-cavitand **10b** (K_a=1370 M^{-1}) [58]. We will see in the next section that the high affinity of the *iiii* isomer of phosphorylated cavitands for the ammonium guests allows the formation of multicomponent complexes.

4
Supramolecular Architectures

4.1
Molecular Capsule by Covalent Association of Cavitands

Molecular capsules composed of cavitands and able to form inclusion complexes have received much attention [29, 77, 78]. They can be formed covalently [78, 79] or reversibly through metal coordination [80–82] or H-bond-

ing [83–90]. To our knowledge, covalently linked phosphorus cavitands leading to molecular capsule or to nano scale cavitand structure, has not been investigated so far. We may mention the proposed dimeric compound **20** obtained by Kazakova et al. made of two resorc[4]arene molecules rim to rim bounded with four phosphite groups [91] (Scheme 21). The structure was established from spectral and elemental analysis data. The cage compound could include eight molecules of diethylamine inside the hydrophobic cavity. The lack of structural data is however quite frustrating.

20

R = -(CH$_2$)$_6$-CH$_3$
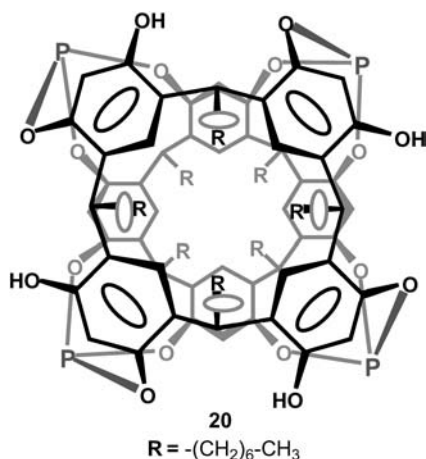
Scheme 21

4.2
Assembly of Cavitands through Silver Ion Coordination

As described above, cavitand **13** is able to extract efficiently silver(I) ion. For a guest to host ratio G/H≥2 a new species was formed and recovered in quantitative yield and was identified as the 2:4 complex **13**$_2$·(AgPic)$_4$. The X-ray crystal structure of the **13**$_2$·(AgPic)$_4$ complex showed a supramolecular assembly made of two cavitands linked by their upper rim with four silver cations through P=S...Ag...S=P coordination (Fig. 9) [70].

The Ag$^+$ cations are coordinated to two sulfur atoms of different cavitands with Ag-S distances in the range 2.47–2.50 Å. In the solid, efficient π-stacking of the P-phenyl groups with the picrate anions stabilizes the supramolecular complex (Fig. 10). The two cavitands are aligned along their common C_4 axis and offset by about 45°, leading to a helical structure. The inner space is reduced by the occupancy of the sulfur atoms, and there is probably not enough room to accommodate small guests inside the cavity.
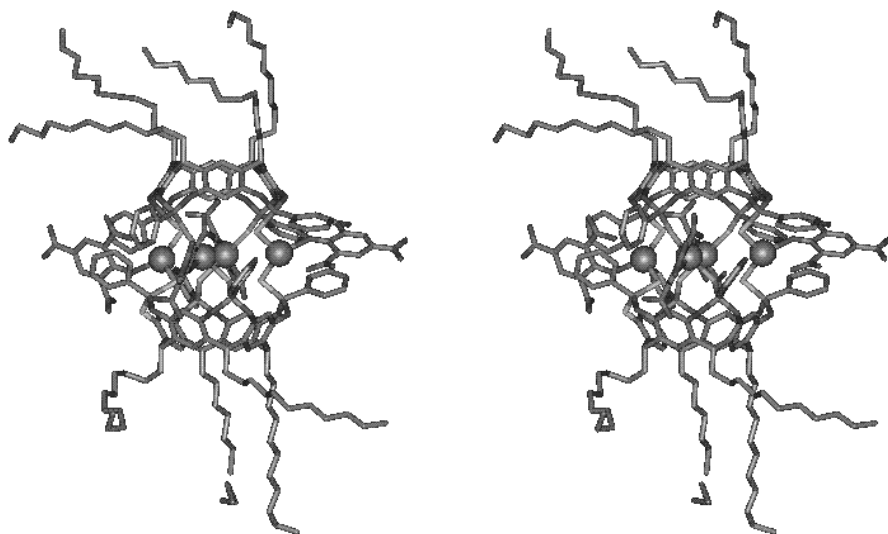
Fig. 9 Stereoview of the X-ray crystal structure of the $13_2 \cdot (AgPic)_4$ complex (hydrogen atoms have been omitted for clarity)
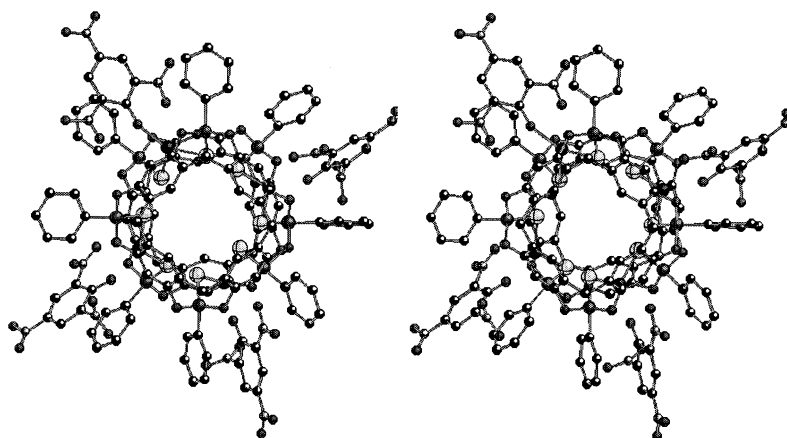
Fig. 10 Top stereoview of the $13_2 \cdot (AgPic)_4$ complex (hydrogen atoms and long chain substituents have been omitted for clarity)

4.3
Assemblies of Cavitands Through Ammonium Ions Complexation

The high affinity of ammonium cations for tetra-bridged phosphorus(IV) P=O cavitands was used to complex bis-ammonium guests. The highly insoluble N,N'-dimethyl-bipyridinium dication [paraquat^{2+}] was readily dissolved in chloroform solution in presence of **12b** in a 2:1 host-guest ratio.
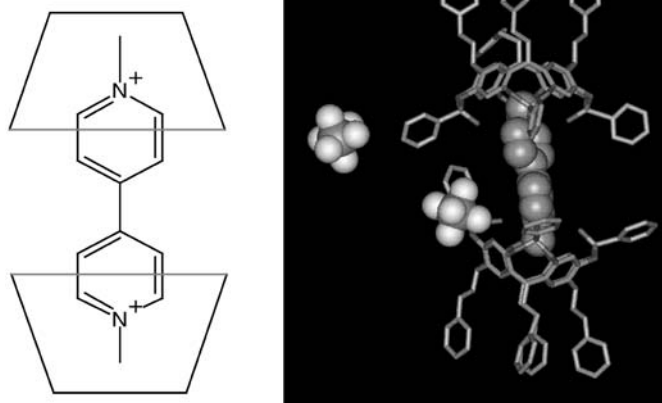
Fig. 11 Schematic representation and molecular structure of the [(**12b**)₂·para-quat²⁺](PF₆⁻)₂ complex (hydrogen atoms have been omitted for clarity)
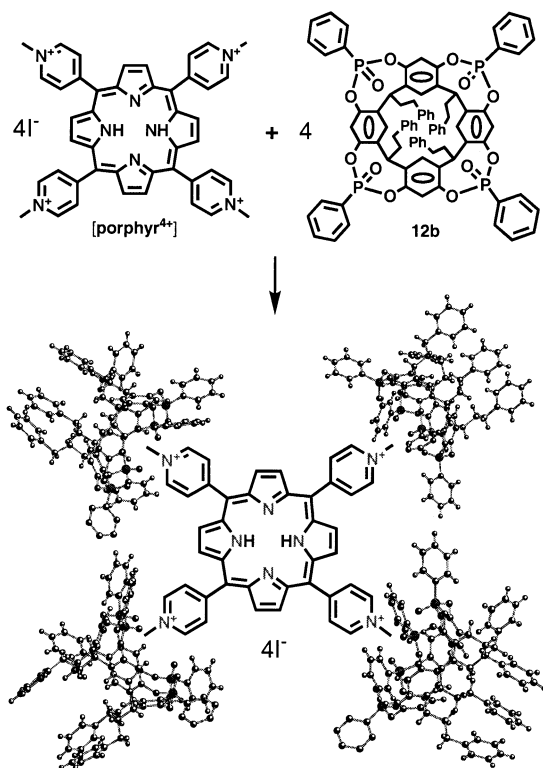
Fig. 12 Schematic representation of the supramolecular assembly [(**12b**)₄·porphyr⁴⁺] (I⁻)₄

Solution NMR evidenced the complexation process and showed the high field shift of the methyl resonance signals of the guest due to the ring current effects of the aromatic rings of the cavity. The solid state structure of the $[(12b)_2 \cdot paraquat^{2+}](PF_6^-)_2$ complex is depicted in Fig. 11. The NCH_3 groups are embedded in the molecular cavities and strongly interact with the P=O groups of the cavitand units [92].

This new type of supramolecular assembly opens the route to the design of more elaborated systems and for instance the propensity of the phosphorylated cavitand 12b to bind to poly-methylammonium guests, was further illustrated by the formation of the supramolecular complex depicted in Fig. 12. The fourfold symmetrical tetrapyridinium porphyrin [porphyr^{4+}] insoluble in chloroform was used as guest and was readily dissolved in chloroform solution in the presence of four equivalents of 12b [93].

It is noteworthy that the encapsulation of the N^+-CH_3 group allowed the dissolution of the guest in organic solvent. This remarkable property can find some application in the field of host-guest recognition processes, where extraction and transport from or through different liquid phases are of interest. Further developments can now be considered in the field of material chemistry. It is conceivable to design a cavitand dimer by lower-rim to low-
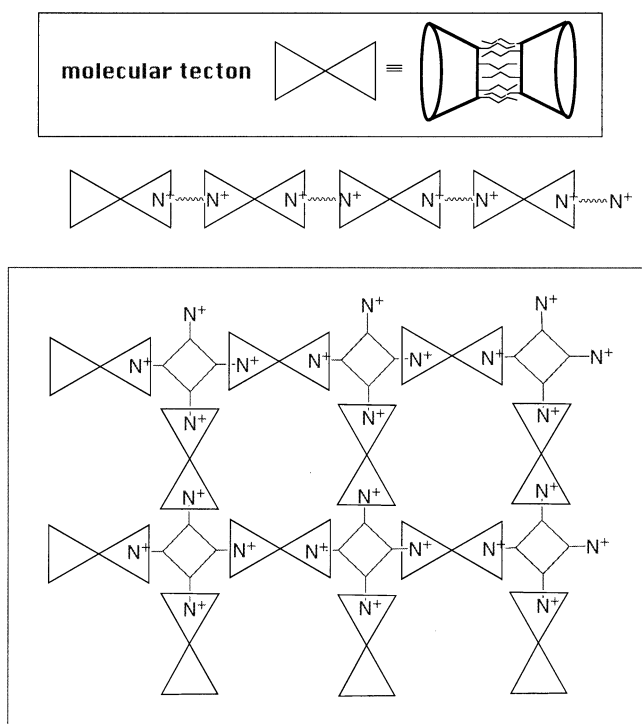
Fig. 13 Schematic representation of supramolecular assemblies of phosphorylated cavitand tectons

er-rim association. Such funtionalized hosts could be used to construct new polymeric capsules ("polycaps") [94]. Two phosphorylated cavitands attached together by their lower rim can be considered as a molecular *tecton* [95] and can therefore lead through poly-cation complexation to linear and bi- or tri-dimensional self assembling supramolecular networks, of which a schematic futuristic view is given in Fig. 13.

The search for cavitand *tectons* can be achieved through covalent binding of cavitands, as well as reversible association through lower rim functionalities, such as H-bonding or metal ion coordination [96].

5
Phosphorylated Hemicryptophanes

5.1
Objective

The considerable interest in the design of container molecules [26, 27, 30], for their potential application as nano-scale chemical reactors has particularly received much attention [97]. In this sense, supramolecular catalysis allowing the chemical transformation of a substrate selectively entrapped within a molecular receptor, will behave as a chemical reactor [98]. One way to obtain a supramolecular catalysis, is to design a molecular receptor containing a lipophilic cavity allowing selective substrate binding, and specific sites for metal ion coordination [97, 99]. Attempts in this direction have
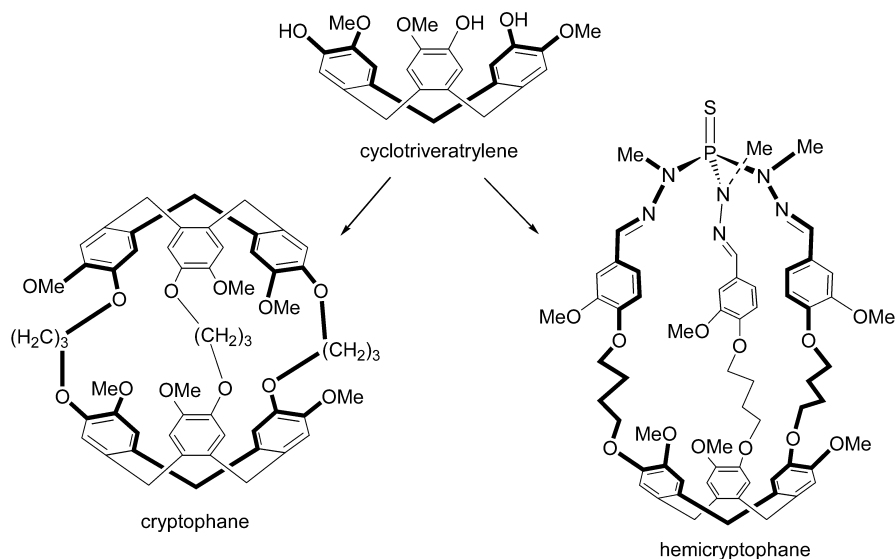
Scheme 22

been developed starting from the cryptophane platform (Scheme 22). Cryptophanes are well known host molecules developed by Collet et al. in the 1980s [100, 101]. Their high propensity to form Van der Waals host-guest complexes are essentially due to the spherical hydrophobic molecular cavity delineated by two cyclotriveratrylene units, which insures the encapsulation of neutral organic guests like chloroform [102], methane [103], or xenon gas [104, 105], as well as tetramethylammonium cation [106]. A recent approach to the synthesis of cyclotriveratrylene based ligands suggests that combining a metal coordination site and a suitable binding pocket for a particular substrate might be overcome by the use of properly designed cryptophanes [107, 108]. The concept of hemicryptophane that introduces dissymmetry at the molecular cavity level offers such an opportunity.

5.2
Synthesis

Recently, the phosphorylated hemicryptophane **22** using the CTV platform and containing a ditopic molecular cavity was prepared according to Scheme 23. The synthesis follows subsequent protection deprotection steps to afford the tri-substituted precursor **23**, which contains the cyclotriveratrylene unit. The phosphotrihydrazide moiety allowing the formation of the molecular cavity was introduced in the last step to give rise to **22** in moderate yield [109]. The strategy using the phosphotrihydrazide reagent is known to produce in fairly good yields original phosphorus macrocycles and cryptands [14], and this is confirmed in the present case where three hydrazone bonds are formed in **22**.
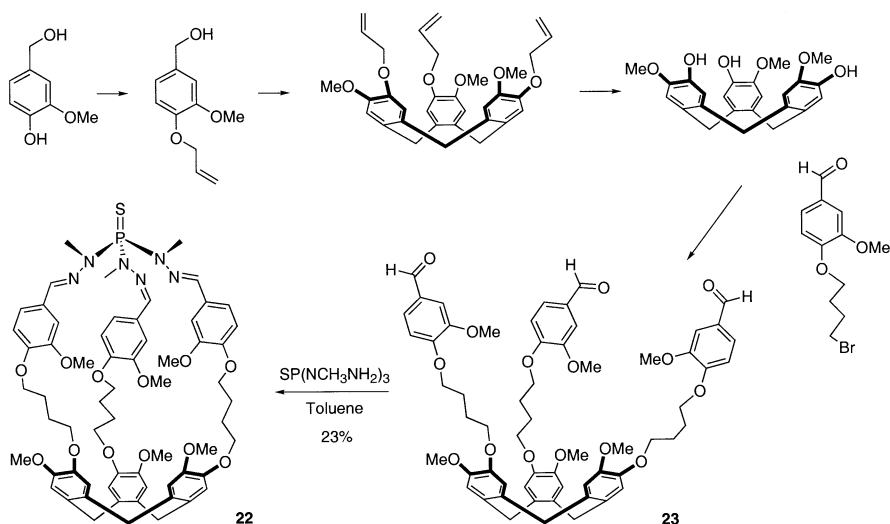
Scheme 23
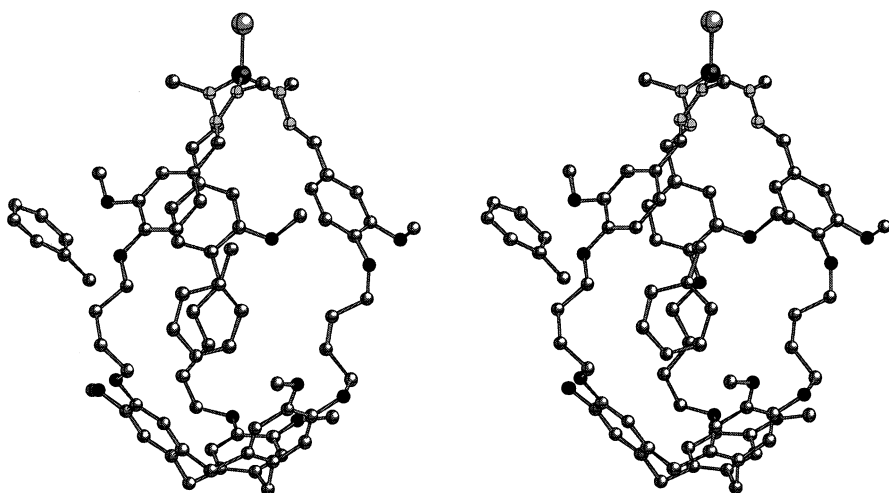
Fig. 14 Stereoview of the molecular structure of the hemicryptophane complex **22**·toluene (hydrogen atoms have been omitted for clarity)

Two isomers were expected according to the outside or inside orientation of the thiophosphoryl group. Only one isomer was characterized showing the P=S bond directed outside. The new hemicryptophane **22** presents a molecular cavity large enough to complex a toluene molecule as shown in the solid state structure depicted in Fig. 14. The toluene complex is stabilized through Van der Waals and specific π-interactions.
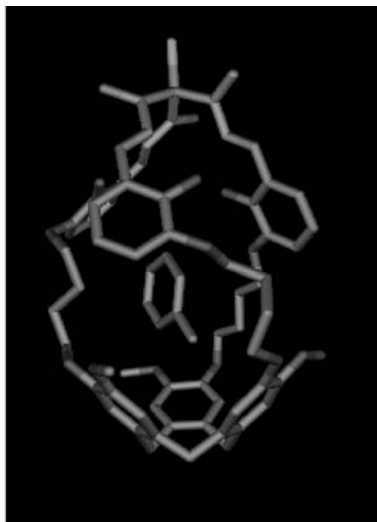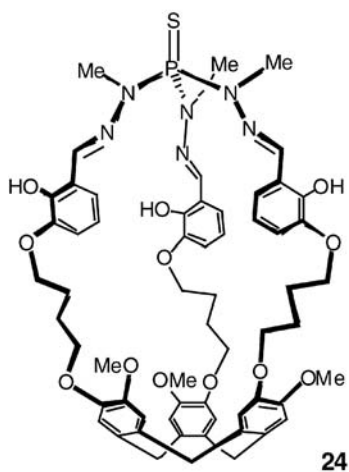
Fig. 15 Molecular structure of the hemicryptophane complex **24**·toluene (hydrogen atoms have been omitted for clarity)

Ditopic supramolecular receptor with catalytic properties should be able first to encapsulate a substrate and/or a reactant, and second, to allow chemical transformations in the specific environment of the molecular cavity. In such an approach, it is thus necessary to modify the structure of the hemicryptophane **22** by adding complexation sites such as phenol groups having affinity for metal cations. This was achieved by designing host **24**, the preparation of which followed a similar sequence to that used for the synthesis of **22** allowing the formation of **24** in 54% yield. Interestingly, the solid state structure of **24** showed the formation of the **24**·toluene complex (Fig. 15) [110]. The thiophosphoryl group in **24** is oriented outward and the hydrophobic pocket delineated by the cyclotriveratrylene and the three butoxy chains is occupied by a solvent guest leaving some room in the more polar part of the molecule defined by the phospho-trihydrazone moiety.

5.3
Metal Complexation and Stereochemistry

The gallium and iron complexes of **24** were obtained by reaction with Ga(acac)$_3$ or Fe(acac)$_3$. The diamagnetic Ga(III) and the paramagnetic Fe(III) complexes were obtained in good yields and their solid state structures show the metal ion bound to the hydrazone nitrogens and the phenolic oxygens in an octahedral environment (Fig. 16) (**24**·Fe and **24**·Ga structures are isomorphous) [110]. Interestingly the complexes possess two stereogenic centers due to the C_3 symmetry of the cyclotriveratrylene platform (M or P configuration), and the octahedral coordination site (Δ or Λ coordination). Thus, two diastereomeric racemates [MΔ/PΛ] and [MΛ/PΔ] are expected, but only
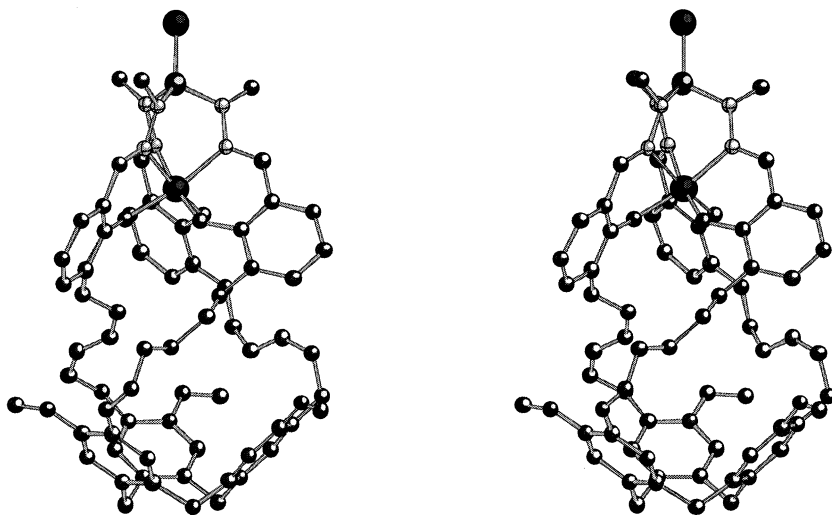
Fig. 16 Stereoview of the molecular structure of the metal hemicryptophane complex **24**·Ga(III) (hydrogen atoms have been omitted for clarity)

one was clearly identified [MΛ/PΔ], suggesting that the formation of the complex might be diastereoselective. This can be explained by non-favorable interactions between the linkers and the methoxy groups in the [MΔ/PΛ] racemate The synthesis of the optically pure ligand with M or P configuration would ascertain this selectivity. These complexes exhibit a lipophilic cavity in close proximity to the metal ion. Unfortunately, the helical structure of the three butoxy chains reduces the size of the cavity, which is essentially occupied by the CH_2 bridges. No solvent molecule was detected inside the host, but increasing the length of the linker chains should allow the encapsulation of neutral substrates.

6
Summary and Outlook

The high affinity of tetra-bridged phosphorylated cavitands for various guests was attributed to the cooperative effects between P=X donor groups (X=lone pair, O, S), H-bonding and π-interactions with the preorganized aromatic cavity of the host. It was thus demonstrated that the *iiii* isomer provided the best structure to take advantage of the properties of the phosphorylated cavitands. The new hemicryptophane structure is also promising and further work in this field will be carried out to synthesize water-soluble hosts, and ditopic receptors for possible applications in catalysis or for properties that are still to discover. It was the purpose of this chapter to illustrate the possibilities of the phosphorylated cage compounds to form new supramolecular associations. This review was essentially restricted to the new cavitand and hemicryptophane hosts, some of them forming strong multi-components associations that anticipate the formation of novel elaborated host-guest systems and new molecular devices for the recognition of neutral substrates or metal and organic cationic species. A new challenge will arise first from the diversity of the phosphorus groups and second from the structure of the molecule, some of them being chiral, precluding some interesting applications in terms of chiral recognition with potential applications in catalysis. The second point will be the preparation of new self-assembling systems based on the complexation or coordination properties of the new phosphorylated hosts that can be important for the development of self-organized molecular networks.

References

1. Cram DJ, Kaneda T, Helgeson RC, Brown SB, Knobler CB, Maverick E, Trueblood KN (1985) J Am Chem Soc 107:3645
2. Cram DJ (1986) Angew Chem Int Ed Engl 12:1039
3. Many reports on this topic have been published. In the area of cage compounds; see, e.g., Kunze C, Selent D, Neda I, Schmutzler R, Spannenberg A, Börner A (2001) Hetero-atom Chem 12:577 and references cited therein
4. Ezell JB, Gilkerson WR (1966) J Am Chem Soc 88:3486
5. Jackson MD, Gilkerson WR (1979) J Am Chem Soc 101:328
6. Sinyavskaya EI (1986) Sov J Coord Chem 12:663
7. Kabachnik MI, Polikarpov YM (1988) J Gen Chem USSR 58:1729
8. Delmau LH, Simon N, Schwing-Weill MJ, Arnaud-Neu F, Dozol JF, Eymard S, Tournois B, Böhmer V, Grüttner C, Musigmann C, Tunayar A (1998) Chem Commun 1627
9. Boerrigter H, Verboom W, Reinhoudt DN (1997) J Org Chem 62:7148
10. Boerrigter H, Verboom W, Reinhoudt DN (1997) Liebigs Ann/Recueil 2247
11. Talanova GG (2000) Ind Eng Chem Res 39:3550
12. Friedrichsen BP, Whitlock HW (1989) J Am Chem Soc 111:9132
13. Friedrichsen BP, Powell DR, Whitlock HW (1990) J Am Chem Soc 112:8931
14. Caminade AM, Majoral JP (1996) Synlett 1019
15. Caminade AM, Kraemer R, Majoral JP (1997) New J Chem 21:627
16. Bauer I, Rademacher O, Gruner M, Habicher WD (2000) Chem Eur J 6:3043
17. Declercq JP, Delangle P, Dutasta JP, Van Oostenryck L, Tinant B (1998) Acta Cryst C53:1484
18. Delangle P, Dutasta JP, Declercq JP, Tinant B (1998) Chem Eur J 4:100
19. Delangle P, Dutasta JP (1995) Tet Lett 36:9325
20. Tsvetkov EN, Bovin AN, Syundyukova VK (1988) Russ Chem Rev 57:776
21. Caminade AM, Majoral JP (1994) Chem Rev 94:1183
22. Declercq JP, Delangle P, Dutasta JP, Van Oostenryck L, Simon P, Tinant B (1996) J Chem Soc Perkin Trans II 2471
23. Mitjaville J, Caminade AM, Mathieu R, Majoral JP (1994) J Am Chem Soc 116:5007
24. Allan CB, Spreer LO (1994) J Org Chem 59:7695
25. Delangle P, Dutasta JP, Van Oostenryck L, Tinant B, Declercq JP (1996) J Org Chem 61:8904
26. Cram DJ, Cram JM (1994) In: Container molecules and their guests. Monographs in supramolecular chemistry, vol. 4. The Royal Society of Chemistry
27. Maverick E, Cram DJ (1996) In: Vögtle (ed) Comprehensive supramolecular chemistry, vol 2. Pergamon, p 367
28. Timmerman P, Verboom W, Reinhoudt DN (1996) Tetrahedron 52:2663
29. Rudkevich DM, Rebek J Jr (1999) Eur J Org Chem 1991
30. Jasat A, Sherman JC (1999) Chem Rev 99:931
31. Böhmer V (1995) Angew Chem Int Ed 34:713
32. Neda I, Kaukorat T, Schmutzler R (1998) Main Group Chem News 6:4
33. Gloede J (1997) Phosphorus Sulfur Silicon 127:97
34. Wieser C, Dieleman CB, Matt D (1997) Coordination Chem Rev 165:93
35. We will use the name resorc[4]arene to design the tetrameric product obtained from the condensation of resorcinol and aldehyde also named resorcinarene or resorcino-larene
36. Högberg AGS (1980) J Am Chem Soc 102:6046
37. Weinelt F, Schneider HJ (1991) J Org Chem 56:5527
38. Tunstad LM, Tucker JA, Dalcanale E, Weiser J, Bryant JA, Sherman JC, Helgeson RC, Knobler CB, Cram DJ (1989) J Org Chem 54:1305
39. The name cavitand refers to the rigidified bridged resorc[4]arene. IUPAC name for the tetra-briged phosphorus cavitand: 5,9,13,17-tetra-R-1,21,23,25-tetrakis-R'-2,20:3,19-

dimetheno-1H,21H,23H,25H-bis[1,3,2]dioxaphosphocino[5,4-i:5′,4′-i′]benzo[1,2-d:5,4-d′]bis[1,3,2]benzodioxaphosphocine (R and R′ are the substituents on the phosphorus atoms and at the lower rim of the resor[4]arene framework, respectively)

40. Abis L, Dalcanale E, Du Vosel A, Spera S (1990) J Chem Soc Perkin Trans II 2075
41. Abis L, Dalcanale E, Du Vosel A, Spera S (1988) J Org Chem 53:5475
42. Stewart KD (1984) PhD thesis. University of California Los Angeles
43. Markovsky LN, Kalchenko VI, Rudkevich DM, Shivanyuk AN (1992) Mendeleev Commun 106
44. Kalchenko VI, Rudkevich DM, Shivanyuk AN, Markovsky LN (1994) Russ J Gen Chem 64:663
45. Xu W, Rourke JP, Vittal JJ. Puddephatt RJ (1993) J Chem Soc Chem Comm 145
46. Xu W, Vittal JJ, Puddephatt RJ (1993) J Am Chem Soc 115:6456
47. Xu W, Vittal JJ, Puddephatt RJ (1995) J Am Chem Soc 117:8362
48. Xu W, Rourke JP, Vittal JJ, Puddephatt RJ (1995) Inorg Chem 34:323
49. Xu W, Vittal JJ, Puddephatt RJ (1997) Inorg Chem 36:86
50. Burilov AR, Nikolaeva IL, Galimov RD, Pudovik MA, Reznik VS (1995) Russ J Gen Chem 65:1602
51. Nifant'ev EE, Maslennikova VI, Panina EV, Bekker AR, Vasyanina LK, Lysenko KA, Antipin MY, Stuchkov YT (1995) Mendeleev Commun 131
52. Maslennikova VI, Panina EV, Bekker AR, Vasyanina LK, Nifanteev EE (1996) Phosphorus Sulfur Silicon 113:219
53. Vollbrecht A, Neda I, Thönnessen H, Jones PG, Harris RK, Crowe LA, Schmutzler R (1997) Chem Ber/Recueil 130:1715
54. Sakhaii P, Neda I, Freytag M, Thönnessen H, Jones PG, Schmutzler R (2000) Z Anorg Allg Chem 626:1246
55. Nikolaeva IL, Burilov AR, Kharitonov DI, Pudovik MA, Habicher WD, Konovalov AI (2001) Russ J Gen Chem 71:379
56. Nifanteev EE, Maslennikova VI, Vasyanina LK, Panina EV (1994) Russ J Gen Chem 64:142
57. Bibal B, Dubessy B, Dutasta JP (unpublished results)
58. Lipmann T, Dalcanale E, Mann G (1994) Tetrahedron Lett 35:1685
59. Lipmann T, Wilde H, Dalcanale E, Mavilla L, Mann G, Heyer U, Spera S (1995) J Org Chem 60:235
60. Dalcanale E, Jacopozzi P, Ugozzoli F, Mann G (1998) Supramol Chem 9:305
61. Jacopozzi P, Dalcanale E, Spera S, Chrisstoffels LAJ, Reinhoudt DN, Lippmann T, Mann G (1998) J Chem Soc Perkin Trans II 671
62. Nuutinen JMJ, Irico A, Vincenti M, Dalcanale E, Pakarinen JMH, Vainiotalo P (2000) J Am Chem Soc 122:10,090
63. Delangle P, Mulatier JC, Tinant B, Declercq JP, Dutasta JP (2001) Eur J Org Chem 3695
64. Ismail RM (1970) Z Anorg Allg Chem 370:252
65. Dubessy B, Dutasta JP (unpublished results)
66. Bibal B, Tinant B, Declercq JP, Dutasta JP (2003) Supramol Chem 15:25
67. Bibal B, Mulatier JC, Valade AG, Dutasta JP (unpublished results)
68. Basler B, Tinant B, Declercq JP, Dutasta JP (unpublished results)
69. Bibal B (2000) Doctorat Thesis. École Normale Supérieure de Lyon—Université de Lyon I
70. Bibal B, Tinant B, Declercq JP, Dutasta JP (2002) Chem Commun 432
71. Bibal B, Declercq JP, Dutasta JP, Tinant B, Valade AG (2003) Tetrahedron 59:5849
72. Nifanteev EE, Maslennikova VI, Goryukhina SE, Antipin MI, Lyssenko KA, Vasyanina LK, (2001) J Organometal Chem 631:1
73. Irico A, Vincenti M, Dalcanale E (2001) Chem Eur J 7:2034
74. Pinalli R, Nachtigall FF, Ugozzoli F, Dalcanale E (1999) Angew Chem Int Ed 38:2377
75. Burgess MA (1978) In: Metal ions in solution, Ellis Horwood, England
76. Dutasta JP, Bibal B, Delangle P, Gosse I, Mulatier JC (1999) Phosphorus Sulfur Silicon 144/146:337

77. Chapman RG, Sherman JC (1998) J Am Chem Soc 120:9818
78. Tucci FC, Renslo AR, Rudkevich DM, Rebek J Jr (2000) Angew Chem Int Ed 39:1076
79. Starnes SD, Rudkevich DM, Rebek JJr (2001) J Am Chem Soc 123:4659
80. Fochi F, Jacopozzi P, Wegelius E, Rissanen K, Cozzini P, Marastoni E, Fisicaro E, Manini P, Fokkens R, Dalcanale E (2001) J Am Chem Soc 123:7539
81. Fujita M, Umemoto K, Yoshizawa M, Fujita N, Kusukawa T, Biradha K (2001) Chem Commun 509
82. Cuminetti N, Ebbing MHK, Prados P, De Mandoza R, Dalcanale E (2001) Tetrahedron Lett 42:527
83. Shivanyuk A, Rebek J Jr (2001) Chem Commun 2374
84. Shivanyuk A, Rebek J Jr (2001) PNAS 98:7662
85. Ma S, Rudkevich DM, Rebek J Jr (1998) J Am Chem Soc 120:4977
86. Mansikkamäki H, Nissinen M, Schalley CA, Rissanen K (2003) New J Chem 27:88
87. Vysotsky MO, Thondorf I, Böhmer V (2001) Chem Comm 1890
88. Prins LJ, Reinhoudt DN, Timmerman P (2001) Angew Chem Int Ed 40:2382
89. Rincón AM, Prados P, De Mendoza R (2001) J Am Chem Soc 123:3493
90. Prins LJ, De Jong F, Timmerman P, Reinhoudt DN (2000) Nature 408:181
91. Kazakova EK, Makarova NA, Zotkina VV, Burilov AR, Pudovik MA, Konovalov AI (1996) Mendeleev Commun 157
92. Bibal B, Tinant B, Dubessy B, Declercq JP, Dutasta JP (unpublished work)
93. Mulatier JC, Dutasta JP (unpublished results)
94. Rebek J Jr (1999) Acc Chem Res 32:278
95. Jouaiti A, Hosseini MW, Kyritsakas N (2003) Eur J Inorg Chem 57 and references cited therein
96. Pirondini L, Bonifazi D, Menozzi E, Wegelius E, Rissanen K, Massera C, Dalcanale E (2001) Eur J Org Chem 2311
97. Kang J, Hilmersson G, Santamaria J, Rebek J (1998) J Am Chem Soc 120:3650
98. Sanders JKM (1998) Chem Eur J 8:1378
99. Blanchard S, Le Clainche L, Rager MN, Chansou B, Tuchague JP, Duprat AF, Le Mest Y, Reinaud O (1998) Angew Chem Int Ed Engl 37:2732
100. Collet A (1996) In: Vögtle F (ed) Comprehensive supramolecular chemistry, vol 2. Pergamon, New York, p 325
101. Collet A, Dutasta JP, Lozach B, Canceill J (1993) Top Curr Chem 165:103
102. Canceill J, Cesario M, Collet A, Guilhem J, Lacombe L, Lozach B, Pascard C (1989) Angew Chem Int Ed Engl 28:1246
103. Garel L, Dutasta JP, Collet A (1993) Angew Chem Int Ed 32:1169
104. Bartik K, Luhmer M, Dutasta JP, Collet A, Reisse J (1998) J Am Chem Soc 120:784
105. Brotin T, Dutasta JP (2003) Eur J Org Chem 973
106. Garel L, Lozach B, Dutasta JP, Collet A (1993) J Am Chem Soc 115:11,652
107. Matouzenko G, Vériot G, Dutasta JP, Collet A, Jordanov J, Varret F, Perrin M, Lecocq S (1995) New J Chem 19:881
108. Vériot G, Dutasta JP, Matouzenko G, Collet A (1995) Tetrahedron 51:389
109. Gosse I, Dutasta JP, Perrin M, Thozet A (1999) New J Chem 23:545
110. Gosse I, Bougault C, Tinant B, Declercq JP, Dutasta JP (unpublished results)

State of the Art. Chemical Synthesis of Biophosphates and their Analogues via P[III] Derivatives

Jan Michalski · Wojciech Dabkowski

Centre of Molecular and Macromolecular Studies, Polish Academy of Sciences,
Sienkiewicza 112, 90-363 Lodz, Poland
E-mail: jmich@bilbo.cbmm.lodz.pl

Abstract This chapter is concerned with preparation and applications of tricoordinate phosphorus compounds in synthesis of biophosphates and their structural analogues and illustrates the recent trends with a series of selected examples.

Keywords Phosphitylating reagents · Phosphites · Bioconjugates · Phosphoroamidites · P-chiralbiophosphates analogues · Phosphorofluoridites

List of Abbreviations

All	Allyl
Ar	Aryl
B	Base nucleoside(protected)
Bn	Benzyl
Beaucage reagent	3*H*-1,2-Benzodithiol-3-one 1,1-dioxide
t-Bu	*tert*-Butyl
i-Pr	Isopropyl
BSA	Bis(trimethylsilyl)acetamide
Bz	Benzoyl
CPBA	*m*-Chloroperoxybenzoic acid
DBU	1,8-Diazabicyclo[5.4.0]undec-7-ene
DCC	*N,N*-Dicyclohexylcarbodiimide
DNP	2,4-Dinitrophenyl
DMTr	4,4′-Dimethoxytrityl
Fm	Fluorenylmethyl
Fmoc	9-Fluorenylmethoxycarbonyl
T	Thymine
TBAF	Tetrabutylammonium fluoride
TBDMS	*tert*-Butyldimethylsilyl
TBDPS	*tert*-Butyldiphenylsilyl
TBHP	*tert*-Butyl hydroperoxide
Tetrazole	1-*H*-Tetrazole
TMCS	Trimethylchlorosilane

1
Introduction

In contrast to tetracoordinate phosphorus compounds P^{IV}, which are involved in the mechanism of life or are related to biophosphates, tricoordinate phosphorus compounds P^{III} have not been found in nature. However, their importance in the synthesis of biophosphates is very great. The introduction of P^{III} compounds as phosphitylation reagents was a turning point in synthetic biophosphate chemistry.

Tricoordinate phosphorus >P-X compounds containing a suitable leaving group are indispensable in the synthesis of biophosphates and their structural analogues. In contrast to phosphoryl >P(O)-X and thiophosphoryl >P(S)-X, compounds they are spectacularly more reactive in nucleophilic displacements at the phosphorus centre. Westheimer has compared reactions of P^{III} compounds with nucleophiles to enzymatic reactions regarding their reactivity [1]. The essential feature of P^{III} compounds is their free electron pair with all the structural, stereochemical and mechanistic consequences that follow. P^{III} compounds have the structure of a trigonal pyra-

mid. The lone electron pair can be considered as an additional ligand forming a kind of tetrahedral structure. Therefore when three different ligands are attached to the P[III] phosphorus atom a chiral centre is formed. Chirality depends on the stability of the pyramidal structure, inversion requires over 30 kcal/mol of free energy of activation. Tricoordinate phosphorus compounds behave as electrophiles when a suitable leaving group L is attached to the phosphorus centre. Countless nucleophilic displacements can be performed on >P-L compounds and this is the most important route to other P[III] compounds. The most likely mechanism of this reaction is the formation of a trigonal bipyramidal transition state (TBP) or intermediate which occurs with inversion of configuration at the phosphorus atom. Due to the presence of a free electron pair, P[III] compounds behave as nucleophiles reacting with a wide range of electrophiles to give P[IV] compounds. This second advantageous property allows conversion of P[III] compounds into biophosphates and their important analogues such as phosphorothioates and phosphonates. This dualistic reactivity of P[III] compounds is governed by electronic stereochemical factors and provides a continuous playground in planning synthetic ventures and choosing suitable protecting groups. Information about both tricoordinate and tetracoordinate phosphorus compounds can be found in several books and monographs [2]. L. D. Quin's "Guide to Organophosphorus Chemistry" is a competent up-to-date introduction to tervalent phosphorus chemistry and organophosphorus chemistry in general [3]. O. Dahl's experiences in the area of "Tervalent Phosphorus Acids Derivatives" in "Specialist Periodical Reports: Organophosphorus Chemistry" are an excellent source of information [4]. Earlier comprehensive review of organic derivatives of phosphorus acid and thiophosphorus acid (up to 1970) are to be find in G. M. Kosolapoff and L. Maier "Organic Phosphorus Compounds" [5].

2
Phosphoroamidites

Phosphoroamidites are the phosphitylating reagents most often used in the synthesis of various biomolecules such as oligonucleotides, sugar phosphates, phosphoinositols and phospholipids [6]. The phosphoroamidite strategy is an ingenious extension of the Letsinger phosphite method [7]. It was originally invented by Caruthers and has since been applied by numerous research groups in the synthesis of nucleotides and other types of biophosphates [8]. Phosphoroamidites do not react readily with alcohols and some other H-nucleophiles unless activated. An indispensable part of the phosphoroamidite strategy is the employment of a proper activator and a suitable protecting group at the phosphorus centre. Efficiency of phosphoroamidite coupling with alcohols is controlled by the steric and electronic effect of both components. Bulky substituents in the amido group like diisopropyl groups can help control selective coupling preventing the formation of symmetrical structures -P(OR)$_2$. Reactivity of phosphoroamidites depends on several factors. For example N,N-dimethylphosphoroamidites

are more reactive than the most frequently used *N,N*-diisopropyl derivatives. The latter are preferred because of their stability. Lower reactivity caused by electronic and steric factors may be compensated by appropriate activation.

The phosphoroamidite approach is being ameliorated over time by optimal use of additional leaving groups, activators, protecting groups and oxidation procedures. This method of phosphorylation was originally devised for nucleotide chemistry and gradually became the most popular synthetic route for biophosphates derived from inositols, sugars, lipids and other important bioalcohols. Significant pieces of information about phosphoroamidite chemistry are included in several excellent reviews. Most of them deals with nucleotide chemistry: E. Uhlman and A. Peyman [6a], S.L. Beaucage and R.P. Iyer [6b,c,e] and Y. Hayakawa [6g]. Synthesis of biophosphates other than nucleotides have been reviewed by: S.L. Beaucage and R.P. Iyer [6d] and E.E. Nifantiev et al. [6f]. The number of papers dealing with phosphoroamidite methodology is enormous and new applications are frequent. For these reasons it is only possible in the scope of this review to illustrate some current trends in the area.

2.1
Activation of Phosphoroamidites and its Relation to the Stereoselective Coupling Procedure

2.1.1
Activation by Azolides, Mechanistic Aspects

Tetrazole is by far the most commonly used activator in coupling reactions of phosphoroamidite with alcohols and other nucleophiles [9]. This activator suffers from several disadvantages. Tetrazole is expensive, explosive, hygroscopic and sparingly soluble in acetonitrile, the solvent most frequently used in the coupling reaction. It may induce transesterification of trialkylphosphites [10]. Tetrazole is not effective [11a] or must be used in large excess [11b] when strongly electronegative ligands are attached to the P^{III} centre. These problems have become even more pronounced in the synthesis of oligonucleotide phosphorothioates on the scale needed for the production of the antisense drugs [11c]. To render the phosphoroamidite approach even more useful several other activators have been investigated [12]. They are substituted 1*H*-azoles and include 5-(4-nitrophenyl)-1*H*-tetrazole [12a,b,f], 5-ethylthio-1*H*-tetrazole [12c,d,g] and 4,5-dicyanoimidazole [12e].

The accepted mechanism for the activation by tetrazole and other *H*-azoles [13], supported by recent stereochemical results, is shown in Scheme 1.
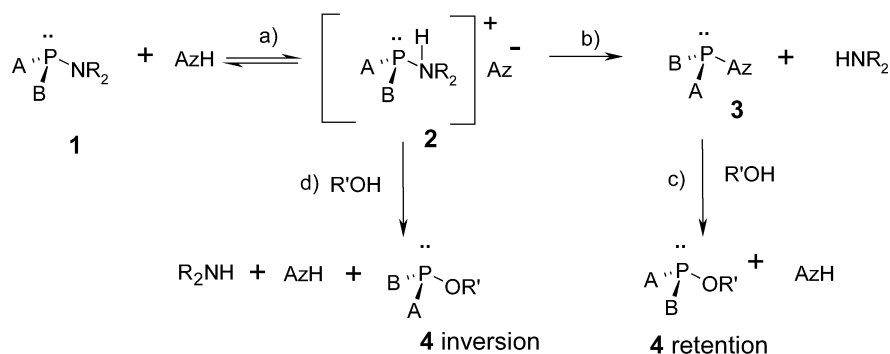
Scheme 1

1-*H*-azole (AzH) protonates phosphoroamidite **1** to produce the salt-like species **2** (step a). Cations of the type **2** were found in model studies to react with alcohols more reluctantly in the presence of strong acids than in weak acids. This observation shows that the fast acid-catalysed alcoholysis of phosphoroamidites must take place by N-protonation[13].

The salt **2** undergoes rearrangement into the highly reactive tetrazolide **3** (step b) by the nucleophilic displacement at the P^{III} centre by an azolide anion. In the case of a chiral phosphoroamidite **1** step b is most likely to proceed with inversion of configuration at the phosphorus centre. In the reaction of azolide **3** with an alcohol (step c) another inversion is to be expected. This should provide the phosphite **4** of the same configuration as the starting phosphoroamidite. Arguments have been advanced from kinetic and stereochemical studies [13, 19] that pathway d is also feasible. In this case the phosphite **4** should be formed by the inversion mechanism. The general picture presented in Scheme 1 is somewhat simplified and a better understanding of the role of the ion-pair **2** is desirable.

Hayakawa and Kataoka have found that 5-(4-nitrophenyl)-1*H*-tetrazole (NPT) can be used in catalytic amounts provided that the amine formed in the coupling reaction can be removed by a suitable scavenger [12b]. This was achieved using molecular sieves MS13X (pore size 10 Å; particle size ca. 2 μm) as amine scavenger. The amine formed is a stronger base than the activator, and so its interaction with the scavenger is stronger than with the phosphoroamidite. The catalytic cycle connected with this catalytic activation is shown (Scheme 2).

This procedure lowers the volume of acetonitrile necessary to dissolve poorly soluble NPT. The latter is expensive and can be explosive.

R= (*i*-Pr)   R'= 4 O$_2$N-Ar
R"= protected nucleoside
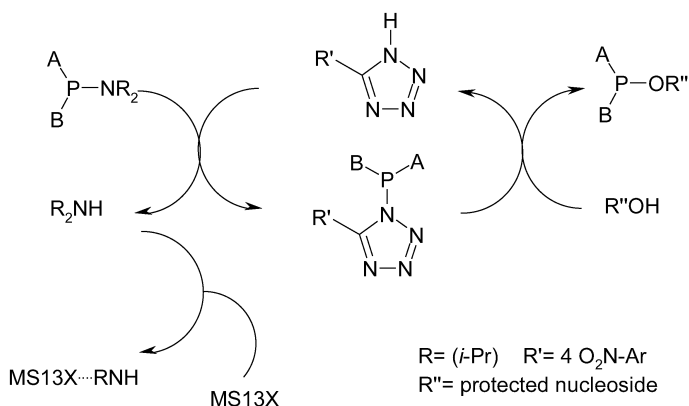
Scheme 2

Example 1: the phosphoroamidite coupling procedure leading to dinucleosides and employing a catalytic amount of 5-(*p*-nitrophenyl)-1*H*-tetrazole (NPT) is illustrated [12b]. Dinucleoside phosphates can be prepared by this procedure at a multigram scale in 92–98% yield. The catalyst NPT (5 mol%) is used in the presence of molecular sieves 13X in acetonitrile at 40 °C (step a).
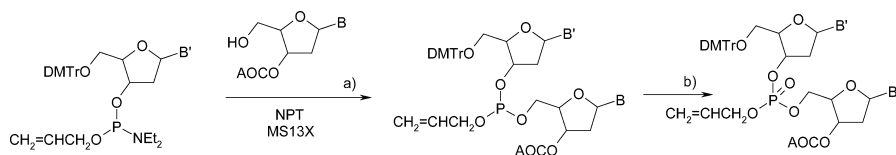
The phosphite obtained was oxidized by bis(trimethylsilyl) peroxide with trimethylsilyl triflate as catalyst to give the corresponding phosphate (step b). In coupling and oxidation procedures (allyloxy)carbonyl (AOC) and allyl protecting groups were left intact. The intermediate phosphate was converted in over 95% yield into the unprotected derivatives. This was accomplished by the usual detritylation with dichloroacetic acid and removal of allyl and AOC protecting groups by Pd[PPh$_3$]$_4$/PPh$_3$ catalyst [14].

2.1.1.1
Activation by Azolides, Stereochemical Aspects

Stereochemical studies on the formation of chiral internucleotide linkages using the phosphoroamidite approach which are relevant to the mechanism of the activation process have been initiated by Stec and Zon [15]. When tetrazole was used as the activator, however, complete epimerization at the phosphorus centre was observed and this was explained by the rapid and multiple ligand exchange at the intermediate tetrazolide. In spite of these early discouraging observations highly promising results have been recently disclosed.

Example 2: it has been assumed that selectivity should be observed when one of diastereomeric products from the azolide intermediate 3 (Scheme 1) is preferentially formed [16]. Engels and Shell demonstrated that in the case of methylphosphonates this goal can be achieved by the use of a specially synthesized activator 4,5-dicyanoimidazole [17]. Due to the fast epimerization, the starting phosphonoamidite can be used without separation into the individual diastereomers.
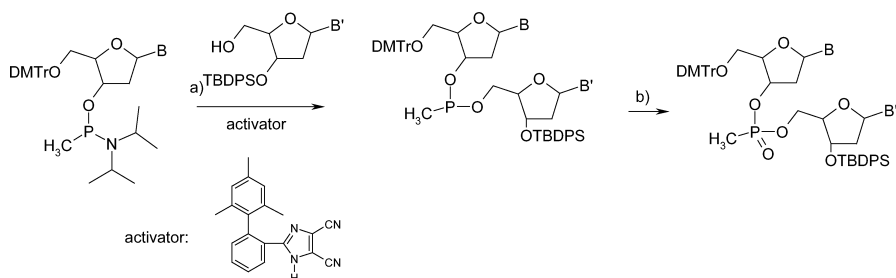
The intermediate phosphonite (step a) was oxidized by TBHP to give the dinucleoside methylphosphonate (step b). Selectivities of this procedure were up to 84/16 (R_P/S_P). According to previous studies by Engels and coworkers a tetrazole containing a chiral activator has little influence on the selectivity of phosphonoamidite coupling [18].

Example 3: different activators derived from 4,5-dicyanoimidazole were prepared and used by Just and Lu in the stereoselective coupling reactions of phosphoroamidites with nucleosides [19]. An easily removable chiral auxiliary derived from D-xylose was synthesized and used for stereoselective construction of dithymidine phosphorothioate. The part of this study is illustrated below.
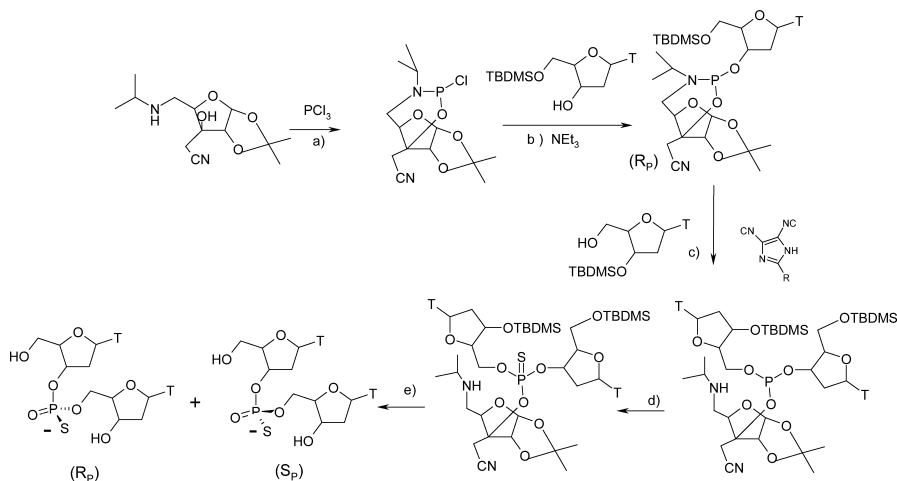
The aminosugar was allowed to react with phosphorus trichloride to give the intermediate cyclic phosphorochloridite (step a). The latter was trans-

formed in situ into the phosphoroamidite by condensation with 5′-O-TB-DMS-thymidine in the presence of triethylamine (step b). The phosphoroamidite that was obtained after chromatographic purification as a single diastereomer was coupled with

3′-O-TBDMS-thymidine in the presence of 2-bromo-4,5-dicyanoimidazole as activator to give two isomeric phosphites in a ratio of 1:6 (step c). Subsequent sulfurization by 3H-1,2-benzodithiol-3-one 1,1-dioxide (Beaucage reagent) gave the phosphorothioates in the same ratio. The chiral auxiliary was removed by the treatment with concentrated ammonia and silyl protecting groups by TBAF to give dithymidine phosphorothioates in the same ratio 1:6 (step d). The minor and major isomers of the phosphorothioates formed were assigned with R_P and S_P configuration respectively. Analysis of the stereochemistry of the intermediate phosphoroamidite (R_P) and the structural determination of the major isomer of dithymidine thiophosphate (S_P) allow to suggest that coupling involves double inversion corresponding to steps b and c in Scheme 1. The cyclic phosphoroamidite (S_P) analogous to the one already described in a similar sequence of reactions gave rise to formation of the phosphite (R_P) and the phosphorothioate (S_P) as major products.
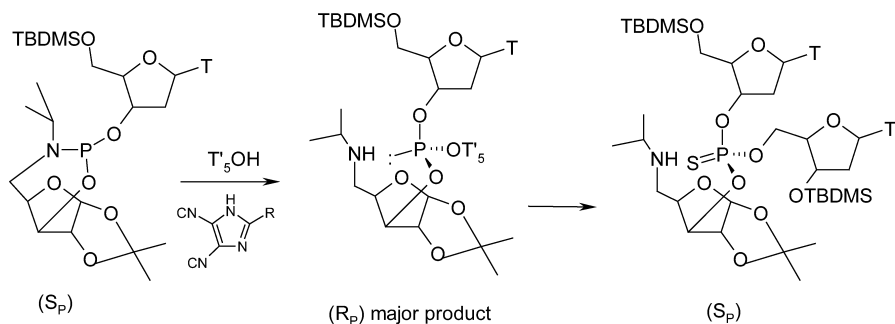
Therefore a mechanistic scheme is proposed which involves the protonated intermediate of the type **2** (Scheme 1), reacting with the alcohol with inversion of configuration at the P^{III} centre (Scheme 1, path d). Factors controlling the change of mechanism are not clear.

2.1.2
Activation by Acids Salts

Several acids salts have been proposed to replace tetrazole as the activator of phosphoroamidite coupling with alcohols. The most popular are benzimidazolium [20a], imidazolium [20b], *N*-methylimidazolium [20c], *N*-methylaniline [20h] triflates, pyridinium hydrochloride [20d,e], hydrobromide [20e], tetrafluorborate [20f], trifluoroacetate [20g] and 2,4,6-collidine trifluoroacetate [20i].

Recently Hayakawa and his colleagues, in their efforts to improve synthesis of oligonucleotides, have introduced several novel acid/azole complexes [20j]. They were selected because they are nonhygroscopic, crystalline compounds with high solubility in acetonitrile and exhibiting very high activity in the liquid phase. The azolium salt allows smooth and high-yield condensation of the nucleoside phosphoroamidite and a 5′-O-free nucleoside, in which equimolar amounts of reactants and promoter are employed in the presence of powdery molecular sieves 3 Å in acetonitrile. The utility of the azolium promoter has also been demonstrated in liquid-phase synthesis of several biologically important biophosphates.

The following mechanism for condensation of a nucleoside phosphoroamidite and a nucleoside activated by an azolium salt AzH$^+$X$^-$ has been proposed [13, 20j]. This Scheme 3 includes the additional pathway d related to recent stereochemical studies.
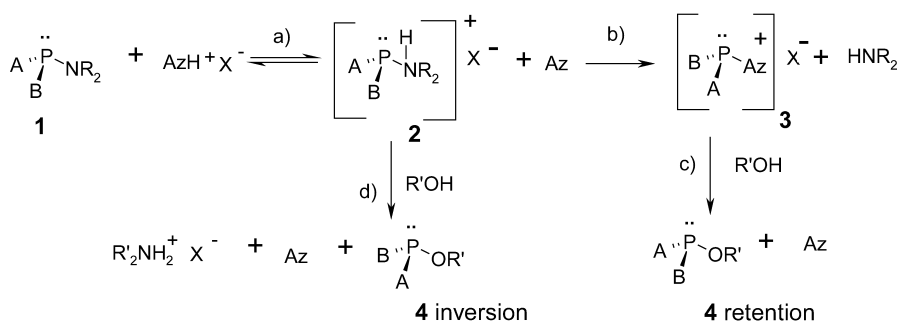
Scheme 3

As in the case of tetrazole the promoter first acts as an acid, activating the phosphoroamidite **1** by protonation and forming the activated species **2** (step a). This activation cogenerates a free azole. Subsequently the resulting azole, but not the less reactive conjugate base X$^-$ of the acid, reacts with **2** to form the phosphorazolidite **3** (step b) which subsequently condenses with a nucleoside R′OH (step c) to provide the dinucleoside phosphite **4** and regenerate the free azole. In this scheme, the second step b is the slowest. From a stereochemical point of view both steps b and c in Scheme 3 should proceed with the inversion of configuration at the chiral phosphorus yielding the phosphite **4** of the same configuration as the starting phosphoroamidite **1**. The direct attack of the alcohol on **2** without passing through **3** should proceed with the inversion of configuration at P^{III}. Mechanistic model studies on this matter have been recently published [13a–d].

Example 4: Wada et al. have been successful in developing a new class of activators dialkyl (cyanomethyl) ammonium tetrafluoroborates [21]. These activators have high proton-donating ability and a counteranion of low nucleophilicity. With this class of salts a remarkably efficient diastereocontrolled synthesis of dinucleoside phosphorothioates has been devised. The power of this method lies in the fact that stereopure monomers can be ob-

tained diastereoselectively from the appropriate amino alcohols. In this respect the method seems be more advantageous than procedures applied by others. Even in the most advanced work of Stec et al. [22] and Beaucage et al. [23] on fully P-stereocontrolled synthesis of oligonucleotides phosphorothioates the diastereopure monomers had to be isolated from the mixture of diastereomers by a troublesome chromatographic separation. The diastereo pure nucleoside 3′-phosphoroamidates were synthesized from enantiopure amino alcohols (*S*)- and (*R*)-2-methylamino-1-phenylethanol to create an oxazaphospholidine ring.

TBDPS= *tert*-butyldiphenylsilyl
TBDMS= *tert*-butyldimethylsillyl
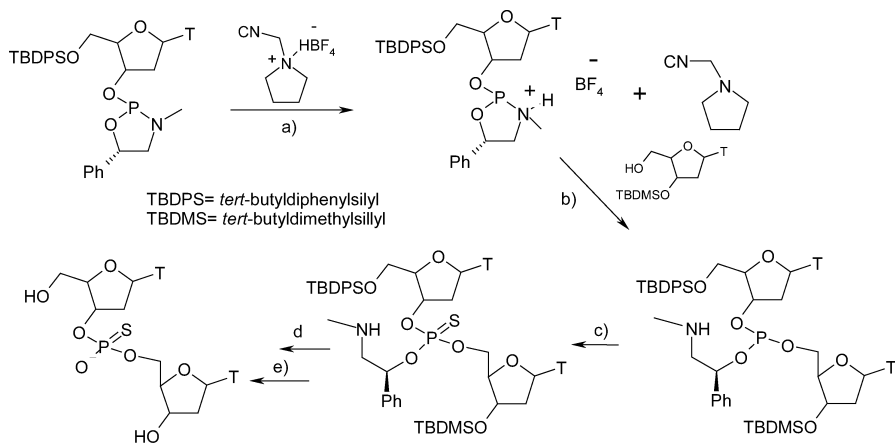
Diastereo pure 3′-phosphoroamidite activated in this novel way forms the intermediate salt (step a) which reacts with 3′-*O*-(*tert*-butyldimethylsilyl)thymidine in acetonitrile at room temperature to give the dinucleoside phosphite (step b). The latter underwent sulfurization by the Beaucage reagent (step c). The phosphorothioate formed in reaction (c) was treated with DBU to remove the chiral auxiliary and then finally by Et$_3$N·HF to remove silyl groups to give the 3′,5′-dithymidine phosphorothioate (steps d and e). The crucial reaction (b) proceeds with the inversion of configuration at the P^{III} chiral center and very high stereoselectivity. In reactions (a), (c) and (d) configuration at the phosphorus centre is unchanged. Other interesting attempts to achieve stereoselection in the synthesis of dinucleoside phosphorothioates have been recently described [24].

Example 5: Hayakawa and Noyori group in their studies on new activators for phosphoroamidite coupling reactions have applied the most effective member of the group of acid/azole complexes *N*-(phenyl)imidazolium triflate (N-PhIMT) in the efficient synthesis of biologically important compounds [20j]. A noteworthy example is synthesis of cytidine-5′-monophospho-*N*-acetylneuraminic acid. This compound is a source of sialic acid in the sialyltransferase-catalysed biosynthesis of sialyl oligosaccharides [25].

OAc

AcO

AcNH

AcO   OAc   COOCH₃

OH

N
/   \
(i-Pr)   (i-Pr)
P—OCH₂CH₂CN
O
O—CH₂
O
Cyt(Ac)
AcO   OAc

N-PhIMT

OAc

AcO
AcNH
AcO   OAc
COOCH₃
O
P—OCH₂CH₂CN
O
O
Cyt(Ac)
AcO   OAc
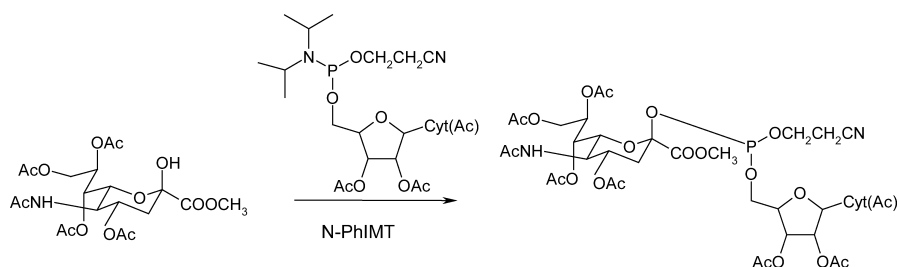
The intermediate phosphite employed in this synthesis was prepared by condensation of duly protected sialic acid with the nucleosidyl phosphoroamidite in the presence of N-PhIMT. Oxidation by TBHP and deprotection according to standard procedures gave the cytidine-5′-monophospho-*N*-acetylneuraminic acid. This synthetic route is claimed to have advantages over procedures published earlier [26]. The same group demonstrated the importance of 3 Å and 4 Å molecular sieves as moisture scavengers in the reaction of nucleoside phosphoroamidite with a nucleotide. This approach should be likely to find application in the synthesis of biophosphates outside nucleotide chemistry.

Example 6: efficient synthesis of deoxyribonucleoside phosphoroamidite eliminating the use of additional activator has been described by Ravikumar and his associates [27].

DMTrO
O
B
HO
+
(i-Pr)₂N
P—Cl
(i-Pr)₂N
a) Et₃N
→
DMTrO
O
B
O—P—N(i-Pr)₂
N(i-Pr)₂
b) ROH/Et₃N
Et₃N·HCl
→
DMTrO
O
B
O—P—N(i-Pr)₂
OR

ROH = p-NCCH₂C₆H₄CH₂OH,   HOCH₂CH₂CN
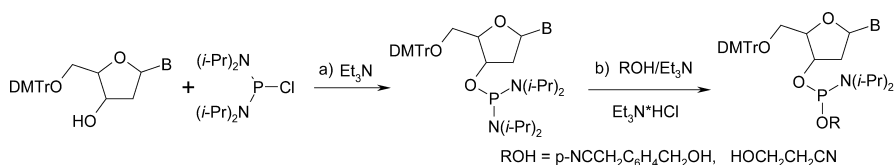
The triethylamine hydrochloride formed in step (a) serves as an activator in step (b) for the reaction with an alcohol (ROH) providing the phosphite containing the desired protecting group. Acetonitrile proved to be a better solvent for this reaction than dichloromethane. It was found that activation by pyridinium hydrochloride was faster but led to formation of dinucleoside phosphite.

2.1.3
Activation by 2,4-Dinitrophenol

Dabkowski et al [28] have found that 2,4-dinitrophenol (DNP), whose pKa=4.1 is close to that of tetrazole pKa 4.9, acts as an efficient activator of phosphate synthesis via the phosphoroamidite procedure. The reaction of P^III amidites with an equivalent amount of nucleoside in the presence of 2,4-dinitrophenol proceeds in very high yield and at rates comparable or higher than those when tetrazole is used. Phosphitylations activated by 2,4-dinitrophenol (DNP) take place at room temperature in aprotic solvents like THF,

CH$_2$Cl$_2$ or MeCN. On average the optimal amount of activator required for efficient coupling is ca. 1.5 equivalent of the stoichiometrical ratio. Numerous examples illustrating this methodology show that DNP is superior to tetrazole when P^{III} amides bear a strongly electron attracting group at the phosphorus centre. Mechanistic features of the DNP activation are shown in Scheme 4.

ArOH: 2,4-dinitrophenol
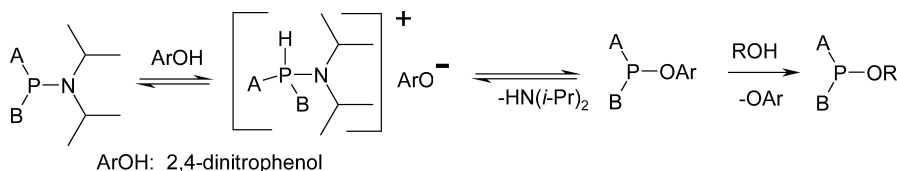
Scheme 4

The mechanistic picture presented here is analogous to that postulated in the activation by 1H-azolides (Scheme 1). Spontaneous reaction of the arylphosphite with alcohols has its analogy with the phosphitylating properties of some phosphorazolides [29]. Additional evidence for the mechanism described in Scheme 4 is that addition of triethylamine dramatically reduces the rate of formation of the phosphite. This inhibition provides evidence for the reversible acid catalysis. The nucleophilic catalysis step is slow and cannot explain the observed inhibition. Two important factors are involved in catalytic properties of DNP: acidity and the ability to form reactive intermediates. The coupling process described in Scheme 4 is not stereoselective for similar reasons which have been discussed in the case of tetrazole activations. Some structural changes in the DNP activator such as introduction of bulky group in the ortho position may inhibit fast ligand exchange in the first step of activation and give rise to a stereoselective coupling [30]. Studies on the activation of phosphoroamidite by DNP have paved the way to a novel type of phosphitylating reagent.

Example 7: the bis(2,4-dinitrophenyl)phosphoroamidite which can be prepared by a standard procedure reacts with alcohols in a non-selective way which leads to a mixture of products [28]. From a mechanistic point of view this result is consistent with spontaneous displacement of a 2,4-dinitrophenoxy group in the reaction with alcohol which liberates free DNP. The latter activates the amino group allowing further ligand exchange. However if phosphitylation by the bis(2,4-dinitrophenyl)phosphoroamidite is performed in the presence of one equivalent of triethylamine, high chemoselectivity is observed, and the nucleoside (2,4-dinitrophenyl)phosphoramidite is formed in over 92% yield.
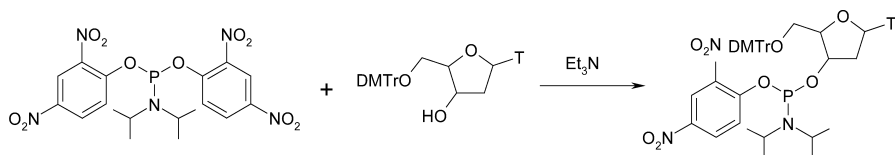
Example 8: when P^{III} amidites bear a strongly electron-attracting group at the phosphorus centre 2,4-dinitrophenol (DNP) is distinctly superior activator to tetrazole [28].
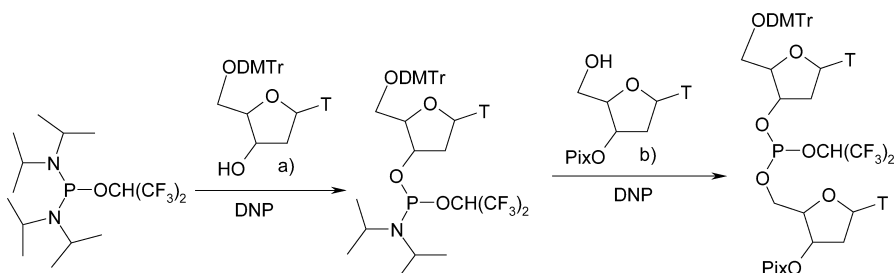
The phosphordiamidite used in this transformation was introduced by Tataku et al. [32]. Both steps a and b are highly selective and the dinucleotide is formed in excellent yield in THF at 20 °C.

2.1.4
Activation by Trimethylchlorosilane

Earlier studies from Michalski et al. [33] on interaction of P^{III}-amides with trialkylhalogenosilanes R$_3$SiX suggested that this type of silane could act as activator in the coupling reaction of phosphoroamidites with alcohols. Indeed it was found by Dabkowski et al. that trimethylchlorosilane (TMCS) is an excellent activator in the synthesis of biophosphates by phosphoroamidite route [34]. The mechanism of activation by TMCS is presumed to involve its reaction with the P^{III} amide. This type of interaction has been discussed in Michalski's paper and more recently by Nifantiev [35]. The first step produces salt-like species R$_2$P$^+$(SiMe$_3$)NR''$_2$Cl$^-$ and R$_2$PN$^+$R''$_2$(SiMe$_3$)Cl$^-$ which react either directly with alcohol to give ester R$_2$POR' or via intermediate formation of R$_2$PCl. In both cases TMSCl is regenerated. The exact nature of this complex deserves further study. A catalytic cycle is proposed in Scheme 5.
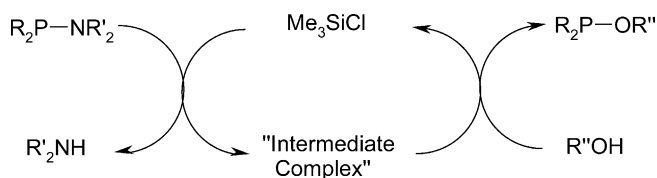
Scheme 5

An alternative mechanistic scheme in which TMCS first reacts with alcohols to form hydrogen chloride which then activates the phosphoroamidite in situ seems to be unlikely. It is known that TMCS reacts very slowly with alcohols unless a catalyst is present [36]. Formation of HCl would effect the removal of an acid labile group like DMTr attached to a base or *tert*-butyl

attached to a phosphorus centre. This is actually observed when commercial TMCS contaminated with HCl is used. This activation works well with sterically hindered alcohols. Superiority of TMCS over tetrazole was clearly visible in case of phosphoroamidites holding strongly electronegative groups at the P^{III} centre. Examples illustrating applications of this unconventional catalytic activator are given at another place.

Example 9: a noteworthy example is the activation of bis(4-nitrophenyl)-*N,N*-diisopropylphosphoroamidite [31] in coupling with alcohols activated by TMCS. This difunctional phosphitylating reagent does not react with alcohols in the presence of tetrazole, but in the presence of TMCS such a coupling becomes possible [37a,b].
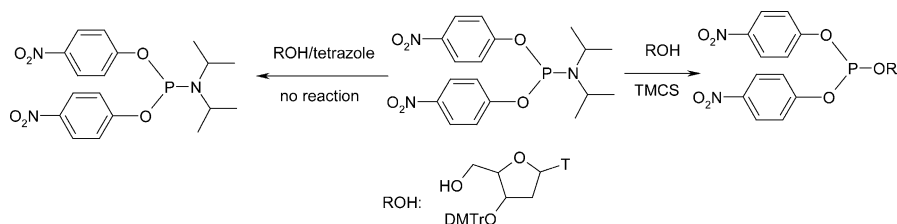
Example 10: trimethylchlorosilane TMCS has been found an effective activator in the typical synthesis of dinucleotides in solution and its utility is comparable with that of tetrazole [34]. An example of this activation is the reaction of thymidine with tris(dimethylamino)phosphine.
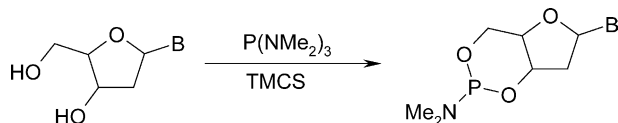
This reaction proceeds in poor yield without an activator [38]. In the presence of TMCS (60 mol%) cyclic thymidine 3′,5′-cyclic dimethylphosphoroamidite is formed in 95% yield.

Example 11: TMCS is also a highly effective activator in typical couplings leading to dinucleotides and similar biophosphates, and is comparable with tetrazole and imidazolium salts [34]. The optimal amount of this activator is below the stoichiometric ratio.
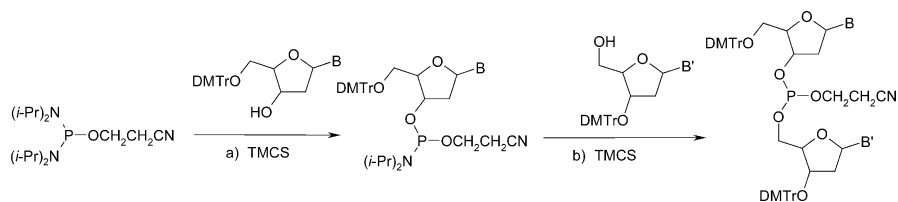
The first coupling (step a) proceeds selectively yielding the nucleoside phosphoroamidite which undergoes a second coupling to give the desired dinucleoside phosphite in very high yield (step b). Both couplings take place in solvents such as THF or acetonitrile at 20 °C.

3
Monofunctional Phosphoroamidites

Monofunctional phosphoroamidites contain the amino function as the sole leaving group. The role of the amino function has already been discussed in the connection with activation in coupling procedures with bioalcohols. The art of phosphorylation via phosphoroamidite comprises the following four elements: choice of a suitable phosphoroamidite, its activation for coupling with bio- or bio-related alcohols, oxidation (sulfurization) to phosphate or phosphate like P^{IV} structures and finally removal of protecting groups. A desirable situation is when protecting group at the phosphorus centre can be removed parallel with other protecting groups. The most frequently used procedures are based on the experience collected from synthetic nucleotide chemistry and its impressive development since 1976. Here are selected examples of the phosphitylation practice which illustrates this area and pay special attention to procedures outside classic nucleotide chemistry.

Example 12: dibenzyl-*N,N*-diisopropylphosphoroamidite has been applied by Lindberg et al. in the efficient synthesis of phospholipids from glycidol phosphates [39].
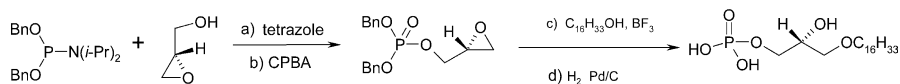
Using this phosphoroamidite, (*S*)-glycidol was phosphorylated to give (*R*)-1-*O*-glycidyl dibenzylphosphates (step a, b). Regiospecific epoxide opening using hexadecanol or a cesium palmitate prior to phosphate deprotection provided the derived phospholipids (step c). The benzyl protecting group was removed in a standard way, by catalytic hydrogenolysis (step d). A similar sequence of reactions was carried out using di(*tert*-butyl)-*N,N*-diisopropylphosphoroamidite.

Example 13: D- and L-myo-inositol 2,4,5-triphosphates and their phosphorothioate analogues have been recently prepared by Potter and his associates [40]. Tribenzyl-myo-inositol was phosphitylated with di(benzyl)-*N,N*-diisopropylphosphoroamidite in the presence of tetrazole (step a) followed by oxidation with *m*-chloroperbenzoic acid (CPBA) to give fully protected phosphate triesters (step b). Removal of the benzyl protecting group was performed by hydrogenolysis catalysed by palladium Pd/C (step c). The phosphorothioate analogues were synthesized in similar way. Intermediate triphosphites were oxidized using elemental sulfur in a mixed solvent of pyridine and DMF (step d). Treatment of fully protected phosphorothioates with sodium in liquid ammonia gave the desired thiophosphates (step e).
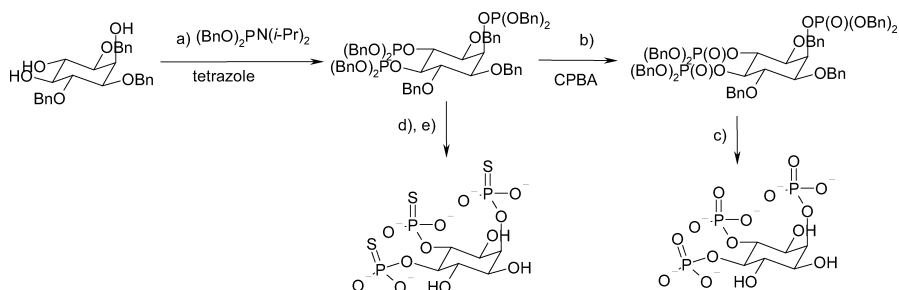
Information concerning inositol phosphates and thiophosphates is included in the review by Potter[41].

Example 14: an efficient strategy has been described by Koganty and his associates for the synthesis of compound which is a novel lipid A mimetic [42] The multi-step synthesis is exemplified from the introduction of the phosphate moiety onwards.
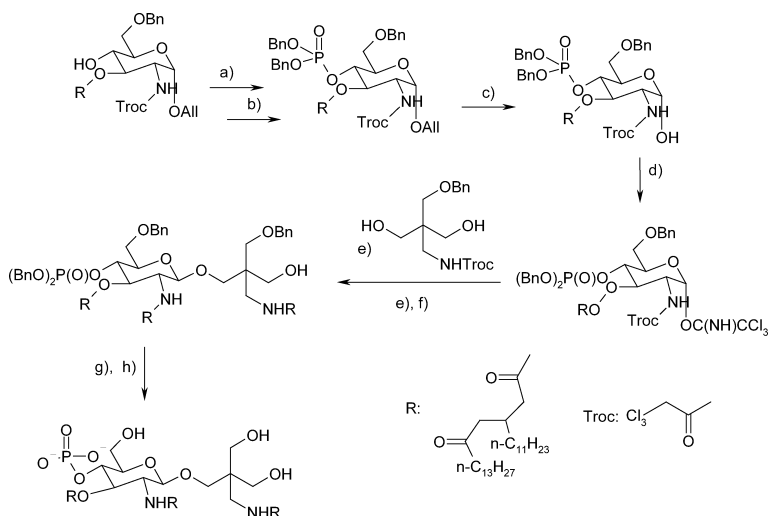
The phosphite group was introduced by a tetrazole activated dibenzyl-N,N-diisopropylphosphoroamidite coupling (step a) followed by oxidation of the corresponding phosphate with CPBA (step b). Removal of the allyl group at an anomeric position without affecting the benzyl protecting group took place by the isomerization of the allyl double bond using an iridium complex followed by hydrolysis of the isomerised aglicone (step c). Conversion of the deprotected sugar into the glycosylating reagent was achieved by treatment with trichloroacetonitrile and cesium carbonate (step d). Glycosylation by the α-isomer-donor of the diol in the presence of TMSOTf provided the corresponding glycoside (step e). Due to steric crowding no diglycosilation product was formed. Reductive cleavage of the Troc- group with Zn/

AcOH (step f) and N-acylation with a suitable fatty acid in the presence of 1,3-dicyclohexylcarbodiimide (DCC) (step g) provided the intermediate which after global debenzylation by hydrogenolysis in the presence of palladium on charcoal provided the desired lipid A mimetic (step h).

Example 15: in connection with studies on thermal stability of proteins and nucleic acids of the methanogen species the cyclodiphospho-D-glycerate (CDPG) has been synthesized by Priestley from n-butyl-D-glycerate employing dibenzyl diisopropylphosphoroamidite (BnO)$_2$PNiPr$_2$ reagent [43].
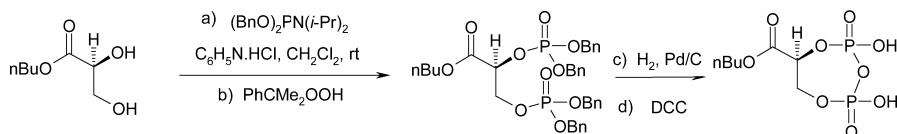
The main goal was to produce CDPG on a large scale. Tetrazole activation was not investigated because acceptable yields were observed when pyridium hydrochloride was employed (step a). Cumene hydroperoxide was used as a useful oxidant (step b). To be successful, deprotection by catalytic hydrogenolysis (step c) must proceed in the absence of P^{III} species. Otherwise the efficiency of catalytic hydrogenolysis is severely diminished.

Example 16: the synthesis of (−)-shikimate-3-phosphate by Shin and Wu [44] using dibenzyl-N,N-diisopropylphosphoroamidite and subsequent oxidation by CPBA (steps a and b) involves the deprotection of the final triester phosphate by trimethylbromosilane (TMBS) which allows simultaneous removal of benzyl 2,2,3,3-tetramethoxybutane and methyl groups (steps c and d).
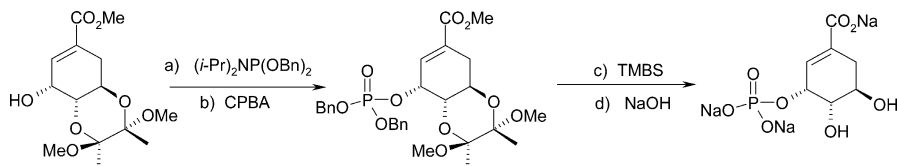
The deprotection procedure is based on transesterification of benzyl phosphate into the corresponding silyl ester followed by hydrolysis or alcoholysis.

Example 17: Bertozzi and associates in their studies on sulfotransferases have performed synthesis of a bisubstrate analogue designed to inhibit estrogen sulfotransferase [45]. Synthesis of this diphosphate depends on the coupling of two phosphates prepared by phosphoroamidite methodology. The synthesis utilizes differently protected 3′-phosphoadenosine-5′-phosphate allowing selective functionalization of the 5′-phosphate with the sulfate acceptor mimic.
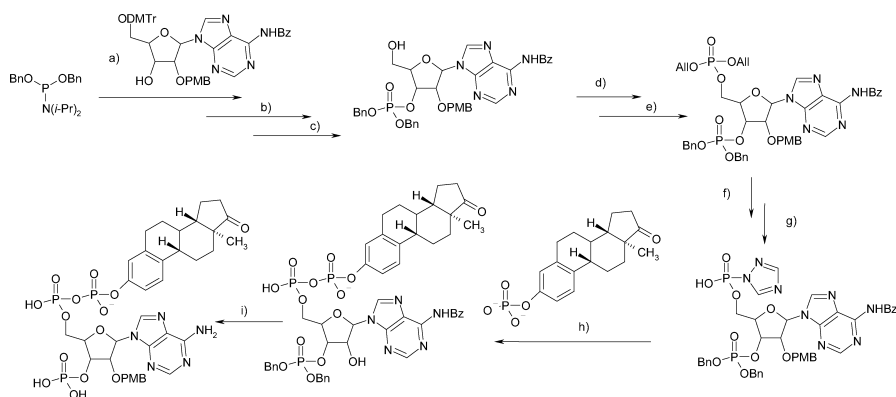
Phosphoroamidite methodology was employed to locate 3′-dibenzylphos-phite by the reaction with dibenzyl-*N,N*-diisopropylphosphoroamidite acti-vated by tetrazole followed by oxidation with CPBA (steps a and b). The 5′-deprotected intermediate (step c) was further phosphitylated by diallyl-*N,N*-diisopropylphosphoroamidite under similar conditions (step d) and oxi-dized (step e). The 5′-phosphate was selectively deprotected with Pd(PPh$_3$)$_4$ (step f) providing the necessary phosphate for the coupling procedure. The estrone 3′-phosphate component was generated by a standard procedure us-ing dibenzyl-*N,N*-diisopropylphosphoroamidite. Phosphitylation of estrone in the presence of tetrazole, oxidation by CPBA and the removal of benzyl protection by catalytic hydrogenolysis (Pd/C) gave the estrone 3′-phosphate component. The latter was coupled with the 5′-phosphate component trans-formed into an activated imidazolium intermediate by carbonyl diimidazole (CDI) (step g) to give the phosphate (step h). Final deprotection was per-formed by a standard catalytic hydrogenolysis (step i).

Example 18: Shuto et al. have prepared 3,7-anhydro-D-glycero-D-ido-octi-tol 1,5,6-trisphosphate as a novel IP$_3$ receptor ligand employing *O*-xylene-*N,N*-diethylphosphoroamidite (XEPA) as phosphitylating reagent [46], [47a,b]. The coupling was performed in the presence of tetrazole (step a). Oxidation of the phosphite by *m*-chloroperbenzoic acid (CPBA) afforded the corresponding phosphate (step b).
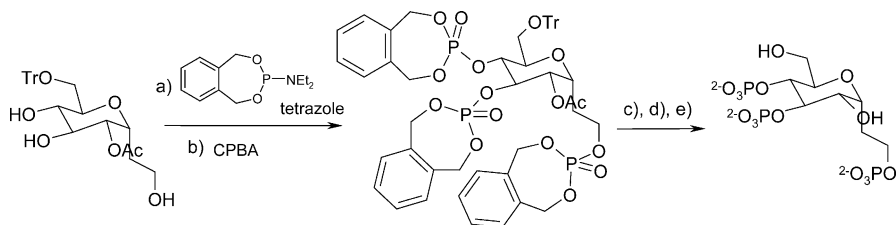
After the deprotection of *O*-xylenephosphate groups by catalytic hydro-genation in the presence of Pd-C (step c) trityl and acetyl groups were re-

moved by consecutive acid and basic hydrolysis to give the target compound as its sodium salt (steps d and e).

Example 19: Crich and Dudkin have used phosphoroamidite containing two different protecting groups: *O*-benzyl-*O*-2-cyanoethyl-*N,N*-diisopropyl-phosphoroamidite [48]. This phosphitylating reagent was prepared in excellent yield from 2-cyanoethyl *N,N* diisopropylchlorophosphoroamidite, which was immediately used for coupling with an appropriate alcohol in the presence of tetrazole and oxidized without delay with TBHP. This kind of phosphorylation procedure was used in the synthesis of 4,8,12,16,20-pentamethyl-pentacosylphosphoryl *β*-D-mannopyranoside, an unusual *β*-mannosyl phosphoisoprenoid from *Mycobacterium avium*.
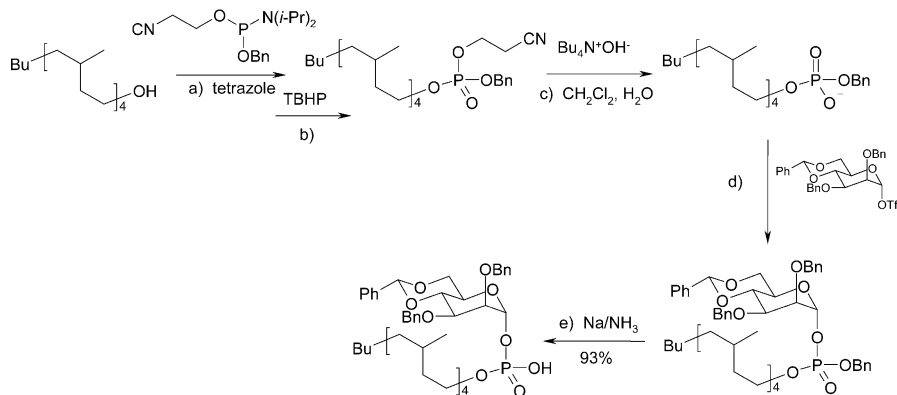
The phosphitylating reagent was coupled with the isoprenoid alcohol in the presence of tetrazole to give the phosphite (step a) which was oxidized in situ with TBHP to yield the corresponding phosphate in 96% overall yield (step b). The phosphate obtained was treated with tetrabutylammonium hydroxide in a dichloromethane/water biphasic system to deprotect the 2-cyanoethyl group (step c). The salt obtained was coupled in a highly *β*-selective manner with mannosyl triflate (step d). Attempted deprotection of the phosphate by catalytic hydrogenolysis gave unwanted side products. However reduction by sodium in liquid ammonia afforded the sodium salt in 97% yield (step e). No anomerization was observed during the deprotection procedure. This chapter includes many important references to carbohydrate phosphates.

Example 20: diallyl-*N,N*-diisopropylphosphoroamidite has been prepared by Bannwarth and Küng and employed in the phosphitylation of the peptide hydroxy function [49]. The phosphitylation by this reagent proceeds in the presence of tetrazole (step a) followed by CBPA oxidation (step b) and removal of allyl protecting groups in the presence of Pd(O)P(C$_6$H$_6$)$_3$ (step c).

Z: -Asp-(OBut)-Ala-Ser-Gly-Glu(OBut)$_2$
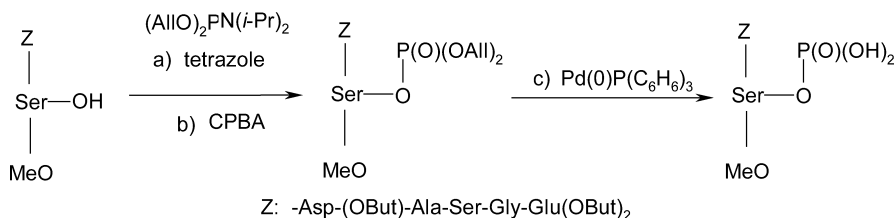
Example 21: combination of allyl and *O*-nitrobenzyl protecting groups in phosphitylation procedures have allowed Prestwich and Chen to perform the effective synthesis of caged inositol-P$_6$ derivatives [50]. The allyl groups were removed in the presence of RhCl(PPh$_3$)$_3$. The *O*-nitrobenzyl group is resistant to this procedure but can be removed by catalytic hydrogenolysis or under the impact of radiation. Phosphoroamidites containing the *O*-nitrobenzyl group were prepared from PCl$_3$ and proved to be reasonably stable if kept at −20 °C in the absence of moisture and oxygen.
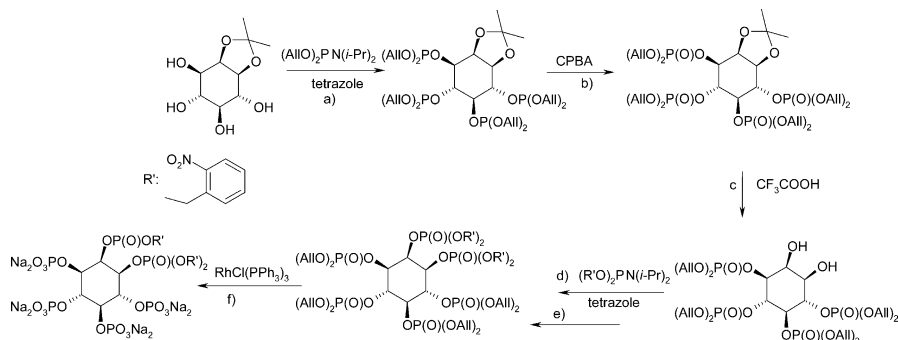
The phosphitylation procedure was performed under standard conditions (steps a and b). The allyl groups were not affected during oxidation by CPBA at low temperature. Standard conditions were applied to phosphorylation employing di-*O*-nitrobenzyl-*N,N*-diisopropylphosphoroamidite (steps d and e). No phosphate migration was observed during the acidic cleavage of the isopropylidene group (step c). Attempts to remove allyl groups using Pd^0 (step f) failed. However the rhodium catalyst RhCl(PPh$_3$)$_3$ allowed efficient cleavage of all allyl groups. The Rh(I) version allowed removal of allyl groups without affecting photolabile groups. This methodology was also used in the synthesis of P-1,1,2,2-tetra-caged Ins P$_6$ [41].

Example 22: removal of allyl group attached to a phosphorus centre with Pd, Pt and Rh complexes is a well established procedure [51] but is inconvenient for synthesis of therapeutic compounds on a large scale. During the deprotection step the palladium catalyst is susceptible to poisoning especially with P-S compounds resulting in loss of catalytic efficiency. Furthermore traces of organometallic compounds remain in the product after deprotection. In the paper of Manoharan et al. other methods of deprotection of allyl

groups which are working with oligonucleotides are presented and discussed. The dinucleoside allyl phosphite is oxidized by Beaucage reagent (step a). The authors have found, that for a practical synthesis of nucleoside phosphates and thiophosphates, allyl protecting group can be easily be removed by concentrated ammonium hydroxide containing 2% mercaptoethanol (step b).
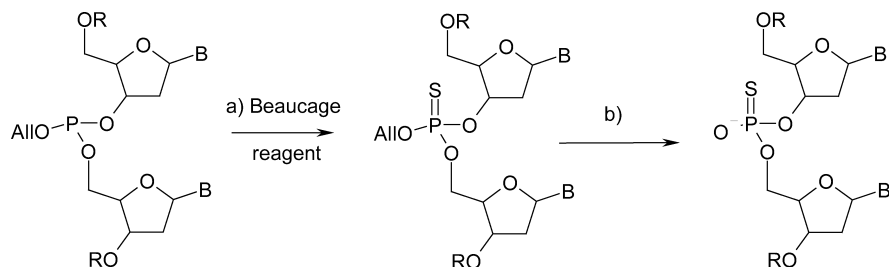
The authors have also studied the deprotection by less basic nucleophiles such as thiophenolate and iodide. Deprotection by the latter anion may lead to a side-reaction when condensation of the allyl iodide formed with the deprotected phosphorothioate leads to the corresponding S-allyl phosphorothioate. To suppress this side reaction thiourea was used to trap the allyl iodide.

Example 23: Phosphoroamidites containing two *tert*-butyl protecting groups. $(t\text{-BuO})_2\text{PN}(i\text{-Pr})_2$ have been used in many phosphorylation procedures. Konradsson and associates have described a new, efficient route to enantiopure phospholipids starting from (S)-glycidol [39]. (R)-bis-(*tert*-butyl)-N,N-diisopropylphosphoramidite was used to prepare (R)-di-*tert*-butyl-phosphoryl glycidol by coupling in the presence of tetrazole (step a) and subsequent oxidation by CPBA (step b).
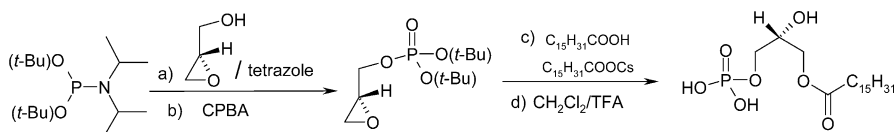
The oxidation with CPBA at 0 °C in CH_2Cl_2 does not effect removal of *tert*-butyl protecting groups [39]. Classic iodine/water oxidation system is not suitable, because it causes extensive *tert*-butyl cleavage [39]. Finally *tert*-butyl protective groups are removed by the action of trifluoroacetic acid TFA. This procedure is complementary to the one in Example 12.

Example 24: preparation of an asymmetrically-protected phosphoroamidite O-*tert*-butyl-O-2-cyanoethyl-N,N-diisopropylphosphoroamidite as a phosphitylating reagent in the synthesis of phosphopeptides has been described by Toth's group. [52]. This reagent allows the efficient synthesis of serine and threoine containing phosphopeptides by the global approach.
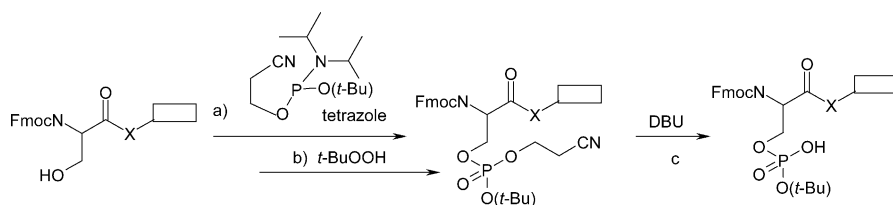
A phosphitylation procedure was carried out in THF using tetrazole as the activator; subsequent oxidation was performed by TBHP in THF (steps a and b). Simultaneous cleavage of 2-cyanoethyl and Fmoc groups was achieved by DBU in dichloromethane solution (step c). Finally the *tert*-butyl group was removed under acidic conditions by trifluoroacetic acid (TFA). In phosphitylation reactions leading to the phosphopeptides, symmetrically protected phosphoroamidites have formerly been used [53].

Example 25: phosphoroamidites containing a 2-cyanoethyl protecting group are very often used in nucleotide chemistry. When only one 2-cya-noethyl group is present, its removal by β-elimination proceeds under the influence of bases and is simple. Phosphates, thio- and selenophosphates containing two 2-cyanoethyl protecting groups are converted into the sec-ondary ester anion, whose electronic character prevents removal of the sec-ond 2-cyanoethyl group. However, expedient silylation of this anion by com-monly used silylation reagents leads to the tertiary phosphate which under-goes further elimination to the desired primary phosphate. Sekine and his associates [54] have employed bis-(2-cyanoethyl)-*N,N*-diisopropylphospho-roamidite in the synthesis of 3′,5′-bisphosphorylated ribonucleosides.

BSA: Bis(trimethylsilyl)acetamide
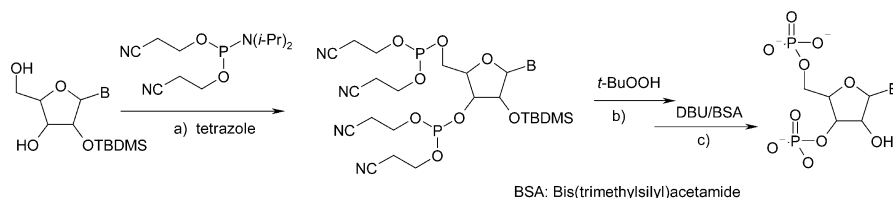
The phosphitylation procedure activated by tetrazole led to the phosphite structure (step a) which was effectively oxidized by TBHP to yield the corre-sponding phosphate (step b). Finally all 2-cyanoethyl protecting group were removed by the action of DBU in the presence of the silylating reagent bis(trimethylsilyl)acetamide BSA (step c). The latter is indispensable to se-cure total deprotection.

Example 26: Bartlett and al [55] have employed the protection strategy de-veloped earlier by Pfleiderer et al. based on the use of the 4-nitrophenylethyl protecting group [56] which is removable by β-elimination in a manner sim-ilar to the 2-cyanoethyl group. It was found that phosphates containing two 4-nitrophenylethyl groups can be deprotected stepwise by DBU in the pres-ence of silylating reagent BSA.
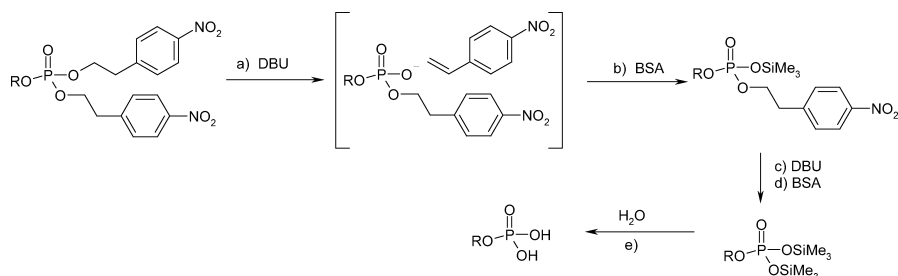
The intermediate formed by action of DBU in the process of β-elimination (step a) is silylated by BSA to produce a neutral phosphate (step b) which undergoes a second β-elimination (step c). The bis-trimethylsilylphosphate formed (step d) can be fully deprotected on exposure to water (step e).

Example 27: Sekine and associates have used bis-O-(2-cyano-1,1-dimethylethyl)-N,N-diethylphosphoroamidite in their studies on steric and electronic control of 2′-3′ phosphoryl migration in 2′-phosphorylated uridine derivatives [57].
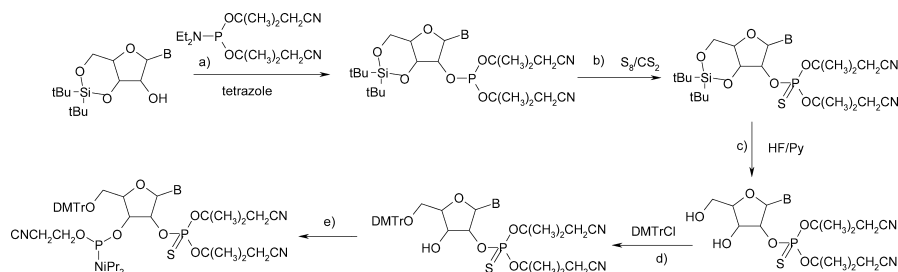
The phosphitylation reaction (step a) and sulfurization leading to the corresponding thiophosphate (step b) proceeded under standard conditions. After deprotection (step c) and selective introduction of the DMTr group (step d) no transphosphorylation 2′→3′ was noted. This fact can be explained by the steric factor combined with the lower activity of thiophosphates in comparison with normal phosphates. This enabled further phosphitylation (step e) by the customary phosphoroamidites. A difficulty in Sekine's procedure is that the phosphitylating reagent must be prepared in situ and has relatively low purity. Luckily the by-products formed are inert tetracoordinate species.

Example 28: a caged compound includes a photocleavable-protecting group that masks an essential functionality upon removal by photolysis [58]. Imperiali and associates have developed an "interassembly" approach for the synthesis of peptides containing 1-(2-nitrophenyl)ethyl-caged phosphamino acids [59]. The peptides described in that paper are based on phosphorylation sites of kinases involved in cell movements.

Following the style of presentation used in Imperiali's paper concerning the synthesis of caged phosphopeptides the general route for synthesis of peptides containing 2-nitrophenylethyl-caged phosphoserine-threonine and tyrosine residue is presented below.
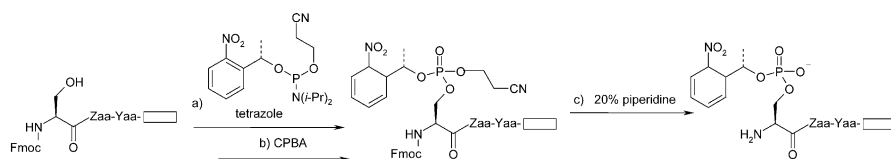
A standard coupling procedure activated by tetrazole (step a) is followed by the oxidation of the phosphite formed by CPBA (step b), This gave the corresponding phosphate which underwent simultaneous removal of a 2-cyanoethyl group at the phosphorus centre and an Fmoc group at the aminoacid function by the action of piperidine in DMF. The tyrosine hydroxyl showed reduced reactivity in the phosphitylation step, so in this case a very large excess of phosphitylating tetrazole and presence of dried 4 Å molecular sieves was required. Also the oxidation of the phosphite derived from tyrosine by CPBA resulted in several side products. Satisfactory oxidation was achieved however with either *tert*-butyl hydroperoxide (TBHP) in decane or hydrogen peroxide in aqueous THF. The phosphitylating reagent O-1-(2-nitrophenyl)-ethyl-O'-2-cyanoethyl-N,N-diisopropylphosphoroamidite was synthesized from 1-(2-nitrophenyl)ethanol and 2-cyanoethyldiisopropyl-chlorophosphoroamidite.
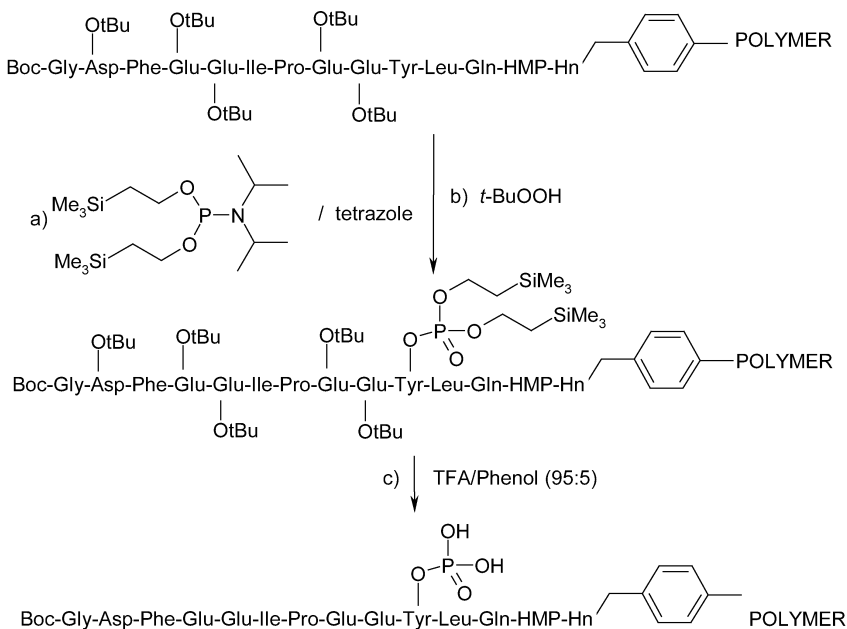
Example 29: *N,N*-diisopropyl-bis[(trimethylsilyl)ethyl]phosphoroamidite have been prepared from commercial available dichloro(diisopropylamino)phosphine and 2-(trimethylsilyl)-ethanol [60] in 65% yield after purification by chromatography. Chao et al. have used this phosphitylating reagent in a way which is compatible with the Fmoc/*tert*-butyl strategy for the synthesis of phosphotyrosine containing peptides [61].

Steps a and b of this synthetic procedure were performed under standard activation and oxidation conditions. It is advantageous that in the final deprotection step c the trimethylsilylethyl group is cleaved by *β*-fragmentation by the action of TBAF simultaneously with *tert*-butyl protective groups present in the oligopeptide chain.

Example 30: Bialy and Waldman in their synthesis of protein phosphates 2A inhibitor (4S, 5S, 6S, 10S, 11S, 12S) cytostatin have found that application of the fluorenylmethyl protecting group (Fm) allowed successful formation of the phosphate moiety [62]. Initial experiments with the methoxybenzyl group, successfully employed in the synthesis of fostriecin [63] failed. The 2-cyanoethyl protecting group was also not suitable because that one 2-cyanoethyl group could be removed without destroying the whole molecule (Examples 25 and 26).
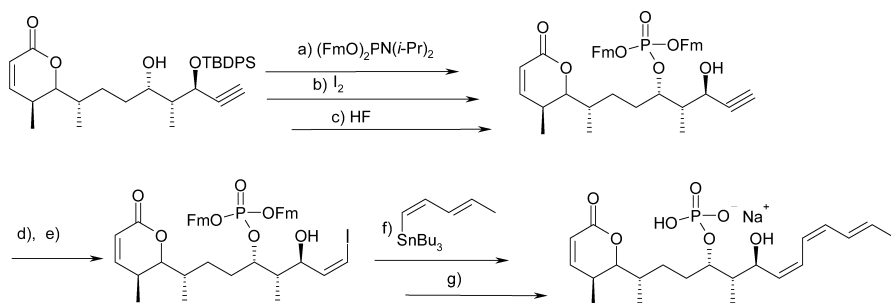
In the sequence of reactions presented above, phosphitylation by bis(fluorenylmethyl)-*N,N*-diisopropylphosphoroamidite proceeds in the presence of tetrazole (step a). The phosphite formed was oxidized by elemental iodine in pyridine, H$_2$O, THF solution (step b). After the removal of the *tert*-butyldiphenylsilyl group (step c) the phosphate formed containing an alkyne moiety was converted into the corresponding alkynyl iodide by *N*-iodosuccinimide in the presence of silver nitrate (step d) followed by reduction of the triple bond by phosphoroamide generated in situ (step e). This intermediate was then subject to Stille coupling with *Z,E*-dienyl-stannan in the presence of [PdCl$_2$(CH$_2$CN)$_2$] catalyst to give (*Z,Z,E*) triene phosphate (step f). Finally the phosphate formed was treated with an excess of Et$_3$N to remove both fluorenylmethyl group and to give the desired isomer of cytostatin (step g). It is interesting to note that the fluorenylmethyl group was able to survive synthetic procedures c–f.

Example 31: Watanabe and Nakatomi in their synthetic studies on unsaturated PI(3,4,5)P$_3$ have employed 9-fluorenylmethyl phosphate derivatives [64].
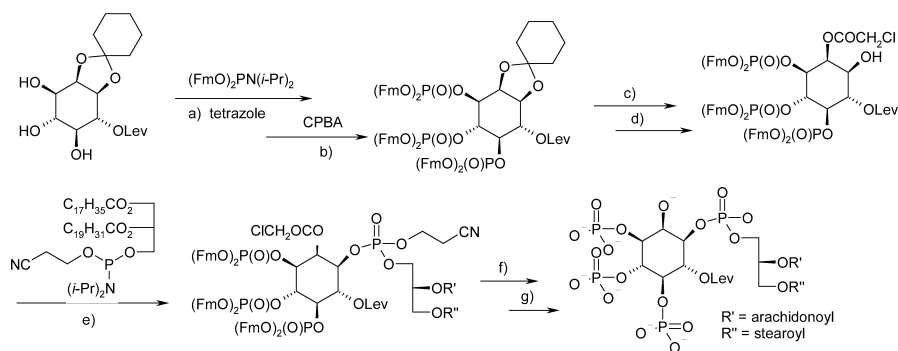
A phosphitylation procedure by bis(9-fluorenylmethyl) *N,N*-diisopropyl-phosphoroamidite follows the usual tetrazole activation (step a) and oxidation to the phosphate by CPBA (step b). After the removal of the diol protecting group (step c) the diol formed was regioselectively acetylated by chloroacetic acid anhydride (step d). The alcohol formed was phosphitylated with 2-*O*-arachidonoyl-1-*O*-stearoyl-*sn*-glycerol 2-cyanoethyl *N,N*-diisopropylphosphoroamidite in the presence of tetrazole (step e). The polyphosphate structure obtained after oxidation with TBHP (step f) was fully deprotected by reaction with a large excess of triethylamine in acetonitrile at 20 °C under anhydrous conditions (step g). The challenging problem in these studies was suitable choice of a phosphate protecting group. The benzyl group which is traditionally used in inositol chemistry could not be used. Its removal by the action of trimethylbromosilane or sodium in liquid NH$_3$ in the final stage of this synthetic procedure was also unsuccessful. 2-Cyanoethyl, 2-(4-nitrophenyl)ethyl and 2-(trimethylsilyl)ethyl removable group by β-elimination or β-fragmentation was also found unsuitable.

4
Polyfunctional Phosphoroamidites

A polyfunctional phosphoroamidite can be defined as one in which there is more than one amido group or one where an amido group is combined with other leaving groups. They also differ, like monofunctional phosphoroamidite by the kind of the protecting group attached to the P^{III} centre. They have received extensive coverage in already mentioned reviews [6]. The application of hexaalkyl-phosphorous amides (R$_2$N)$_3$P (R=Me, Et) in the phosphitylation of polyols (sugars) has been described in a recent review by Nifantiev et al [6f].

Compounds ROP(NR$_2$)$_2$ are standard reagents in the synthesis of oligonucleotides and their thioanalogues. The most popular are diamidites contain-

ing the diisopropyl amido group. They are relatively stable and they allow effective regioselective phosphorylation by virtue of the steric hindrance.

Phosphoroamidites holding an additional leaving group like chloride are also of great importance. They may serve, like dichloroamidophosphines R_2NPCl_2, as substrates in the synthesis of other phosphitylating reagents. Two other popular types are $R'OP(NR_2)_2$ and $R'OP(NR_2)Cl$. The latter phosphitylating reagent allows stepwise phosphitylation: first by exchange of the chloro group and then by substitution of the activated amido group. Substitution of the chloro group may be facilitated by nucleophilic catalysis [65]. Bromo and iodo derivatives are impractical as phosphitylating reagents. Fluoro derivatives will be discussed separately because of their unusual properties. Phosphoroamidites containing an aryloxy leaving group are of interest because of their stability and their ability to exchange an amido group under acidic conditions and an aryloxy group under basic conditions. Cyclic phosphoroamidites containing a five-member ring can also be classified as bifunctional phosphorylating reagents because the corresponding P^{III} ester, formed by amidite coupling after it has been oxidized to the P^{IV} structure may undergo ring opening with other nucleophiles.

Example 32: Fraser-Reid and his associates in their synthetic approaches to lipidated phosphoglyceroinositides have introduced the phosphate backbone via phosphoroamidite method employing *O*-benzyl-bis(*N,N*-diisopropyl)phosphorodiamidite [66].
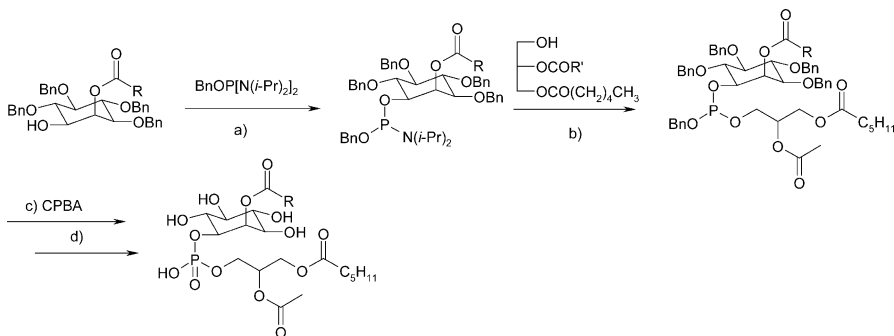
First phosphitylation was performed by *O*-benzyl-bis(*N,N*,-diisopropyl)-phosphoroamidite in the presence of diisopropyl-ammonium tetrazolide at room temperature in dichloromethane solution (step a). The intermediate phosphoroamidite was coupled with a glycerol moiety in the presence of tetrazole in boiling CH_2Cl_2 to give the benzyl phosphite (step b), which was oxidized by CPBA in CH_2Cl_2 into the corresponding phosphate (step c). In the final step d total debenzylation was achieved by Pd/C transfer hydrogenolysis in the presence of formic acid and methanol at room temperature.

Example 33: trimethylchlorosilane (TMCS) has been found to be a highly effective activator in typical couplings leading to dinucleotides and similar biophosphates, and is comparable with tetrazole and imidazolium salts [34]. The optimal amount of this activator is below the stoichiometric ratio.
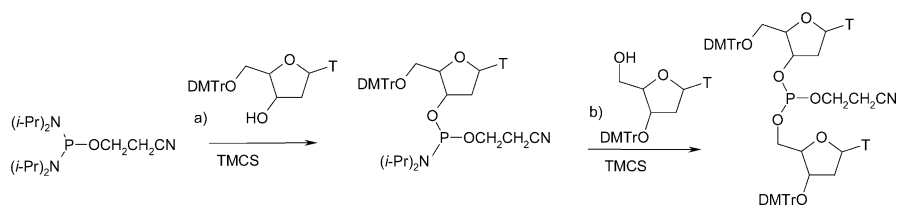
The first coupling of β-cyanoethyl tetraisopropylphosphorodiamidite (step a) proceeds selectively yielding the nucleoside phosphoroamidite which undergoes a second coupling to give the desired dinucleoside phosphite in very high yield (step b). Both couplings take place in solvents such as THF or acetonitrile at 20 °C.

Example 34: bis(N,N-diisopropylamino)trimethylsiloxyphosphine was prepared from readily available chlorobis(diisopropylamino)phosphine in almost quantitative yield [67]. Michalski et al. have observed that this trimethylsilyloxy-bis-(diisopropylamino)phosphine has the ability to undergo highly selective nucleophilic substitution at the P^{III} atom without affecting the silicon centre. A number of 3′,5′-dinucleoside trimethylsilylphosphites have been prepared in this way in very high yield without isolation of the mononucleotide intermediate.
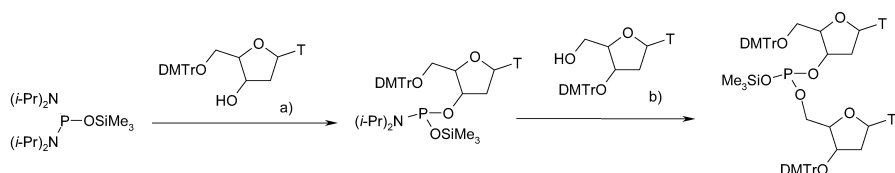
The formation of dinucleoside trimethylsilylphosphite proceeds in the presence of tetrazole in a one flask-procedure (steps a and b). The trimethylsilyloxy-P^{III} esters are very susceptible to hydrolysis and so they must be prepared and employed under strictly anhydrous conditions. The dinucleoside trimethylsilyloxyphosphites are identical with those prepared by Seela et al. from dinucleoside H-phosphonates [68].

Example 35: Li and Shaw [69] in their synthesis of nucleoside 3′,5′-cyclic boranophosphorothioate have used 3′,5′ cyclic phosphoroamidite.
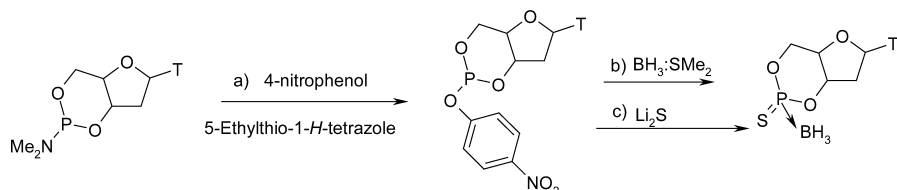
The reaction with 4-nitrophenol activated by 5-ethylthio-1-H-tetrazole led to formation of the 4-nitrophenyl phosphite (step a). Among several boronating reagents tested borane-dimethyl sulfide gave the optimal yield of

the borano complex (step b) which was transformed in a very high yield by lithium sulfide into the desired nucleoside-3′,5′-cyclic boranophosphorothioate (step c).

Example 36: Beaucage and associates have performed stereocontrolled syntheses of oligothymidine and oligodeoxycytidine phosphorothioates [23].
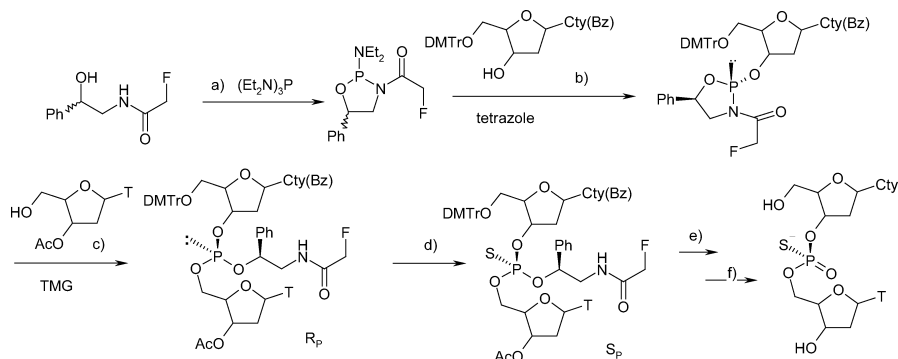
The synthesis begins with the preparation of cyclic *N*-acyl phosphoroamidite using hexaethylphosphorotriamidite (step a) which was allowed to react with N^4-benzoyl-5′-*O*-DMTr-2′-deoxycytidine (step b). The crude cyclic phosphoroamidite was purified by silica gel chromatography. The separated R$_P$ and S$_P$ diastereomers underwent stereoselective coupling with 3′-*O*-acetyl-thymidine in the presence of *N,N,N′,N′*-tetramethylguanidine (TMG) (step c). For simplicity only the S$_P$ isomer is indicated in presenting the further course of the synthesis. The sulfurization step with Beaucage reagent gave the corresponding thiophosphate (step d). Purified by silica gel chromatography this was deprotected first by concentrated NH$_4$OH at 55 °C (step e) and then by 80% aq. AcOH (step f). The details of the final deprotection and suggestions of its mechanism are described in this elegant study.

Example 37: the 4-cyano-2-butenyl protecting group has been described by Ravikumar et al. in the synthesis of oligodeoxy ribonucleosides by the phosphoroamidite approach [70]. This group is resistant to acids conditions and its removal proceeds under mild basic conditions by aqueous ammonia.
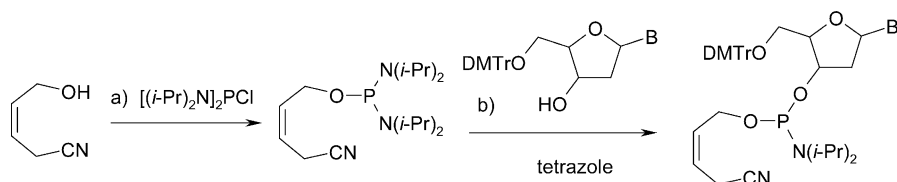
The 5′-nucleosido-4-cyano-2-butenylphosphoroamidite is formed in steps a and b under the usual conditions. The applicability of this new phosphoroamidite was demonstrated by the synthesis of heterodimers containing the thiophosphate moiety.

Example 38: the application of 2-cyanoethyl diisopropylchlorophospho-roamidite Cl-P(OCH$_2$CH$_2$CN)N(i-Pr)$_2$ in the synthesis of constructs contain-ing acyclic nucleoside inserts has been described by Damha and associates [71]. 5$'$-O-MMT-2$'$3$'$-seco-β-D-uridine was prepared by NaIO$_4$ oxidation leading to the dialdehyde followed by in situ reduction of the dialdehyde with NaBH$_4$ (steps a and b). Monoprotection of any of the free hydroxyl functions was achieved non-selectively by reaction with *tert*-butyl-dimethylchlorosilane and the mixture of regioisomers formed was separated by silica gel column chromatography (step c).
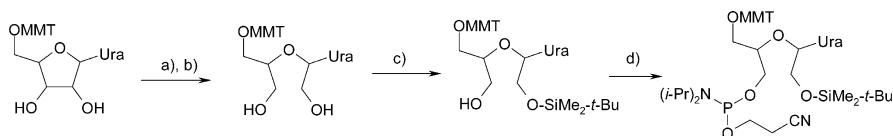
The phosphitylation proceeded in the presence of a catalytic amount of 4-(dimethylamino)pyridine as a nucleophilic [65] activator and-N,N-diiso-propylethylamine as hydrogen chloride scavenger (step d). The desired phosphoro-amidite was prepared in almost quantitative yield.

Example 39: biotin is used for DNA detection due to the exceptionally high biotin-streptavidin interaction [72]. Rothschild and associates [73] have reported the synthesis of photocleavable biotin phosphoroamidite em-ploying 2-cyanoethyl-N,N-diisopropylchlorophosphoroamidite.
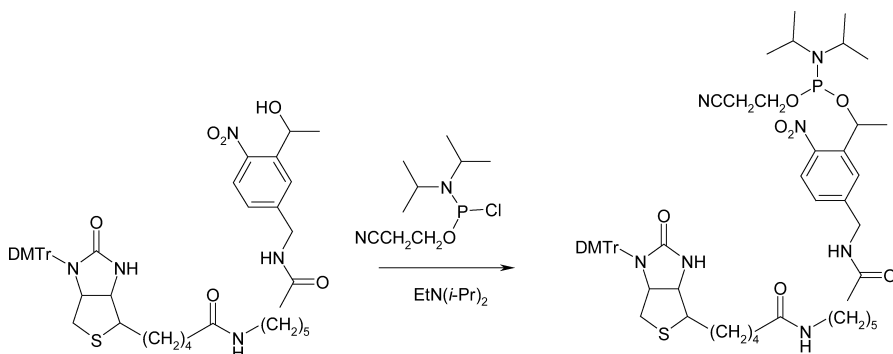
No phosphitylation of biotin nitrogen N$_2$ was observed under these reac-tion conditions. The phosphoroamidite formed was designed for direct use in automated DNA synthesized using standard phosphoroamidite chemistry to introduce a photocleavable biotin label on the 5$'$-terminal phosphate of synthetic oligonucleosides.

Example 40: mononucleoside phosphotriester derivatives with S-acyl-2-thioethyl bioreversible phosphate-protecting groups have been synthesized by Imbach and his associates [74a,b] in their research on intracellular deliv-ery of 3$'$-azido-3$'$-dideoxythymidine-5$'$-mono-phosphate.
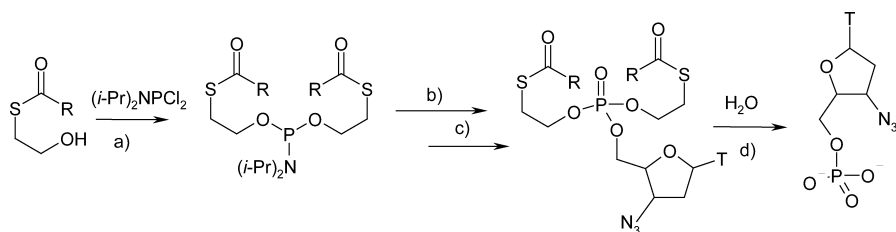
Phosphitylating reagents derived from a spectrum of R groups have been prepared from $(i\text{-Pr})_2\text{NPCl}_2$ and $\text{RC(O)SCH}_2\text{CH}_2\text{OH}$ in the presence of Et_3N followed by flash silica gel chromatography (step a). The coupling procedure with 3′-azido-2′,3′-dideoxythymidine activated by tetrazole led to the intermediate phosphite (step b) which subsequently was oxidized to the corresponding phosphate by CPBA (step c). Within this concept enzymatic hydrolytic removal of a protecting group in vivo proceeds with the elimination of ethylene episulfide.

5
Phosphoroamidites Containing Aryloxy Leaving Group

Phosphoroamidites containing aryloxy ligands attached to the P^{III} centre are special class of phosphitylating reagents. In contrast to the amido group which is activated under acidic conditions the aryloxy group resistant to acid conditions can be exchanged by alcohols and other nucleophile under influence of strong bases without affecting the amido group. Phosphoroamidites of this class have been applied as synthons for preparation of natural and modified internucleoside linkages. They play a very important role in the synthesis of P^{III}-F compounds.

Example 41: based upon the early observation that the *O*-chlorophenoxy group can be selectively eliminated from a dinucleoside *O*-arylphosphite triester [75], Caruthers and associates have used *O*-arylphosphoroamidites in the synthesis of dinucleoside *H*-phosphonates [76].
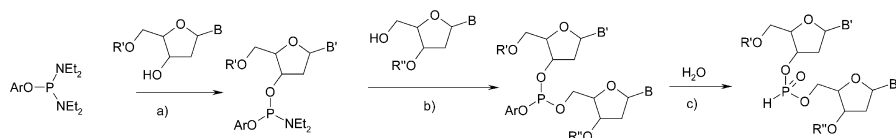
Steps a and b were performed in the presence of tetrazole from the appropriate phosphoroamidites in a good yield. The hydrolysis (step c) requires the presence of 5-(2′-nitrophenyl)tetrazole and ZnBr_2.

Example 42: *O*-methyl-*O*-4-nitrophenyl-*N,N*-diisopropylphosphoroamidite is readily available and shows high stability. Michalski et al. have applied this reagent in the synthesis of natural and modified dinucleotides [77].
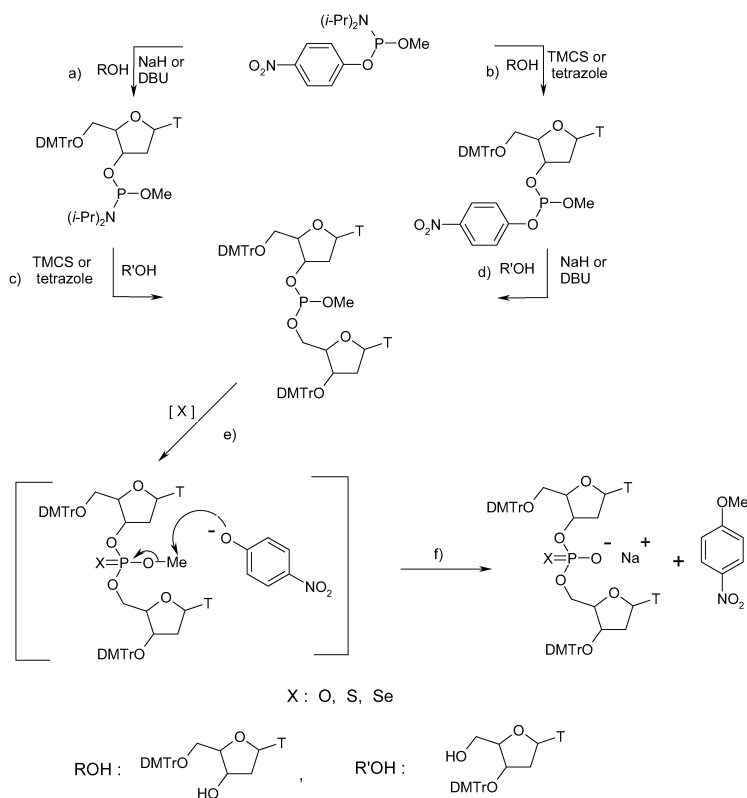
The intermediate mononucleoside phosphates are formed either via activation of the 4-nitrophenoxy group by DBU (step a) or of the diisopropylamido group by tetrazole or trimethylchlorosilane (step b). Dinucleoside methylphosphate was prepared from the corresponding monophosphite in a similar manner (steps c and d). Fast oxidation by dry air or elemental sulfur (selenium) was observed and attributed to the presence of 4-nitrophenoxide anion (step e). Even more remarkable is high capability of the 4-nitrophenolate anion to demethylate the intermediate phosphate (step f). This step is so rapid that Michalski et al. failed to observe the intermediate methylphosphate or corresponding sulfur or selenium analogues. This series of reactions that can be performed as a one-flask procedure, and the total yield is over 90%.

Example 43: Michalski et al. have described a synthetic approach to modified oligonucleotides based on N,N-diisopropyl-di-(4-nitrophenyl)phosphoroamidite. The procedure involves displacement of either the 4-nitrophenoxy or the diisopropylamino ligand [78].
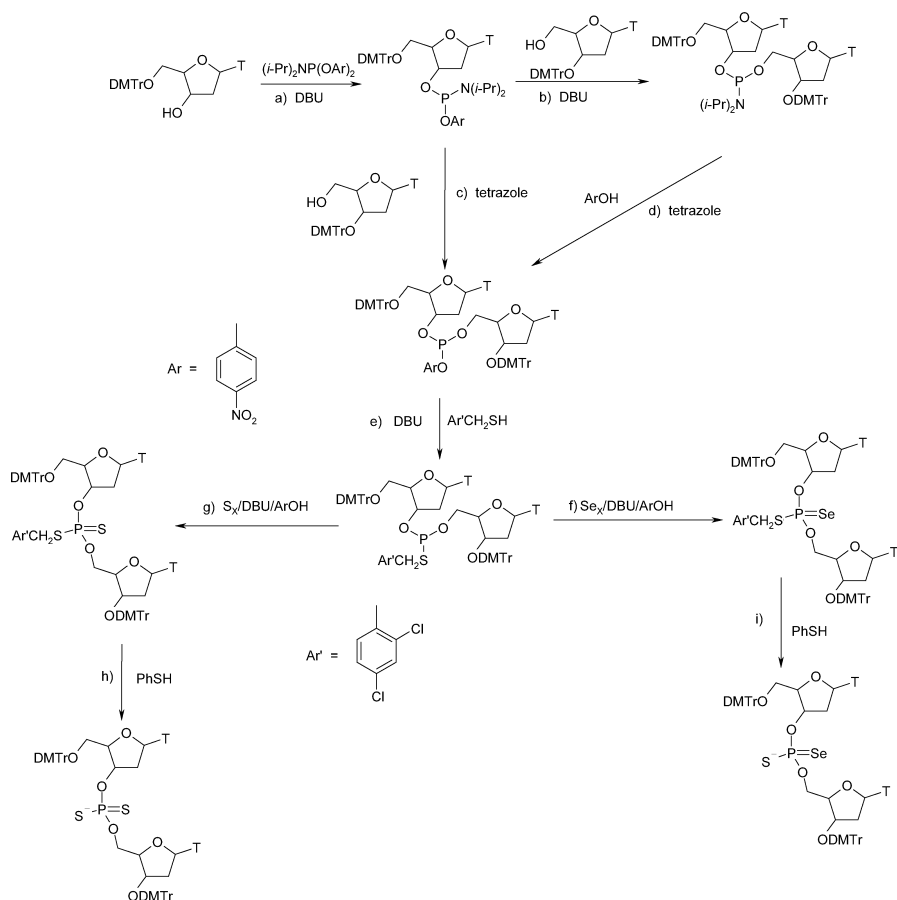
The phosphitylation procedure starts by coupling of mononucleoside with the phosphitylating reagent in the presence of DBU (step a). The nucleoside 4-nitrophenylphosphoroamidite undergoes a second coupling via the N(i-Pr)$_2$ group in the presence of tetrazole to give the dinucleoside arylphosphite (step c). Reaction with 2,4-dichlorobenzyl mercaptan activated by DBU gave the corresponding thiophosphite (step e). This intermediate can either add sulfur (step g) or selenium (step f) to give the dinucleoside dithiophosphate or thioselenophosphate. Removal of the 2,4-dichlorobenzyl residue acting (as a sulfur protecting group) by the reaction with thiophenol gave the corresponding dinucleoside dithiophosphate salt (step h) or dinucleoside thioselenophosphate salt (step i). All these synthetic operations can be performed as a one-flask procedure in an overall yield of isolated product greater than 90%.

The phosphitylation described in the step b leads to the dinucleoside phosphoroamidite that gave the dinucleoside phosphoroamidite which was turned into the dinucleoside arylphosphite by the reaction with 4-nitrophe-

nol in the presence of tetrazole (step d). More detailed studies of step d by
^{31}P NMR spectroscopy revealed that DBU behaves in this case not only as a
strong base but also as a nucleophile [78a]. The proposed structure of the
intermediate salt is consistent with that for the adduct of chloro bis(diiso-
propylamino)phosphine with DBU found out by Bertrand et al. [79].
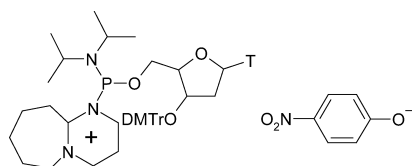
Example 44: another extension of the strategy shown in Examples 42 and
43 is the synthesis of trinucleotide containing thiophosphate and se-
lenophosphates internucleotide links [77].
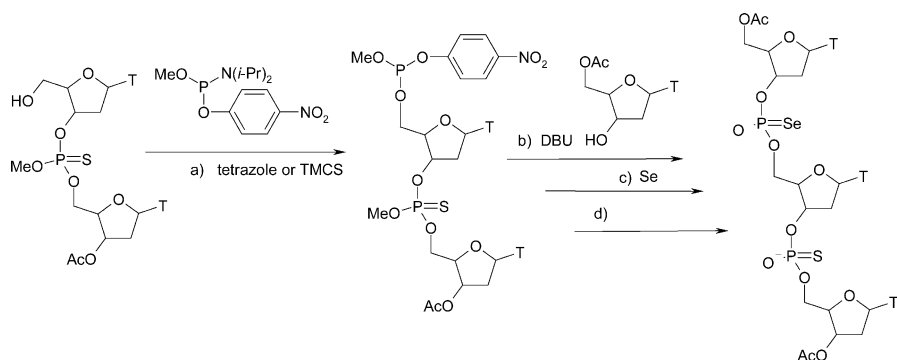
The thionucleoside with a free 5′-hydroxy group was phosphitylated in
the presence of tetrazole or TMCS (step a) and the intermediate formed cou-
pled with 5′-O-acetylthymidine activated by DBU (step b). The addition of
elemental selenium (step c) is followed by the fast demethylation in the pres-
ence of 4-nitrophenoxide (step d). All these operations can be performed as
a one-flask procedure to give the desired product in over 90% yield.

Example 45: Mizuguchi and Makino have observed stereoselective phos-
phitylation of thymidine by P-aryloxy nucleotide separated into diastere-
omers [80].
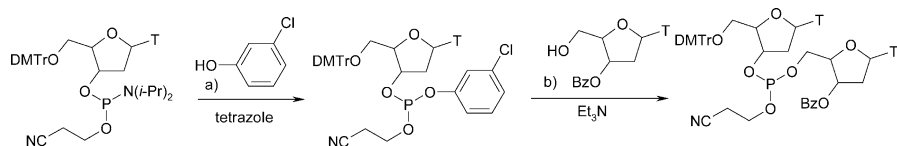
The mononucleoside was condensed with 3-chlorophenol in the presence
of tetrazole (step a). The aryloxyphosphite obtained was separated into

"fast" and "slow" isomers and was allowed to react with 5′-O-thymidine in the presence of triethylamine in pyridine or acetonitrile solution (step b). Although the latter phosphitylation reaction seems to be highly stereoselective, its final stereochemical output is lowered by P-epimerization. This transphosphorylation is likely to proceed with inversion of configuration at the phosphorus centre. No further applications of this method were revealed.

6
Fluorophosphoroamidites

Formally fluorophosphoroamidite ROP(F)NR′$_2$ could be classified as bifunctional phosphitylating reagents, but it is useful to discuss them separately. The rate of nucleophilic displacement at the P^{III}-X centre is relatively low for fluorine ligand in comparison with other halogens. In general, compounds containing the P^{III}-F moiety exhibit surprising chemical and stereochemical stability. In special cases, however, it is possible to exchange fluorine ligands for other groups.

Example 46: Dabkowski et al. have developed a very useful way of generating the P^{III}-F moiety by exchange of an aryloxy group attached to the P^{III} centre for a fluoride anion [31].

This reaction proceeds with a variety of aryloxy ligands and a spectrum of substituents R and R′ at the phosphorus centre. Alkalimetal fluorides, tetrabutylammonium fluoride (TBAF), hypervalent silicon Ph$_3$SiF$_2$ and tin Ph$_3$SnF$_2$ difluorides are suitable fluoride anion donors. The exchange of aryloxy ligand proceeds efficiently in solvents such as THF, MeCN and CH$_2$Cl$_2$.

Example 47: Dabkowski et al. have devised a strategy for the synthesis of nucleoside phosphorfluoridites based on the replacement of a 4-nitrophenoxy group attached to a P^{III} centre by fluoride anion [11b, 31].
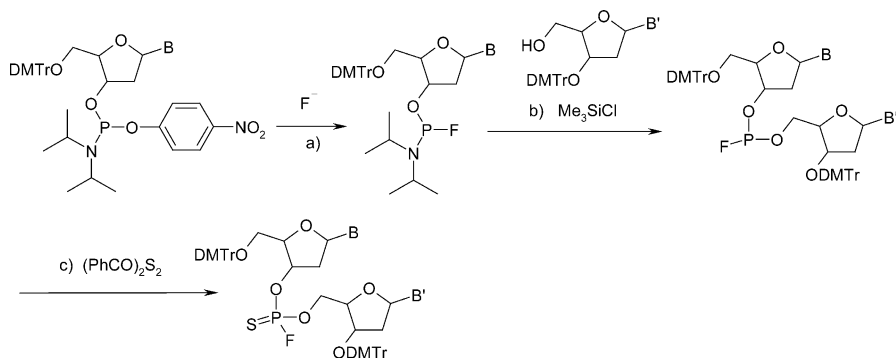
The exchange of 4-nitrophenoxy groups by fluoride anion using tetra-butylammonium fluoride (TBAF) proceeded in almost quantitative yield and the mononucleoside fluorophosphoroamidite was formed with some degree of stereoselectivity (step a) and was separated into the pure diastereoisomers. However, the coupling reaction in the presence of tetrazole or TMCS affords dinucleoside phosphorofluoridite (step b) as 1:1 mixtures of diastereoisomers in almost quantitative yields. The chromatography of dinucleoside phosphorofluorides on silica gel gave pure "fast" isomers of high configurational stability. The configurational stability of phosphorofluoridates can be explained by the presence of the strong P^{III}-F bond and steric hindrance exerted by nucleoside groups. P-Chiral P-F compounds racemize in the presence of anionic fluoride donors probably via achiral intermediates containing two fluorine ligands in apical positions. Dinucleoside phosphorfluoridites have been used in the stereospecific synthesis of dinucleosides phosphorofluoridothionates. This is illustrated by the reaction of a dinucleoside phosphorofluoridite with bis-benzoyl disulfide which leads to a single diastereomer (step c). It is likely that this transformation proceeds with retention of configuration at the chiral phosphorus atom. It was also observed that dinucleoside phosphorofluoridites can also be oxidized in a highly stereoselective manner by a suitable oxygen donor such as camphoro-derived oxoaziridines into the corresponding dinucleoside phosphorofluoridate [81].

Example 48: Dabkowski and Tworowska have applied phosphitylating reagents containing a P^{III}-F bond to the highly efficient synthesis of phosphorofluoridoates and phosphorofluoridothioates [82a]. These compounds, of general formula RO-P(X)(OH)F (X: O, S), are of interest because of their biological activity [82b]. *O-tert*-butyl-*N,N*,-diisopropylfluorophosphoroamidite was prepared from bis-*O,O*-(4-nitrophenyl)-*N,N*-diisopropylphosphoroamidite. Coupling with *tert*-butanol took place in the presence of sodium hydride (step a) and replacement of the aryloxy group was performed by tetrabutylammonium fluoride TBAF (step b). The phosphitylating reagent was formed in over 90% yield.
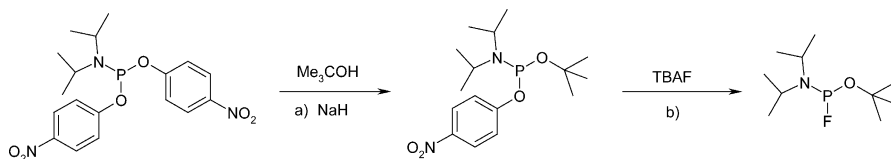
The synthesis of *O*-(2-cyanoethyl) *N,N*,-diisopropylphosphorofluoramidite starts from *O*-(2-cyanoethyl) *N,N,N′N′*-tetraisopropylphosphorodiamidite or *O*-(2-cyanoethyl) *N,N*,-diisopropylchlorophosphoroamidite and proceeds in overall 95% yield.
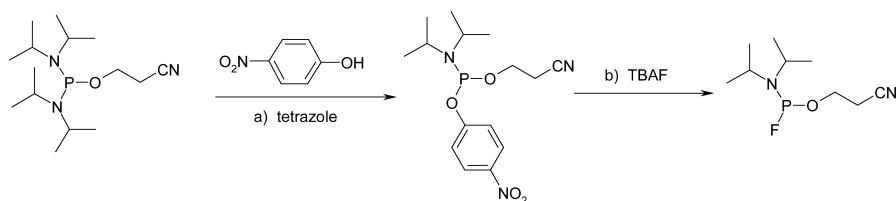
Both fluorophosphitylating reagents react with alcohols in the presence of tetrazole or TMCS (steps a and b).
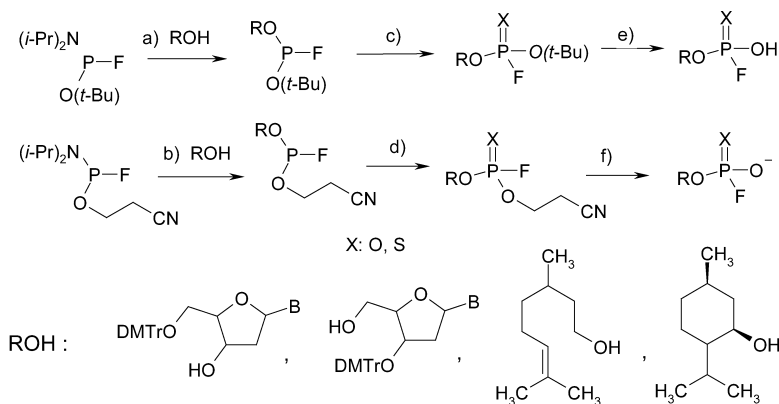
The phosphorus-fluorine bond is not affected by this procedure and subsequent synthetic steps. TMCS proved to be a better activator than tetrazole which must be used in large excess. Synthetic procedures leading to the phosphorofluoridites and employing these new phosphitylating reagents are illustrated above. Coupling reactions a and b proceeded in the presence of TMCS or tetrazole. Phosphorofluoridites obtained were oxidized by TBHP or elemental sulfur to give the corresponding phosphorofluoridoates or phosphorofluoridothioates (steps c and d). The *tert*-butyl group was removed thermally (step e) and the 2-cyanoethyl group by β-elimination in the presence of triethylamine (step f). The desired products were obtained in over 90%yield.

Example 49: fluorophosphoroamidites in particular cases can be exchanged for a fluoride group. For example 3′-O-thymidine-O-methyl-N,N-diisopropylphosphoroamidite has been prepared by the condensation of lithium methoxide with the corresponding fluorophosphoroamidite [30].
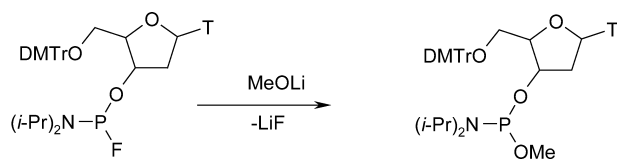
Example 50: as shown in several examples trimethylchlorosilane (TMCS) acts as a highly efficient catalytic activator for the replacement of a P^{III}-NR_2 amino group by alcohols to form the corresponding esters. Michalski and associates have noticed that P^{III}-F compounds can also react as reagents for the replacement of a fluorine ligand by an appropriate alcohol when at least one equivalent of TMCS is used. This reaction is relatively slow. Its driving force is the formation of trimethylfluorosilane [83].
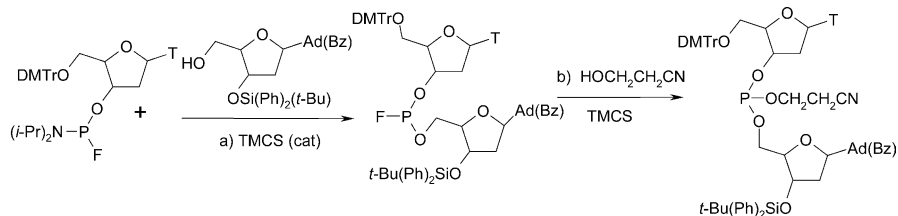
In the sequence of reactions shown above TMCS acts in step a as catalytic activator in the coupling leading to the dinucleoside phosphorfluoridite. In step b the same compound acts as a reagent to give the corresponding phosphite, Me₃SiF and HCl. Hydrogen chloride formed can be trapped by 4-Å molecular sieves or trialkylamine.

Example 51: Michalski and associates have found that P^{III}-F compounds react with Ruppert reagent (Me₃SiCF₃) at 20 °C in THF in an almost quantitative yield [84]. This efficient reaction was applied to synthesize trifluoromethylphosphonate analogues of dinucleosides.
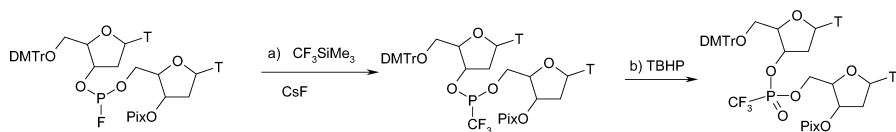
Dinucleoside phosphorofluoridites are readily available (Example 47). The Me₃SiCF₃ reagent reacts with this type of compounds in the presence of a catalytic amount of CsF (step a) and the trifluoromethylphosphonite formed was oxidized to trifluoromethylphosphonate by TBHP (step b). The method is particularly valuable as it is compatible with a sequential procedure combining the formation of phosphorus-fluorine compounds from P^{III}-aryloxy precursors with the reaction leading to P^{III}-CF₃ groups. Both reactions require the presence of fluorine ions as a substrate or catalyst.

Example 52: replacement of the fluorine ligand by the alkyl (aryl) group by the action of organometallic reagent has been studied by Michalski and associates. Preliminary successful results have been achieved with Grignard reagents [30].
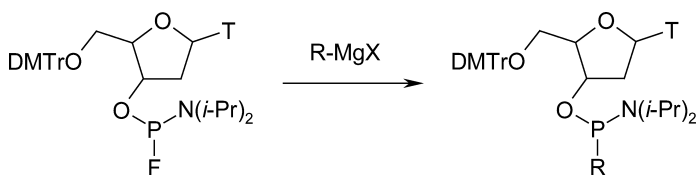
Examples 51 and 52 could be placed in the section dealing with the synthesis of P^{III}-C systems. However, it seemed appropriate to discuss them in the conjunction with general properties of P^{III}-F systems.

7
C-Phosphonoamidites and Related Structures

A synthesis of alkyl (aryl) C-P^{III} compounds derived from bioalcohols is based on three principal strategies. In the first approach starting material contains a C-P^{III} bond, as alkyl(aryl)chlorophosphine RPCl$_2$ and chlorophosphonoamidites R-P(Cl)NR$'_2$ is used. Another standard approach employs the Arbuzov-Michaelis reaction in which alkyl(aryl)phosphonites RP(OR$'$)$_2$ are allowed to react with alkyl halides at a somewhat elevated temperature (60 °C or higher) [85]. Tricoordinate phosphorus compounds containing a P^{III}-OSiR$_3$ moiety react with alkyl halides at ambient temperature with a very high yield. Since compounds of this type are readily available from H-Phosphonates, it is possible to predict their increasing use [68, 86]. The third approach is based on the reaction of P^{III}-X compounds with organometallic reagents, e.g. Grignard reagents. (Example 59). In nucleophilic displacement reactions C-P^{III}-X compounds are more reactive than the corresponding phosphites and have a very high affinity toward oxygen. Therefore synthetic work in this area calls for even more preventive measures than in the case of phosphite structures.
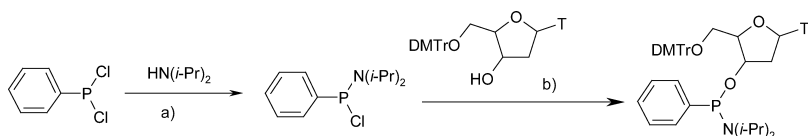
Example 53: Engels and associates have synthesized monomeric phenylphosphonoamidites building blocks that serve as synthons for the introduction of phenylphosphono and phenylphosphonothioate linkages into oligonucleotides [87].

Dichlorophenylphosphine was transformed into chloro-P-phenyl-*N,N*-diisopropylphosphonoamidite, which was purified by distillation in vacuo over a Vigreux column (step a). The subsequent condensation with 5$'$-DMTr-thymidine in the presence of (i-Pr)$_2$NEt at 20 °C in CH$_2$Cl$_2$ solution gave the desired synthons for further applications as 1:1 mixture of diastereomers in 76% yield.

Example 54: hydrogen *O-l*-(−)-methylphenylphosphinothioate R$_P$, S$_P$ has been prepared by Michalski et al. from phenyldichlorophosphine [88] by the following sequence of reactions. Phenyldichlorophosphine when allowed to

react with *l-(−)*-menthol in pyridine solution gave the crude *O-l-(−)*-men-thyl-P-phenylphosphonochloride RₚSₚ (step a). The latter compound was converted into hydrogen *O-l-(−)*-menthyl-P-phenylphosphinothioates RₚSₚ by reaction with hydrogen sulfide (step b). The overall yield, when both re-actions were performed as a one-flask procedure, was very high.
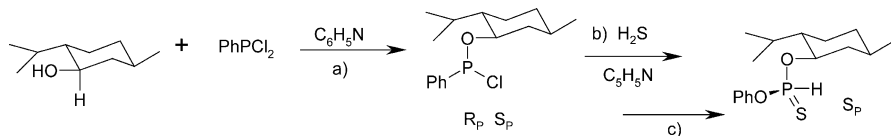
The crystalline diastereomer Sₚ was separated by crystallization from *n*-hexane (step c) and is an excellent starting material for the synthesis of other P-chiral thioanalogues of biophosphates.

Example 55: *N,N*-diisopropyl-4-nitrophenylmethylphosphonoamidite has been applied in the synthesis of oligonucleoside methylphosphonates [89]. This stable crystalline compound prepared from methyldichlorophosphine, was employed in two ways in a procedure similar to that presented in the Examples 42 and 43.
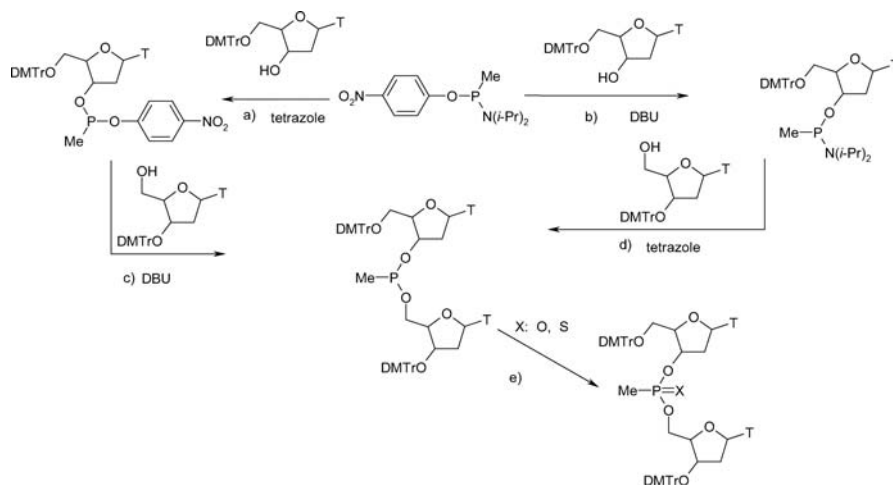
3′-*O*-Nucleoside was allowed to react with the phosphonoamidite via acti-vation of the diisopropylamino group by TMCS or tetrazole to give the 4-ni-trophenyl methylphosphonate (step a) or activation of the 4-nitrophenyl group by DBU to give the corresponding phosphonoamidite (step b). A sim-ilar type of coupling via activation of an amido or aryloxy group with 5′-*O*-nucleoside gave the dinucleoside methylphosphonate (step c, d) which was finally oxidized, by air or elemental sulfur (step e). Both alternative proce-dures are very efficient providing the desired dinucleosides methylphospho-nate or methylphosphonothioates in excellent yield.

Example 56: the Isis Pharmaceutical group in their extensive investigations of antisense oligonucleotides as therapeutics has described the synthesis of 3′-C-methylene nucleoside phosphonoamidites for the new backbone modification of oligonucleotides [90]. This paper gives good insight into tricoordinate phosphorus and related H-phosphonate chemistry in the service of nucleotide synthesis.
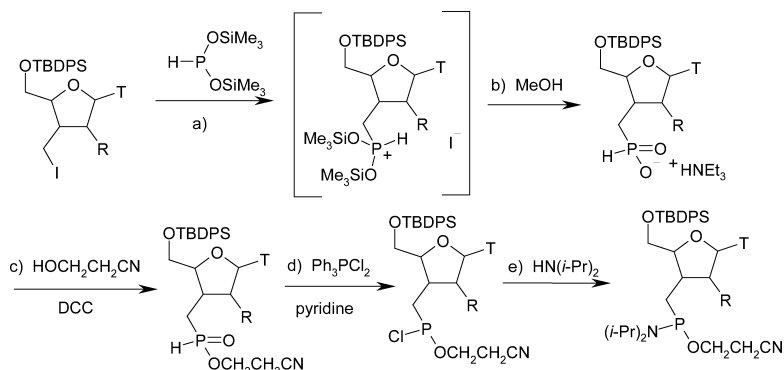
An Arbuzov-Michaelis type reaction of 3′-C-methyliodo nucleoside with bis(trimethylsilyl)phosphonite (BTSP) gave an intermediate product (step a) which was transformed by MeOH and subsequently by Et$_3$N into the desired H-phosphinic acid salt (step b). BTSP has already been employed in the synthesis of other small molecules outside nucleoside chemistry [91a–c]. The triethylammonium salt of the phosphinic acid was condensed at elevated temperature using dicyclohexylcarbodiimide (DCC) to give the intermediate H-phosphinate as a mixture of two diastereoisomers at the phosphorus centre (step c). This intermediate was allowed to react with triphenylphosphine dichloride (Ph$_3$PCl$_2$) prepared in situ from triphosgene and triphenylphosphine [94] to give the intermediate chloro-2-cyanoethylphosphine (step d) which was finally transformed into the desired phosphonoamidite (step e). The transformation of hydrogen phosphonates into the corresponding phosphorohalidites R$_2$P(O)H→R$_2$PX has been used recently also by other authors, e.g. [71].
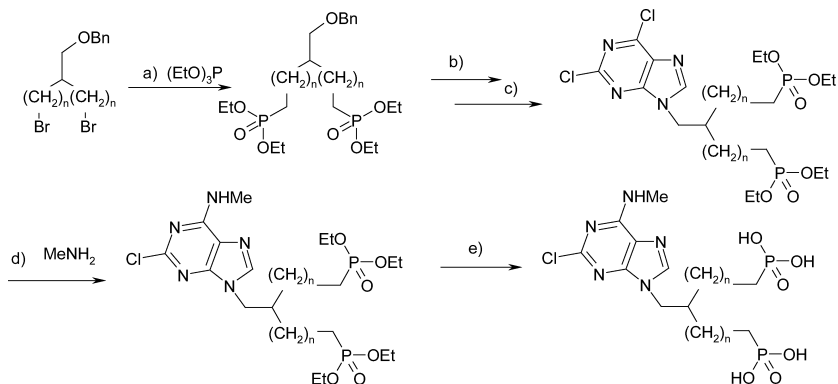
Example 57: the synthesis of 2-chloro-N^6-methyladenine-9-(2-methyl-propyl)bis phosphonate, analogous to the corresponding bisphosphate, has been performed by Jacobson and associates [93]. The key step in this synthesis is the Arbuzov-Michaelis reaction.

The starting diol was transformed into the dibromide by elemental bromine with triphenyl phosphine adduct which undergoes the Arbuzov-Michaelis reaction under somewhat drastic conditions at 150 °C (step a). Catalytic removal of the benzyl group was performed by a Pd/C catalyst (step b) and the alcohol formed was allowed to react with dichloropurine in the presence of triphenylphosphine and diethylazodicarboxylate (Mitsunobu reaction) (step c). Finally the desired product was obtained by reaction with methylamine (step d) and the removal of ethyl groups at the phosphorus centre was performed by transilylation using trimethyliodosilane (step e).

Example 58: a general route to phosphorodithioic acid derivatives was described by Martin and al. [94]. The method involves the reaction of Grignard reagents with 2-chloro-1,3,2-dithiophospholane to give intermediate dithiophosphinate. The latter was oxidized by elemental sulfur to give an intermediate cyclic dithiaphospholane, which undergoes nucleophilic ring opening according to methodology reported by Stec and his associates[95]. The procedure is illustrated by the preparation of choline-derived phosphorodithioates.
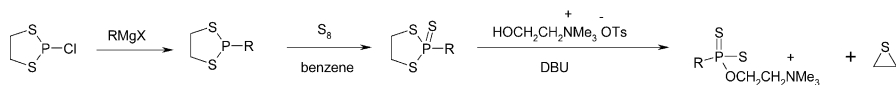
Example 59: Caruthers and his associates have synthesized esterified acetic acids phosphonodiamidites under Reformatsky reaction conditions [96].
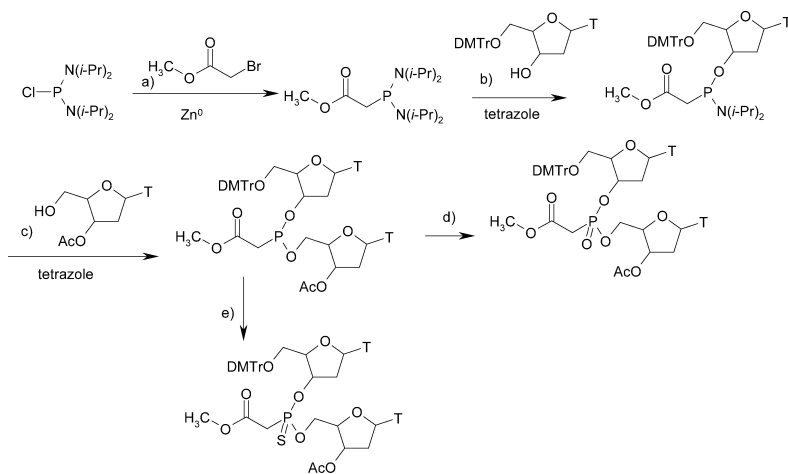
The Reformatsky type of reaction with Zn(0) was performed in situ and led to somewhat unstable phosphonodiamidite (step a) which was coupled with 5′-DMTr-thymidine to give the intermediate mononucleoside phosphonoamidite (step b). The latter was further coupled with 3′-acetyl-thymidine (step c). Couplings described in steps b and c were activated by tetrazole. The intermediate dinucleoside phosphonite was oxidized with (1S)-(+)-(10-camphorsulphonyl)oxaziridine (step d) or sulfurized with Beaucage reagent. The phosphonoamidites mentioned above were used in the solid-phase chemical synthesis of phosphonoacetate and thiophosphonoacetate oligonucleotides.

8
Miscellaneous Phosphitylating Reagents

Phosphorus trichloride PCl$_3$ and related structures ROPCl$_2$ and (RO)$_2$PCl are increasingly important as phosphitylating reagents. Cyclic phosphorus chloridites and the corresponding phosphoroamidites can be classified as bifunctional phosphorylating reagents. This allocation is based on the fact that, after initial coupling and subsequent oxidation, the cyclic P^{IV} compounds formed are prone to react with another nucleophile via ring opening.

Example 60: a simple one-pot route for the synthesis of 2′,3′-didehydro-2′3′-dideoxythymidine (d4T) or 3′-azido-2′,3′-dideoxythymidine (AZT) hydrogen phosphate derivatives via reaction of d4T or AZT with phosphorus trichloride has been described by Zhao et al. [97].
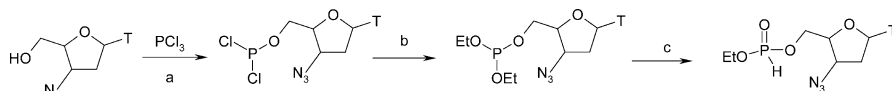
Formation of the nucleoside phosphorodichloridite at −30 °C by PCl$_3$ in CH$_2$Cl$_2$ solution (step a) is followed by reaction with ethanol (step b). Subsequently dealkylation occurs with the assistance of hydrogen chloride formed in reaction (a) to give the desired 5′-nucleoside H-phosphonate (step c). It was found that a mixture of ethanol and *tert*-butanol (1:1) as alcoholysis agent prevented side reactions and gave a higher yield than when ethanol alone was used.

Example 61: phosphitylating reagents phosphorodichloridites ROPCl$_2$ derived from bioalcohols or containing a protecting group R are readily available by the synthetic procedure of Claesen et al. [98]. These compounds can be prepared in acetonitrile solution from the corresponding alcohols and excess of PCl$_3$ without the use of base. After removal of the solvent the residue is distilled or crystallized to give the desired phosphorodichloridites often in over 90% yield.

$$ROH \xrightarrow[\text{20}^0\text{C, 10 min.}]{\text{7 PCl}_3/\text{CH}_3\text{CN}} ROPCl_2$$
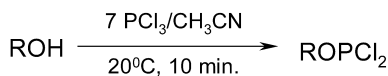
Regarding the mechanism of reaction in which acetonitrile is used as solvent, this solvent has a low tendency to bind hydrogen ions. The result is that hydrogen ions are available for protonation of phosphorus or oxygen in the transition state. An interesting representative of this class of compounds is 1,1-dimethyl, 2,2,2-trichloroethyl phosphorodichloridite. This phosphitylating reagent reacts selectively with nucleosides at −78 °C in THF/pyridine. The deprotection of trichloroethyl phosphorotriesters was achieved with tributylphosphine [92]. Alternative reducing agents such as Zn metal can also be used [100].
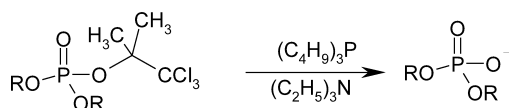
Example 62: commercially available diethylphosphorochloridite (EtO)$_2$PCl has been used by Mills and Potter in the synthesis of myo-inositol 1,2,4,5-tetrakisphosphate [101].
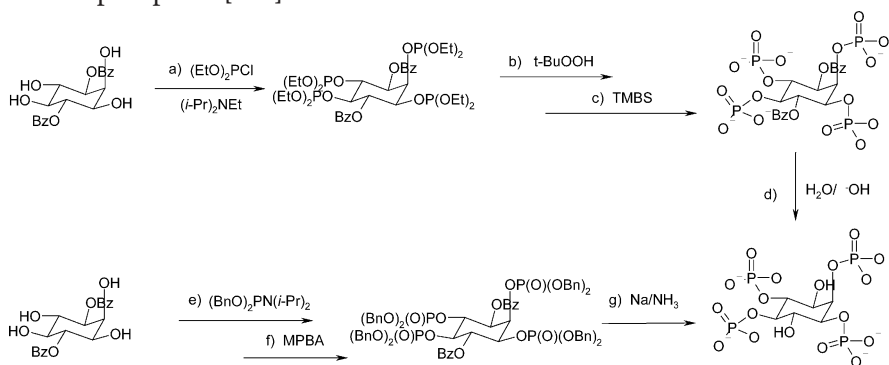
The coupling led to the intermediate phosphite (step a) which was oxidized by TBHP (step b). The phosphate formed containing eight ethoxy groups was deprotected by *trans*-esterification using trimethylbromosilane and subsequent hydrolysis by water (step c). Two benzoyl groups were removed by basic hydrolysis (step d). The same tetrakis phosphate was prepared by phosphitylation with dibenzyl-*N,N*-diisopropylphosphoroamidite in the presence of tetrazole (step c) followed by oxidation with CPBA (step f). The removal of all benzyl and benzoyl groups was achieved in one step by sodium in liquid ammonia (step g).

Example 63: Meier in his studies on potential prodrugs derived from biologically active nucleoside monophosphates used the cyclic chlorophosphites 2-chloro-4-*H*-1,3,2,-benzodioxa-phosphinines for the synthesis of the cyclic phosphotriesters having two ligands of different hydrolytic stability: benzyloxy and aryloxy [102].
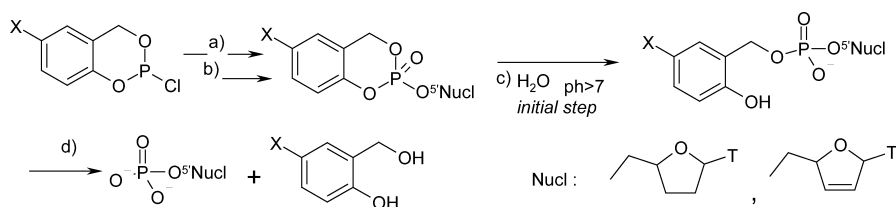
The phosphitylation procedure (step a) proceeds in the presence of EtN(i-Pr)$_2$ (DPEA) and the subsequent oxidation by TBHP (step b). The cyclic phosphate is deprotected stepwise (steps c and d) and serves as a "model for the physiological milieu". It has been possible to deliver phosphate mono-esters via steps c and d in a controllable manner from cyclic phosphotri-esters at physiological pH.

Example 64: Lin and Shaw have performed the synthesis of the triphos-phate analogue: nucleoside α-P-borano, α-P-thiotriphosphate [103] based on Eckstein and Ludwig methodology [104]. Cyclic phosphorochloridite de-rived from salicylic acid 2-chloro-4H-1,3,2-benzodioxaphosphorin-4-one was used as phosphitylating reagent in the reaction with 3′-O-acetylthymi-dine (step a). The intermediate P^{III}-esters formed as a mixture of di-astereoisomers were allowed to react with tributylamine pyrophosphate to give the cyclic anhydride (step b). The borane group was introduced in the reaction with excess of a borane-diisopropylamino complex (step c).
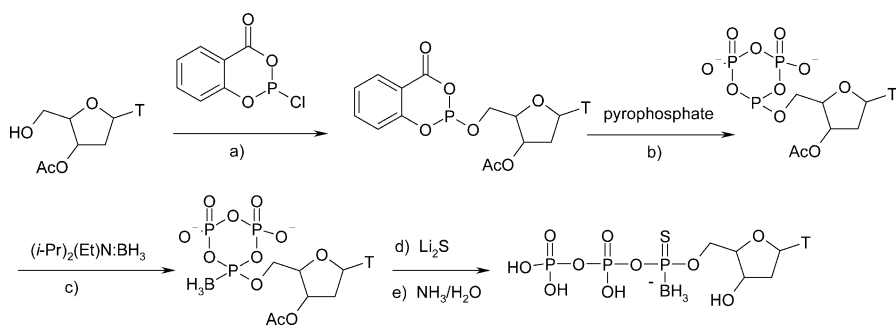
Ring opening of the cyclic boronated triphosphate was achieved by the action of lithium sulfide (step d) and the 3′-OH group was deprotected by an NH$_3$-H$_2$O-MeOH system (step e).

Example 65: the phosphorylation of bioalcohols according to the metho-dology developed by Stec and his associates uses 2-N,N-diisopropylamino-1,3,2-oxathiaphospholane [105].
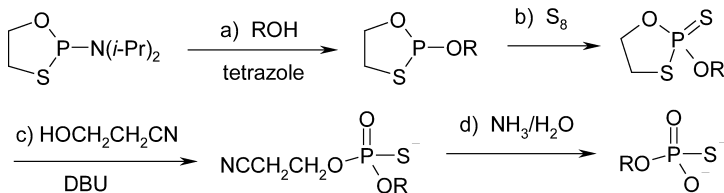
This synthetic procedure steps a–d can be performed as a one-flask process. The simplicity of this method and its high yield observed makes this approach competitive with the most widely used method based on sulfurization of phosphite intermediate prepared on phosphoroamidite route. An analogous dithiaphospholane approach was applied earlier for the synthesis of phosphorodithioates derived from deoxyribonucleosides [105]. The oxathiophospholane strategy which allows stereoselective synthesis of P-chiral thioanalogues of oligonucleotides was most recently described by Guga, Okruszek and Stec [105].

Example 66: the phosphoroamidite route has been used to prepare phospholipid analogues holding biocompatible properties. Brown et al. [106] have prepared the 2-(methacryloyloxy)ethylphosphorylcholine monomer using the 2-*N,N*-diisopropyl-1,3,2-dioxaphospholane which was coupled with 2-hydroxyethyl methacrylate (step a) in the presence of 4,5-dichloroimidazole.
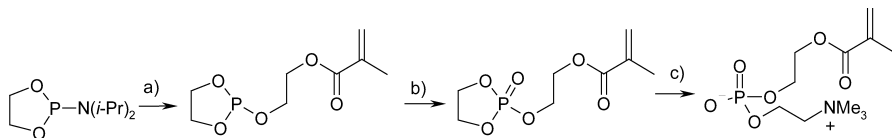
The phosphite formed was efficiently oxidized by MPBA (step b). Use of trimethylamine N-oxide as an oxidant was investigated in the hope that this reagent would oxidize the cyclic phosphite and that trimethylamine formed would be employed in the ring opening reaction (step c) to produce the phosphorylcholine in a one-flask procedure. In this case to avoid the residual oxidant in the product less than one equivalent of the oxidant was used and it was necessary to add an additional amount of trimethylamine to form the desired 2-(methacryloxy)ethylphosphorocholine in good yield.

Example 67: Martin and Wagman have developed a general procedure for the synthesis of lipid phosphorodithioate analogues as phosphate mimic for the study of biological pathways and enzyme mechanisms [107]. They observed that readily available phosphitylating reagent 2-chloro-1,3,2-dithiaphospholane is superior than the corresponding 2-dialkylamino analogues for the synthesis of phospholipids derivatives.
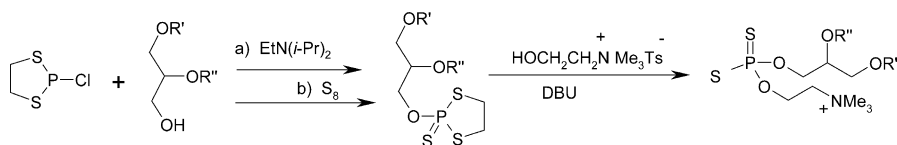
The first coupling was performed in CH$_3$CN or THF in the presence of EtN(i-Pr)$_2$ at −38 °C in 3 h (step a). Formation of the P^{IV} intermediate took place by addition of elemental sulfur in carbon disulfide solution (step b). The desired phosphorodithioate analogue of phosphatidylcholine was prepared by treatment of the latter with choline tosylate in the presence of DBU.

Example 68: Salomonczyk et al. have performed the synthesis of (±)-my-oinositol 1,2-bis- and 1,2,3-tris-(carboxymethylphosphonates) using the Arbuzov-Michaelis reaction [108].
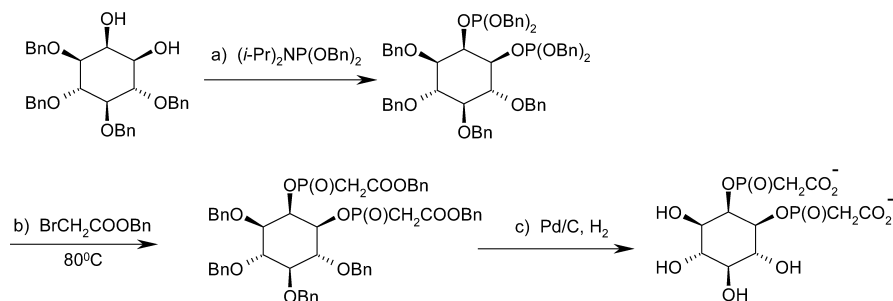
Phosphitylation of inositol 3,4,5,6-tetra-O-benzyl myo-inositol by dibenzyl-N,N-diisopropylphosphoroamidite gave the corresponding bis-dibenzylphosphite (step a). After 12 h at 80 °C the Arbuzov-Michaelis reaction with the excess of benzyl bromoacetate at 80 °C gave after 12 h the fully protected bis-1,2-diphosphonate (step b), which was totally deprotected by catalytic hydrogenolysis to give the desired product (step c).

Example 69: Mlotkowska and Olejnik have described the synthesis of rac-S-(2-acetoxy-3-hexadecyloxypropyl)thiophospholine using an Arbuzov-Michaelis type reaction [109].
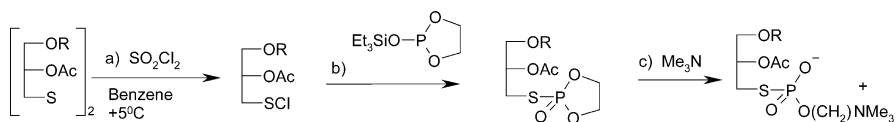
The disulfide derived from a thioglycerol was converted into the corresponding sulfenyl chloride (step a) and allowed to react with 2-triethylsilyloxy-1,3,2-dioxaphospholane to give a cyclic thiophosphate (step b). Reactions a and b were performed as a one-flask procedure and the crude thiophosphate was transformed into the desired thiophosphocholine by opening the phospholane ring with trimethylamine (step c).

9
Final Remarks

The synthesis of PS chiral analogues of biophosphates via P^{III} compounds required as therapeutic continues to attract attention. It is apparent that future perspectives in this fascinating area will focus on finding easy access to chiral P^{III} compounds other than the separation of diastereoisomers and improvements in the stereoselective coupling procedures. So far research efforts in synthesis of new drugs with a phosphorus backbone has paid insufficient attention to cost and difficulties of large scale production [110]. This chapter illustrated the trends with a series of selected examples.

At the same time, procedures based on tetracoordinate phosphorus reagents remain indispensable, for example in the synthesis of polyphosphates [111]. The same refer to procedures based on H-phosphonate chemistry [112]. Emil Fischer found the synthesis of biophosphates fascinating when he first studied them 80 years ago [113]. That fascination has continued ever since drawing into the field a great number of eminent chemist and looks set to intensify.

References

1. Westheimer FH (1992) In: Walsh EN, Griffith EJ, Parry RW, Quin LD (eds) Phosphorus chemistry developments in American sciences. ACS Symposium Series 486, ACS, Washington, DC, pp 1–18
2. a) Kosolapoff MG, Maier L (1972) (eds) Organic phosphorus compounds, vol 1-7. Wiley-Intersciences, New York; b) Edmunson RS. (1988) Dictionary of organophosphorus compounds. Chapman& Hall, London; c) Regitz M (ed) (1982) Methoden der Organischen Chemie (Houben-Weyl), Band E(1) and E(2) (Organischen Phosphorverbindungen), Georg Thime Verlag, Stuttgart, Germany, 1982; d) Hartley FR (1990) The chemistry of organophosphorus compounds, vol 1–4. Wiley, New York; e) Emsley J, Hall D (1976) The chemistry of phosphorus. Harper & Row, London; f) Goldwhite H (1981) Introduction to phosphorus chemistry. Cambridge University Press, Cambridge, UK; g) Hudson RF (1965) Structure and mechanism in organo-phosphorus chemistry. Academic Press, New York; h) Kirby AJ, Warren SG (1967) The organic chemistry of phosphorus. Elsevier, Amsterdam; i) Grayson M, Griffith EJ (eds) (1964–1983) Topics in phosphorus chemistry, vol 1–11. Wiley, New York; j) Engel R (ed) (1992) Handbook of organophosphorus chemistry. Marcel Dekker, New York; k) Pudovik AN (1989) (ed) Chemistry of organophosphorus compounds. MIR Pulishers, Moscow
3. Quin LD (2000) A guide to organophosphorus chemistry. Wiley-Intersciences, Wiley Publication
4. Royal Society of Chemistry (1970–2000) Organophosphorus chemistry. Specialist Periodical Report, Royal Society of Chemistry, London
5. Kosolapoff GM, Maier L (eds) (1973) Organic phosphorus compounds. Wiley, New York London Sydney Toronto
6. The comprehensive source of informations concerning oligonucleotides and other biophosphates up to 1990 are reviewed by: a) Uhlman E, Peyman A (1990) Chemical Reviews 90:453; b) Beaucage SL, Iyer RP (1992) Tetrahedron 48:2223; c) Beaucage SL, Iyer RP (1993) Tetrahedron 49:1925; d) Beaucage SL, Iyer RP (1993) Tetrahedron 49:6123; e)

Beaucage SL, Iyer RP (1993) Tetrahedron 49:10441; f) Nifantiev EE, Grachev MK, Burmistrov SY (2000) Chem Rev 100:3755; g) Hayakawa Y (2001) Bull Chem Soc Jpn 74:1547

7. a) Letsinger RL, Finnan JL, Heavner GA, Lunsford WB (1975) J Am Chem Soc 97:3278; b); Letsinger RL, Lunsford WB (1976) J Am Chem Soc 98:3655

8. a) Beaucage SL, Caruthers MH (1981) Tetrahedron Lett 22:1859; b); Sinha ND, Biernat J, McManus J, Köster H (1984) Nucleic Acids Res 12:4539

9. a) Dahl O (1983) Phosphorus Sulfur 18:201; b) Dahl BH, Nielsen J, Dahl O (1987) Nucleic Acids Res 15:1729; c) Berner S, Mühlegger K, Seliger H (1989) Nucleic Acids Res 17:853

10. Watanabe Y, Maehara S-I, Ozaki S (1992) J Chem Soc Perkin Trans 1 1879

11. a) Karl RM, Richter W, Klösel R, Mayer M, Ugi I (1996) Nucleotides Nucleotides 15(1/3):379; b) Dabkowski W, Tworowska I, Michalski J, Cramer F (1995) J Chem Soc Chem Commun 1435; c) Sanghvi YS, Guo Z, Pfundheller HM, Converso A (2000) Org Proc Res Dev 4:175

12. a) Froehler BC, Matteucci MD (1983) Tetrahedron Lett 24:3171; b) Hayakawa Y, Kataoka M (1997) J Am Chem Soc 119:11758; c) Wright P, Lloyd D, Rapp W, Andrus A (1993) Tetrahedron Lett 34:3373; d) Wincott F, DiRenzo A, Schaffer C, Grimm S, Tracz D, Workman C, Sweedler D, Gonzales C, Scaringe S, Usman N (1995) Nucleic Acids Res 23:2677; e) Vargeese C, Carter J, Yegge J, Krivjansky S, Settle A, Kropp E, Peterson K, Pieken W (1998) Nucleic Acids Res 26:1046; f) Moriguchi T, Yanagi T, Kunimori M, Wada T, Sekine M (2000) J Org Chem 65:8229; g) Graham SM, Pope SC (1999) Organic Lett 1:733

13. a) Nurminen EJ, Mattinen JK, Lönnberg H (1998) J Chem Soc Perkin Trans 2 1621; b) Nurminen EJ, Mattinen JK, Lönnberg H (1999) J Chem Soc Perkin Trans 2 2551; c) Nurminen EJ, Mattinen JK, Lönnberg H (2000) J Chem Soc Perkin Trans 2 2238; d) Nurminen EJ, Mattinen JK, Lönnberg H (2001) J Chem Soc Perkin Trans 2 2159; e) Nifantyev EE, Gratchev MK, Burmistrov SY, Vasyanina LK, Antipin MY, Struchkov YT (1991) Tetrahedron 47:9839

14. a) Tanigawa Y, Nishimura K, Kawasaki A (1982) Tetrahedron Lett 23:5549; b) Hayakawa Y, Uchiyama M, Kato H, Noyori R (1985) Tetrahedron Lett 26:6505

15. Stec WJ, Zon G (1984) Tetrahedron Lett 25:5279

16. Noyori R, Tokunaga M, Kitamura M (1995) Bull Chem Soc Jpn 68:35

17. Schell P, Engels JW (1998) Tetrahedron Lett 39:8629

18. Schell P, Engels JW (1997) Nucleosides Nucleotides 16(5/6):769

19. Lu Y, Just G (2001) Tetrahedron 57:1677

20. a) Hayakawa Y, Kataoka M, Noyori R (1996) J Org Chem 61:7996; b) Hayakawa Y, Kataoka M (1998) J Am Chem Soc 120:12,395; c) Hostomsky Z, Smrt J, Arnold L, Tocik Z, Paces V (1987) Nucleic Acids Res 15:4849; d) Gryaznov SM, Letsinger RL (1992) Nucleic Acids Res 20:1879; e) Beier M, Pfleiderer W (1999) Helv Chim Acta 82:879; f) Brill WK-D, Nielsen J, Caruthers MH (1991) J Am Chem Soc 113:3972; g) Eluteri A, Capaldi DC,. Krotz AH, Cole DL, Ravikumar VT (2000) Org Proc Res Dev 4:182; h) Fourrey JL, Varenne J (1984) Tetrahedron Lett 25:4511; i) Salamończyk GM, Kuznikowski M, Poniatowska E (2002) Tetrahedron Lett 43:1747; j) Hayakawa Y, Kawai Y, Hirata A, Sugimoto J, Kataoka M, Sakakura A, Hirose M, Noyori R (2001) J Am Chem Soc 123:8165

21. Oka N, Wada T, Saigo K (2002) J Am Chem Soc 124:4962

22. Stec WJ, Karwowski B, Boczkowska M, Guga P, Koziołkiewicz M, Sochacki M, Wieczorek MW, Blaszczyk J (1998) J Am Chem Soc 120:7156

23. Wilk A, Grajkowski A, Phillips LR, Beaucage SL (2000) J Am Chem Soc 122:2149

24. Yu D, Kandimalla ER, Roskey A, Zhao Q, Chen L, Chen J, Agrawal S (2000) Bioorg Med Chem 8:275

25. Beyer TA, Sadler JE, Rearick JI, Paulson JC, Hill RL (1981) Adv Enzymol Relat Areas Mol Biol 52:23

26. Kajihara Y, Ebata T, Koseki K, Kodama H, Hashimoto H (1995) J Org Chem 60:5732

27. Eleuteri AE, Capaldi DC, Cole DL, Ravikumar VT (1999) Nucleosides Nucleotides 18(80):1879
28. Dabkowski W, Tworowska I, Michalski J, Cramer F (2000) Tetrahedron Lett 41:7535
29. Zhang Z, Tang JY (1996) Tetrahedron Lett 37:331
30. Unpublished preliminary results from this laboratory
31. Dabkowski W, Tworowska I (1995) Tetrahedron Lett 36:1095
32. Tataku H, Watanabe T, Hamamoto S (1988) Tetrahedron Lett 29:81
33. Cypryk M, Chojnowski J, Michalski J (1985) Tetrahedron 41:2471
34. a) Dabkowski W, Tworowska I, Michalski J, Cramer F (1997) Chem Commun 877; b) Dabkowski W, Tworowska I, Michalski J, Poniatowska E, Cramer F (1999) Phosphorus Sulfur Silicon 144:109
35. Grachev MK, Mishina VY, Nifantiev EE (1993) Zh Obshch Khim 60:2638
36. Snyder DS (1995) J Org Chem 60:2638
37. a) Dabkowski W (unpublished result); b) Marsault E, Just G (1998) Nucleosides Nucleotides 17(5):939
38. Baschang G, Kvita V, (1973) Angew Chem 44
39. Lindberg J, Ekeroth J, Konradsson P (2002) J Org Chem 67:194
40. Mills SJ, Liu C, Potter BV (2002) Carbohydr Res 337:1795
41. Potter BVL, Lampe D (1995) Angew Chem Int Ed Engl 34:1933
42. a) Jiang ZH, Budzynski WA, Skeels LN, Krantz MJ, Koganty RR (2002) Tetrahedron 58:8833; b) Jiang ZH, Bach MV, Budzynski WA, Krantz MJ, Koganty RR, Longenecker BM (2002) Bioorg Med Chem Lett 12:2193
43. Earle MJ, Abdur-Rashid A, Priestley ND (1996) J Org Chem 61:5697
44. Shin TL, Wu SH (2000) Tetrahedron Lett 41:2957
45. Armstrong JI, Verdugo DE, Bertozzi CR (2003) J Org Chem 68:170
46. Shuto S, Yahiro Y, Ichikawa S, Matsuda A (2000) J Org Chem 65:5547
47. a) Watanabe Y, Komoda Y, Ebisuya K, Ozaki S (1990) Tetrahedron Lett 31:25,546; b) Watanabe Y, Komoda Y, Ozaki S (1992) Tetrahedron Lett 33:1313
48. Crich D, Dudkin V (2002) J Am Chem Soc 124:2263
49. Bannwarth W, Küng E (1989) Tetrahedron Lett 30:4219
50. Chen J, Prestwich GL (1997) Tetrahedron Lett 38:969
51. Manoharan M, Lu Y, Casper MD, Just G (2000) Org Lett 2(3):243
52. Kupihár Z, Váradi G, Monostori É, Tóth GK (2000) Tetrahedron Lett 41:4457
53. a) Bannwarth W, Trzeciak A (1987) Helv Chim Acta 70:175; b) Starker G, Jakobsen MH, Olsen EC, Holm A (1991) Tetrahedron Lett 32:5389
54. Kadokura M, Wada T, Seio K, Sekine M (2000) J Org Chem 65:5104
55. Alberg DG, Lauhon CT, Nyfeler R, Fässler A, Bartlett PA (1992) J Am Chem Soc 114:3535
56. Himmelsbach F, Schulz BS, Trichtinger T, Charubala R, Pfleiderer W (1984) Tetrahedron 40:59
57. Sekine M, Tsuruoka H, Iimura S, Kusuoku H, Wada T (1996) J Org Chem 61:4087
58. Bochet CG (2002) J Chem Soc Perkin Trans 1 125
59. Rothman DM, Vazquez ME, Vogel EM, Imperiali B (2002) Org Lett 4:2865
60. Perich JW, Johns RB (1988) Synthesis 142
61. Chao H-G, Bernatowicz MS, Klimas CE, Matsueda GR (1993) Tetrahedron Lett 34:3377
62. Bialy L, Waldmann H (2002) Angew Chem Int Ed Engl 41:1748
63. Boger DL, Ichikawa S, Zhong W (2001) J Am Chem Soc 123:4161
64. Watanabe Y, Nakatomi M (1999) Tetrahedron 55:9743
65. Murugan R, Scriven EFV (2003) Aldrichimica Acta 36:21
66. Schluster U, Lu J, Fraser-Reid B (2003) Org Lett 5:255
67. Dabkowski W, Michalski J, Qing W (1990) Angew Chem Int Ed Engl 29:522
68. Seela F, Kretschmer U (1990) J Chem Soc Chem Commun 1154
69. Li P, Shaw BR (2002) Chem Commun 2890
70. Ravikumar VT, Cheruvallath ZS, Cole DL (1997) Nucleosides Nucleotides 16(7/9):1709

71. Mangos MM, Min K-L, Viazovkina E, Galarneau A, Elzagheid MI, Parniak MA, Damha MJ (2003) J Am Chem Soc 125:654
72. McInnes JL, Symons RS (1989) In: Symons RH (ed) Nucleic acid probes. CRC Press, Boca Raton FL, p 33
73. Olejnik J, Krzymanska-Olejnik E, Rothschild K (1996) Nucleic Acids Res 24:361
74. a) Lefebver I, Périgaud C, Pompon A, Aubertin A-M, Girardet J-L, Kirn A, Gosselin G, Imbach J-L (1995) J Med Chem 38:3941; b) Peyrottes S, Coussot G, Lefebvre I, Imbach J-L, Gosselin G, Aubertin A-M, Perigaud C (2003) J Med. Chem 46:782
75. Letsinger RL, Schott ME (1988) J Am Chem Soc 103:7394
76. Eritja R, Smirnov V, Caruthers MH (1990) Tetrahedron 46:721
77. Helinski J, Dabkowski W, Michalski J (1993) Nucleosides Nucleotides 12(60):597
78. Helinski J, Dabkowski W, Michalski J (1993) Tetrahedron Lett 34:6451
79. Reed R, Reau R, Dahan F, Bertrand G (1993) Angew Chem Int Ed Engl 32:399
80. Mizuguchi M, Makino K (1996) Nucleosides Nucleotides 15(1/3):407
81. Tworowska I (2001) PhD thesis, PAN CBMM Lodz
82. a) Dabkowski W, Tworowska I (2001) J Chem Soc Perkin Trans 1 2462; b) Dyatkina N, Arzumanov A, Krayevsky A, O'Hara B, Gluzman Y, Baron P, MacLow C, Polsky B (1994) Nucleosides Nucleotides 13(1/3):325
83. Tworowska I, Dabkowski W, Kazmierczak L, Michalski J (2002) J Organomet Chem 643/644:490
84. Tworowska I, Dabkowski W, Michalski J (2001) Angew Chem Int Ed 40:2898
85. Stec WJ, Zon G, Egan W, Byrd RA, Philips LR, Gallo K (1985) J Org Chem 50:3908
86. de Vroom E, Spierenburg ML, Dreef CE, van der Marel GA, van Boom JH (1987) Recl Trav Chim Pays-Bas 106(2):65
87. Mag M, Muth J, Jahn K, Peyman A, Kretzschmar G, Engels WJ, Uhlmann E (1997) Bioorg Med Chem 5:2213
88. Luczak L, Lopusinski A, Michalski J (1998) Tetrahedron 54:9731
89. Helinski J, Dabkowski W, Michalski J (1991) Tetrahedron Lett 32:4981
90. An H, Wang T, Maier MA, Manoharan M, Ross BR, Cook PD (2001) J Org Chem 66:2789
91. Boyd EA, Regan AC (1994) Tetrahedron Lett 35:4223; Reiter LA, Jones BP (1997) J Org Chem 62:2808; Rivero IA, Somanathan R, Hellberg LH (1993) Synth Commun 23:711
92. Wada T, Ishikawa K, Hata T (1993) Tetrahedron 49:2043
93. Xu B, Stephens A, Kirschenheuter G, Greslin AF, Cheng X, Sennelo J, Cattaneo M, Zighetti ML, Chen A, Kim S-A, Kim HS, Bischofberger N, Cook G, Jacobson KA (2002) J Med Chem 45:5694
94. Martin SF, Wagman AS (1993) J Org Chem 58:5897
95. Okruszek A, Sierzchala A, Sochacki M, Stec WJ (1992) Tetrahedron Lett 33:7585
96. Dellinger D, Sheehan DM, Christensen NK, Lindberg JG, Caruthers MH (2003) J Am Chem Soc 125:940
97. Sun XB, Kang JX, Zhao YF (2002) Chem Commun 2414
98. Claesen CAA, Segers RPAM, Tesser GI (1985) Recl Trav Chim Pays-Bas 104:119
99. Letsinger RL, Groody EP, Lander N, Tanaka T (1984) Tetrahedron 40:137
100. Eckstein F, Rizk I (1967) Angew Chem In Ed Engl 6:949
101. Mills SJ, Potter BVL (1997) J Chem Soc Perkin Trans 1 1279
102. Meier C (1996) Angew Chem Int Ed Engl 35:70
103. Lin JL, Shaw BR (2000) Chem Commun 2115
104. Ludwik J, Eckstein F (1991) J Org Chem 56:1777
105. Guga P, Okruszek A, Stec WJ (2002) Recent advances in stereocontrolled synthesis of P-chiral analogues of biophosphates. In: Majoral J-P (ed) Top Curr Chem 220:169
106. Brown JE, Driver MJ, Russell JC, Sammes PG (2000) J Chem Soc Perkin Trans 1 653
107. Martin SF, Wagman AS, Zipp GG, Gratchev MK (1994) J Org Chem 59:7957
108. Salomonczyk G, Rehnberg N, Krawiecka B, Michalski J (1997) Tetrahedron Lett 38:647
109. Mlotkowska B, Olejnik B (1995) Liebigs Ann 1467

110. Mihaichuk JC, Hurley BH, Vagle KE, Smith RS, Yegge JA, Pratt GM, Tompkins CJ, Sebesta DP, Pieken WA (2000) Org Proc Res Dev 4:214
111. a) Burgess K, Cook D (2000) Chem Rev 100:2047; b) Reese CB (2002) Tetrahedron 58:8893
112. Stawinski J (1992) Some aspects of H-phosphonate chemistry. In: Engel R (ed) Handbook of organophosphorus chemistry. Marcel Dekker, New York, p 377; Stawinski J, Kraszewski A (2002) Acc Chem Res 35:952
113. Fischer E (1914) Ber Dtsch Chem Ges 3193

Hybrid Organic-Inorganic Materials Based on Organophosphorus Derivatives

André Vioux · Jean Le Bideau · P. Hubert Mutin · Dominique Leclercq

UMR CNRS 5637, Université de Montpellier 2, Case 007, Place E. Bataillon,
34095 Montpellier 5, France
E-mail: vioux@univ-montp2.fr

Abstract Because P-O-Metal and P-C linkages are quite stable, organophosphorus derivatives offer a general alternative to silicon-based coupling in the field of organic/inorganic hybrid materials, covering a wide range of application: ion exchange, proton conductors, catalysts, sensors, membranes etc. This review surveys two classes of hybrid solids in which the organic part is introduced through phosphorus groups. In the first class (which includes metal phosphonates, metal phosphinates, and related mono- and dialkylphosphates) the organic and inorganic parts are linked in the repeated structural unit ordered in a crystal network (molecular crystals, one-, two-, or three-dimensional solids). The second class corresponds to inorganic substrates (mainly metal oxides) modified by organophosphorus groups that are grafted on the surface; alternatively organophosphorus groups may be incorporated into metal oxides by sol-gel processing.

Key words Phosphonate · Phosphinate · Phosphate · Surface modification · Sol-gel

1
Introduction

The development of organic-inorganic hybrid materials, which is currently booming [1], aims at combining the physical and chemical properties of inorganic and organic components, for applications such as scratch resistance coatings, contact lenses, dental filling, sensors, membranes, catalysis, chromatography, ion extraction, etc. The binding of organic moieties within inorganic matrices or on inorganic supports mainly relies on the use of silicon-based precursors, owing to the hydrolytic stability of Si-C bond. Organo-functional silanes (typically $RSi(OEt)_3$) are widely used in sol-gel processing, either as a single precursor, or copolymerized with another alkoxide precursor (usually tetraethoxysilane). Materials named "ormosils" (organically modified silicas) or "ormocers" (organically modified ceramics) are prepared in this manner. Organosilanes are also used as coupling agents, for instance to modify the surface of particulate fillers or fibers in the field of composite materials, to make molecular catalysts heterogeneous, or to prepare self-assembled monolayers on silica surfaces.

The aim of this survey is to highlight that organophosphorus compounds, such as phosphonic and phosphinic acids and their derivatives (salts, esters), offer an attractive alternative to organosilanes coupling molecules. Actually the P-C bond is as stable as the Si-C bond toward hydrolysis and the versatile phosphorus chemistry makes a wide range of functional organic groups available. Moreover, unlike Si-O-C bonds, P-O-C bonds are cleaved only under harsh hydrolytic conditions, such as refluxing in concentrated HCl solution, which makes it possible to use monoalkyl and dialkyl phosphoric acids as tri- and bidentate reagents, respectively, as well as phosphonic and phosphinic derivatives (Fig. 1).

Unlike silanol groups, acidic P-OH groups cannot self-condense in solution, which discards the formation of P-O-P bonding. The formation of frameworks including phosphorus groups involves P-O-Metal linkages (as in
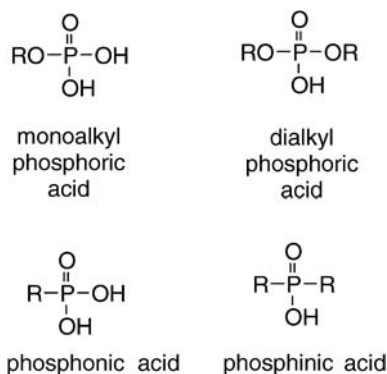
Fig. 1 Tridentate and bidentate organophosphorus reagents

inorganic metal phosphates), or P=N-linkages as in polyphosphazenes. Polyphosphazenes $(R_2P=N-)_n$ are often compared to polysiloxanes for their physical properties. They form an important class of polymers that has been widely reviewed [2–4], and therefore they are not covered here. The scope of the present review is limited to two classes of hybrid solids in which the organic part is introduced through phosphorus groups.

In the first class (which includes metal phosphonates, metal phosphinates, and related mono- and dialkylphosphates) both the organic and inorganic moieties belong to a structural unit repeated in an ordered 1-D, 2-D, or 3-D arrangement.

In the second class the organic moiety is bonded through a phosphorus group to the surface of an inorganic substrate (metal oxide or salt). This corresponds to the grafting of organophosphorus groups on the surface of preformed inorganic supports. Alternatively, in the case of metal oxides the inorganic substrate may be formed in situ by sol-gel processing or precipitation.

2
Metal Phosphonates and Phosphinates, and Related Mono- and Dialkylphosphates

The development of the large family of microporous metal phosphates has prompted many works with organophosphorus precursors over the past decade. In metal phosphonates, the phosphonate tetrahedron O_3PC features a basal plane defined by the three oxygen atoms and a corner bearing a more or less bulky and hydrophobic organic group; such pattern favors layered (two-dimensional) assembly. However one-dimensional and three-dimensional metal phosphonates may be obtained depending on the metal atoms, the organic groups and the synthesis parameters. Lowering the connectivity around the phosphorus atom can be done by introducing a second P-C bond, i.e., by using phosphinic acids $R_2P(O)OH$, which leads to metal phosphinates that mostly present chain arrangements. Finally, playing with the choice of the organic moiety as well as with the synthesis parameters may produce molecular (zero-dimensional) compounds. We will hereafter illustrate these points without intention to be exhaustive in the presentation of known phosphonates, phosphinates, and alkylphosphates.

2.1
Metal Phosphonates

2.1.1
Layered Structures

Metal phosphonates are usually prepared by reaction of phosphonic acids with metal salts under hydrothermal conditions [5–7]. Layered structures are predominant for most metals, the organic group being oriented more or
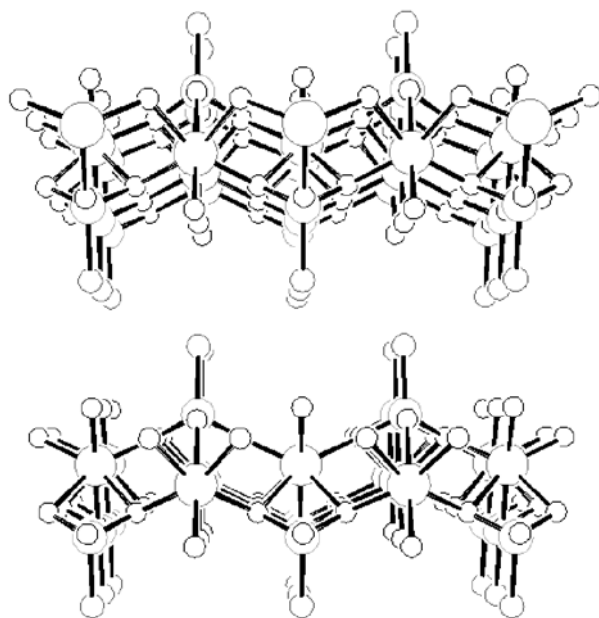
Fig. 2 Layers of $Zn(O_3PCH_3) \cdot H_2O$ showing pending methyl groups

less perpendicularly into the interlamellar region. However, divalent metal phosphonates are noticeable by the high number of compounds with fully determined isotype crystallographic structures.

One typical structure is obtained with most divalent metals phosphonates $M^{II}(O_3PR) \cdot H_2O$ [8–10]. This structure consists of quite compact layers of metals in an octahedral environment of oxygen atoms (Figs. 2 and 3). These octahedrons share four corners with neighboring octahedrons, one corner with a phosphonate tetrahedron and one edge with another phosphonate tetrahedron. The last corner is occupied by a coordinated water molecule. The phosphonate tetrahedron, made of three oxygen atoms and one carbon atom, has its oxygen atoms base nearly parallel to the inorganic layer, the carbon atom (hence the organic group) pointing toward the interlamellar space (thus, the interlayer distance is directly related to the size of the organic group). However it is noteworthy that the propensity of the metal atom for a peculiar coordination geometry may be strong enough to depart from the typical structural arrangement described above, as observed for the copper atom in $Cu^{II}(O_3PR) \cdot H_2O$, which adopts a two-dimensional structure with a square pyramidal environment for the metal atom [11].

Due to the number of isotype compounds, systematic studies of physical properties of divalent metals phosphonates are of interest. For instance, systematic studies of magnetic properties could be carried out by varying the paramagnetic metal center [8, 12]. The organic part may also be varied systematically in order to determine the origin of a cooperative effect yielding
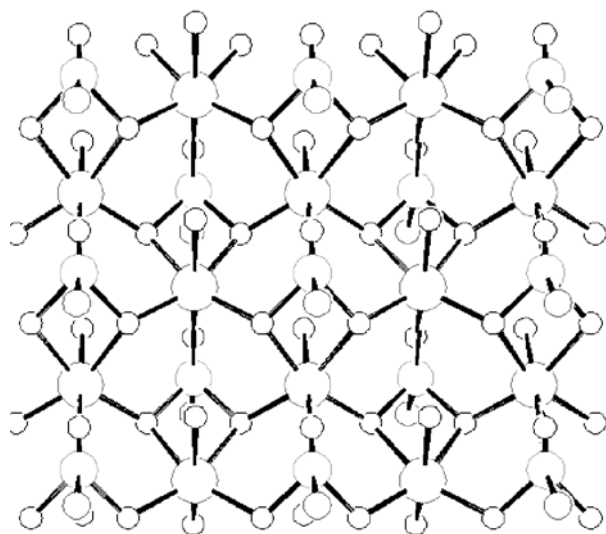
Fig. 3 Top side view of a layers of Zn(O$_3$PCH$_3$)·H$_2$O; Zn atoms are in octahedral environment and share four corners with neighboring octahedrons

a macroscopic property: modification of the interlamellar distance as in (VO)^{II}(O$_3$PR)·H$_2$O [13] and in Fe^{II}(O$_3$PR)·H$_2$O [14], or modification of the electronic energy levels on the phosphorus atom as in (VO)^{II}(O$_3$PR)·H$_2$O [15], without any modification of the structure of the inorganic layers.

Layered structures are also common in trivalent metal phosphonates [16–18], and practically the sole ones in tetravalent metal phosphonates. Most metal IV phosphonates, such as Zr(O$_3$PPh)$_2$ [19, 20], present a structure in which the metal atom is coordinated to six different phosphonate groups through the oxygen atoms.

2.1.2
Other Structures

Crystalline self-assembly does not always result in layered arrangement. Several microporous compounds with tubular channels have been obtained, such as β-Cu(O$_3$PCH$_3$) (Fig. 4) [21], and β-Al$_2$(O$_3$PCH$_3$) [22, 23]. The diameters found in the channels ranged from 6 to 10 Å, the methyl groups pointing toward the center of the channels, giving them a hydrophobic character. The microporous aluminum methylphosphonate β-Al$_2$(O$_3$PCH$_3$) has also been synthesized in the presence of 1,4-dioxane, part of which is found included in the resulting compound. It was shown that the dioxane molecules could be removed upon heating, and that further heating in the presence of water resulted in the transformation into the closely related α-Al$_2$(O$_3$PCH$_3$) [24].
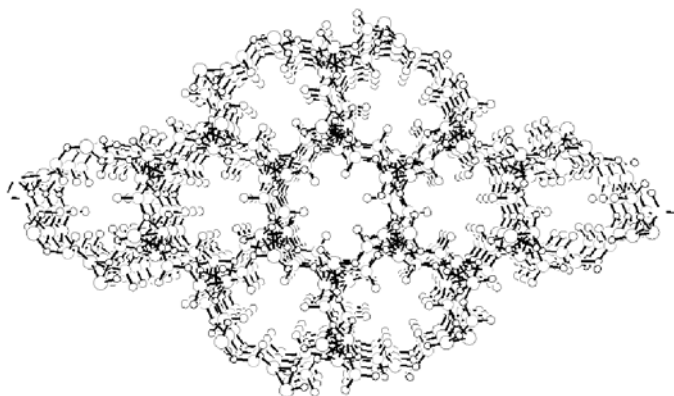
Fig. 4 Hydrophobic channels of β-Cu(O$_3$PCH$_3$); the methyl groups point toward the center of the channels (after [21])

Besides this, one-dimensional compounds such as several uranyl phosphonates, among which UO$_2$(O$_3$PC$_6$H$_5$)·0.7H$_2$O (Fig. 5) [25], and one vanadyl phosphonate, (H$_3$O)((V$_3$O$_4$)(H$_2$O)(O$_3$PC$_6$H$_5$)$_3$)·2.33H$_2$O [26], feature molecular tubes with a hydrophilic character. In these cases, the phenyl rings point outside and away from each inorganic tubes and the water molecules are located at the center of the tubes. The diameter of the tubes in these compounds was around 12 Å. It is noteworthy that the uranyl/oxygen/phos-
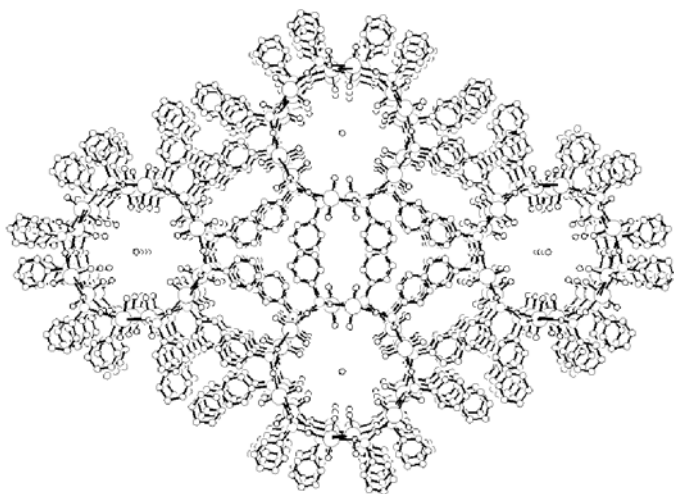
Fig. 5 Hydrophilic channels of UO$_2$(O$_3$PC$_6$H$_5$)·0.7H$_2$O; for clarity, an oxygen atom from a water molecule have been schematically drawn at the center of the channels in order to feature the average water position (after [25])

phorus bonding within the walls of the tube was similar to that found in the lamellar compound $UO_2(O_3PCH_2Cl)$ [27].

2.1.3
Influence of the Organic Group on the Structure

The effect of bulky organic groups on the structure is well illustrated in the vanadyl series, where two different layered structures, $(VO)(O_3PR)\cdot H_2O$ and $(VO)(O_3PR)\cdot 1.5H_2O$, were obtained for a phenyl group, and a chlorinated or a methylated phenyl group, respectively. The surface available on the layer per phosphonate group was 32 Å^2 in $(VO)(O_3PR)\cdot H_2O$ and 36 Å^2 in $(VO)(O_3PR)\cdot 1.5H_2O$, reflecting the bulkiness of the organic groups [13]. Either a more hydrated phase or the use of a bulkier group gave the structural type $(VO)^{II}(O_3PR)\cdot 2H_2O$, with 52 Å^2 available per phosphonate group. In this structure, the vanadyl octahedra are separated from each other by phosphonato bridges [28]. Another interesting illustration of the effect of the bulkiness of the organic group is brought by cobalt II phosphonates. Whereas these metal phosphonates exhibit the common flat lamellar arrangement with alkyl and phenyl groups, with *tert*-butyl group the bulkiness of the organic moiety leads to a lamellar but corrugated arrangement, in which cobalt atoms are found in octahedral as well as in tetrahedral sites (Fig. 6) [29].
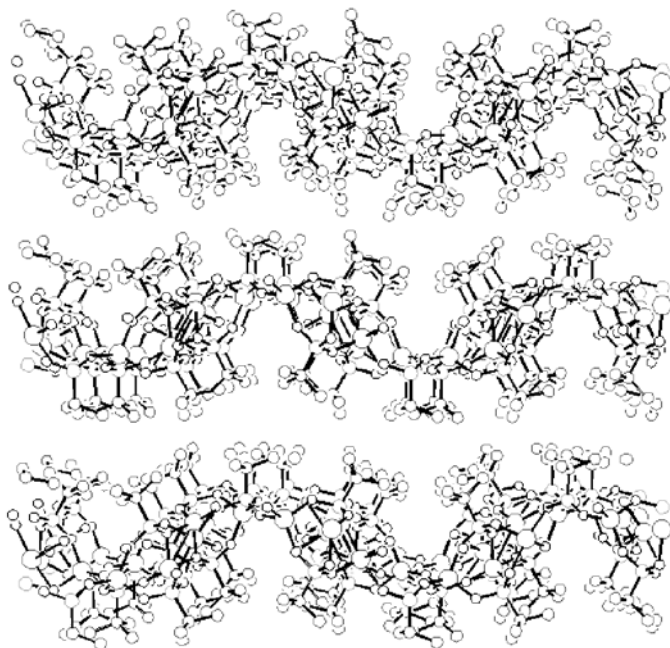
Fig. 6 Corrugated layers of $Co(O_3P\text{tert-Bu})\cdot H_2O$ (after [29])
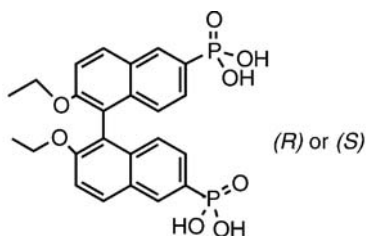
Fig. 7 (*R*)- or (*S*)-2,2′-diethoxy-1,1′-binaphtalene-6,6′-bis(phosphonic acid)

Striking examples of the way by which the organic moiety drives the coordination chemistry of phosphonic acids with metals are given by the preparation of enantiomerically pure metal phosphonates. Thus, the reaction of pure enantiomeric (R)-PhRP*(O)CH$_2$PO$_3$H$_2$ with zinc nitrate in aqueous solution yielded enantiomerically pure layered zinc phosphonates keeping the same configuration on the phosphorus atom of the phosphine oxide [30, 31]. It is noteworthy that the layered arrangement was drastically different in the racemic series. Moreover the reaction of (*R*)- or (*S*)-2,2′-diethoxy-1,1′-binaphtalene-6,6′-bisphosphonic acid (Fig. 7) with MnCO$_3$, CoCO$_3$, 2Ni-CO$_3$·3Ni(OH)$_2$·4H$_2$O, CuO, and Zn(ClO$_4$)$_2$·6H$_2$O led to the corresponding metal phosphonates with open-framework structures. Solid-state circular dichroism indicated the formation of supramolecular enantiomers. Such homochiral porous metal phosphonates may find applications in enantioselective separation and asymmetric catalysis [32].

2.1.4
Use of Bi- and Trifunctional Phosphonate Groups. Pillared Structures

One way to induce structural variations is to increase the hapticity of the phosphonate group, that is using organic groups with a functional end, such as hydroxyl, amine, amide, carboxylate, and carboxylic acid groups, which can coordinate to the metal atoms. In many cases, this way results in the formation of two-dimensional inorganic layers connected by the organic groups forming pillars, which gives a three-dimensional character to the structure. Carboxyphosphonic acids most often produce such pillared structures. This is illustrated by Zn$_3$(O$_3$PC$_2$H$_4$CO$_2$)$_2$ [33] or Co$_3$(O$_3$PC$_2$H$_4$CO$_2$)$_2$ [34] where metal atoms are found in tetrahedral as well as in octahedral coordination sites, by Mn$_3$(O$_3$PCH$_2$CO$_2$)$_2$ where manganese atoms are found in octahedral, square pyramidal and tetrahedral coordination sites [35, 36] and by Pb$_3$(O$_3$PCH$_2$CH$_2$CO$_2$)$_2$ where divalent lead atoms are found in three, four and five-coordination sites [37, 38]. Other functional phosphonate groups have led to microporous crystalline solids, such as the amine derivative Zn(O$_3$PC$_2$H$_4$NH$_2$) [39], the hydroxy derivative Zn(O$_3$PCH$_2$OH) [40], and the amide derivative Zn(O$_3$PCH$_2$C(O)NH$_2$)·H$_2$O [41], whose structures exhibit open three-dimensional inorganic frameworks as in β-Cu(O$_3$PCH$_3$) cited above. Nevertheless, once the second functional group is involved in the co-

ordination to the metal atom, it cannot bring anymore functionality to the material: therefore it is interesting to increase the number of functional groups. Phosphonate groups bearing aminoacid [42, 43] or iminodiacetate [44] functionalities have been used for this purpose.

Bis(phosphonic acid)s $H_2O_3PRPO_3H_2$ (R=rigid aryl, flexible alkyl, or alkyl-aryl group) are widely used to form covalent pillars between layers. The zirconium derivatives have been presented in a recent review [7]. The latest works on bis(phosphonate)s may be illustrated by the synthesis of $Ti(O_3P(CH_2)_nPO_3)$ (n=2, 3) [45], $Cu_2(O_3PCH_2PO_3)$ [46], and $Ga_4(O_3PC_2H_4PO_3)_3$ [18]. Moreover a variety of templates along with bis(phosphonic acid)s have been introduced, aiming at directing the organization. A good example is given by the family of templated vanadyl bisphosphonates, which presents 1D, 2D, and 3D structures depending on the template as well as on the phosphonic acid used [47]. A lot of compounds have been obtained with templates such as alkyldiamines among which compounds are such as $(NH_3(CH_2)_2NH_3)Zn(hebpH_2)_2)\cdot 2H_2O$ (hebpH$_2$=1-hydroxyethylidenebisphosphonate) [48] or $(NH_3(CH_2)_2NH_3)Cu_3(hebp)_2$ [49].

2.1.5
Some Applications of Layered and Pillared Metal Phosphonates

The rich structural variety described above initiated numerous studies aiming at designing structural arrangements with attainable functional groups, for applications such as ion exchange, sensing, proton conductivity, catalysis, etc. However, most applications to date have focused on layered (and pillared) metal phosphonates, which show high potential for intercalation, exchange and in situ chemistry.

Intercalation of chemical species has been widely studied in layered phosphonates. Vanadyl phosphonate $(VO)^{II}(O_3PR)\cdot 2H_2O$ exhibits the capability of exchanging water by primary alcohols with alkyl chains from 2 to 18 carbon atoms [50]. In layered vanadyl naphthylphosphonate, the interdigited naphthalene chromophores can form excimers; the fluorescent emission was shown to vary with the length of the intercalated alcohol, which opens possible applications as sensors [51]. The same approach has been carried out for the intercalation of primary alkylamines and alkanediols in $(VO)^{II}(O_3PR)\cdot 2$-H_2O and $(VO)^{II}(O_3PR)\cdot 1.5H_2O$ [52, 53]. The exchange of coordinated water by primary amines in copper, zinc, cobalt, and cadmium phosphonates has already been reviewed [5]. One noteworthy feature in these intercalation reactions is the shape selectivity since only primary alcohols or amines are intercalated, while secondary and tertiary alcohols and amines are excluded due to steric impossibilities for them to migrate up to the coordination site.

Layered metal IV phosphonates are widely used, particularly zirconium phosphonates, because their synthesis is versatile and their structural arrangement may be tailored to applications. Zirconium phosphonates are usually prepared by heating an aqueous solution of a metal IV salt (e.g., $ZrOCl_2$) with a phosphonic acid at 60–80 °C; synthesis in the presence of HF permits one to increase significantly the crystallinity of the final products.
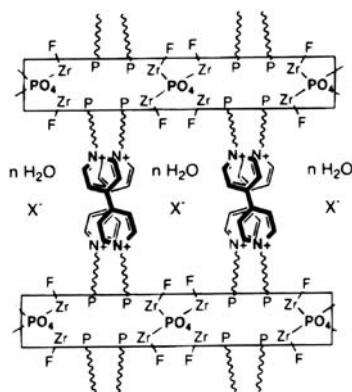
Fig. 8 Schematic representation of $Zr_2(PO_4)(O_3PCH_2CH_2(bipyridyl)CH_2CH_2PO_3)X_3 \cdot 3-H_2O$ (X=halide) (from [57] with permission)

Metal IV layered compounds may be used as mixed forms: mixed phosphate/phosphonate, mixed phosphite/phosphonate, mixed phosphonates. Mixed zirconium phosphate/phosphonate may be prepared by the classical way (which leads to α-ZrP type compounds), or from γ-ZrP, by exchange of $O_2PR(OH)$ phosphonate groups for $O_2P(OH)_2$ phosphate groups [54–56]. Recently a third type has been obtained by co-precipitation, depending on the phosphoric acid relative amount, where both PO_4 bridging orthophosphate sites (γ-ZrP type) and O_3PR bridging phosphonate sites (α-ZrP type) are present [44, 57, 58] (Fig. 8).

Good proton conductivities were found in sulfophenyl and sulfobenzyl zirconium phosphonates obtained by exchange reactions from γ-ZrP [54] as well as in α-ZrP type $Zr(O_3PC_6H_4SO_3H)_2$ [59], with values ranging from 0.02 to 0.05 Ω^{-1} cm^{-1} at room temperature. The conductivity is thought to result from adsorbed water and fluorine ions (ammonium fluoride is used in the synthesis) as well as from the presence of the sulfonic acid groups. Zirconium phosphonates containing sulfophenyl groups, alone or mixed with hydrophobic alkyl groups, also found applications as acid catalysts in organic synthesis [60, 61].

The lack of accessibility of the organic groups in layered metal phosphonates often hinder their use in applications such as catalysis or ion exchange. Several strategies have been used in order to enhance the accessibility. The idea of creating porosity by alternating pillar groups and small functional pendent groups (POH, PH), which was originally proposed by Dines and coworkers, gave rise to many studies that have been recently reviewed [7, 62, 63]. It appears that the synthesis by co-precipitation of crystalline mixed phases with both pillars and pendent groups homogeneously distributed in the same layers is not straightforward, because segregation often takes place in the presence of HF. Alberti et al. proposed to overcome this tendency to segregation by using pillars with broad bases, namely 4,4′-(3,3′,5,5′-tetramethylbiphenylene) bis(phosphonate), to force the alternation
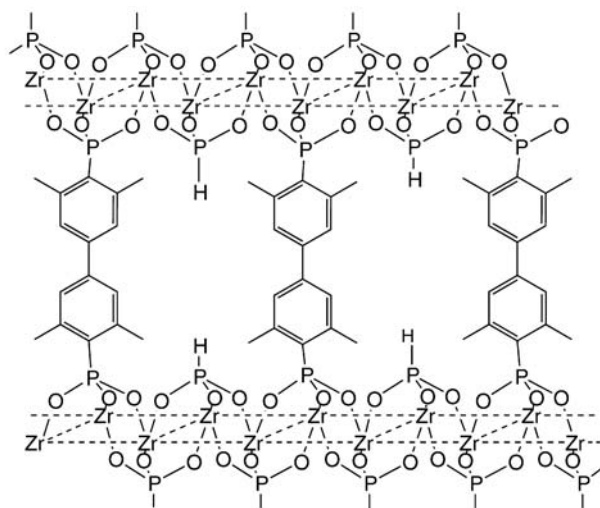
Fig. 9 Schematic representation of pillared α-zirconium phosphite-4,4'-(3,3',5,5'-tetramethylbiphenylene)bis(phosphonate) [64, 65]

of pillars and phosphite groups (Fig. 9) [64, 65]. Another possibility is to avoid the use of HF. Thus, microporous zirconium phosphate/biphenylenebis(phosphonate) were obtained by a nonhydrolytic sol-gel route followed by a mild hydrothermal treatment. [66] Actually, it seems that the key point is to avoid aqueous synthesis, as suggested by Clearfied's work [7, 62]. However all these approaches are rather limited: in practice only small micropores are attainable, which restricts the range of organic functions that can be incorporated and the size of the substrates that can be accommodated in the pores.

Functional pillars may be also introduced for specific applications. For instance bipyridine pillars (namely 2,2'-bipyridyne-5,5'bis(phosphonate)) have been introduced in zirconium and indium phosphonates [67, 68]. In the case of zirconium, two strategies were investigated for gaining porosity, leading either to mixed phosphite/phosphonate compounds of the α-ZrP type, or to phosphate/phosphonate compounds derived from γ-ZrP [67]. The compound $Zr(PO_4)(H_2PO_4)_{0.5}(O_3P\text{-bipy-}PO_3H)_{0.5} \cdot 2H_2O$ was found to be essentially microporous with a narrow distribution of pore size centered around 5 Å. The accessibility of bipyridine complexing sites was evidenced with the two types of materials by a rapid uptake of Cu(II) and Fe(II) from methanolic solutions. Such materials offer promising prospects in metal ions removal and supported catalysis.

Pillared polyethers and polyimines have been also described, which present sorbent and ion exchange properties [7, 56]. Immobilization of crown ethers and diaza crown ethers has been carried out with the bisphosphonate pillars strategy by using the co-precipitation synthesis [44, 58]. Exchange re-

actions on γ-ZrP led to pillared layered ion exchangers showing selective recognition [69].

Zirconium compounds pillared by a viologen-containing group have been prepared using N,N'-ethyl-4,4'-bipyridyl bis(phosphonic) acid [70, 71]. Compound $Zr_2(PO_4)(O_3PCH_2CH_2(bipyridyl)CH_2CH_2PO_3)X_3·3H_2O$ (X=fluoride; Fig. 8), prepared by hydrothermal synthesis, was crystalline and its structure was solved from powder diffraction data [57]. The exchange of anionic metal halides, $(MX_4)^-$, for the halide ions, followed by reduction with dihydrogen gas, yielded colloidal metal M (Pt, Pd) particles, while viologen groups turned blue or purple. Exposure to air resulted in bleaching of the solid. However Pt and Pd colloids are able to act as microelectrodes for the reduction of viologen by dihydrogen, and subsequent electron transfer to dioxygen gives hydrogen peroxide. The catalytic system also reduces hydrogen peroxide to water in the presence of dihydrogen, but at a much slower rate. So, bubbling a mixture of H_2/O_2 through an aqueous suspension of the reduced material led to very efficient production of H_2O_2 (up to 40% yield based on H_2 consumed) [72].

2.2
Metal Phosphinates and Related Chain Compounds

There are some cases in which phosphonate groups act as bidentate bridging ligands. Thus, one-dimensional uranyl phosphonate $(UO_2(HO_3PC_6H_5)_2 (H_2O))_2·8H_2O$ presents linear chains formed by uranium atoms in a square pyramidal environment of five oxygen atoms: four coming from four different phosphonato groups and one from one coordinated H_2O molecule [73]. Aryl groups point away from the same side of each chain in a symmetric manner so that alternating hydrophobic and hydrophilic regions are formed. A proton conductivity of $3.25×10^{-3}\ \Omega^{-1}\ cm^{-1}$ was measured at room temperature. The linear chain of zirconium fluorophosphonate $(NH_4)Zr(F_2) [H_3\{O_3PCH_2NH(CH_2CO_2)_2\}_2]·3H_2O·NH_4Cl$ involves bridging bidentate phosphonate groups, the coordination of the zirconium atom being completed by the presence of two fluorine atoms [74]. Nevertheless phosphinate groups are the most convenient organophosphorus ligands to generate chain compounds.

Polymeric metal phosphinates, $M(O_2PRR')_n$, among which the most studied are divalent metal phosphinates [75], form a unique class of inorganic polymers. The interest in these compounds lies in the following features:

- The one-dimensional framework is completely inorganic
- Phosphinate groups are solid bridging ligands and metal phosphinates are usually resistant to oxidation and hydrolysis
- The versatile coordination of metal centers may result in a variable number of bridging phosphinate groups
- The properties result from both the nature of the metal atom and the nature of the organic substituents on the phosphorus atom
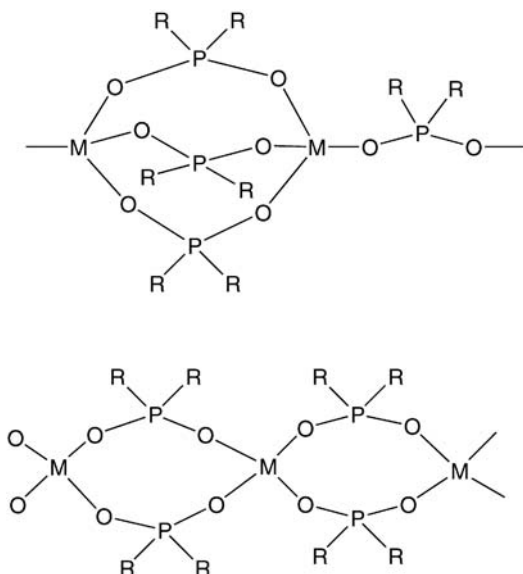
Fig. 10 Schematic representation of the linear chain of poly metal(II) phosphinates, alternating triple and single bridging phosphinate groups, and double bridging phosphinate groups

Metal phosphinates have found applications as coatings and lubricants [76], as flame retardant additives in thermosetting compositions [77], and as pigments [78]. The possibility to introduce specific properties by the organic groups has not been exploited yet.

Polymeric metal phosphinates are usually prepared by reaction of a metal salt with two equivalents of a sodium or potassium salt of the phosphinic acid:

$$MX_2 + 2R_2POONa \rightarrow [M(O_2PR_2)]_n + 2NaX$$

$$M = Be, Co, Cr, Fe, Ni, Mn, Pb, Zn$$

$$X = CH_3COO, Cl, ClO_4, SO_4, NO_3$$
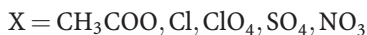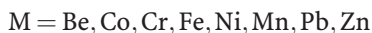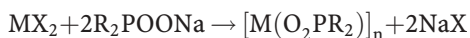
The reaction is usually performed in water, but sometimes without solvent or in EtOH, THF, and benzene. Organometallic precursors like diethyl zinc have also been used (in THF at −70 °C). The nature of the precursors does not seem to have any marked influence on the polymer properties of the metal phosphinates.

The linear chain of polymeric metal(II) phosphinates consists of metal atoms linked either by alternating single and triple bridging phosphinate groups [79–81], or by double bridging phosphinate groups [82–86] (Fig. 10).

Most efforts have been directed toward the preparation of soluble or tractable (hence processable) metal phosphinates for applications as inor-
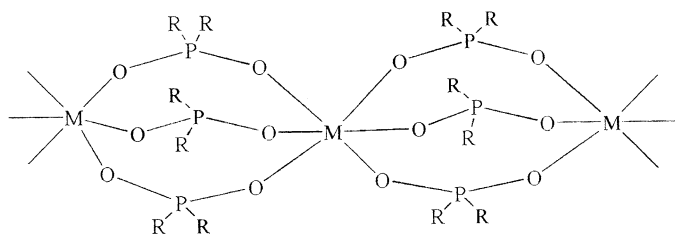
Fig. 11 Schematic representation of a linear chain of polymeric metal(III) phosphinates with triple bridging phosphinate groups

ganic polymers. The organic substituents on the phosphinate moieties have a very pronounced effect on the polymer properties. Polymers with CH_3, n-C_5H_{11}, and C_6H_5 groups are usually insoluble, high-melting and brittle; polymers with n-alkyl groups with six or more carbons are partially soluble and melt at low temperature. Unsymmetric phosphinates and mixtures of phosphinates result in polymers with increased solubility. The thermal stability of polymeric metal phosphinates also depends upon the carbon substituents. The methyl and phenyl phosphinates are the most stable, with incipient decomposition above 450 °C. As the size of the alkyl groups increases, the thermal stability decreases.

Trivalent metal phosphinates have also been prepared. The chain structure was assumed to consist of triple-bridging phosphinate according to Fig. 11.

Like the divalent metal phosphinates they are often insoluble. However, soluble polymers have been obtained with long chain dialkylphosphinic acid such as $Al(O_2P(C_8H_{17})_2)_3$ and the copolymers $Al(O_2PCH_2C_6H_5,C_4H_9)$ $(O_2P(C_8H_{17})_2)_2$ and $Cr(O_2PMePh)_2(O_2P(C_4H_9)_2$ [87].

Soluble metal phosphinates have been obtained by introducing a stable ligand, such as acetylacetonate, which decreases the functionality of the metal, hence the number of phosphinate bridges. Soluble $[Cr(Acac)(O_2PPh_2)_2]_n$ was prepared by adding two equivalents of diphenylphosphinic acid to chromium(III) acetylacetonate at 175–250 °C [88]. Starting from chromium(II) acetate in water, soluble $Cr(OH)(O_2PPh_2)_2 \cdot H_2O$ was obtained after addition of two equivalents of Ph_2POOK in water and oxidation by exposure to the atmosphere [87]. A series of soluble chromium(III) diphosphinate polymers $[Cr(L)(O_2PRR')_2]_n$ was obtained from $CrCl_3$, phosphinic acid, triethyl amine, and LH, L being CH_3O, $(OCH_2CH_2)_{0.5}$, $OCH_2CH_2NH_2$ [89]. The same strategy was applied to the preparation of polymeric fluoroaluminum bisphosphinates [90] and polymeric titanium(IV) phosphinates [91]. Another synthesis has been recently reported for the preparation of a polymeric aluminum phosphinate [92]. This synthesis involves the use of chelated aluminum compounds bearing only one reactive group that can be substituted by a phosphinic acid, according to Scheme 1.
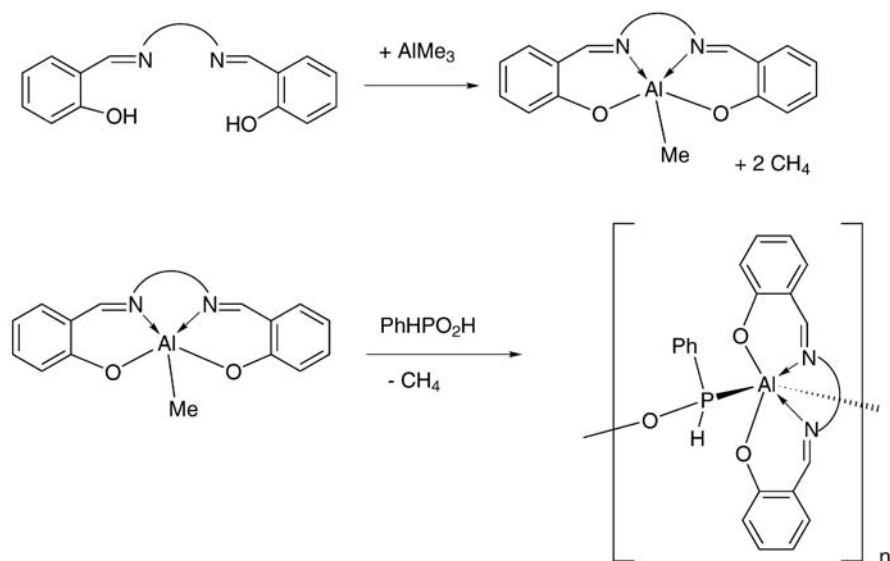
Scheme 1 Preparation of a polymeric aluminum phosphinate [92]

Depending on the number of carbon atoms between the two nitrogen atoms, dimers or infinite polymers have been obtained, the crystallographic structures of which have been reported [92].

It is worth mentioning that there are few examples of related polymeric metal dialkyl phosphates. The structures of polymeric magnesium, zinc, barium and cadmium diethylphosphates have been reported [93–97]. In the magnesium and zinc derivatives, chains are formed by double phosphate bridges (similar to Fig. 10). For the Cd structure, each 6-coordinated cadmium is linked to preceding and succeeding metal by two bridging phosphates forming height membered rings and two bridging μ_2-oxygen atoms forming four-membered rings (Fig. 12). In the case of the barium structure each bar-
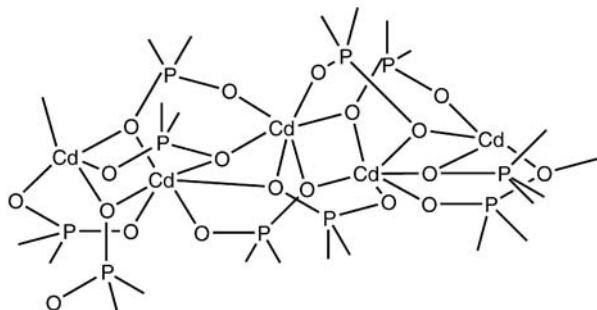
Fig. 12 Schematic representation of polymeric cadmium diethylphosphates

ium atom is made 8-coordinate by additional bonding of two OEt donor groups.

Polymers with alternating triple and single bridging phosphate groups (Fig. 10) have been obtained by reacting di-*tert*-butylphosphoric acid with manganese acetate [98, 99]. However the addition of the same phosphoric acid to copper acetate or cadmium acetate led to the formation of double bridged polymers (Fig. 10) [99]. Polymers metal dialkylphosphates show poor thermal stability, decomposition occurring before 140 °C, which allows one to convert them into metal phosphate materials under mild conditions [98, 99].

2.3
Molecular Crystalline Compounds

In the field of materials, soluble molecular compounds may be of interest as model compounds, or as precursors to higher dimension compounds. In recent years original molecular compounds have been reported, with cage-like structures arising from the linkage of metal centers by bridging organophosphorus groups: phosphonates [100–106], phosphinates [106–108], and dialkylphosphates [98, 109, 110]. Some phosphonates of the group 13 elements (Scheme 2), characterized by X-ray diffraction, may be regarded as models of secondary building units (SBUs) of microporous metallophosphates [107, 111], especially single four-ring units (4R or 4), double four-ring units (D4R or 4-4), and double six-ring units (D6R or 6-6) [100, 112–114].

$$4\ RP(O)(OH)_2 + 4\ MR'_3 \xrightarrow{-8\ R'H}$$

M= B, Al, Ga, In;
R'= alkyl or NMe$_2$;
R= alkyl or phenyl

4--4 or D4R

M= Al; R'=Me; R= ^{t}Bu

6-6 or D6R
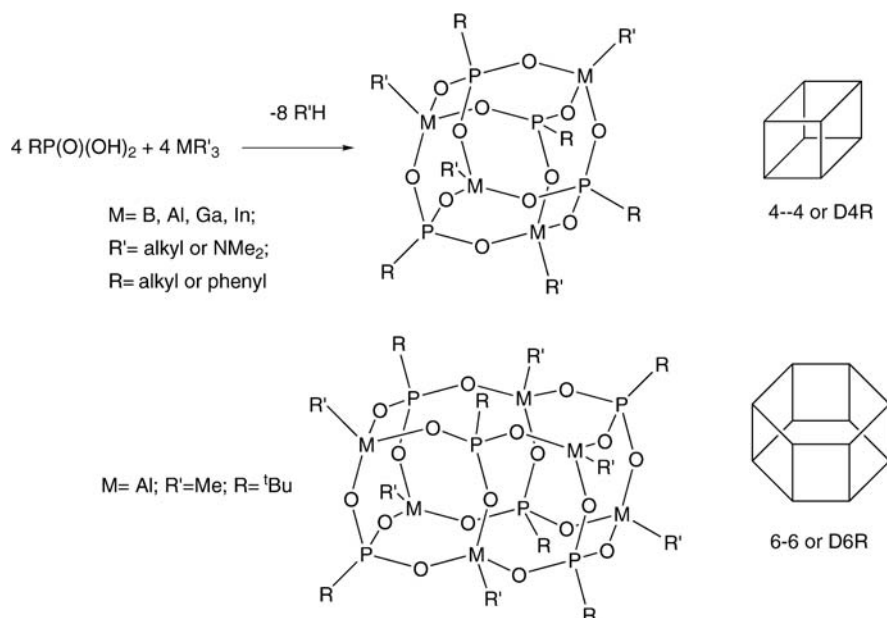
Scheme 2 Syntheses of cage-like group 13 phosphonate [111]

The organic groups pointing out of the polyhedral core most often make these molecular compounds soluble in organic solvents. An attractive prospect is to use these compounds as precursors in the preparation of materials by means of functional groups on metal centers, through cage-fusion reactions or low-temperature condensation processes. Unexpectedly the cubic compounds featured in Scheme 2, with alkyl groups bonded to the metal atoms, are stable toward air and moisture. However cubic compounds with actual functional groups were obtained by using amido groups instead of alkyl groups, compounds [*tert*-BuPO$_3$M(NMe$_2$)]$_4$ (M=Al, Ga) being highly reactive toward reagents containing acid hydrogen atoms [111]. The phosphonato-bridged titanium oxo-alkoxide displayed in Scheme 3 [115], has been used as a single-source precursor in sol-gel processing [116].
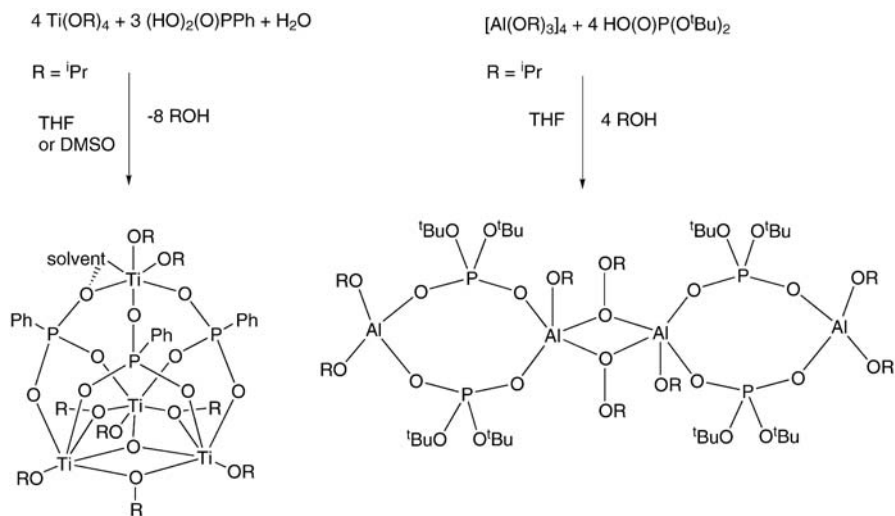
Scheme 3 Syntheses of metal alkoxide polynuclear complexes [110, 115]

Another approach is to use functional groups on phosphorus atoms. Interesting precursors have been designed by using *tert*-butylphosphate groups (Schemes 2 and 3), which undergo facile isobutene elimination, often as early as 100–150 °C, resulting in the in situ formation of P-OH groups; applications have been recently developed:

- In nonhydrolytic sol-gel processing, by low-temperature thermolysis of the precursor (Al compound in Scheme 3) in solution [110]
- For the preparation of coordination polymers (see above) by rearrangement reactions of di-*tert*-butyl phosphate complexes containing the M$_4$(μ_4-O) core (Fig. 4) in the presence of an acid or a base [98, 99] (Scheme 4)
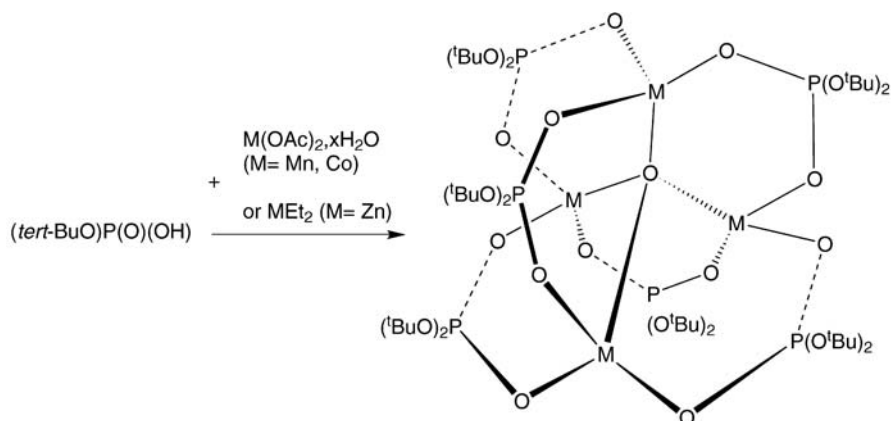
Scheme 4 Syntheses of metal di-*tert*-butyl phosphate complexes containing the M_4 (μ_4-O) core [98, 99, 117, 118]

- For the preparation of two-dimensional materials by reaction of the same type of complex (M=Zn) in anhydrous organic solvent in the presence of 1,6-hexylamine at room temperature, or in the presence of long-chain primary amines near 200 °C [98, 109]
- For the preparation of metal phosphate ceramics by solid-state thermolysis [99, 117, 118] or for the preparation of thin films by CVD [110]

3
Inorganic Substrates Modified by Organophosphorus Coupling Agents

3.1
Surface Modification of Inorganic Supports

The surface modification of an inorganic support with organophosphorus coupling agents (OPCA) is an extremely versatile route to hybrid materials. This route has been applied to a variety of supports, including metal oxides, metals, aluminosilicates, silica, metal hydroxides, and carbonates.

The grafting of OPCA to metal oxide surfaces is well documented. OPCA bind strongly to the surface of transition metal oxides such as TiO_2 [119–131], ZrO_2 [120, 121, 127, 130, 132, 133], SnO_2 [125, 126, 134], Ta_2O_5 [127, 135], Nb_2O_5 [127], Fe_2O_3 [136], or indium-tin oxide (ITO) [137–139]. OPCA also exhibit good affinity for Al_2O_3 [121, 140–145] as well as anodized Al [127, 146]. In the same way, OPCA can be used to modify the native oxide layer at the surface of metals, such as titanium, aluminum, iron, steel, copper, and brass [147–156]. Aluminosilicates, such as mica [157] and imogolite [158], have been modified using phosphonic acids. However, in the case of

mica, contact angles measurements suggested that the monolayer is not very robust.

The bonding of phosphonic acids to SiO_2 surfaces has also been reported: in an organic solvent, Si-O-P bonds are formed by Si-OH/P-OH condensation [159]; however, in an aqueous medium, no bonding was observed [127]. This behavior, which may be ascribed to the sensitivity of Si-O-P bonds to hydrolysis, has been utilized for the micro- and nanopatterning of surfaces by selective surface modification of TiO_2 patterns within a matrix of SiO_2 [128].

Hydroxides are also prone to surface modification by OPCA, as shown by the results reported for boehmite (γ-AlOOH) [142, 160, 161] and goethite (α-FeOOH) [162, 163].

Phosphate and phosphonate molecules have a very high affinity for calcium carbonate surfaces, as shown by their influence on the precipitation and growth of calcite [164–166]. Accordingly, organophosphorus compounds such as alkylphosphoric acids [167–169] and phosphonic acid-terminated polyoxyethylene [170, 171] have been used to modify the surface of $CaCO_3$ powders.

3.2
Grafting Reactions

In the above-mentioned studies, the OPCA are in most cases potentially tridentate species, phosphonic acids and monoalkylphosphoric acids (or the corresponding ammonium salts). Only a few works deal with potentially bidentate species such as phosphinic acids and dialkylphosphoric acids [124, 172]. The anchoring of the OPCA to oxide surfaces most probably involves the formation of M-O-P bridges. These bridges result from the condensation of surface hydroxyl groups with P-OH (or $P-ONH_4$) groups and from the complexation of the phosphoryl oxygen surface metal atoms. In the case of titanium and aluminum oxide, FTIR experiments suggest that phosphonate surface species are predominantly tridentate $RP(OM)_3$ species (Scheme 5) [120, 124, 143, 173].
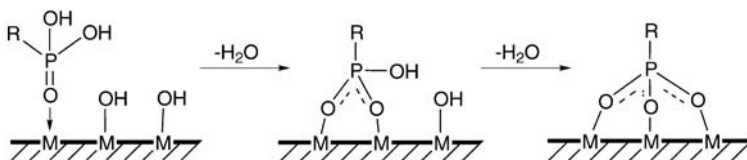
Scheme 5 Schematic representation of the formation of a tridentate phosphonate surface species by coordination and condensation to the surface

However, the bonding mode of OPCA surface species appears to depend strongly on the nature of both the OPCA and the surface, and on the conditions of the surface modification. For instance, from a combination of XPS,
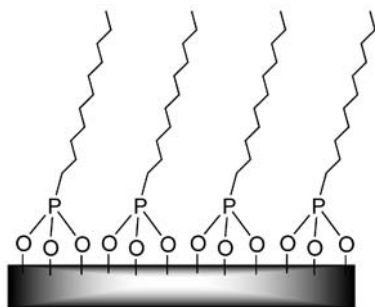
Fig. 13 Schematic representation of the creation of a self-assembled monolayer by adsorption of a long-chain OPCA

ToF-SIMS, and AFM results, the formation of ordered monolayers of octadecylphosphoric acid on a Ta_2O_5 surface involves both monodentate and bidentate phosphate species [135]. In the case of goethite, (γ-AlOOH), it was found that methylphosphonic acid bound to the surface as a monodentate or a bidentate species depending on the pH and the concentration [163].

The formation of P-O-P bridges by homocondensation of OPCA is not observed, with two important consequences:

– The surface modification can be done in water (contrary to organosilane coupling agents)
– The formation of multilayers by homocondensation of the OPCA can be discarded, and under mild conditions only (partial) monolayers are formed
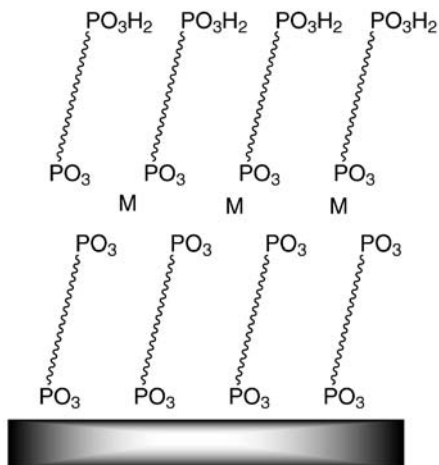
Fig. 14 Schematic representation of the creation of a bilayer by alternatively reacting the surface with a bisphosphonic acid and a metal salt

Thus, the adsorption of phosphonate or phosphate bearing long alkyl chains (typically from 8 to 18 C atoms) on metal oxide or metal surfaces leads to the formation of self-assembled monolayers (Fig. 13) [121, 127, 131, 132, 135, 150, 154, 174].

When bisphosphonic acids are used, multilayers can be formed in a controlled way by alternatively reacting the surface with the bisphosphonic acid and a metal salt (Fig. 14) [139, 174–181].

However, in the case of phosphonic and phosphinic acids it was shown that, depending on the oxide chemical stability and on the grafting conditions (temperature, pH, concentration of OPCA), a dissolution-precipitation mechanism can be operative, leading to the formation of a metal phosphonate or phosphinate phase (Scheme 6), even in the case of chemically stable TiO_2 [121, 124, 172]. This mechanism implies the cleavage of the Ti-O-Ti bridges by the organophosphorus acid; considering the excellent chemical stability of TiO_2, assistance to the cleavage by coordination of the phosphoryl group was proposed [124]. The same dissolution-precipitation mechanism has been reported in the surface modification of calcium carbonate powders by alkylphosphoric acids [167].

OH OH OH OH OH OH
M M M M M M

Low T and C

High T and C

R
HO—P
R
P
O O OH O O O
M M M M M M

Surface Modification

Metal Phosphonate

Metal oxide

Dissolution / Precipitation
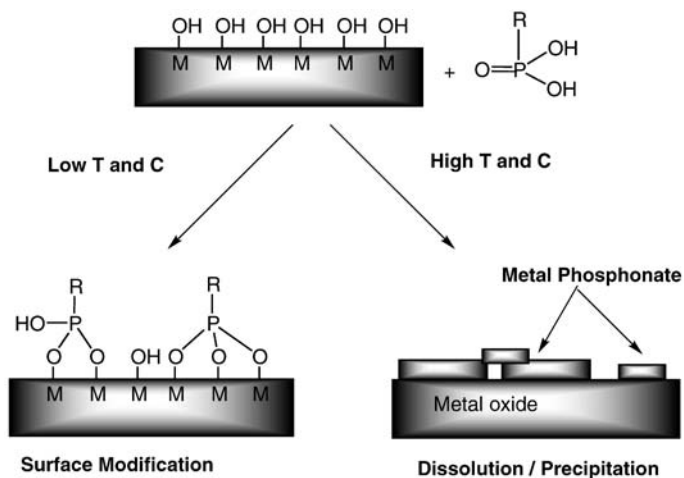
Scheme 6 Schematic representation of the competition between surface modification and dissolution-precipitation

Quite recently it was shown that phosphonic esters, trimethylsilyl [124, 143] and alkyl esters [124, 143, 145] could also be used to modify the surface of titanium or aluminum oxide in organic solvents at moderate temperatures. Unlike Si-O-C bonds, P-O-C bonds are not easily hydrolyzed, and their cleavage on an oxide surface was unexpected. Most probably, coordination of the phosphoryl oxygen to the surface assists the condensation by increasing the electrophilicity of the P atom, thus facilitating the condensation of P-O-R groups with surface hydroxyls (Scheme 7) [124]. The chemisorption of

gaseous phosphonate or phosphate esters on metal oxide surfaces has been extensively studied for the detection and the decontamination of pesticides and chemical warfare agents [182–184]. It is noteworthy that in the case of diethylphosphonate coupling molecules, the dissolution-precipitation mechanism discussed above was not observed for TiO_2 and Al_2O_3 supports, even under severe conditions.
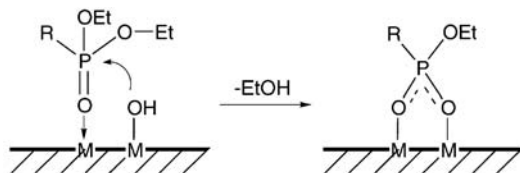
Scheme 7 Schematic representation of the reaction of a diethyphosphonate on the surface of a metal oxide

3.3
Some Applications of Surface Modification

At the present time, covalent hybrid materials based on OPCA have found relatively few applications. However, several examples can be found in fields as different as composite materials, separation, catalysis, optics, electronics, or biomedical. For instance, about 20 years ago, OPCA have been used to improve the mechanical properties of composite materials based on $CaCO_3$ filler and various polymer matrices [168, 169, 185, 186]. OPCA have been used since many years as corrosion inhibitors [147, 153, 187–192] and adhesion promoters [152, 187, 193]. In the separation domain, OPCA have been used to modify inorganic membranes [120, 141, 194, 195] or supports for chromatography [120, 196–198]. Several recent works have been devoted to the bonding of transition metal complexes (e.g., ruthenium(II) polypyridine) to nanocrystalline TiO_2 using phosphonic acid anchors for the elaboration of photovoltaic [119, 122, 123, 138, 199] and optical devices [200–202]. There are very few examples of OPCA based hybrid materials in heterogeneous catalysis, although OPCA allow to bind organometallic catalysts [145, 203, 204] and enzymes [197, 205] to a large variety of supports other than SiO_2. It is in the biomedical area that OPCA are expected to find increasing applications, for instance to design bio-sensors [128] or to modify the surface of titanium implants [156].

3.4
Sol-Gel Route

One advantage of sol-gel processing over surface modification is to create the inorganic oxide support in situ. Hence, without the limitation of the surface area of particles, more organic groups can be incorporated, even though their accessibility is not warranted. Another advantage is the possibility to

shape the final material before the liquid-to-gel transition (film coating for instance) and to control the porosity of materials during the sol-gel synthesis, by micelle-assisted templating for instance. Over the last decades a great deal of research has been devoted to the preparation of silica-based organic-inorganic hybrid materials by sol-gel processes involving organosilicon precursors. However, to-date sol-gel processing has not been extensively developed with organophosphorus precursors, except a few works recently reported on the incorporation of organophosphorus groups within titanium, zirconium and aluminum oxides [143, 203, 206, 207].

As shown in Schemes 8 and 9, one-step and two-step sol-gel routes have been used. In the two-step method a metal alkoxide was first mixed with a solution of phosphonic or phosphinic acid (P-O-M bonds form at this stage by condensation reaction), then neutral water was added to hydrolyze the residual alkoxide groups. A detailed study was carried out with $Ti(O^iPr)_4$, using diphenyl phosphinic (DPPA) and phenyl phosphonic acids (PPA), which act as chemical modifiers [206, 208]. Depending on the P/Ti and H_2O/Ti ratios, and on the nature of the modifier, molecular Ti oxo-alkoxo-phosphonates or phosphinates, sols, gels, or precipitates were obtained. Whatever the H_2O/Ti ratio, the P/Ti ratio was retained, showing that there was no removal of the PPA or DPPA ligands upon hydrolysis. Phenylphosphonate-containing gels were also prepared from zirconium and aluminum alkoxides [143, 207]. In all cases solid-state ^{31}P MAS NMR spectroscopy indicated a homogeneous dispersion of phosphonate groups within the oxide matrix; the formation of a metal phosphonate phase remained negligible.
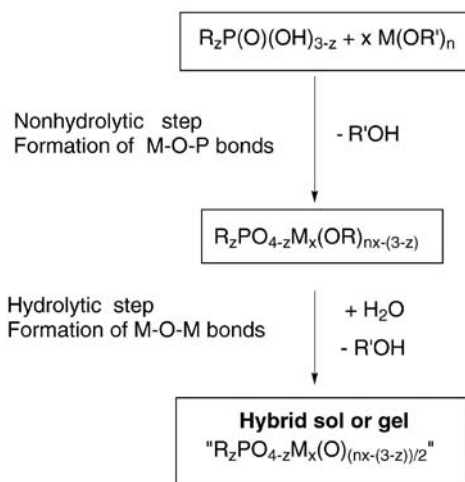
Scheme 8 Two-step sol-gel route to hybrid organic-inorganic materials based on organophosphorus derivatives [206, 208]
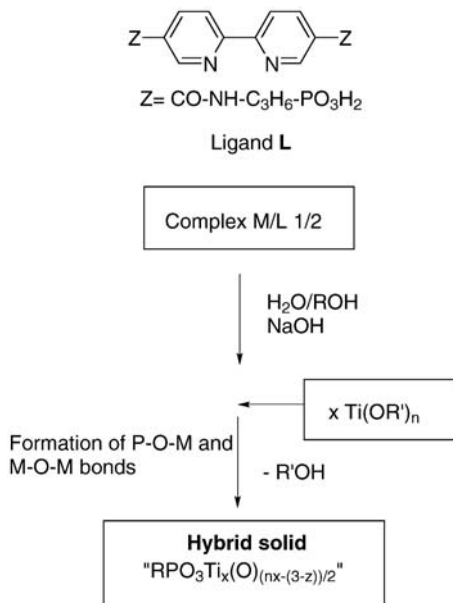
Scheme 9 One-step sol-gel route to hybrid organic-inorganic materials based on organo-phosphorus derivatives [203]

The one-step method (Scheme 9) was used to immobilize rhodium and iridium 2,2′-bipyridine complexes onto in situ generated titanium dioxide particles, to prepare supported catalysts for hydrogenation reactions under dihydrogen pressure [203]. Interestingly, the authors reported that direct grafting of preformed TiO_2 led to very poor activities with low complex incorporation. Accordingly the experimental sol-gel procedure was optimized on the basis of the catalytic performances: 2,2′-bipyridine ligand L (Scheme 8) was suspended in a water-2-propanol mixture and was dissolved by adding NaOH. $[M(cod)Cl_2]_2$ (M=Rh, Ir) was then added and the mixture was stirred for 48 h at room temperature. The titania precursor $(Ti(O^iPr)_4)$ was added in one portion (a Ti/P molar ratio of 5.6 was found to be optimal). The excellent activities of the resulting supported catalysts compare well with the homogeneous parent systems; no significant metal leaching was observed on recycling.

4
Conclusion

Because Metal-O-P and P-C linkages are quite stable, organophosphorus precursors offer a general alternative to silicon-based coupling agents in the field of organic/inorganic hybrid materials. Different classes of compounds are achievable depending on the target application. Metal phosphonates

form a fascinating class of hybrid organic-inorganic solids with intermingled architectures in which the nature of the organic moiety plays a determining role. Taking advantage of the versatility of phosphorus chemistry, which permits one to tailor functional organic groups (complexing groups, chromophore groups etc), metal phosphonates may be applied to various areas: ion exchange, proton conduction, catalysis, sensing, etc. However the main limitation lies in the lack of accessibility of the organic group in metal phosphonates, in which an uniform mesoporosity is difficult to achieve. Grafting of organophosphorus reagents opens up the possibility to functionalize practically any metal oxide support with the desired physical and chemical properties. Alternatively, the in situ formation of the inorganic part may be carried out by sol-gel processing in the presence of the organophosphorus reagents. In these approaches, one advantage of organophosphorus precursors over organosilicon precursors lies in the absence of self-condensation between P-OH groups whereas self-condensation between Si-OH groups may lead to the formation of separate domains under the same conditions. Organophosphorus coupling agents (OPCA) are quite complementary of organosilane coupling agents: organosilanes are more efficient with silicon containing inorganic supports such as silica, whereas OPCA appear best suited for the preparation of hybrid materials based on metals, metal oxides, and carbonates.

References

1. Eckert H, Ward M (2001) Chem Mater 13:3059
2. Neilson RH, Wisian-Neilson P (1988) Chem Rev 88:541
3. Allcock HR (1999) Macromol Symp 144:33
4. Gleria M, De Jaeger R (2001) J Inorg Organomet Polym 11:1
5. Clearfield A (1998) Progr Inorg Chem 47:371
6. Maeda K, Mizukami F (1999) Catal Surveys Jpn 3:119
7. Clearfield A, Wang ZK (2002) J Chem Soc Dalton Trans 2937
8. Bujoli B, Pena O, Palvadeau P, Le Bideau J, Payen C, Rouxel J (1993) Chem Mater 5:583
9. Cao G, Lee H, Lynch VM, Mallouk TE (1988) Inorg Chem 27:2781
10. Martin KJ, Squattrito PJ, Clearfield A (1989) Inorg Chim Acta 155:7
11. Zhang Y, Clearfield A (1992) Inorg Chem 31:2821
12. Le Bideau J, Payen C, Bujoli B, Palvadeau P, Rouxel J (1995) J Magnetism Magnetic Mater 140/144:1719
13. Huan G, Jacobson AJ, Johnson JW, Corcoran EW (1990) Chem Mater 2:91
14. Le Bideau J, Payen C, Bujoli B (1995) CR Acad Sci Paris Série II 320:141
15. Le Bideau J, Papoutsakis D, Jackson JE, Nocera DG (1997) J Am Chem Soc 119:1313
16. Chaplais G, Le Bideau J, Leclercq D, Mutin PH, Vioux A (2000) J Mater Chem 10:1593
17. Morizzi J, Hobday M, Rix C (2000) J Mater Chem 10:1693
18. Bujoli-Doeuff M, Evain M, Janvier P, Massiot D, Clearfield A, Gan Z, Bujoli B (2001) Inorg Chem 40:6694
19. Poojary DM, Hu H-L, Campbell FL, Clearfield A (1993) Acta Cryst B 49:996
20. Poojary DM, Bhardwaj C, Clearfield A (1995) J Mater Chem 5:171
21. Le Bideau J, Payen C, Palvadeau P, Bujoli B (1994) Inorg Chem 33:4885
22. Maeda K, Kiyozumi Y, Mizukami F (1994) Angew Chem Int Ed Engl 33:2335
23. Maeda K, Kiyozumi Y, Mizukami F (1997) J Phys Chem B 101:4402

24. Carter VJ, Wright PA, Gale JD, Morris RE, Sastre E, Perez-Pariente J (1997) J Mater Chem 7:2287
25. Poojary DM, Grohol D, Clearfield A (1995) Angew Chem Int Ed Engl 34:1508
26. Bonavia G, Haushalter RC, O'Connor CJ, Sangregorio C, Zubieta J (1998) Chem Commun 2187
27. Poojary DM, Grohol D, Clearfield A (1995) J Phys Chem Solids 56:1383
28. Johnson JW, Jacobson AJ, Brody JF, Lewandowski JT (1984) Inorg Chem 23:3842
29. Le Bideau J, Jouanneaux A, Payen C, Bujoli B (1994) J Mater Chem 4:1319
30. Fredoueil F, Evain M, Bujoli-Doeuff M, Bujoli B (1999) Eur J Inorg Chem 1077
31. Fredoueil F, Evain M, Massiot D, Bujoli-Doeuff M, Bujoli B (2001) J Mater Chem 11:1106
32. Evans OR, Manke DR, Lin W (2002) Chem Mater 14:3866
33. Drumel S, Janvier P, Barboux P, Bujoli-Doeuff M, Bujoli B (1995) Inorg Chem 34:148
34. Rabu P, Janvier P, Bujoli B (1999) J Mater Chem 9:1323
35. Stock N, Frey SA, Stucky GD, Cheetham AK (2000) J Chem Soc Dalton Trans 4292
36. Cabeza A, Aranda MAG, Bruque S (1998) J Mater Chem 8:2479
37. Ayyappan S, Diaz de Delgado G, Cheetham AK, Férey G, Rao CNR (1999) J Chem Soc Dalton Trans 2905
38. Cabeza A, Aranda MAG, Bruque S (1999) J Mater Chem 9:571
39. Drumel S, Janvier P, Deniaud D, Bujoli B (1995) J Chem Soc Chem Comm 1051
40. Hix GB, Kariuki BM, Kitchin S, Tremayne M (2001) Inorg Chem 40:1477
41. Hix GB, Turner A, Kariuki BM, Tremayne M, MacLean EJ (2002) J Mater Chem 12:3220
42. Jaimez E, Hix GB, Slade RCT (1997) J Mater Chem 7:475
43. Hartman SJ, Todorov E, Cruz C, Sevov SC (2000) Chem Commun 1213
44. Clearfield A, Sharma CVK, Zhang B (2001) Chem Mater 13:3099
45. Serre C, Ferey G (2001) Inorg Chem 40:5350
46. Barthelet K, Nogues M, Riou D, Férey G (2002) Chem Mater 14:4910
47. Soghomonian V, Chen Q, Haushalter RC, Zubieta J (1995) Angew Chem Int Ed Engl 34:223
48. Song HH, Zheng LM, Wang Z, Yan CH, Xin XQ (2001) Inorg Chem 40:5024
49. Zheng LM, Song HH, Duan CY, Xin XQ (1999) Inorg Chem 38:5061
50. Johnson JW, Jacobson AJ, Butler WM, Rosenthal SE, Brody JF, Lewandowski JT (1989) J Am Chem Soc 111:381
51. Torgerson MR, Nocera DG (1996) J Am Chem Soc 118:8739
52. Gendraud P, de Roy ME, Besse JP (1996) Inorg Chem 35:6108
53. Gendraud P, Bigey L, Gueho C, de Roy ME, Besse JP (1997) Chem Mater 9:539
54. Alberti G, Boccali L, Casciola M, Massinelli L, Montoneri E (1996) Solid State Ionics 84:97
55. Alberti G, Giontella E, Murciamascaros S (1997) Inorg Chem 36:2844
56. Alberti G, Brunet E, Dionigi C, Juanes O, De la Mata MJ, Rodriguez-Ubis JC, Vivani R (1999) Angew Chem, Int Ed Engl 38:3351
57. Byrd H, Clearfield A, Poojary D, Reis KP, Thompson ME (1996) Chem Mater 8:2239
58. Clearfield A, Poojary DM, Zhang B, Zhao B, Derecskei-Kovacs A (2000) Chem Mater 12:2745
59. Stein SEW, Clearfield A, Subramanian MA (1996) Solid State Ionics 83:113
60. Curini M, Epifano F, Marcotullio MC, Rosati O, Nocchetti M (2002) Tetrahedron Lett 43:2709
61. Segawa K, Ozawa T (1999) J Mol Catal A Chem 141:249
62. Clearfield A (1998) Chem Mater 10:2801
63. Alberti G, Vivani R, Marmottini F, Zappelli P (1998) J Porous Mater 5:205
64. Alberti G, Marmottini F, Murciamascaros S, Vivani R (1994) Angew Chem Int Ed Engl 33:1594
65. Alberti G, Costantino U, Marmottini F, Vivani R, Zapelli P (1998) Microporous Mesoporous Mater 21:297
66. Medoukali D, Mutin PH, Vioux A (1999) J Mater Chem 9:2553

67. Odobel F, Bujoli B, Massiot D (2001) Chem Mater 13:163
68. Morizzi J, Hobday M, Rix C (2001) J Mater Chem 11:794
69. Brunet E, Huelva M, Vazquez R, Juanes O, Rodriguez-Ubis JC (1996) Chem Eur J 2:1578
70. Vermeulen LA, Thompson ME (1992) Nature 358:656
71. Poojary DM, Vermeulen LA, Vicenzi E, Clearfield A, Thompson ME (1994) Chem Mater 6:1845
72. Reis KP, Joshi VK, Thompson ME (1996) J Catal 161:62
73. Grohol D, Subramanian MA, Poojary DM, Clearfield A (1996) Inorg Chem 35:5264
74. Zhang B, Poorajy DM, Clearfield A (1998) Inorg Chem 37:249
75. Block BP (1970) Inorg Macromol Rev 1:115
76. Yamakawa H, Hayashi T, Kaneshige Y (1989) Jpn Kokai 01,065,137 (Tosoh Corp., Japan)
77. Horold S (2000) EP 10,241,168 (Clariant GmbH, Germany)
78. Venezky DL (1972) US 3,654,189
79. Giordano F, Randaccio L, Ripamonti A (1967) Chem Commun 19
80. Giordano F, Randaccio L, Ripamonti A (1967) Chem Commun 1269
81. Giordano F, Randaccio L, Ripamonti A (1969) Acta Cryst B 25:1057
82. Colamarino P, Orioli PL, Benzinger WD, Gillman HD (1976) Inorg Chem 15:800
83. Cini R, Orioli P, Sabat M, Gillman HD (1982) Inorg Chim Acta 59:225
84. Betz P, Bino A (1988) Inorg Chim Acta 149:171
85. Shieh M, Martin KJ, Squattrito PJ, Clearfield A (1990) Inorg Chem 29:958
86. Sergienko VS (2001) Zh Neorg Khim 46:946
87. Nannelli P, Block BP, King JP, Saraceno AJ, Sprout OS Jr, Peschko ND, Dahl GH (1973). J Polym Sci Polym Chem 11:2691
88. Block BP, Simkin J, Ocone LR (1962) J Am Chem Soc 84:1749
89. Gillman HD, Nannelli P (1977) Inorg Chim Acta 23:259
90. Schmidt DL, Flagg EE (1969) J Polym Sci Part A 1 7:865
91. Dahl GH, Block BP (1967) Inorg Chem 6:1439
92. Wang Y, Parkin S, Atwood D (2002) Inorg Chem 41:558
93. Ezra FS, Collin RL (1973) Acta Crystallogr B29:1398
94. Harrison WTA, Nemoff TM, Gier TE, Stucky GD (1992) Inorg Chem 31:5395
95. Harrison WTA, Nemoff TM, Gier TE, Stucky GD (1994) J Mater Chem 4:1111
96. Kyogoku Y, Iitaka Y (1966) Acta Crystallogr 21:49
97. Miner VW, Prestegard JH, Faller JW (1983) Inorg Chem 22:1862
98. Lugmair CG, Tilley TD, Rheingold AL (1997) Chem Mater 9:339
99. Sathiyendiran M, Murugavel R (2002) Inorg Chem 41:6404
100. Walawalkar MG, Murugavel R, Roesky HW, Schmidt H-G (1997) Inorg Chem 36:4202
101. Walawalkar MG, Murugavel R, Roesky HW, Schmidt H-G (1997) Organometallics 16:516
102. Walawalkar MG, Murugavel R, Voigt A, Roesky HW, Schmidt H-G (1997) J Am Chem Soc 119:4656
103. Walawalkar MG, Horchler S, Dietrich S, Chakraborty D, Roesky HW, Schafer M, Schmidt HG, Sheldrick GM, Murugavel R (1998) Organometallics 17:2865
104. Landry CC, Cleaver WM, Guzei IA, Rheingold AL (1998) Organometallics 17:5209
105. Yang Y, Pinkas J, Noltemeyer M, Schmidt H-G, Roesky HW (1999) Angew Chem Int Ed Engl 38:664
106. Guerrero G, Mehring M, Mutin PH, Dahan F, Vioux A (1999) J Chem Soc Dalton Trans 1537
107. Mason MR (1998) J Cluster Sci 9:1
108. Chakraborty D, Chandrasekhar V, Bhattacharjee M, Kratzner R, Roesky HW, Noltemeyer M, Schmidt HG (2000) Inorg Chem 39:23
109. Lugmair CG, Tilley TD (1998) Inorg Chem 37:6304
110. Lugmair CG, Tilley TD, Rheingold AL (1999) Chem Mater 11:1615
111. Walawalkar MG, Roesky HW, Murugavel R (1999) Acc. Chem Res 32:117

112. Yang Y, Pinkas J, Noltemeyer M, Roesky HW (1998) Inorg Chem 37:6404
113. Yang Y, Pinkas J, Schafer M, Roesky HW (1998) Angew Chem Int Ed Engl 37:2650
114. Yang Y, Walawalkar MG, Pinkas J, Roesky HW, Schmidt HG (1998) Angew Chem Int Ed Engl 37:96
115. Mehring M, Guerrero G, Dahan F, Mutin PH, Vioux A (2000) Inorg Chem 39:3325
116. Mutin PH, Mebring M, Guerrero G, Vioux A (2001) Mater Res Soc Symp Proc 628:CC2.4.1
117. Murugavel R, Sathiyendiran M (2001) Chem Lett 84
118. Murugavel R, Sathiyendiran M, Walawalkar MG (2001) Inorg Chem 40:427
119. Pechy P, Rotzinger FP, Nazeeruddin MK, Kohle O, Zakeeruddin SM, Humphrybaker R, Gratzel M (1995) Chem Commun 65
120. Randon J, Blanc P, Paterson R (1995) J Membrane Sci 98:119
121. Gao W, Dickinson L, Grozinger C, Morin FG, Reven L (1996) Langmuir 12:6429
122. Zakeeruddin SM, Nazeeruddin MK, Pechy P, Rotzinger FP, Humphrybaker R, Kalyana-sundaram K, Gratzel M, Shklover V, Haibach T (1997) Inorg Chem 36:5937
123. Campus F, Bonhote P, Gratzel M, Heinen S, Walder L (1999) Solar Energy Mater Solar Cells 56:281
124. Guerrero G, Mutin PH, Vioux A (2001) Chem Mater 13:4367
125. Frantz R, Durand J-O, Lanneau GF, Jumas J-C, Olivier-Fourcade J, Cretin M, Persin M (2002) Eur J Inorg Chem 1088
126. Merrins A, Kleverlaan C, Will G, Rao SN, Scandola F, Fitzmaurice D (2001) J Phys Chem B 105:2998
127. Hofer R, Textor M, Spencer ND (2001) Langmuir 17:4014
128. Michel R, Lussi JW, Csucs G, Reviakine I, Danuser G, Ketterer B, Hubbell JA, Textor M, Spencer ND (2002) Langmuir 18:3281
129. Michel R, Reviakine I, Sutherland D, Fokas C, Csucs G, Danuser G, Spencer ND, Textor M (2002) Langmuir 18:8580
130. Pawsey S, Yach K, Reven L (2002) Langmuir 18:5205
131. Zwahlen M, Tosatti S, Textor M, Haehner G (2002) Langmuir 18:3957
132. Gao W, Dickinson L, Grozinger C, Morin FG, Reven L (1997) Langmuir 13:115
133. Crepaldi EL, Soler-Illia GJAA, Grosso D, Sanchez C, Albouy P-A (2001) Chem Commun 1582
134. Frantz R, Granier M, Durand J-O, Lanneau GF (2002) Tetrahedron Lett 43:9115
135. Textor M, Ruiz L, Hofer R, Rossi A, Feldman K, Haehner G, Spencer ND (2000) Langmuir 16:3257
136. Chaneac C, Tronc E, Jolivet J-P (2001) Mater Res Soc Symp Proc 628:CC6.4.1
137. Gardner TJ, Frisbie CD, Wrighton MS (1995) J Am Chem Soc 117:6927
138. Trammell SA, Moss JA, Yang JC, Nakhle BM, Slate CA, Odobel F, Sykora M, Erickson BW, Meyer TJ (1999) Inorg Chem 38:3665
139. Stockhause S, Neumann P, Schrader S, Kant M, Brehmer L (2002) Synth Met 127:295
140. Wieserman LF, Wefers K, Cross K, Martin ES (1991) US 4994429 (Aluminum Co. of America)
141. Caro J, Noack M, Kolsch P (1998) Microporous Mesoporous Mater 22:321
142. Persson P, Laiti E, Ohman L-O (1997) J Colloid Interface Sci 190:341
143. Guerrero G, Mutin PH, Vioux A (2001) J Mater Chem 11:3161
144. Hector LG Jr, Opalka SM, Nitowski GA, Wieserman L, Siegel DJ, Yu H, Adams JB (2001) Surf Sci 494:1
145. Villemin D, Moreau B, Simeon F, Maheut G, Fernandez C, Montouillout V, Caignaert V, Jaffres PA (2001) Chem Commun 2060
146. Nitowski GA, Wieserman LF, Wefers K (1994) US 5277788 (Aluminum Co. of America)
147. Mueller B, Foerster I (1996) Corrosion Sci 38:1103
148. Rohwerder M, Stratmann M (1999) MRS Bull 24:43
149. Maege I, Jaehne E, Henke A, Adler H-JP (1999) Chemia 140:29
150. Van Alsten JG (1999) Langmuir 15:7605
151. Gawalt ES, Avaltroni MJ, Koch N, Schwartz J (2001) Langmuir 17:5736

152. Jahne E, Henke A, Adler H-JP (2000) Coating 33:218
153. Rajendran S, Apparao BV, Palaniswamy N, Periasamy V, Karthikeyan G (2001) Corrosion Sci 43:1345
154. Lewington TA, Alexander MR, Thompson GE, McAlpine E (2002) Surf Eng 18:228
155. Tosatti S, Michel R, Textor M, Spencer ND (2002) Langmuir 18:3537
156. Viornery C, Chevolot Y, Leonard D, Aronsson BO, Pechy P, Mathieu HJ, Descouts P, Gratzel M (2002) Langmuir 18:2582
157. Woodward JT, Ulman A, Schwartz DK (1996) Langmuir 12:3626
158. Yamamoto K, Otsuka H, Wada S, Takahara A (2001) Chem Lett 5:1162
159. Lukes I, Borbaruah M, Quin LD (1994) J Am Chem Soc 116:1737
160. Laiti E, Oehman L-O (1996) J Colloid Interface Sci 183:441
161. Laiti E, Persson P, Oehman L-O (1998) Langmuir 14:825
162. Nowack B, Stone AT (1999) J Colloid Interface Sci 214:20
163. Barja BC, Tejedor-Tejedor MI, Anderson MA (1999) Langmuir 15:2316
164. Hamza SM, Hamdona SK, Mahmoud TH (1993) J Mater Sci 28:1607
165. Reyhani MM, Oliveira A, Parkinson GM, Jones F, Rohl AL, Ogden MI (2002) Int J Modern Phys B 16:25
166. Ojo SA, Slater B, Catlow CRA (2002) Molec Simul 28:591
167. Nakatsuka T, Kawasaki H, Itadani K, Yamashita S (1981) J Colloid Interface Sci 82:298
168. Nakatsuka T, Kawasaki H, Itadani K, Yamashita S (1982) J Appl Polym Sci 27:259
169. Nakatsuka T, Kawasaki H, Yamashita S (1985) Rubber Chem Tech 58:107
170. Mosquet M, Chevalier Y, Brunel S, Guicquero JP, Le Perchec P (1997) J Appl Polym Sci 65:2545
171. Mosquet M, Chevalier Y, Le Perchec P, Foissy A, Guicquero JP (1999) Colloid Polym Sci 277:1162
172. Guerrero G, Chaplais G, Mutin PH, Le Bideau J, Leclercq D, Vioux A (2001) Mater Res Soc Symp Proc 628:CC6.6.1
173. Coast R, Pikus M, Henriksen PN, Nitowski GA (1996) J Adhesion Sci Technol 10:101
174. Neff GA, Page CJ, Meintjes E, Tsuda T, Pilgrim WC, Roberts N, Warren WW Jr (1996) Langmuir 12:238
175. Lee H, Kepley LJ, Hong HG, Akhter S, Mallouk TE (1988) J Phys Chem 92:2597
176. Hong HG, Sackett DD, Mallouk TE (1991) Chem Mater 3:521
177. Byrd H, Pike JK, Talham DR (1993) Chem Mater 5:709
178. Katz HE, Bent SF, Wilson WL, Schilling ML, Ungashe SB (1994) J Am Chem Soc 116:6631
179. O'Brien JT, Zeppenfeld AC, Richmond GL, Page CJ (1994) Langmuir 10:4657
180. Fang MM, Kaschak DM, Sutorik AC, Mallouk TE (1997) J Am Chem Soc 119:12184
181. Neff GA, Helfrich MR, Clifton MC, Page CJ (2000) Chem Mater 12:2363
182. Rusu CN, Yates JT (2000) J Phys Chem B 104:12,292
183. Kim CS, Lad RJ, Tripp CP (2001) Sens Actuators B 76:442
184. Wagner GW, Procell LR, O'Connor RJ, Munavalli S, Carnes CL, Kapoor PN, Klabunde KJ (2001) J Am Chem Soc 123:1636
185. Nakatsuka T, Kawasaki H, Yamashita S, Kohjiya S (1983) J Colloid Interface Sci 93:277
186. Nakatsuka T, Yamashita S (1983) J Appl Polym Sci 28:3549
187. Matienzo LJ, Shaffer DK, Moshier WC, Davis GD (1986) J Mater Sci 21:1601
188. Davis PK, Hoye PAT, Williams MJ, Woodward G (1996) Phosphorus Sulfur Silicon Relat Elem 109/110:197
189. Friedfeld SJ, He SL, Tomson MB (1998) Langmuir 14:3698
190. Maege I, Jaehne E, Henke A, Adler HJP, Bram C, Jung C, Stratmann M (1998) Macromol Symp 126:7
191. Kowalik T, Adler H-JP, Plagge A, Stratmann M (2000) Macromol Chem Phys 201:2064
192. Felhosi I, Telegdi J, Palinkas G, Kalman E (2002) Electrochim Acta 47:2335
193. Maege I, Jaehne E, Henke A, Adler H-JP, Bram C, Jung C, Stratmann M (1998) Progr Org Coatings 34:1

194. Wieserman LF, Wefers K, Cross K, Martin ES, Hsieh HP, Quayle WH (1990) US 4,957,890 (Aluminum Co. of America)
195. Randon J, Paterson R (1997) J Membrane Sci 134:219
196. Wieserman LF, Novak JW, Conroy CM, Wefers K (1988) US 4,786,628 (Aluminum Co. of America)
197. Wieserman LF, De Young DH, Whitesides GM (1990) UK 2,221,466 (Aluminum Co. of America)
198. Clausen AM, Carr PW (1998) Anal Chem 70:378
199. Bonhote P, Moser J, Humphry-Baker R, Vlachopoulos N, Zakeeruddin SM, Walder L, Gratzel M (1999) J Am Chem Soc 121:1324
200. Will G, Nagaraja Rao JSS, Fitzmaurice D (1999) J Mater Chem 9:2297
201. Felderhoff M, Heinen S, Molisho N, Webersinn S, Walder L (2000) Helv Chim Acta 83:181
202. Sotomayor J, Will G, Fitzmaurice D (2000) J Mater Chem 10:685
203. Maillet C, Janvier P, Pipelier M, Praveen T, Andres Y, Bujoli B (2001) Chem Mater 13:2879
204. Benitez IO, Bujoli B, Camus LJ, Lee CM, Odobel F, Talham DR (2002) J Am Chem Soc 124:4363
205. Duval R, Yvin JC (1999) FR 2,773,171 (Societe Civile Ase et Bio)
206. Guerrero G, Mutin PH, Vioux A (2000) Chem Mater 12:1268
207. Mutin PH, Delenne C, Medoukali D, Corriu R, Vioux A (1998) Mater Res Soc Symp Proc 519:345
208. Mehring M, Lafond V, Mutin PH, Vioux A (2003) J Sol Gel Sci Technol 26:99

"Zwitterionic Phospholide Derivatives— New Ambiphilic Ligands"

Dietrich Gudat

Institut für Anorganische Chemie der Universität Stuttgart, Pfaffenwaldring 55,
70550 Stuttgart, Germany
E-mail: gudat@iac.uni-stuttgart.de

Abstract Attachment of one or two phosphonio substituents converts a phospholide anion not only into a zwitterion or cation but induces as well a redistribution of the π-electrons in the ring. The result of these changes is an eventual reduction of π-nucleophilicity and a simultaneous increase in π-electrophilicity, and, as a consequence, the chemical properties of these species exhibit some notable differences from those of the original anions. This review gives an account on the current knowledge on the synthesis, physical properties, and—in particular—chemical behaviour of phosphonio-substituted phospholide derivatives. With respect to the significance of the use of phospholides as ligands in coordination chemistry, the substituent induced tuning of the ligand properties of the zwitterionic and cationic species, and the resulting effects on the molecular and electronic structure of the complexes formed, will be given special attention.

Keywords Aromatic phosphorus heterocycles · Phospholides · P ligands · Zwitterions · σ-Donor/π-acceptor properties

1
Introduction

The discovery of ferrocene [1] marked the beginning of a—still continuing—story of complexes that are distinguished by the presence of one or several cyclopentadienyl (Cp) ligands interacting with the metal by their π-electron system. Over the years, these species experienced a tremendous development, and until today, cyclopentadienyl moieties evolved into one of the most abundant classes of multipurpose ligands in organometallic chemistry [2–4]. One of the reasons for this versatility lies indisputably in the unique propensity of the Cp-unit to tolerate a variety of different bonding situations, from the predominance of electrostatic interaction between the anionic ligand and a metal cation in complexes of alkaline and alkaline earth metals, to bonding modes involving mainly covalent interaction of the ligand π-electron system with metal d-orbitals [4]. The latter situation is realized in transition metal complexes that may according to their topology be classified as η^n-complexes where n denotes the number of ring carbon atoms interacting with the metal ("interacting" and "non-interacting" carbon atoms in cases where n<5 may rapidly interchange, leading to the well known fluxional behaviour) [2–4]. All complexes have in common that the most important bonding contributions arise from interaction of filled ligand π- with empty metal-d-orbitals. In the frame of the Dewar-Chatt-Duncanson model which analyses metal-ligand interactions in terms of "ligand-to-metal" and "metal-to-ligand" charge transfer contributions, respectively, cyclopentadienyl moieties behave as strong donor ligands but exhibit low to negligible acceptor qualities [4]. As a consequence, the metal atoms in cyclopentadienyl complexes are generally electron rich, up to the point that they exhibit considerable Lewis-base character such as the iron atom in ferrocene.

With the development of the chemistry of cyclopentadienyl complexes, attempts were made to modify systematically the functionality of the ligand by attachment of specific substituents, or by the formal replacement of a ring carbon by an isoelectronic heteroatom. One modification that is of relevance for the topic covered here involves the formal replacement of one of the C_5H_5-hydrogen atoms by a positively charged phosphonio group (mostly Ph_3P) [5], thus leading to a compensation of the overall charge of the former anion. While this effect improves, on one hand, the chemical stability of the ligand (as compared to $C_5H_5^-$, neutral $C_5H_4PPh_3$ is inert towards hydrolysis

[5] and can be handled in aqueous solution), it is also considered to make the zwitterion a weaker donor towards transition metals. Nonetheless, zwitterionic phosphonio-cyclopentadienides still possess a tendency towards η^5-complexation of transition metals, and quite a few complexes have been prepared whose structural features bear close resemblance to those of cyclopentadienyl-complexes with anionic ligands [6]. Furthermore, the use of the salt $[Co(CO)_2(\eta^5-Ph_3PC_5H_4)][Co(CO)_4]$ in the catalytic cyclotrimerisation of alkynes demonstrated that the attachment of a zwitterion to a metal is robust enough to survive a catalytic cycle [7].

A more pronounced modification of ligand properties proved feasible by direct incorporation of heteroatoms into the five-membered ring. A particularly fruitful approach involved the replacement of a CH-unit by an isoelectronic phosphorus atom. Following the first synthesis of a pspholyl anion of this type by Braye in 1971 [8] it was in particular the group of Mathey who studied systematically the complexation behaviour of these species [9, 10]. The results of these investigations served to establish that replacement of a carbon by a phosphorus atom of similar electronegativity and comparable valence p-orbital energy induces only minor perturbations of the occupied π-orbitals, but effects a significant energetic stabilization of antibonding π^*-orbitals. As a consequence, both anions exhibit similar degrees of aromaticity and comparable Lewis-basicities [11] but a phospholyl is a better π-acceptor than a cyclopentadienyl ligand, and induces a much lower net electron transfer to the metal atom [12, 13].

The phosphorus atom in a π-coordinated phospholyl ligand still exhibits a lone-pair of electrons that is capable of binding a second metal atom, so that a phospholyl complex such as phosphaferrocene is—in contrast to ferrocene—itself a ligand. This special property which has no direct correspondence in the chemistry of cyclopentadienyl complexes has recently been fruitfully exploited as the underlying principle which allowed the introduction of phosphaferrocenes as effective ligands in catalytic applications [10, 13, 14].

The scope of this review is to outline the recent development of the chemistry of phosphonio-substituted phospholide derivatives which combine both the attachment of exocyclic phosphonio-substituents and formal substitution of one (or several) CH-units of a cyclopentadienyl ring by phosphorus atom(s). The area includes derivatives with benzannulated ring systems that can be considered hetero-analogues of indenyl ligands. It will be shown that phosphonio-substituted phospholide derivatives differ in their chemical properties from phospholides or cyclopentadienyls, in particular as their complexation behaviour is concerned: whereas the coordination chemistry of cyclopentadienyl and phospholyl anions is dominated by the formation of π-complexes, phosphonio-substituted phospholide derivatives are distinguished by a competition between σ- and π-nucleophilicity. As a consequence, complexes formed may not only contain "side-on" or "end-on" coordinated ligands, but the ligands in many complexes display further a unique mobility and may switch between different coordination modes, thus showing aspects of a reactivity that may be potentially useful for applications in catalysis.

2
Syntheses of Cationic and Neutral Phosphonio-Phospholide Derivatives

All phosphonio-substituted phospholide and heterophospholide derivatives discussed in this chapter have in common that the phosphonio-substituents are attached to the carbon atom(s) next to the dicoordinate phosphorus atom(s). A great deal of work has been dedicated to benzannulated compounds whose five membered rings carry a benzene moiety fused to the edge opposite to the two-coordinate phosphorus atom. Using the systematic nomenclature, these condensed heterocycles may be denoted as benzo[*c*]phospholides or benzo[*c*]-1,2-diphospholides, respectively. In the following, these denominations will be abbreviated as benzophospholide or -diphospholide for the sake of simplicity.

2.1
By Condensation Reactions

The door to the chemistry of phosphonio-substituted phospholide derivatives was pushed open by a publication by Schmidpeter and Thiele in 1991 who reported on the synthesis of the cationic diphosphonio-isophosphindole 1 (Scheme 1) [15]. Even though the product was originally formulated as a stabilised phosphenium ion and its bonding situation characterised by a resonance between canonical structures **1a–c** which attested a highly ambiphilic (i.e. both electrophilic and nucleophilic) nature by assigning both positive and negative formal charges to the two-coordinate phosphorus atom, it turned out later that a description as a doubly phosphonio-substituted phospholide with a delocalised aromatic π-electron system (**1d**) was preferable (a more detailed discussion of the electronic structure will be given below) [16, 17].
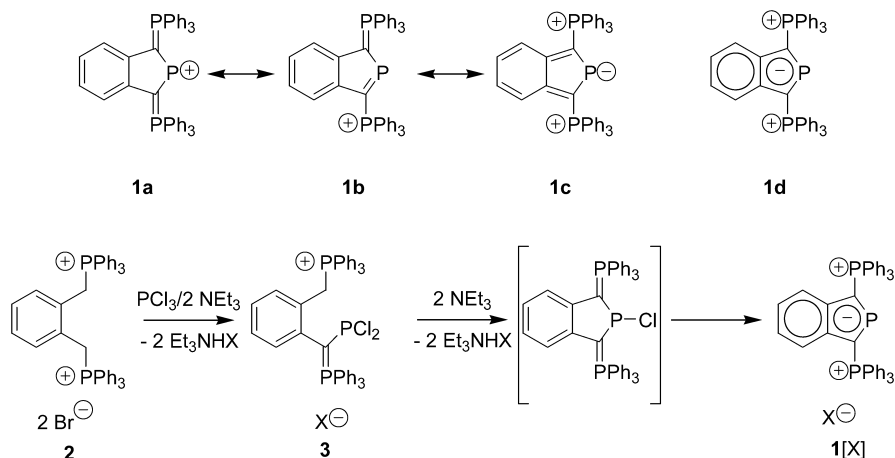
Scheme 1 Resonance structures of the cation **1**(X=Cl, Br) according to [15, 16]

The formation of the heterocycle 1 from the xylylene-bis-phosphonium salt **2** and PCl$_3$ proceeds via a detectable intermediate **3** in a cascade of condensation reactions that is terminated by spontaneous heterolysis of the last remaining P-Cl bond in a cyclic bis-ylide-substituted chlorophosphine formed (Scheme 1) [15]. The reaction scheme is applicable to an arsenic analogue of 1 [15] and to bis-phosphonio-benzophospholides with different triaryl-, aryl-alkyl- and aryl-vinyl-phosphonio groups [16, 18, 19], but failed for trialkylphosphonio-substituted cations; here, insufficient acidity prohibited obviously quantitative deprotonation of the phosphonium salts, and only mixtures of products with unreacted starting materials were obtained [19]. The cations were isolated as chloride or bromide salts, but conversion of the anions by complexation with Lewis-acids or metathesis was easily feasible [16, 18, 19] and even salts with organometallic anions ([Co(CO)$_4$]$^-$, [CpM(CO)$_3$]$^-$ (M=Mo, W) were accessible [20].
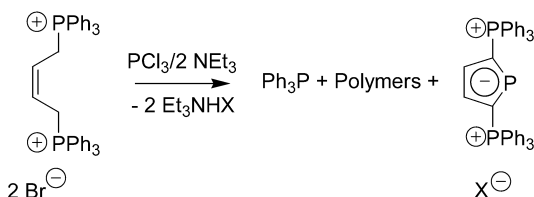
Scheme 2 Products arising from base-induced condensation from PCl$_3$ with xylylene- and butenylidene-bis-phosphonium salts (X=Cl, Br)

Reactions of butenylidene-bis-phosphonium salts with PCl$_3$/triethylamine under similar conditions proceeded predominantly via base-induced fragmentation to triphenyl phosphine and polymeric products of unknown constitution (Scheme 2). Monocyclic bis-phosphonio-phospholides formed only as spectroscopically detectable but hardly isolable byproducts [18, 19].

The base-induced reactions of xylylene- and butenylidene-bis-phosphonium salts may be rationalised by a common mechanism that involves initial deprotonation to give the intermediate ylide 4 which may either suffer fragmentation to R$_3$P and a transient butadienyl-phosphonium salt (Scheme 3, (a)), or transform via an addition/elimination sequence to a new ylide (Scheme 3, (b)) that undergoes subsequent ring closure. The evident preference of xylylene-bis-phosphonium salts for heterocycle formation is under this hypothesis attributable to the fact that the fragmentation path requires the energetically unfavourable conversion of the benzenoid into a chinoid ring which should add considerably to the activation energy for this step [19].
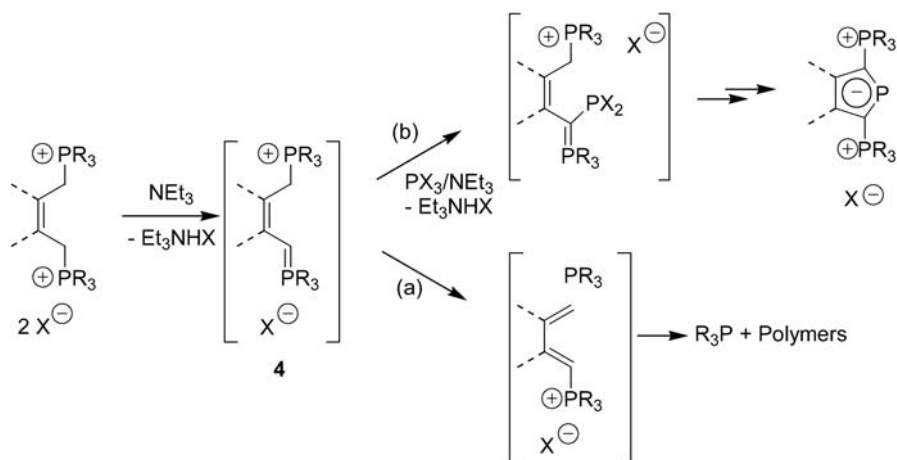
Scheme 3 Proposed mechanism for the base-induced condensation of PCl₃ with butenylidene-bis-phosphonium salts

In contrast to monocyclic bis-phosphonio-pospholides, the 1,2-di- and 1,2,4-triphospholide derivatives were more easily available by condensation reactions under formation of P-P bonds. The group of Schmidpeter reported that reaction of two equivalents of PCl_3/triethylamine with the bis-triphenylphosphonio-propenide 5 in the presence of triphenyl phosphine afforded as main product the isolable 2,3-dihydro-1,2-phosphole bromide 7 whose dechlorination with an equimolar amount of tributyl phosphine gave the cationic bis-phosphonio-1,2-diphospholide 8 (Scheme 4) [21, 22]. The reaction proceeds via initial condensation of 5 and PCl_3 to give a four-membered heterocycle 6 which reacts then with PPh_3 and a second equivalent of PCl_3 via ring expansion to give 7. A closely related mechanism was discussed for the condensation of the bis-trimethylsilylated phosphonium ylide 9 with 1.5 equivalents of PCl_3 in the presence of tributyl phosphine as reductive dechlorination agent which afforded first the 1,2-dihydro-1,2,4-triphospholide 10 and subsequently, with excess tributyl phosphine, the unsaturated triphospholide 11 as final product [23]. Both 10 and 11 were isolated in modest yields as moderately air and water stable halide salts which were easily convertible into other salts via anion metathesis.
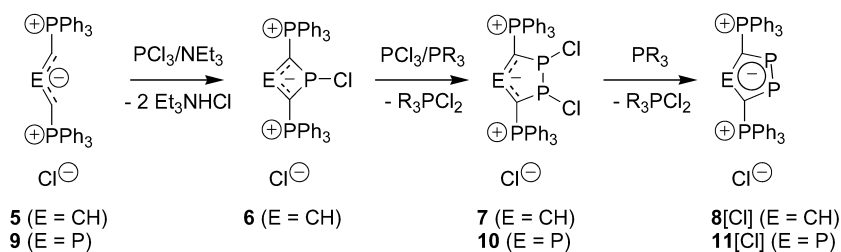
Scheme 4 Synthesis of bis-phosphonio-1,2-di- and 1,2,4-triphospholides (R=Bu, Ph)

The bis-phosphonio-1,2,4-diazaphospholide **15** which is isoelectronic to **11** was—last, but not least—prepared by condensation of the ylidyl-dichlorophosphine **12** with trimethylsilyl azide. Depending on the ratio of the reactants, the zwitterionic triazaphospholide **14** formed as by-product [24]. The formation of both products was explained by a common mechanism which proceeded via initial [2+3] cycloaddition of both reactants followed by cleavage of ClSiMe$_3$ to give the heterocycle **13** as key intermediate. The generation of **14** was then completed by a second dechlorosilylation while **15** was postulated to arise from elimination of a Me$_3$SiNPCl fragment to give an intermediate diazo-ylide which was then quenched by a [2+3] cycloaddition with **12** and a final dechlorosilylation (Scheme 5).
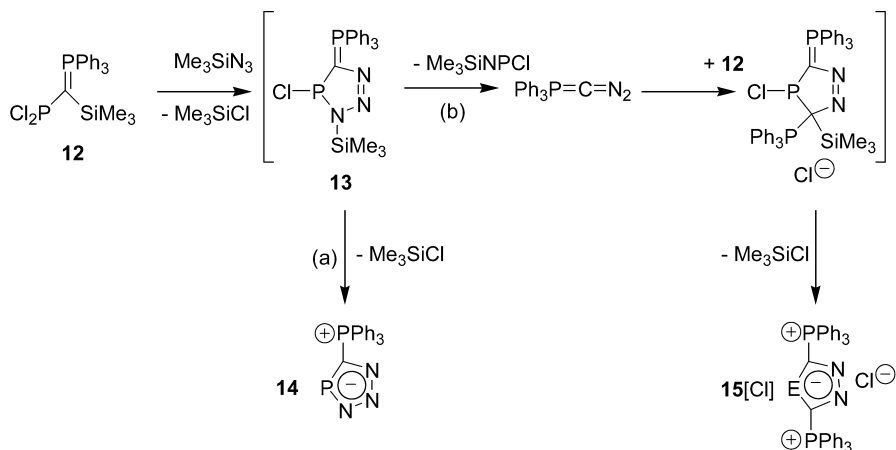
Scheme 5 Condensation reactions leading to the phosphonio-1,2,3,4-triazaphospholide and bis-phosphonio-1,2,4-diazaphospholide system

Ylidyl-dichlorophosphines such as **12** are not only accessible from condensation of PCl$_3$ with C-silylated ylides, but also via base induced dehydrohalogenation of phosphonium salts with active methylene groups in the presence of phosphorus trihalides. The attempt to employ this strategy to prepare C-phenylated ylidyl-dichlorophosphines **16** leads to the discovery of an unexpected side reaction that provided a surprisingly simple access to the benzo-1,2-diphospholide (or 1,2-diphosphaindenide) system (Scheme 6) [25]. Even if the mechanism was not unveiled in all details, the reaction involves presumably a further base-promoted condensation of PX$_3$ with **16** to give transient diphosphines **17** whose C-phenyl rings undergo intramolecular electrophilic phosphinylation to the 3-phosphonio-1,2-dihydro-benzodiphospholides **18**. Although the transformation **16**→**18** remained incomplete, the latter were isolated in around 30% yields by fractional crystallisation and were finally converted into the fully unsaturated 3-phosphonio-benzo-1,2-diphospholide **19** by reductive dehalogenation [25].
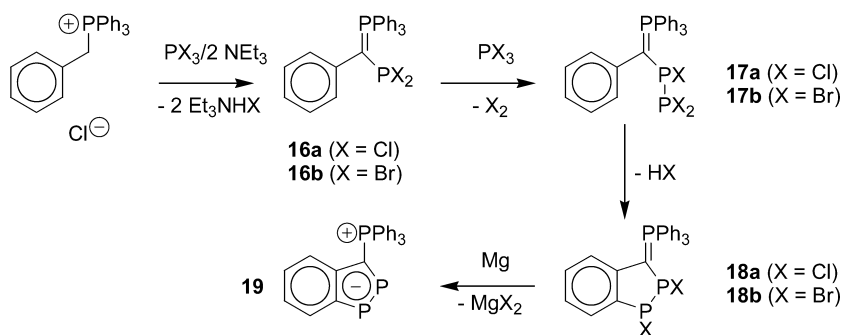
Scheme 6 Synthesis of 3-phosphonio-benzo-1,2-diphospholides according to [23]

2.2
By Ring Metathesis Reactions

Ring metathesis via formal exchange of a single atom in a pre-formed ring is a common strategy for the synthesis of inorganic heterocycles. The use of this approach for the preparation of bis-phosphonio-benzophospholides was first reported by the group of Schmidpeter who found that the stannain-dene **20** and PCl_3 reacted selectively with exchange of a neutral tin by a cat-ionic phosphorus atom to give **1** [26] (Scheme 7). Even though this reaction was mainly of mechanistic interest and offered no synthetic advantage as compared to the condensation route outlined above, metathesis may be the method of choice if other routes fail. This was demonstrated for the ω-phos-phinoalkyl-functionalised bis-phosphonio-benzophospholide **23** which was readily isolated from a two-step reaction involving conversion of the precur-sor phosphonium salt **21** into a sila-heterocycle **22** and subsequent metathe-sis with PCl_3; attempts to the direct synthesis of **23** via condensation of **21**
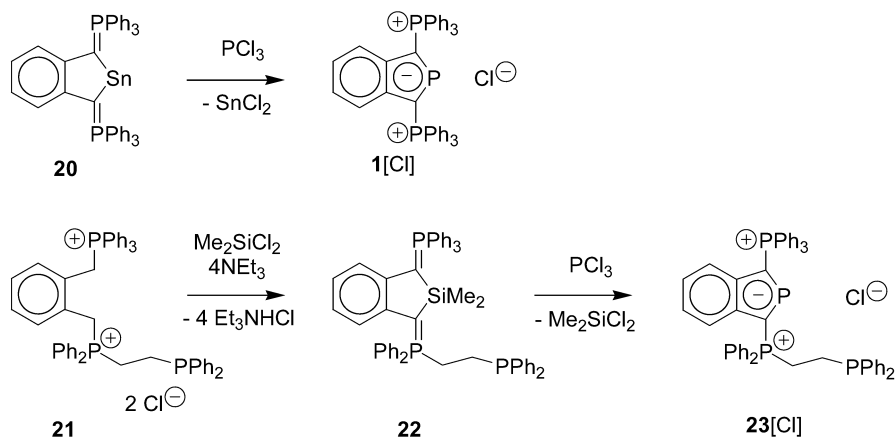
Scheme 7 Syntheses of bis-phosphonio-benzophospholides by ring metathesis

with PCl$_3$ yielded impure products that could not be further purified [27]. Regarding that **22** is essentially a silylated phosphonium ylide whose preparation from a phosphonium salt is feasible via well known and generally applicable routes, it is conceivable that the "silyl-ylide" route may evolve into a useful protocol for the preparation of further functionalised bis-phosphonio-benzophospholides.

2.3
Transformation Between Phosphonio-Pholides by Modification of Substituents

Transformation of a phosphonio-substituted pholide derivative under conservation of the π-electron system has been demonstrated in a number of cases which include substitution of a ring-hydrogen atom, replacement of a PR$_3^{(+)}$-moiety by a hydride, or reductive de-arylation of a Ph$_3$P$^{(+)}$- to a phosphinyl substituent PPh$_2$. Subsequent re-quaternisation of the latter allows the formal substitution of a Ph$_3$P$^{(+)}$- by a modified Ph$_2$(R)P$^{(+)}$-moiety in a two-step reaction. The application of this scheme is not only perfectly suitable for the synthesis of bis-phosphonio-benzophospholides with different phosphonio-moieties but, since the last reaction stage tolerates a variety of functional groups in the electrophile, offers as well a convenient pathway for the synthesis of side-chain functionalised phosphonio-pholide derivatives from more simple substituted precursors.

2.3.1
Substitution of Hydrogen Atoms

Reaction of the bis-phosphonio-benzophospholide **1** with bromine in the presence of triethyl amine afforded the 5,6-dibromo-substituted derivative **24b** [28]. Detailed studies revealed that the reaction proceeds in a similar way as the "indirect" electrophilic substitution of λ^3-phosphinines [29] where the actual substitution is preceded by oxidative addition of Br$_2$ to the two-coordinate phosphorus (see also below). The mono-substitution product **24a** was observed as intermediate, but could not be isolated (Scheme 8).
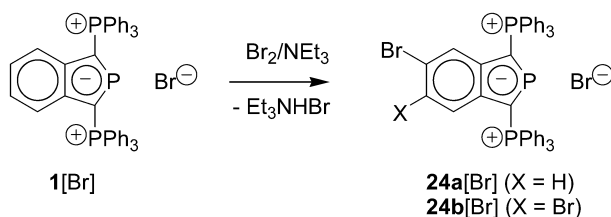
Scheme 8 Bromination of a bis-phosphonio-benzophospholide

2.3.2
Reduction of Phosphonio-Substituents

Phosphonium ions R_4P^+ react with a variety of reducing agents via P-C bond cleavage to give, after quenching of the initial carbanionic products, a mixture of a tertiary phosphine R_3P and a hydrocarbon RH [30]. As phosphonio-substituted phospholide derivatives exhibit at least two topologically different P-C bonds, their reduction may yield more complicated mixtures: bond cleavage can occur either at the P-C bond between the R_3P-substituent and the ring to give R_3P and a H-substituted phospholide, or, alternatively, at an internal P-C bond in the R_3P-moiety to give an R_2P-substituted phospholide and RH. Furthermore, cations with two phosphonio-moieties may react with reduction of one or both positively charged substituents. Although the high complexity of possible reactions might imply at a first glance that the synthetic benefit of reductions of phosphonio-substituted phospholides is questionable, this is actually not the case. To date, several procedures have been reported where either the reduction proceeds highly selective, or procedures for the separation of a single desired product are available [31–34]. Although most reductions reported so far dealt with phosphonio-benzophospholides, the extension to other heterocyclic systems has been demonstrated [34], and a more general applicability is conceivable.

Starting from readily available cationic bis-phosphonio-benzophospholides, the most useful reactions from a synthetic point of view proved those involving reductive cleavage of a single phosphonio-group; the reasons are obviously that these reactions occur under relatively mild conditions, the number of possible products is limited, and the neutral products formed are robust and easily separated from the reaction mixture. Studies of various reactions of the cation 1 revealed that the method of choice for the selective cleavage of a phenyl moiety to give the zwitterion **25** (Scheme 9) involved treatment of a suspension of **1** in THF with active magnesium [33] while cleavage of Ph_3P and formation of the H-substituted zwitterion **26** was preferred when the reduction was carried out with $NaBH_4$ in iPrOH, respectively [32, 33]. The BH_4-reduction proceeded chemoselectively, but the magnesium reduction yielded actually a mixture of **25** and **26** which had to be separated during the work-up. The product ratio varied with the method of activation of the metal; the highest relative yields of 25 (>50% of reduction products) were achieved by employing magnesium powder obtained by reduction of $MgCl_2$ with potassium [33], whereas magnesium generated by thermal decomposition of Mg-anthracene, or the use of Mg-anthracene itself, gave between 25 and 50% of the undesired by-product 26 [31].

The reductive cleavage of phosphonio-substituents attached to other heterocyclic frameworks was first demonstrated in the reaction of the 3,5-bis-phosphonio-1,2,4-diazaphospholide **15** with $NaBH_4$ or $LiBEt_3H$ to yield the zwitterionic borane-complexes **27**. Liberation of the "free" zwitterion **28** was readily feasible by treatment of the complexes with an excess of NEt_3 (Scheme 9) [34].
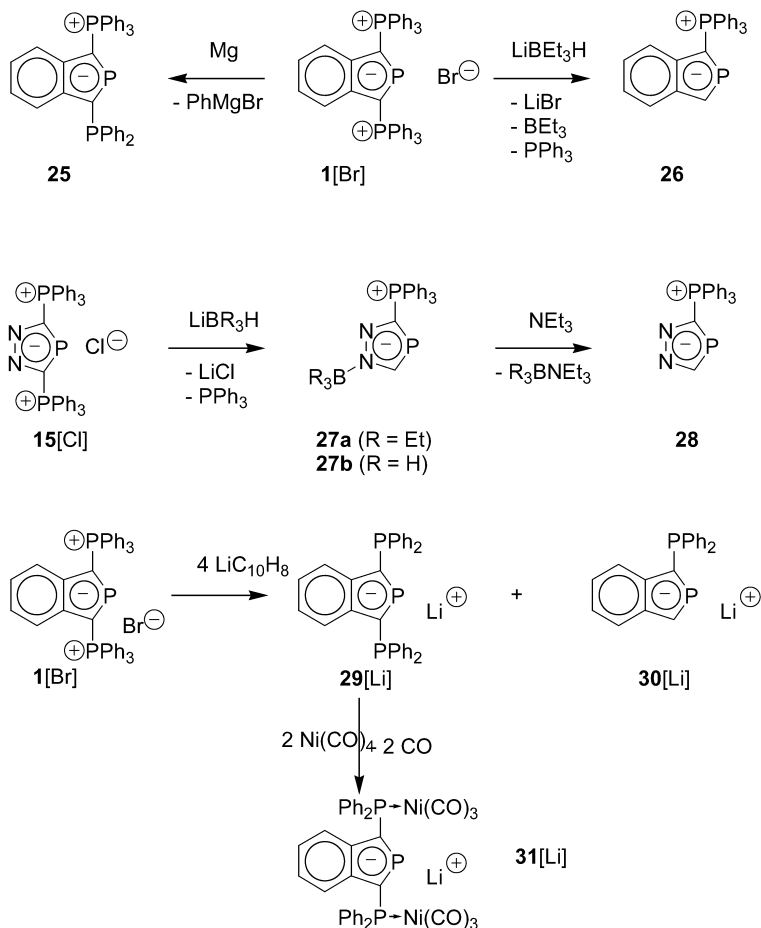
Scheme 9 Reduction of cationic bis-phosphonio-benzophospholides and -diazaphospholides

Reduction of both phosphonio-substituents of a cationic, or the remaining phosphonio-group of a zwitterionic benzophospholide requires more powerful reducing agents than magnesium. Reactions with alkaline metals turned out to follow a more complicated pathway and yielded inseparable product mixtures [31]. Although highly interesting from a mechanistic point of view (see below), these reactions were thus of little synthetic value. However, when alkaline metal naphthalenides $MC_{10}H_8$ (M=Li, Na, K) rather than the pure metals were used, the reactions proceeded under reduction of all Ph_3P-substituents to give as main products mono- or bis-phosphinyl-benzophospholide anions (Scheme 9) [31, 35] which were convertible into novel zwitterions or cations by subsequent quaternisation steps (see following section). As in the reaction with magnesium, the reduction afforded mixtures

of compounds where the former Ph$_3$P-moiety had formally been replaced by a hydrogen or a Ph$_2$P-group, respectively. Isolation of a pure product was so far only possible in the case of the nickel complex **31** which represents to date the first example of a free benzophospholide anion that was characterized by a single-crystal X-ray diffraction study [31].

2.3.3
Quaternisation of Phosphinyl-Substituents

Phosphinyl-substituted (benzo)phospholides are in principle ambident nucleophiles whose attack by an electrophile may occur both at the exocyclic and the endocyclic phosphorus atom. However, as the former is more nucleophilic [33], the initial attack occurs normally highly regioselective under quaternisation of the phosphinyl-moiety. Since the generation of a new electron withdrawing phosphonio-substituent further deactivates the ring phosphorus atom, the product formed is generally stable under the reaction conditions. Quaternisation of the ring phosphorus is not principally unfeasible, but appears to require the action of a strong electrophile such as methyl triflate [36].

Reactions under quaternisation of exocyclic R$_2$P-substituents have so far been applied exclusively to benzophospholide derivatives. The most convenient approach involves treatment of the substrate with an appropriate alkyl halide [27, 31, 35] or acrylic acid (Scheme 10) [27]. The quaternisation products formed are in general isolable without complication if pure starting materials have been employed as is normally the case for zwitterionic substrates. Anionic benzophospholides such as **29** and **30** are, in contrast, normally only accessible as crude product mixtures whose quaternisation affords mixtures of several phosphonium salts. Separation of the desired product may in these cases require lengthy work-up procedures and result in substantially lower yields [31].
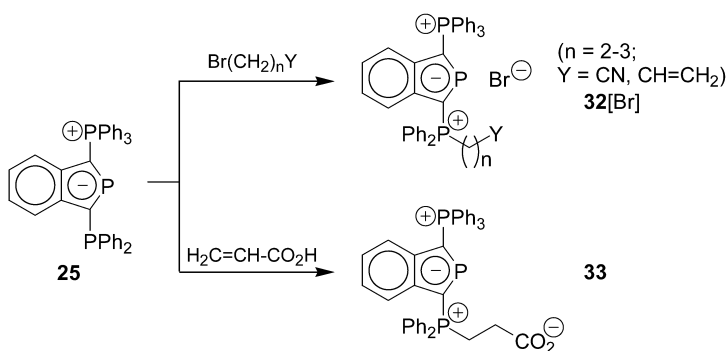
Scheme 10 Phosphonio-benzophospholides by quaternisation of phosphine-type precursors

In addition to the electrophilic alkylation, the phosphinyl-benzophospholide **25** reacted also with sulphur, BH$_3$·thf, and trimethylsilyl azide under selective conversion of the Ph$_2$P-moiety to give the corresponding thioxophosphorane, borane-adduct, and iminophosphorane, respectively [33, 37], and quaternisation with chloro-acetonitrile followed by deprotonation gave access to a zwitterionic phosphonio-benzophospholide with an exocyclic ylide-substituent [37].

3
Physical Properties and Bonding Situation

3.1
Molecular Structures

Determination of the molecular structures by single-crystal X-ray diffraction studies has been carried out for 3,5-bis-phosphonio-1,2-di- and -1,2,4-triphospholides [21, 23], 3-phosphonio- and 3,5-bis-phosphonio-1,2,4-diazaphospholides [24, 34], and several 1,3-bis-phosphonio- and 1-phosphonio-benzophospholides [16, 20, 27, 33]. The ring systems of all compounds exhibit at best small deviations from planarity which are attributable to crystal packing effects. An overview of important bond lengths is given in Table 1. The C-C and C-N bonds are in the typical range for aromatic systems and similar as in indoles or indolyl anions. Endocyclic P-C and P-P bonds are intermediate between the values of pure single and double bonds, respectively, and compare to appropriate distances in phospholides and phosphinines. Exocyclic P-C bonds to the phosphorus atoms in phosphonio-substituents are somewhat shorter than pure single bonds, but match comparable distances in electronically stabilised phosphonium ylides [16, 20, 27, 33].

The variation of individual C-C bond lengths in different compounds is generally small and structure correlations are obstructed by the fact that the differences observed are frequently of similar magnitude than those between

Table 1 Average values of selected bond distances in phosphonio-substituted phospholide derivatives (data from [16, 20–24, 27, 33, 34]). "Endocyclic" bonds refer exclusively to those in the phosphole rings if annulated ring systems are present

Type of bond	Average distance/pm	Standard deviation/pm
Endocyclic bonds		
P-P	207.5	0.3
P-C	174.1	1.5
C-C	143.0	1.3
C-N	138.6	7.3
N-N	135.9	2.4
Exocyclic bonds		
P-C	175.1(4)	1.9
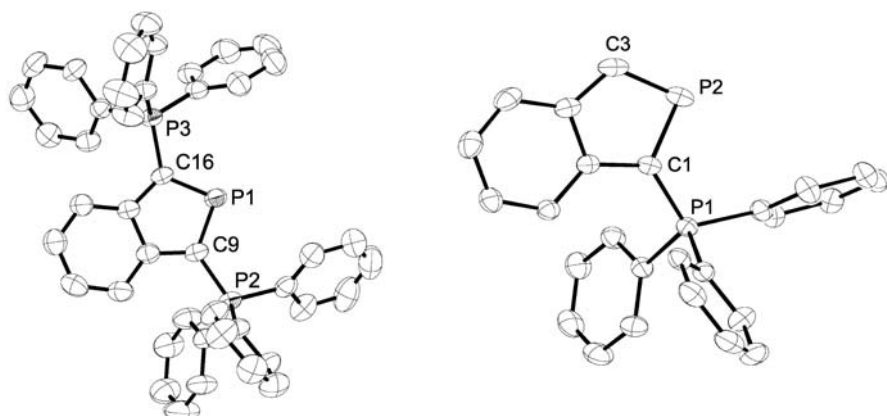
Fig. 1 ORTEP-representation of the molecular structure of the cation 1 [20] (*left*) and the zwitterion 26 [33] (*right*). Hydrogen atoms were omitted for clarity. Selected bond distances (in pm): 1: P1-C9 172.8(4), P1-C16 172.9(4), P2-C9 174.7(4), P3-C16 174.9(4); 26: C1-P2 176.62(11), P2-C3 171.71(14), P1-C1 172.55(11)

crystallographically distinguishable instances of the same molecule [33]. The P-C bond distances display a somewhat larger variability, and in this case a clear cut transmission of structural changes on bond lengths emerges if one compares the two P-C bonds in the benzophospholide or diazaphospholide moiety of the same molecule: both bonds are indistinguishable within experimental error in 1,3-bis-phosphonio-substituted cations, but zwitterions with a single phosphonio-moiety display a shortening of the bond to the carbon atom adjacent to the positively charged substituent and a concomitant lengthening of the remote one (Fig. 1). The observed trend is easily explained in terms of substituent induced shifts of π-electron distributions [33] and will be discussed in the context of appropriate computational studies below.

3.2
Spectroscopic Properties

The phosphonio-substituted phospholide derivatives known to date were characterised routinely by multinuclear NMR and UV-VIS spectroscopy, and mass spectrometry. Beside serving the purpose of compound identification, the spectroscopic data allowed some important conclusions concerning trends in electronic structures of different molecules.

Both the ^{31}P and ^{13}C NMR shifts for the two-coordinate phosphorus and the adjacent carbon atoms are highly diagnostic of the bonding situation. The known ranges of ^{31}P chemical shifts lie around 360 ppm for 1,2,4-triphospholides [23], between 320 and 230 ppm for (benzo)-1,2-diphospholides [21, 25], between 250 and 180 ppm for benzophospholides [15, 16, 27, 28, 32] and close to 180 ppm for diazaphospholides [24, 34]; in comparing

Table 2 Substituent influences on $\delta^{31}P$ of the two-coordinate phosphorus atom in benzophospholide derivatives

R^1	R^2	$\delta^{31}P$	Ref.
H	H	135	[37]
PPh_2	H	174	[31]
PPh_3^+	H	190	[31]
		216	[31]
PPh_2	PPh_2	218	[31]
PPh_3^+	PPh_2	242	[15]
PPh_3^+	PPh_3^+		
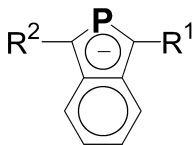
these data it must be noted that the narrow expectation ranges for 1,2,4-triphospholides and -diazaphospholides owe presumably to the small number of known compounds. Attaching an increasing number of substituents to the α-carbon atoms adjacent to a two-coordinate phosphorus atom induces a continuous deshielding of the latter, and this effect is somewhat larger if the substituent is a positively charged $R_3P^{(+)}$- rather than a neutral R_2P-moiety [33] (see Table 2). The ^{13}C chemical shifts of α-carbon atoms appear generally between 85 and 115 ppm for those with $Ph_3P^{(+)}$- and between 135 and 145 ppm for those with Ph_2P- or H-substituents. On the whole, the values of $\delta^{13}C$ for the carbon atoms with formally neutral (H, Ph_2P) substituents match those in phosphinines or phospholides whereas those of phosphonio-substituted carbon atoms range between the values of phos-
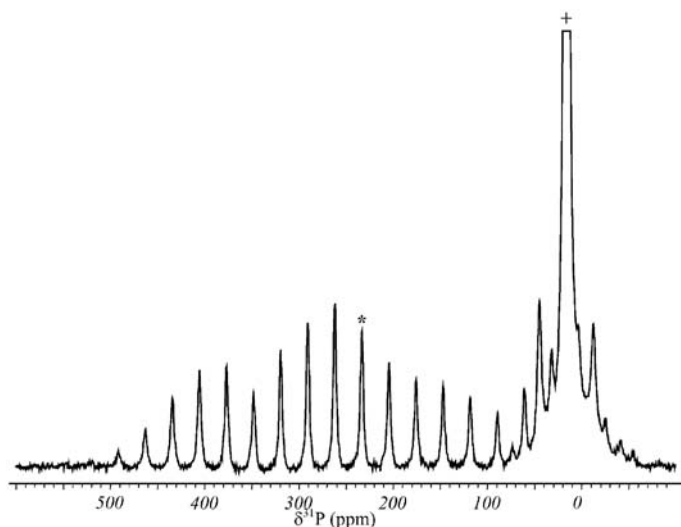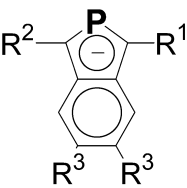
Fig. 2 Solid-state $^{31}P\{^1H\}$ MAS-NMR spectrum of 1[Br]. The *asterisk* and *cross* denote the isotropic lines attributable to the two- and four-coordinate phosphorus atoms, respectively (according to [37])

Table 3 Energies of π-$\pi^\star$ transitions in the benzophospholide chromophor (ΔE in 10^3 cm^{-1}) of phosphonio-benzophospholides (data from [18, 28, 33])

R^1	R^2	R^3	ΔE^1	ΔE^2	Ref.
PPh$_3$$^+$	PPh$_3$$^+$	H	28.3	29.8	[18]
P(py)Ph$_2$$^+$	P(py)Ph$_2$$^+$	H	28.3	29.8	[18]
P(Me)Ph$_2$$^+$	P(Me)Ph$_2$$^+$	H	28.3	29.8	[18]
PPh$_3$$^+$	PPh$_3$$^+$	Br	27.0	29.0	[28]
PPh$_3$$^+$	PPh$_3$$^+$	H	26.9	30.3	[33]
PPh$_3$$^+$	PPh$_2$	H	28.2	31.8	[33]
PPh$_3$$^+$	H				

phinines and acyclic phosphonio-phosphaalkenes or stabilised phosphonium ylides [33].

A solid-state ^{31}P NMR study of the bis-phosphonio-benzophospholide bromide **1**[Br] revealed that the large isotropic chemical shift of the ring phosphorus atom owes mainly to the deshielding of a single principal tensor component (see Fig. 2) whose axis points according to quantum chemical calculations into a direction perpendicular to the axes of the phosphorus lone-pair and the p-orbital involved in the benzophospholide π-electron system [37]. This situation is common for a phosphorus atom in a multiple bond system [38]. An explanation may be given [38] by considering that chemical shifts of non-hydrogen nuclei are normally dominated by the paramagnetic shielding term whose magnitude depends on the availability of excited states that are connected with the ground state by magnetic-dipole allowed transitions. In the present case, the dominant contribution of this type is associated with an n$\rightarrow$$\pi^\star$ excitation, and low transition energies correlate with large deshieldings. The increase of δ^{31}P upon replacement of a neutral Ph$_2$P- or H- substituent by a positively charged Ph$_3$P$^{(+)}$-moiety is thus best rationalised by assuming that the $\pi^\star$-orbital experiences a stronger electronic stabilisation by the electron withdrawing substituent than the phosphorus lone-pair orbital.

Studies of UV-VIS spectra are to date restricted to mono- and bis-phosphonio-benzophospholides [18, 28, 33]. The first two electronic excitations in all compounds were assigned to π-$\pi^\star$ transitions of the benzophospholide chromophor and occur at similar energies as the π-$\pi^\star$ transitions in 2-phospha-naphthalenes (Table 3) [18, 33]. Interpretation of the observed substituent effects confirmed the description of the bonding situation in terms of a delocalised "naphthalene-analogue" 10π-electron system and suggested further a low degree of hyperconjugation with $\sigma^\star$-orbitals in peripheral R$_3$P$^{(+)}$-substituents [18, 28].

3.3
Computational Studies of the Bonding Situation

Computational studies of the bonding situation have so far focussed on two issues, namely the π-electron delocalisation and its perturbation by phos-

Fig. 3 Resonance description of the π-electron structure in (benzo)phospholides (R=H, PH$_3^{(+)}$)

phonio-substituents in (as yet) hypothetic 1,3-bis-phosphonio-phospholides, and in mono- and bis-phosphonio-benzophospholides. The π-delocalisation was assessed from NBO population analyses of the results of ab initio and DFT calculations, and by comparing computed energies of suitable isodesmic reactions [16, 33].

The π-delocalisation in the parent phospholide anion **I** (Fig. 3, R^1=R^2=H) can be expressed in the valence bond picture by resonance between the canonical structures **IA-IC** (and their mirror images). Phosphonio-substituents (R^1=R^2=PH$_3^{(+)}$) increase the weight of the 1,2-dipolaric canonical structure **IB** and induce thus, in essence, a partial π-bond localisation and a shift of π-electron density from the phosphorus to the adjacent carbon atoms [16]. Consequences of this effect are the decrease in delocalisation energy for reaction (1) depicted in Fig. 4, and lower C2-C3/C4-C5 and higher C3-C4 bond orders which are reproduced in concomitant variations of computed bond distances [16].

The bonding in the parent benzophospholide features an extended π-delocalisation around the ring perimeter which is expressed by dissipation of the excess charge on a larger number of canonical formulae such as **IIA-IIE** (and their mirror images of which all but **IIB'** were omitted). Phosphonio-substituents in 1- and 3-positions increase the weight of the symmetry equivalent canonical structures **IIB, IIB'**. As before, this implies a partial π-bond localisation and a reduction of the energy of the isodesmic reaction (2) in Fig. 4 [16].

If only a single phosphonio-group is present (R^1=PH$_3^{(+)}$; R^2=H), the degeneracy of canonical structures **IIB, IIB'** is raised, and **IIB'** obtains less

Fig. 4 Delocalisation energies $\Delta E_{1,2}$ (in kcal mol^{-1}) in (benzo)phospholides as computed from the isodesmic reactions (1) and (2). (R=H, PH$_3$$^{(+)}$; from [16])
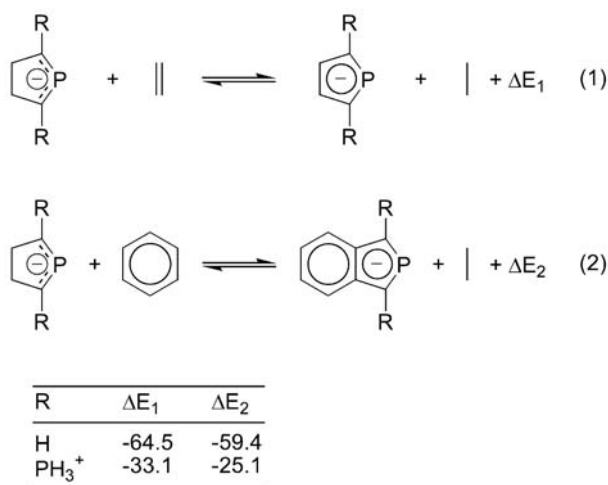
weight than the remaining 1,2-dipolaric structure **IIB**. The exocyclic C-P bond adjacent to the PH$_3$-substituent resembles then more closely that of a phosphonium ylide while the remote endocyclic C-P bond gains more double bond character. At the same time, a higher rating of structure **IIC** indicates increased π-conjugation between the fused rings [33]. Differential tuning of these trends is achieved with growing inductive power of R^2 in the series R^2=PH$_2$, P(BH$_3$)H$_2$, P(S)H$_2$) [33].

Hyperconjugation between the π-electron system and σ*-orbitals in the substituents appears to be generally small and was found to occur to a similar extent in both phosphinyl- and phosphonio-substituted species. This suggests that the dominance of 1.2-dipolaric canonical structures in the latter is attributable to the smaller charge separation and underlines that the shift in π-electron distributions can be understood mainly by electrostatics [33].

Finally, a short account on nature and energies of frontier orbitals should allow some predictions on the ligand properties of benzophospholides [33]. HOMO and LUMO in mono- and bis-phosphonio-benzophospholide can be described as the 5π and 6π* orbitals of a heteronaphthalenic 10π-electron system. The highest σ-orbitals lie approximately 2 eV below the HOMO and are assigned to non-bonding orbitals centred mainly at the ring phosphorus atoms (phosphorus "lone-pairs"). The energies of the latter (-7.3 to -7.5 eV) are similar to those calculated for phosphinine (-7.3 eV) or PH$_3$ (-7.5 eV) at the same level of theory. Generally, all occupied and unoccupied orbitals are as expected stabilised with increasing overall positive charge of the ligand, but the HOMO-LUMO gap changes hardly. Based on these findings it can be predicted that the donator-capability of benzophospholide ligands will decrease and their π-acceptor capability will increase with the number of positively charged phosphonio groups [33].

4
Chemical Reactivity

The reactivity of compounds with phosphorus containing multiple bond systems is coined by the presence of high lying π- and energetically accessible π^*-orbitals which enables these species to act both as nucleophiles and electrophiles [10]. As a consequence of this ambiphilicity, the compounds undergo not only a variety of addition reactions with electrophiles and nucleophiles and may easily engage in redox reactions, but are in particular sought for as highly efficient σ-donor-π-acceptor ligands in coordination chemistry. As will be shown below, these general criteria may also serve as key guidelines for the development of a chemistry of phosphonio-substituted pholide derivatives. In contrast to the broader focus of the synthetic explorations which have been outlined at the beginning of this review, the majority of studies of chemical reactivities have as yet concentrated on phosphonio-substituted benzophospholides.

4.1
Reactions with Nucleophiles and Electrophiles

In spite of the general ambiphilicity of phosphonio-substituted phospholide derivatives, the aromaticity of the phospholide ring [10, 11] tends to reduce their electrophilicity while the intramolecular compensation of the negative charge by the phosphonio-substituents lowers at the same time their nucleophilicity [15, 16]. Bis-phosphonio-benzophospholides and -1,2,4-diazaphospholides are therefore less reactive towards electrophiles and nucleophiles than other types of phosphorus containing multiple-bond systems and lack the notorious hydrolytic instability of many of these species [15, 16, 24]. Reactions are observed, however, with sufficiently strong electrophiles such as triflic acid or methyl triflate, or nucleophiles such as OH⁻ or lithium alkyls, respectively.

The attack of nucleophiles on the bis-phosphonio-benzophospholide 1 occurs invariably at the two-coordinate phosphorus atom and gives a bis-ylide (Scheme 11) which may then undergo further reactions (i.e. rearrangement to a secondary phosphine oxide) [15, 31]. Protonation of 1 by an acid HX appears to occur, in contrast to earlier assumptions, exclusively at the ring carbon next to the phosphorus atom which represents the site of highest electron density in the HOMO [39]. The unstable primary adduct 35 which is observable for X=OTf is easily quenched by nucleophiles such as halide ions or H_2O, and the overall reaction to 36 corresponds thus to a 1,2-addition to the phosphole ring. Alkylation of 1 by methyl triflate was not observed, presumably due to steric protection of the α-carbon by the Ph_3P-moieties (claims to the P-methylation by $[Me_3O][BF_4]$ were later corrected and the product formed was identified as arising from reaction of 1 with $HBF_4/MeOH$ which had been formed by previous hydrolysis of Meerwein's salt) [39]. The activation of a bis-phosphonio-benzophospholide to undergo

similar 1.2-addition reactions may not only be accomplished by previous action of a Brønsted acid as in the above examples, but also by Lewis-acidic transition metal cations (see below) or oxidising agents [37].
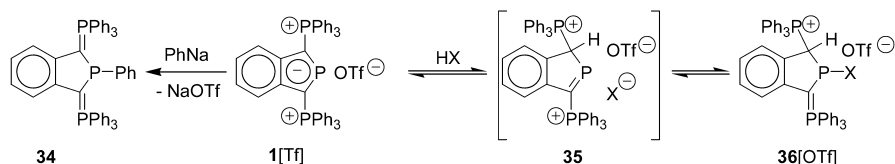
Scheme 11 Reactions of the cation **1** with nucleophiles and electrophiles

Electrophilic alkylation of other phosphonio-substituted phospholide derivatives was studied in the case of the di- and triazaphospholides **14**, **15**, and the 1,2-diphospholide **8**. P-Alkylation of **8** with methyl triflate gave the dication **37** which is distinguished by a flat pyramidal coordination geometry at the tri-coordinate phosphorus atom and represents a bonding situation that is intermediate between a phosphane and a bis(methylene)phosphorane, i.e. between P^{III} and P^{V} (Scheme 12) [36]. Both the triazaphospholide zwitterion **14** and the diazaphospholide cation **15** displayed a preference for N- over P-alkylation upon reaction with methyl triflate [24], and the formation of borane-adducts of the phosphonio-1,2,4-diazaphospholide zwitterion **27** via formation of B-N rather than B-P bonds has already been mentioned (Scheme 9) [34]. The electrophilic attack at nitrogen in the last three examples is comprehensible if one considers that the disposition of nitrogen to adopt a trigonal planar coordination geometry allows to maintain the full π-delocalisation in the ring whereas an attack at a phosphorus or carbon atom would generate a pyramidal or tetrahedral ring node and interrupt the π-delocalisation.
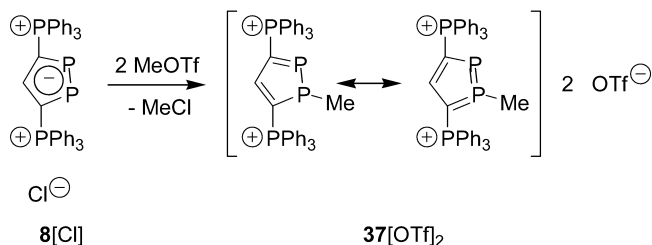
Scheme 12 Alkylation of the phosphonio-substituted 1,2-diphospholide **8**

4.2
Oxidation and Reduction

Oxidation and reduction of the bis-phosphonio-benzophospholide **1** were studied in some detail. Oxidation proceeds via oxidative 1,1-addition of two

halogens or alkoxy groups at the ring phosphorus atom to yield λ^4-benzophospholides and resembles thus similar reactions of phosphinines [29]. The λ^4-benzophospholides may be described, as is suggested in Schemes 13 and 14, as bis-ylides which receive additional stabilisation by hyperconjugation into the central phosphonium moiety.
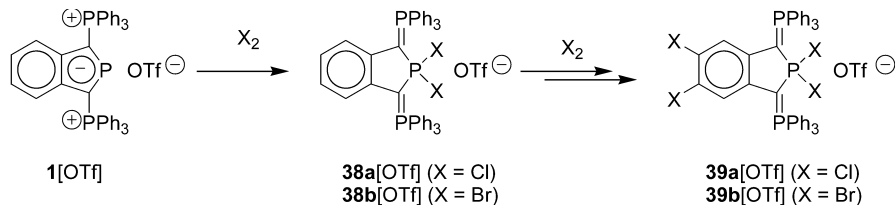
Scheme 13 Halogenation of the bis-phosphonio-benzophospholide **1**

Halogenation of **1** was feasible by treatment with $PhICl_2$ that served as a Cl_2-transfer agent, or Br_2, respectively [28]. Both processes were complicated by side-reactions involving substitution in 5,6-position of the benzophospholide ring (Scheme 13). In the case of the Cl_2-oxidation, the rate of substitution was slower than the oxidation step and the initial product **38a**[OTf] was isolable. In the reaction with Br_2, the rate of the substitution exceeded that of the oxidation step and only the tetrabromide **39b**[OTf] was accessible in pure form. Both **38a** and **39b** reacted with triethyl amine or zinc under reductive dehalogenation to the λ^2-benzophospholides **1** and **24** (see above). Iodine did not oxidize **1**, and attempts to prepare a 2,2-diiodo-λ^4-benzophospholide via Cl/I-exchange from **38a** resulted in immediate decay to I_2 and **1**, suggesting that the oxidation potential of I_2 is already lower than that of **1** [28].
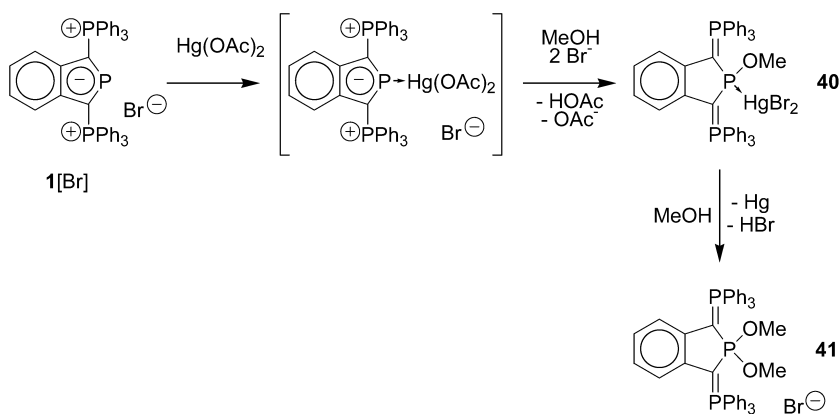
Scheme 14 Hg^{II}-promoted oxidation of the cation **1** (according to [40])

Oxidative alcoholysis of **1** to give dialkoxy-λ^4-benzophospholides was feasible by using either stoichiometric amounts of metal ions such as Hg^{2+}, Cu^{2+}, Pd^{2+} [40, 41], or oxygen in the presence of a catalytic amount of a Cu^I-salt as oxidising agents [41]. The metal promoted oxidation of 1[Br] with Hg^{II}-acetate in methanol was studied in some detail (Scheme 14) [40]. The reaction was postulated to involve initial formation of a Hg^{II}-complex of **1** as key intermediate. As metal coordination activates the phosphole ring for addition of nucleophiles (see previous section), this product was considered unstable and quenched immediately in a reaction sequence involving addition of methanol, deprotonation by an acetate, and OAc/Br-ligand exchange at the metal to afford the isolable complex **40**. The overall reaction is completed by decomposition of **40** in the presence of methanol to yield mercury and the final product **41**[Br].

As has already been mentioned above, reduction of 1,3-bis-phosphonio-benzophospholide cations occurs not at the two-coordinate phosphorus atom but involves rupture of P-C single bonds in the phosphonio-substituents [31]. Beside magnesium, hydridoboranates or alkaline metal naphthalenides whose use has already been discussed, alkaline metals were also applicable reducing agents, and it may be considered as intriguing that reductions with the pure metals yielded different products than those with the naphthalenides [31]. Thus, treatment of 1[Cl] with Li or Na afforded during the early stages of the reaction beside the anions **29**, **30** and cleavage products C_6H_5M and Ph_3P also the P-substituted bis-ylide **34** (Scheme 15) which was converted into the phosphanide-substituted benzophospholide 42[M$_2$] (M=Li, Na) when the reaction advanced. Enrichment of **29**, **30** and **42** up to 90% of all phosphorus containing species was feasible, but quantitative conversion or isolation of any of the products was prevented by unspecific side reactions and slow decomposition to leave phosphanides $MPPh_2$ as only defined phosphorus containing products after prolonged reaction times.
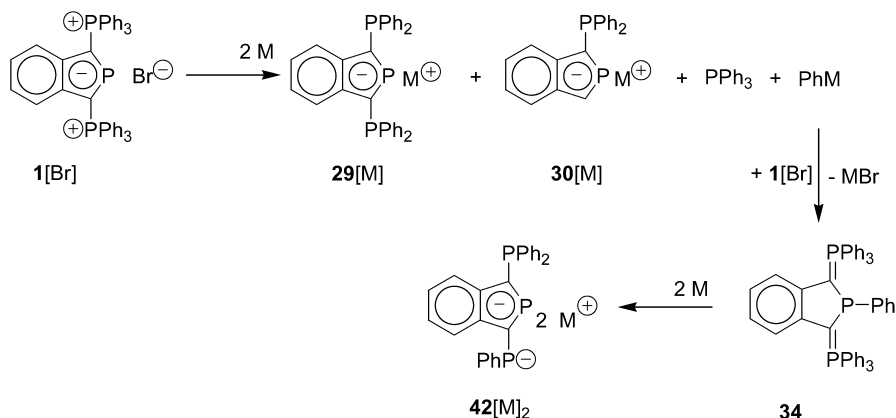
Scheme 15 Proposed mechanism of the reduction of the bis-phosphonio-benzophospholide **3** with alkaline metals (M=Li, Na; according to [31])

The different outcome of reductions of **1** with alkaline metals in the presence or absence of naphthalene is comprehensible if one considers two competing reaction channels, namely (i) reduction to the anions **29, 30,** and (ii) substitution of 1 by the metal phenyl formed leading to **34,** respectively [31]. The selection between both pathways depends obviously on kinetics: the reduction proceeds at a much lower rate when solid metals instead of soluble metal naphthalenides are used so that the slower substitution of still present starting material to give **34** can compete. In view of the low regioselectivity of the reductive disassembly of phosphonio-substituents, the absence of the parent benzophospholide anion—whose formation should result from cleavage of both Ph$_3$P fragments in the cation 1—must further be considered remarkable. A tentative explanation has been given by assuming that either the destruction of the last phosphonio-group occurs with specific fission of an internal P-C bond or, more likely, the benzophospholide decomposes under the reaction conditions [31].

4.3
Coordination Chemistry

Coordination of phosphonio-substituted phospholide derivatives may in principle occur either via the lone-pairs of the two coordinate phosphorus atom (or any other heteroatom in the heterocycle) or via the delocalised π-electron system. Both alternatives have been observed, and it turned out that the actual reactivity of a certain ligand depends frequently on, and is controlled by, the choice of the transition metal fragment. In order to elaborate on the special properties of the complexes formed, the following report is divided into four sections. In the first two parts, focus will be on species whose ligands bind exclusively through the lone-pairs of phosphorus or nitrogen atoms in the ring ("σ-complexes") or the π-electron system ("π-complexes"), respectively. The third section will deal with mixed complexes, and the last one will give a short account on the use of complexes of bis-phosphonio-benzophospholides as hydroformylation catalysts.

4.3.1
Pure σ-Complexes

(Poly)phospholide anions strongly prefer to coordinate transition metals via the π-electron system. Complexation via the phosphorus lone-pair is—apart from rare examples of phospholyl-complexes whose ligand behaves formally as 1e-donor towards a 17e-metal fragment—generally only feasible after the π-electron system has been saturated [9, 10]. This preference is distinctly altered in singly or doubly phosphonio-substituted benzophospholides where coordination via the phosphorus lone-pair becomes competitive or even energetically more favourable than π-coordination [32, 42]. The origin of this effect owes presumably to the polarisation of the π-electron distribution towards 1.2-dipolaric resonance structures (cf. above). This results, in essence,

in a concentration of π-electron density in vicinity to the positively charged substituents, and the resulting intramolecular Coulomb stabilisation may render the π-system less accessible for external electrophilic attack. Even if the details of this deactivation are not yet fully understood and steric effects may also intervene, it is beyond doubt that the preference for π-coordination of a phospholide ring is eventually lost upon attaching an increasing number of phosphonio-moieties [42].

The formation of σ-complexes of bis-phosphonio-benzophospholides has been observed upon reaction with a variety of reagents including (i) suitable precursors capable of transferring 16VE metal carbonyl fragments such as $M(CO)_5$ (M=Cr, Mo, W), $Fe(CO)_4$, $Ni(CO)_3$, $MCl(CO)_4$ (M=Mn, Re), $CpMn(CO)_2$ [27, 32, 35, 43], (ii) olefin complexes of metal atoms with a d^8-configuration and square planar coordination environment such as Rh^I, Pd^{II}, and Pt^{II} [27, 44], and (iii) salts of the coinage metal cations Cu^I, Ag^I, and Au^I with a d^{10} electron count [20, 35, 45, 46]. Intermediate formation of σ-complexes has likewise been inferred from the nature of the products formed in the reaction of 1 with Hg^{II}-salts even though the complexes themselves were considered too instable to be observable [40]. σ-Complexes of a phosphonio-1,2,4-diazaphospholide were formed in the reaction of $[M(CO)_5(thf)]$ (M=Cr, W) with the zwitterion **28** or its triethyl borane adduct [34]. Quite surprisingly, the borane is easily replaced by a transition metal fragment, and the ligand reveals a marked preference to bind two $M(CO)_5$-fragments via the lone-pairs of the phosphorus and one nitrogen atom.

The two-coordinate phosphorus atom of a phosphonio-phospholide moiety is generally a weaker Lewis-base than a tertiary phosphine; as a consequence, the complexes are thermally less stable (this holds in particular for metal fragments with low back donation capability, e.g. $Mn(CO)_4Cl$ [35, 43], benzophospholide ligands are easily displaced by tertiary phosphines such as Ph_3P [27, 44], and bidentate ligands comprising a phosphonio-benzophospholide and a phosphine site react with transition metal fragments preferentially at the phosphine site; coordination of both phosphorus atoms is only observed if the substrate offers two vacant coordination sites [27, 47].

While the low Lewis-basicity of bis-phosphonio-benzophospholides was generally no obstacle, their coordination behaviour turned out to be severely constrained by steric screening of the coordination site by the R_3P-moieties. Unrestricted complex formation was only observed for coinage metal atoms with linear or trigonal-planar coordination spheres where the metal fragment may be arranged to fit into the narrow cleft between the phosphonio-substituents [20, 45]. A remedy for the inaccessibility of metal fragments with tetrahedral, trigonal-bipyramidal, or octahedral coordination spheres was found, however, in the use of ligands featuring a second donor site in one of the phosphonio-moieties. Upon complex formation, these species permit incorporation of one residue as ligand into the metal coordination sphere and turn thus a former repulsive interaction between the metal fragment and an "innocent" R_3P group into an attractive interaction [27]. Examples of the successful application of this approach comprise not only metal

complexes of the phosphinyl-functionalised cation **23** [27], but also such surprising examples as the complexes **45** where the metal atom is chelated by a σ-coordinated benzophospholide moiety and a BH-σ-bond (Scheme 16) [42]. In the case of Pt- and Pd complexes with square planar coordinated d^8-metals, chelating coordination served not only for the stabilisation of the products formed, but also to overcome the kinetic inhibition of complex formation by stabilising a preceding pentacoordinate transition state [27, 44].
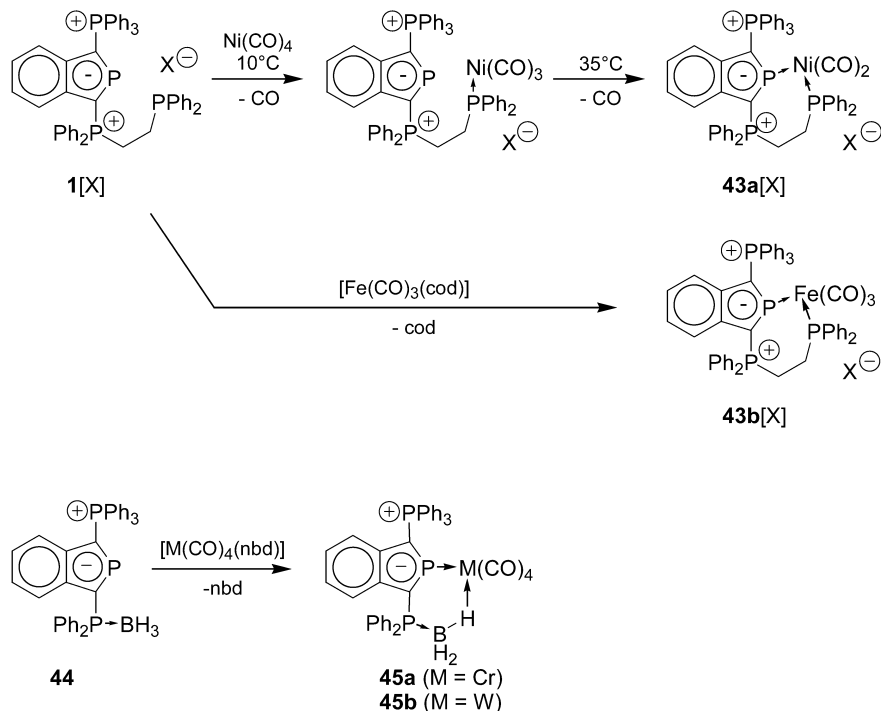
Scheme 16 Formation of complexes with chelating phosphonio-benzophospholide ligands (X=BPh$_4$, Br, OTf)

The σ-coordination of phosphonio-phospholide based ligands induces small coordination shifts of the ^{31}P and ^{13}C NMR signals of the ring atoms, and X-ray diffraction studies revealed hardly any effect on internal bond distances and angles [20, 44–47]. The observed shortening of M-P bond distances with respect to comparable complexes of tertiary phosphines has been considered to reflect more a small covalency radius of the formally sp$_2$-hybridised phosphorus atom rather than high covalent bond orders [20, 27, 43, 45]. Comparison of M-C bond lengths in carbonyl complexes indicates that M-C bonds trans to a phosphonio-benzophospholide are shorter than those in *cis* position [32, 43, 47]. This suggests that a phosphonio-benzophospholide is a weaker π-acceptor than CO and agrees with IR data indi-

cating that phosphonio-benzophospholides exhibit similar π-acceptor power as triaryl phosphines [27, 32, 43, 47].

In summary, it may be concluded that σ-coordinated phosphonio-benzophospholides are both weak to moderate σ-donors and π-acceptors. Back donation is important [40], but even if the π-acceptor capability is not extraordinary [32], the metal atom in a phosphonio-benzophospholide complex must be considered as less electron rich than in a phosphine complex as also the contribution from L→M CT via the σ-bond is lower.

4.3.2
Pure π-Complexes

By far the most important class of π-complexes with anionic phospholide ligands comprises η^5-complexes with a "side-on" attachment of the metal atom to the phosphole ring and participation of all five ring atoms in metal-ligand bonding [9, 10]. Similar η^5-complexes have likewise been observed for phosphonio-benzophospholide zwitterions; in addition, however, both the zwitterions and bis-phosphonio-substituted cations are capable of forming η^2-complexes with coordination of the metal to an endocyclic P-C double bond. A comparable coordination mode is known for organic arenes [48] but is very unusual for phosphorus heterocycles, and the few known exemptions comprise bridging tri- or penta-phospholide rings whose π-electron systems are involved in bonding to further metal atoms [9, 10]. Electronically, the η^2-coordination of a phosphonio-benzophospholide moiety requires some π-bond localization in the aromatic ring system which is presumably facilitated by the lower resonance energies as compared to phosphinines and phospholides (cf. above) [49].
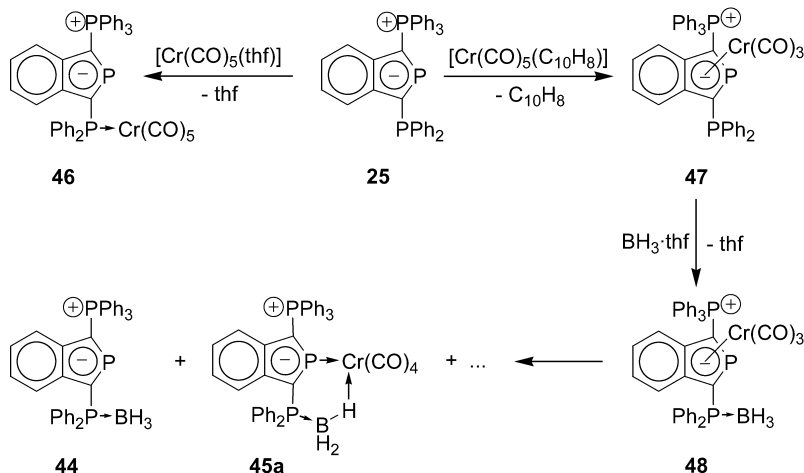
Scheme 17 Selective formation and decay of a η^5-complex of a phosphonio-benzophospholide

The synthesis of η^5-complexes was accomplished by reacting zwitterionic phosphonio-benzophospholides such as **25** and **26** with metal-arene complexes [M(arene)(CO)$_3$] (M=Cr, Mo, Mn$^+$) in a non-coordinating solvent (Scheme 17). The reactions proceeded with high regioselectivity and gave no evidence for the formation of σ-complexes involving phosphorus lone-pairs [32, 42, 43].

The formation of π-complexes was evaded, however, for zwitterions with an additional thioxophosphoranyl, phosphine-borane, or for bis-phosphonio-substituted cations [42]. In these cases, the benzophospholide unit carries two substituents which have—at least in a formal sense—phosphonium character, and complexation occurs exclusively at the phosphorus lone-pair (see the previous section). Attempts to generate appropriate π-complexes by quaternisation of the pendant Ph$_2$P-moiety of the π-complex **47** failed and yielded short-lived intermediates such as **48** which were at best spectroscopically observable and decayed via decomplexation or isomerisation reactions (Scheme 17) [42]. Mechanistic studies suggested that the instability of the primary intermediates correlates with increasing phosphonium character of the substituents at the benzophospholide ring. The spontaneous occurrence of the isomerisation **48**→**45a** deserves attention since it implies that the unusual coordination through a phosphorus lone-pair and a BH-σ-bond is thermodynamically preferable to π-coordination by the five-membered ring and emphasises that the instability of the η^5-complex owes presumably mainly to electronic rather than steric reasons [42].

The known η^5-complexes of phosphonio-benzophospholides are distinguished by large positive coordination shifts for the phosphorus and α-carbon atoms in the ring and similar molecular structures [32, 42, 43] as have been observed for π-phospholyl-complexes [9, 10]. Comparison of the bond distances in π-coordinated and free phosphonio-benzophospholide ligands disclosed that the coordination causes a substantial lengthening of the P-C bonds emerging from the ring phosphorus atom [32, 42, 43]. This is readily understood if one considers that the η^5-coordination implies L→M charge transfer out of the HOMO, and M→L charge transfer into the LUMO, of the ligand. As the largest coefficients of both orbitals are located at the phosphorus and the adjacent carbon atoms, both the weakening of the π-bonding and escalation of π-antibonding interactions in the ring will predominantly affect the P-C bonds.

Formation of η_2-complexes is known for both mono- and bis-phosphonio-benzophospholides and has been observed (Scheme 18) in the reactions of the cation **23** with Jonas' reagent to give the cobalt complex **49** [49], addition of the zwitterion **25** to a Mo-Mo triple bond to afford the dinuclear complex **50** [47], and finally, upon treatment of **26** with copper iodide to yield the complex **51** [46] which is peculiar because of the presence of the same ligand in two different coordination modes. Whereas it is clear that the metal atoms in all complexes supply inappropriate templates for the formation of η^5-complexes, the preference of $\eta^2(\pi)$- over a possible σ-coordination is less well understood [49].
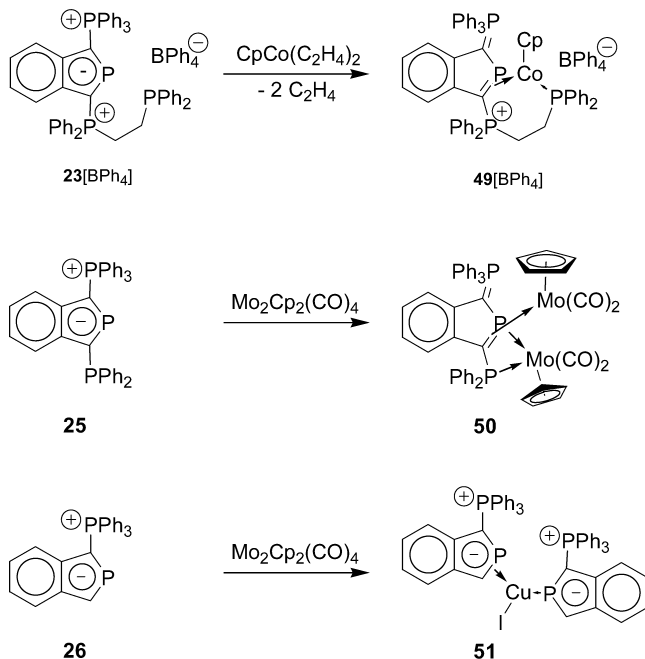
Scheme 18 Formation of η^2-complexes of phosphonio-benzophospholides

Complexes **49** and **50** display a considerable elongation of the coordinated P-C bond, a notable pyramidalisation of the carbon atom, and large positive ^{13}C and ^{31}P coordination shifts with respect to the appropriate free ligands [47, 49]. These effects suggest a considerable degree of M→L back donation and thus a substantial metallacycle character. It has been proposed that the η^2-coordination mode may be favoured since (i) it tolerates a larger extent of charge transfer than σ(P)-coordination, thus allowing a more effective release of the electron pressure on the electron rich metal fragments, and (ii) the partial π-bond localisation is facilitated by a low aromatic stabilisation energy and the possibility to compensate for the loss of resonance energy by increased ylidic character of the exocyclic C–P(phosphonio) bond [47, 49]. Comparison of the ligand properties of the zwitterion **25** with those of 2-diphenylphosphinyl-phosphinines suggested that the phosphinines behave as better π-acceptors towards electron poorer metals whereas **25** is apparently the stronger acceptor if the metal is electron rich [49]. The apparent contradiction in these statements was resolved by considering that their lower LUMO energy makes the phosphinines better intrinsic π-acceptors whereas the 10π-system of a benzophospholide is easier polarisable and may accommodate a larger amount of excess charge. As a consequence, the ranking of both ligands eventually changes under the influence of different charge-capacities when the extent of M→L charge-transfer increases.

The copper complex **51** displays only a moderate bond lengthening, planar coordination geometries, and the absence of significant positive coordination shifts for the atoms in the π-coordinated double bond [46]. Such modest structural distortions upon π-coordination resemble similar features in Cu[I]-arene complexes [48] and were interpreted in terms of a much lower degree of π-bond localization and M→L($\pi^\star$) charge-transfer than in the complexes discussed previously [46]. Computational studies suggested that the energies of isomers with σ- and η^2-coordinated ligands are in this case nearly equal and the unusual η^2-coordination was, in absence of a clear preference, attributed to minor influences such as crystal packing forces. This hypothesis was corroborated by solution NMR studies which showed that both ligands are now equivalent on the NMR time scale and bind presumably both via the phosphorus lone-pairs [46].

The unprecedented absence of a significant coordination shift for a π-coordinated phosphorus-containing double bond deserves some further consideration. Bearing in mind that the deshielding of the ^{31}P NMR signal of a phosphorus atom in a multiple bond system is associated with a lower n→$\pi^\star$ excitation energy (see above), the generally observable decrease of δ^{31}P upon σ(P)-coordination is attributable to combined lowering of the n- and raising of the $\pi^\star$-orbital by the effects of L(lone-pair)→M and M→L($\pi^\star$) charge-transfer. While π-coordination renders little stabilisation of the n-orbital, the $\pi^\star$-orbital may here face severe destabilisation due to π-bond pyramidalisation and concurrent σ/π-rehybridisation effects associated with M→L charge-transfer. Trends in ^{31}P coordination shifts in π-complexes reflect thus mainly changes in M→L charge-transfer and allow to gauge the degree of M→L back-donation [46]. In principle, this approach to the analysis of ^{31}P coordination shifts should be more general, and likewise applicable to π-complexes of other types of unsaturated phosphorus ligands.

4.3.3
Mixed σ/π-Complexes

The capability to use both its phosphorus lone-pair and π-electron system as metal binding site enables a phospholide to act as ambidentate bridging ligand that connects several transition metal atoms in different bonding situations. In accord with this conjecture, phospholides form a variety of complexes **IIIA-IIIE** by donating between four and eight electrons to two or more metal atoms (Fig. 5) [9, 10]. Two types of complexes deserve particular interest: complexes **IIIE** with μ_2-η^5:η^1-bridging ligands are the most abundant ones and have certainly attracted the greatest deal of attention [10]; complexes **IIIB** with μ_2-η^1:η^1-bridging ligands, although rare, are special since the formation of two electron precise M-P bonds induces a breakdown of cyclic π-conjugation and enhances the reactivity of the remaining diene system for further complexation or cycloaddition reactions [9].

For phosphonio-benzophospholides it should be expected that combination of the known σ-coordination of the phosphorus lone-pair to one metal with η^2- or η^5-attachment of the π-electron system to a second metal atom
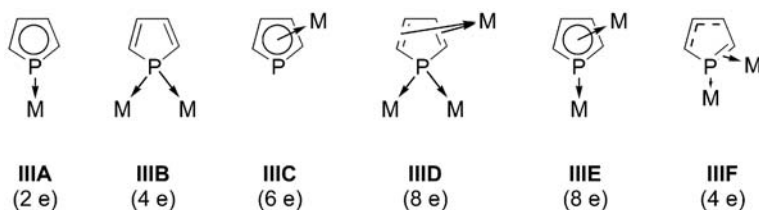
Fig. 5 Schematic representation of different bridging coordination modes for phospholide rings

gives rise to two classes of stable dinuclear complexes (**IIIC** and the novel type **IIIF**) both of which have actually been prepared. Cationic bis-phosphonio-benzophospholides turned out to be further capable of forming a third type of dinuclear complexes which are topologically related to complexes **IIIB** with μ_2-η^1:η^1-bridging phospholyl anions, but exhibit actually a quite different bonding situation.
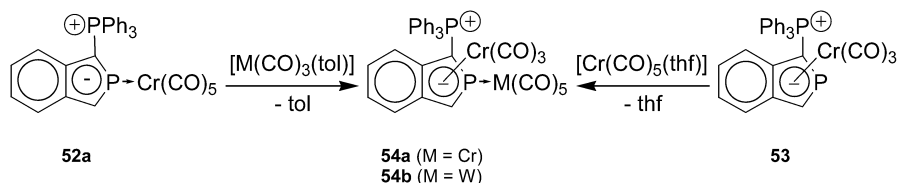
Scheme 19 Formation of complexes with a μ_2-η^1,η^5-bridging phosphonio-benzophospholide

The assembly of the dinuclear complex **54a** with a μ_2-σ:η^5-bridging phosphonio-benzophospholide was feasible by transfer of a 12VE-Cr(CO)$_3$-fragment on the stable precursor σ-complex **52a** or, vice versa, by attachment of a 16VE-Cr(CO)$_5$-fragment to the likewise stable precursor π-complex **53** [50] (Scheme 19). Although both transformations appear deceptively simple, studies aiming at the synthesis of hetero-bimetallic complexes revealed that the reaction is presumably more complicated than a simple transfer of M(CO)$_n$ fragments. For example, the σ-complex **52a** reacted with [W(CO)$_3$(-tol)] via several spectroscopically detectable intermediates to give finally not the expected substitution product but rather the isomeric complex **54b** where the metal atoms have formally changed place [35]. The available data indicate that the reaction is initiated by decarbonylation of **52a** (Scheme 20, reaction (a), the liberated CO is presumably trapped as [W(CO)$_5$(thf)]) to give the π-complex **53** whose reaction with the previously generated [W(CO)$_5$(thf)] then yields **54b** (reaction (b)). Alternatively, **53** may react with remaining starting material to give the homo-bimetallic complex **54a** and the ligand **26** (reaction (c)) which is quenched by [W(CO)$_5$(thf)] to give the tungsten σ-complex **52b** (reaction (d)). Reaction of **53** and **52b** may likewise afford **54b**, and step (c) is obviously reversible so that all intermediates

are finally converted to **54b.** A similar competition between a transfer of intact $M(CO)_n$ fragments and single CO ligands seems to be a general characteristic of analogous reactions and lead in cases of other metal/ligand combinations to the formation of product mixtures whose presence impeded the isolation of the target compounds and imposes a limitation to the accessibility of mixed complexes with μ_2-σ:η^5-coordinated benzophospholides that has not yet been resolved [35].

$$\overset{\oplus PPh_3}{\underset{\textbf{52a}}{\text{[benzophospholide]}}} P{\rightarrow}Cr(CO)_5 + [W(CO)_3(tol)] \xrightarrow[-\ tol]{thf} \overset{Ph_3P^\oplus}{\underset{\textbf{53}}{\text{[benzophospholide]}}} \overset{Cr(CO)_3}{P} + [W(CO)_5(thf)] \quad (a)$$

$$\overset{Ph_3P^\oplus}{\underset{\textbf{53}}{\text{[benzophospholide]}}} \overset{Cr(CO)_3}{P} + [W(CO)_5(thf)] \xrightarrow[-\ thf]{} \overset{Ph_3P^\oplus}{\underset{\textbf{54b}}{\text{[benzophospholide]}}} \overset{Cr(CO)_3}{P}{-}W(CO)_5 \quad (b)$$

$$\overset{Ph_3P^\oplus}{\underset{\textbf{53}}{}} \overset{Cr(CO)_3}{P} + \overset{\oplus PPh_3}{\underset{\textbf{52a}}{}} P{\rightarrow}Cr(CO)_5 \longrightarrow \overset{Ph_3P^\oplus}{\underset{\textbf{54a}}{}} \overset{Cr(CO)_3}{P}{\rightarrow}Cr(CO)_5 + \overset{Ph_3P^\oplus}{\underset{\textbf{26}}{}} P \quad (c)$$

$$\overset{Ph_3P^\oplus}{\underset{\textbf{26}}{}} P + [W(CO)_5(thf)] \xrightarrow[-\ thf]{} \overset{\oplus PPh_3}{\underset{\textbf{52b}}{}} P{-}W(CO)_5 \quad (d)$$
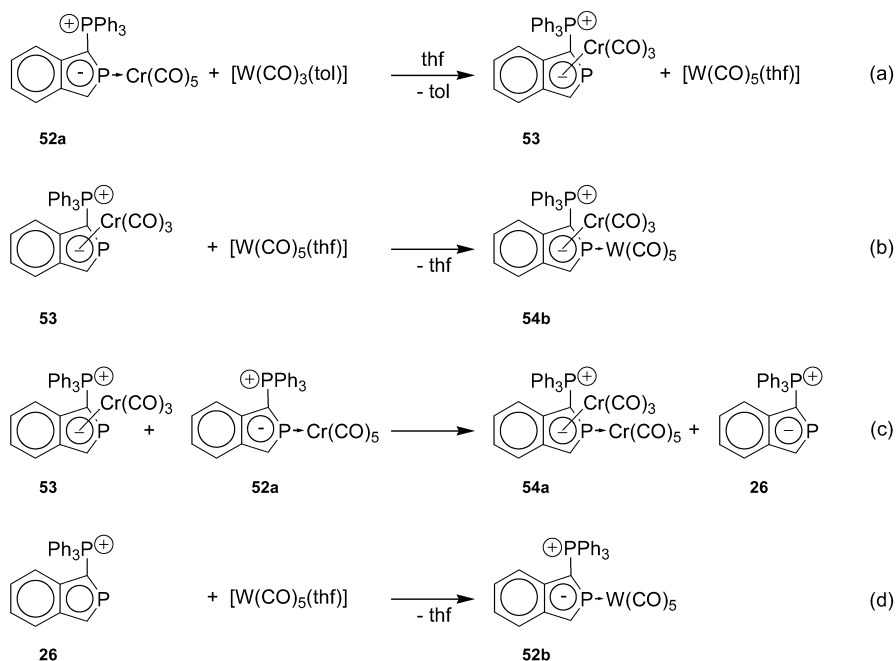
Scheme 20 Observed reaction steps during the formation of complexes with a μ_2-η^1,η^5-bridging phosphonio-benzophospholide

Serendipitous formation of bimetallic complexes **55, 56** with σ:η^2-coordinated phosphonio-benzophospholides was observed in the reaction of the zwitterion **26** with $[M_2(CO)_{10}]$ (M=Mn, Re) [43]. Complexes **56a,b** were characterised by spectroscopic data and single-crystal X-ray diffraction studies whose results pointed to a low degree of $d(M){\rightarrow}\pi^\star(L)$ charge-transfer and thus low metallacycle character, suggesting that, similar as in the copper π-complex **51**, the coordinated double bond acts predominantly as π-donor rather than an as π-acceptor [43].

Considering that the composition of **56a** and of two equivalents of the cationic η^5-complex **57** deviate only by a count of two electrons, mutual redox reactions between both complexes should be feasible. In accord with this hypothesis, **57** was accessible by oxidation of **56a** with ferrocenium hexafluorophosphate while the reverse conversion was accomplished by treating the

cation **57** with activated magnesium (Scheme 21) [43]. Studies of electrochemical reductions/oxidations suggested that the oxidation **56a**→**57** involves two consecutive one-electron steps. The first step is electrochemically reversible and produces a radical intermediate which was detectable by ESR-spectroscopy and was formulated as a dinuclear metal-centred radical cation with a one-electron M-M bond. The second, irreversible step is immediately followed by a chemical reaction [43]. In contrast to the reduction of bisphosphinine complexes where additional electrons are transferred to ligand-centred orbitals [51], the phosphaarene is in this case not directly involved in the redox process. This inert behaviour is in accord with the previously reported oxidation stability of phospholyl-π-complexes [10].
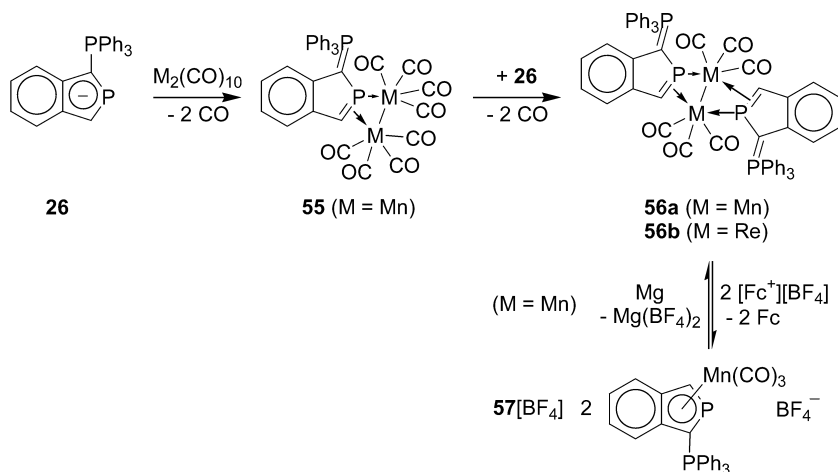
Scheme 21 Formation and redox-induced coordination-isomerisation of complexes with a μ_2-σ:η^2- bridging phosphonio-benzophospholide (Fc=Ferrocene)

Dinuclear complexes **58**, **59** (Scheme 22) with μ_2-η^1: η^1-bridging bis-phosphonio-benzophospholides were isolated from reactions of salts of the cation 1 with silver triflate [52] and copper halides [45, 53], respectively, and the formation of similar complexes was also inferred from spectroscopic studies of the reactions of other Cu^I, Ag^I, and Au^I salts with bis-phosphonio-benzophospholides [19, 52]. Complexes derived from copper halides have cyclic structures and contain beside the μ-benzophospholide a further μ-halide ligand (Fig. 6). A similar structure with an additional bridging trifluoroacetate was also inferred by spectroscopic studies for a silver trifluoroacetate complex, whereas complexes derived from silver triflate contain no further bridging ligand beside the benzophospholide [52]. Spectroscopic investigations revealed that the presence of a second bridging ligand yields a marked kinetic and energetic stabilisation of the dinuclear complexes which were frequently found as dominant reaction products even if much less then two equivalents of the metal were present [45, 52].
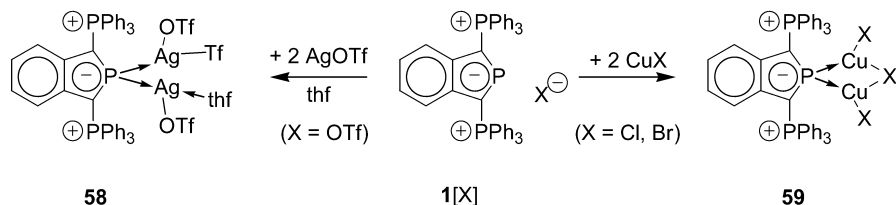
Scheme 22 Coinage-metal complexes with μ_2-η^1:η^1-bridging bis-phosphonio-benzophospholides

Despite the topological similarity between dinuclear complexes with μ_2-η^1:η^1-bridging benzophospholide and phospholide ligands, the bonding situations are actually different. Phospholyl complexes display short M-P distances and a reorganisation of bond distances in the five-membered ring which reflect the formation of two electron-precise M-P bonds and a change from a phosphaarene to a diene structure of the π-electron system [9]. In contrast, the M-P bonds in bis-phosphonio-benzophospholide complexes are longer, the internal bonds in the ligand are hardly affected at all, and the Cu_2PX cores of some copper complexes show often a unique asymmetry (Fig. 6) [45, 52, 53]. Similar features have been observed for copper and silver aryls and aryl cuprates with μ_2-bridging aryls [54] and can be explained by assuming that the M-P bonding interaction is dominated by L→M charge transfer from the lone-pair of the bridging heterocycle. The bonding in the M_2P core may then be rationalised in terms of a 2-electron-3-centre bond which is further stabilised by subsidiary L→M and M→L interactions involving π- and π^*-orbitals of the ligand [17, 54].

The key to the understanding of this situation lies in the realisation that the phosphorus lone-pair in a phosphaarene has considerably more s-character than in a tertiary phosphine. As a consequence, its shape is less direc-
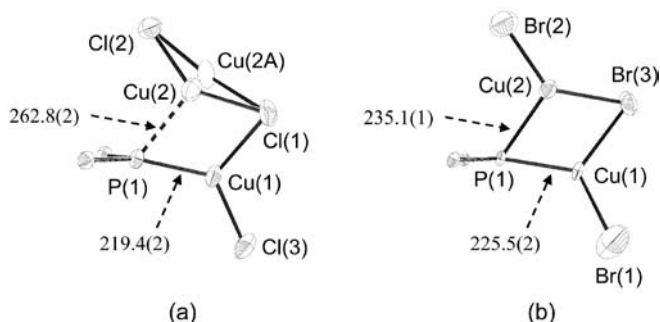
Fig. 6 Representation of the metal and phosphorus environments in copper halide complexes with a η^1:η^1-bridging bis-triphenylphosphonio-benzophospholide. The unsymmetric bridging mode is exemplified by the different P-Cu distances (in pm, data from [45] (a) and [53] (b))
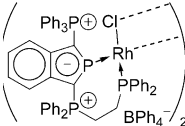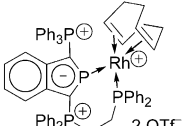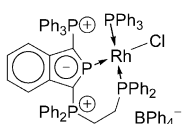
tional but resembles more closely the spherical profile of an s-orbital [55] and overlap may be accomplished even if the M-P vector deviates considerably from the axis of the orbital. Comparable cases of "bent" M-P bonds and μ_2-bridging coordination via a phosphorus lone-pair have in recent years turned out to be quite common in the chemistry of phosphaarenes with formally sp^2-hybridised phosphorus atoms [10, 56]. The finding that η^1:η^1-bridging coordination with electron deficient M-L bonds was only observed for bis-phosphonio-benzophospholide cations whereas zwitterions prefer under similar conditions obviously a μ_2-σ:η^2-binding mode suggests that the η^1:η^1-bridging mode is presumably enforced by a combination of a high degree of steric hindrance and low π-nucleophilicity of the cationic ligands.

4.3.4
Catalytic Applications

Rhodium complexes of phosphorus based ligands are of considerable importance as (pre-)catalysts in hydroformylation which has developed into one of the most important homogeneous catalytic processes [57]. A recent advantage in this field involved the use of phosphinines as ligands whose low-lying π^*-orbitals provide for similar π-acceptor qualities as for phosphites [13, 58].

Table 4 Catalytic activity of rhodium complexes of the bis-phosphonio-benzophospholide **23** in catalytic hydroformylation of hexane using a H$_2$:CO (1:1) mixture (data from [44])

Catalyst	amount catalyst [mol-%]	T [°C]	p [bar]	reaction time [h]	Conversion to aldehydes [%]	Ratio linear:branched aldehyde	TON	TOF [h^{-1}]
60[BBh$_4$]$_2$	0.10	20	40	24	85	1.6	850	35
61[OTf]	0.10	20	40	24	27	2,7	270	11.2
62[BPh$_4$]	0.10	20	40	24	<1	3	<10	<0.4

Considering that bis-phosphonio-benzophospholides behave likewise as π-acceptor ligands, a first study of their use as hydroformylation catalysts was initiated with Rh^I complexes of the phosphine-functionalised cation **23** [44]. Examination of the hydroformylation of hexene at ambient temperature showed that complexes **60** and **61** (Table 4) are active pre-catalysts while **62** displayed negligible activity. As rhodium complexes with more than two phosphorus ligands perform frequently very poorly during hydroformylation, it was suggested that the mild reaction conditions disfavour cleavage of a Rh-P bond in **62** which is required for the generation of a catalytically highly active species [44].

None of the reactions gave rise to the formation of hexane, indicating that the complexes were under the chosen conditions inactive as hydrogenation catalysts. The catalytic activity of the most active complex **60** was considered better than that of the reference system [Rh(CO)$_2$(acac)]/PPh$_3$ (1:5) and roughly similar to that of complexes of monodentate 2.6-disubstituted phosphabenzenes, but the inferior regioselectivity for n-aldehydes as compared to other catalysts makes further optimisation of the catalyst system mandatory [44].

5
Conclusions

Zwitterionic and cationic phosphonio-substituted phospholide derivatives with isolated or benzannulated phospholide, polyphospholide, or heterophospholide rings have been introduced as a new class of phosphaarenes. The chemical and molecular properties of these compounds display some reminiscences to known heterocycles such as phosphinines or phospholides and are governed by a subtle balance between electrophilic and nucleophilic character which can be deliberately tuned by varying the number of phosphonio-substituents. In the same manner as cyclopentadienyl and phospholide anions, the new zwitterions and cations exhibit some potential as ligands in organometallic chemistry. Even if this area is as yet far less developed than the well established coordination chemistry of their anionic counterparts, and up to date only a few of the newly accessible ring systems have been employed as ligands, the results that have already been secured appear interesting and promising and should stimulate further studies.

In regard of the ligand properties, two aspects deserve special attention: (i) attachment of an increasing number of positively charged substituents to a phospholide moiety induces a decrease in π-nucleophilicity and a simultaneous increase in π-acidity which implies a change from a preference for π-coordination in phospholyl anions to one for σ-coordination via the phosphorus lone-pair in bis-phosphonio-substituted cations; (ii) in particular mono-phosphonio-substituted zwitterions display a high degree of coordinative mobility; this allows both shifts between different coordination modes and—in connection with the lack of a permanent electrostatic attraction between the metal ion and the neutral ligands—facilitates intermolecular exchange and ligand-transfer reactions. Both features are of interest with

respect to applications of these ligands in catalysis, and a first report on the use of rhodium complexes of bis-phosphonio-benzophospholides as hydro-formylation catalysts suggests that the further exploration of this area may beyond any academic curiosity also be attractive for real applications.

Even though at the current state a considerable amount of work is still needed to broaden the knowledge on the properties of known types of zwitterionic and cationic phosphonio-phospholide derivatives, there are also challenges and perspectives for new developments. Two particular appealing lines of progress involve the exploration of phosphonio-polyphospholide or -heterophospholide zwitterions as bridging ligands, and the incorporation of zwitterionic phospholide moieties into the framework of phosphametallocenes. The use of monocyclic phosphonio-polyphospholides or heterophospholides with notable π-acceptor capabilities as bridging ligands should offer interesting possibilities for ligand-mediated electronic communication between different metal atoms. Incorporation of zwitterionic phospholides into a metallocene framework should not only extend the known representatives of this class of compounds to new metal/ligand combinations (i.e., coordination of a zwitterionic phospholide to a CpMn fragment should give rise to a neutral complex that is isoelectronic to ferrocene but features a Mn^I instead of the Fe^{II} central atom) but the recent developments in the chemistry of phosphaferrocenes make this area an interesting playground for the development of new applications in catalysis.

References

 1. Kealy TJ, Pauson PL (1951) Nature 168:1039
 2. Wilkinson G, Stone FGA, Abel AW (eds) (1982) Comprehensive organometallic chemistry. Pergamon Press, Oxford
 3. Pearson AJ (1985) Metallo-organic chemistry. Wiley, Chichester
 4. Elschenbroich C, Salzer A (1993) Organometallchemie. Teubner, Stuttgart
 5. Ramirez F, Levy S (1956) J Org Chem 21:488
 6. Selected references: Abel EW, Singh A, Wilkinson G (1959) Chem Ind (London) 1067; Nesmeyanov AN, Kolobova NE, Zdanovich VI, Zhakaeva A (1976) J Organomet Chem 107:319; Tresoldi G, Recca A, Finocchiaro P, Faraone F (1981) Inorg Chem 20:3103
 7. Holy NL, Baenziger NC, Flynn RM (1978) Angew Chem 90:732
 8. Braye EH, Caplier I, Saussez R (1971) Tetrahedron 27:5523
 9. Mathey F (1994) Chem Rev 137:1
10. Dillon KB, Mathey F, Nixon JF (1998) Phosphorus the carbon copy. Wiley, Chichester
11. Nyulászi L (2001) Chem Rev 101:1229
12. Mathey F, Mitschler A, Weiss R (1978) J Am Chem Soc 100:5748
13. Weber L (2002) Angew Chem Int Ed Engl 41:563
14. Ganter C (2001) J Chem Soc Dalton 3541

15. Schmidpeter A, Thiele M (1991) Angew Chem Int Ed Engl 30:308
16. Gudat D, Bajorat V, Nieger M (1995) Bull Soc Chim Fr 132:280
17. Gudat D (1997) Coord Chem Rev 173:71
18. Gudat D, Schrott M, Bajorat V, Nieger M (1996) Phosphorus Sulfur Silicon Rel Elem 109:125
19. Schrott M (1996) PhD Thesis. University of Bonn, Bonn
20. Gudat D, Nieger M, Schrott M (1995) Chem Ber 128:259
21. Jochem G, Schmidpeter A, Nöth H (1996) Chem Eur J 2:221
22. Schrödel HP, Schmidpeter A (1997) Chem Ber Recueil 130:1519
23. Schrödel HP, Schmidpeter A, Nöth H, Schmidt M (1996) Z Naturforsch 51b:1022
24. Schrödel HP, Schmidpeter A (1997) Chem Ber Recueil 130:89
25. Jochem G, Schmidpeter A, Thomann M, Nöth H (1994) Angew Chem Int Ed Engl 33:663
26. Schmidpeter A, Schrödel HP, Knizek J (1998) Heteroatom Chem 9:103
27. Gudat D, Häp S, Bajorat V, Nieger M (2001) Z Anorg Allg Chem 627:1119
28. Gudat D, Holderberg AW, Nieger M (1998) Eur J Inorg Chem 101
29. Märkl G (1990) Phosphinines. In: Regitz M, Scherer OJ (eds) Multiple bonds and low coordination in phosphorus chemistry. Georg Thieme Verlag, Stuttgart, p 220, and references cited therein
30. Cristau HJ, Plénat F (1994) Preparation, properties and reactions of phosphonium salts. In: Hartley FR (ed) The chemistry of organophosphorus compounds. Wiley, New York, vol. 3, chap 2
31. Gudat D, Bajorat V, Häp S, Nieger M, Schröder G (1999) Eur J Inorg Chem 1169
32. Gudat D, Häp S, Szarvas L, Nieger M (2000) Chem Commun 1637
33. Häp S, Szarvas L, Nieger M, Gudat D (2001) Eur J Inorg Chem 2763
34. Szarvas L, Bajko Z, Fusz S, Burck S, Daniels J, Nieger M, Gudat D (2002) Z Anorg Allg Chem 628:2303
35. Szarvas L (2002) PhD Thesis. University of Bonn, Bonn
36. Jochem G, Nöth H, Schmidpeter A (1996) Chem Ber 129:1083
37. Gudat D, Bajko Z (unpublished results)
38. Gudat D, Hoffbauer W, Niecke E, Schoeller WW, Fleischer U, Kutzelnigg W (1994) J Am Chem Soc 116:7325; Burford N, Cameron TS, Clyburne JAC, Eichele K, Robertson KN, Sereda S, Wasylishen RW, Whitla AW (1996) Inorg Chem 35:5460
39. Holderberg AW, Schröder G, Gudat D, Schrödel HP, Schmidpeter A (2000) Tetrahedron 56:57
40. Gudat D, Nieger M, Schrott M (1997) Inorg Chem 36:1476
41. Gudat D, Schrott M, Holderberg AW, Bajorat V, Nieger M (1999) Phosphorus Sulfur Silicon Relat Elem 144:457
42. Bajko Z, Daniels J, Gudat D, Häp S, Nieger M (2002) Organometallics 21:5182
43. Gudat D, Lewall B, Nieger M, Detmer I, Szarvas L, Saarenketo P, Marconi G (2003) Chem Eur J 9:661
44. Häp S, Nieger M, Gudat D, Betke-Hornfeck M, Schramm D (2001) Organometallics 20:2679
45. Gudat D, Holderberg AW, Korber N, Nieger M, Schrott M (1999) Z Naturforsch 54b:1244
46. Gudat D, Nieger M, Schmitz K, Szarvas L (2002) Chem Commun 1820
47. Gudat D, Häp S, Nieger M (2002) J Organomet Chem 643:181
48. Hubig SM, Lindeman SV, Kochi JC (2000) Coord Chem Rev 200/202:831 and references cited therein
49. Gudat D, Häp S, Nieger M (2001) Z Anorg Allg Chem 627:2269
50. Häp S (2000) PhD Thesis. University of Bonn, Bonn
51. Choua S, Sidorenkova H, Berclaz T, Geoffroy M, Rosa P, Mézailles N, Ricard L, Mathey F, Le Floch P (2000) J Am Chem Soc 122:12,227; Rosa P, Mézailles N, Ricard L, Mathey F, Le Floch P, Jean Y (2001) Angew Chem Int Ed Engl 40:1251
52. Gudat D, Schrott M, Bajorat V, Nieger M, Kotila S, Fleischer R, Stalke D (1996) Chem Ber 129:337

53. Gudat D, Schrott M, Nieger M (1995) Chem Commun 1541
54. van Koten G (1990) J Organomet Chem 400:283 and references cited therein
55. Frison G, Mathey F, Sevin A (2002) J Phys Chem 106A:5653
56. Sava X, Ricard L, Mathey F, Le Floch P (2000) Organometallics 19:4899
57. Weissermel K, Arpe H-J (1988) Industrielle Organische Chemie. VCH, Weinheim, p 133
58. Breit B (1996) Chem Commun 2071; Breit B, Winde R, Harms K (1997) J Chem Soc Perkin Trans 1:2681; Breit B (1999) J Mol Catal A 143:143

Ribozyme Mechanisms

Yasuomi Takagi[1, 3] · Yutaka Ikeda[1, 2] · Kazunari Taira[1, 2]

[1] Gene Function Research Center, National Institute of Advanced Industrial Science
and Technology (AIST), Central 4, 1-1-1 Higashi, 305-8562, Tsukuba Science City, Japan
[2] Department of Chemistry and Biotechnology, School of Engineering,
The University of Tokyo, 113-8656, Hongo, Tokyo, Japan
E-mail: taira@chembio.t.u-tokyo.ac.jp
[3] iGENE Therapeutics Inc., Central 4, 1-1-1 Higashi, 305-8562, Tsukuba Science City,
Ibaraki, Japan

Abstract The last few years have seen a considerable increase in our understanding of catalysis by naturally occurring RNA molecules, called ribozymes. The biological functions of RNA molecules depend upon their adoption of appropriate three-dimensional structures. The structure of RNA has a very important electrostatic component, which results from the presence of charged phosphodiester bonds. Metal ions are usually required to stabilize the folded structures and/or catalysis. Some ribozymes utilize metal ions as catalysts while others use the metal ions to maintain appropriate three-dimensional structures. In the latter case, the correct folding of the RNA structures can perturb the pK_a values of the nucleotide(s) within a catalytic pocket such that they act as general acid/base catalysts. The various types of ribozyme exploit different cleavage mechanisms, which depend upon the architecture of the individual ribozyme.

Keywords Ribozymes · Catalyst · Mg^{2+} · A nucleobase · pK_a

List of Abbreviations

aa-tRNA	Amino-acyl tRNA
EDTA	Ethylenediaminetetraacetic acid
HDV	Hepatitis delta virus
sn RNA	Small nuclear RNA
TS	Transition state

1
Introduction

It had long been known that RNA acts as a mediator for coding genetic information into proteins, and that proteins exhibit enzymatic activities. In the early 1980s, however, Cech et al. discovered the self-splicing of premRNA in *Tetrahymena thermophila* [1], while Guerrier-Takada et al. discovered the processing of tRNA precursors by the RNA moiety of RNase P [2]. This catalytic RNA was named "ribozyme " (<u>ribo</u>nucleic acid+en<u>zyme</u>). Since then, many naturally-existing ribozymes have been discovered, including group II intron ribozymes [3 as review], hammerhead ribozymes [4], hairpin ribozymes [5–8], genomic and antigenomic hepatitis delta virus (HDV) ribozymes [9–12] and Varkud satellite (VS) ribozymes [13]. RNA components of a spliceosome and of a ribosome are also thought to be ribozymes [14–18]. Many scientists are attempting to elucidate their mechanisms of actions. Interestingly, artificial ribozymes which can catalyze amino-acylation, RNA polymerization, C-C bond formation and redox reactions have been also found by sophisticated selection systems [19–22]. All of these findings are adding strength in support of the idea of the existence of an RNA world as the origin of life.

When we focus on RNA cleavage, a number of factors affect the acceleration of the cleavage. These factors include an acidic group (Lewis acid) or a basic group that aids in the deprotonation of the attacking nucleophile (in effect enhancing the nucleophilicity of the nucleophile), an acidic group that can neutralize and stabilize the leaving group, and any environment that can stabilize the pentavalent species that is either in a transition state or a short-lived intermediate. The catalytic properties of ribozymes are caused by factors that are derived from the complicated and specific structure of the ribozyme-substrate complex. Recent findings have clearly demonstrated the diversity of the mechanisms of ribozyme-catalyzed RNA-cleavage reactions. Such mechanisms include the metal-independent cleavage that occurs in reactions catalyzed by hairpin ribozymes [21–26] and the general double-met-

al-ion mechanism of catalysis in those reactions catalyzed by the *Tetrahyme-na* group I ribozyme [27]. Furthermore, the architecture of the complex between the substrate and the HDV (hepatitis delta virus) ribozyme enables the perturbation of the pK_a value of the ring nitrogens of cytosine and adenine [28]. The resulting perturbed ring nitrogens appear to be directly involved in acid/base catalysis. Moreover, while high concentrations of monovalent metal ions or polyamines can facilitate cleavage by hammerhead ribozymes, divalent metal ions have the best acid/base catalyst effect under physiological conditions.

In this review, we emphasize the mechanism responsible for the action of cleavage of RNA by representative naturally-existing ribozymes after an explanation of non-enzymatic cleavage of RNA. We would also like to refer to the mechanisms of the spliceosome and ribosomes as ribozymes.

2
Basic Information

2.1
Cleavage of the Phosphodiester Bond

For the cleavage of RNA phosphodiester linkages, three types of large ribozymes, namely group I and II introns and the catalytic RNA subunit of RNase P (Fig. 1), accept external nucleophiles (the 2′-OH group of an internal adenosine in the case of the group II intron). In contrast, small ribozymes, such as hammerheads, hairpins, HDV (Fig. 1) and the VS ribozyme, use an internal nucleophile, namely the 2′-oxygen of the ribose moiety at the cleavage site, with resultant formation of a 3′-terminal 2′,3′-cyclic phosphate [28–35]. Ribozymes in general catalyze the endonucleolytic transesterification of the phosphodiester bond, requiring structural and/or catalytic divalent metal ions under physiological conditions. The reactions catalyzed by small ribozymes are considered to be roughly equivalent to the non-enzymatic hydrolysis of RNA, with inversion of the configuration at a phosphorus atom suggesting a direct in-line attack with the development of a pentacoordinate transition state or intermediate (Fig. 2). The chemical cleavage requires two events, which can occur either via a two-step mechanism or via a concerted mechanism [29, 30, 36, 37].

In the first step of the non-enzymatic hydrolysis of RNA [30, 38–40], the 2′-OH attacks the adjacent scissile phosphate, acting as an internal nucleophile (transition state 1: TS1 in Fig. 2). In the second step, the 5′-oxygen of the leaving nucleotide is released to produce a 3′-end 2′,3′-cyclic phosphate and a 5′-OH terminus (transition state 2: TS2). Of the two putative transition states, TS2 is the overall rate-limiting state [in other words, attack by the 2′-OH on the phosphorus atom is easier than cleavage of the P-O(5′) bond and, thus, TS2 always has higher energy than TS1; for details, see [30]. This conclusion was confirmed in experiments with an RNA analog with a 5′-mercapto leaving group. If the formation of the intermediate was the rate-limit-

A. Hammerhead ribozyme

B. Hairpin ribozyme

C. HDV ribozyme (genomic)

D. Group I ribozyme

E. Group II ribozyme

F. RNase P ribozyme
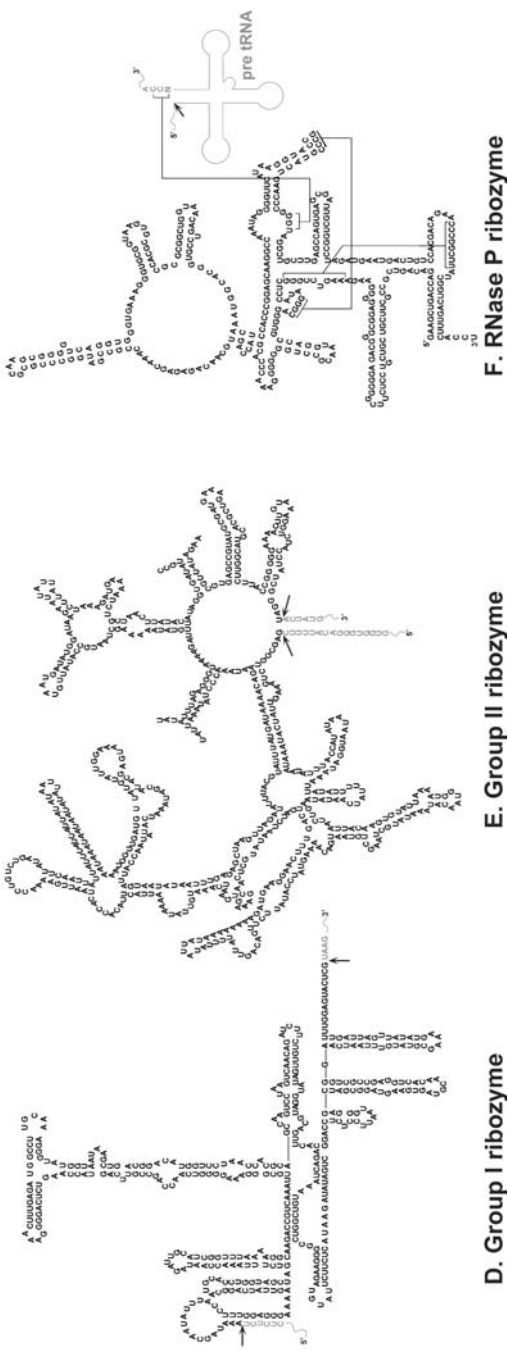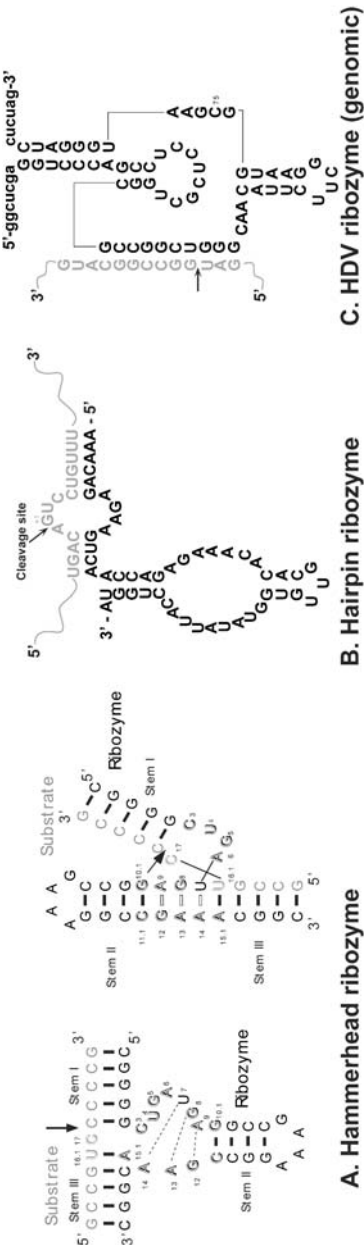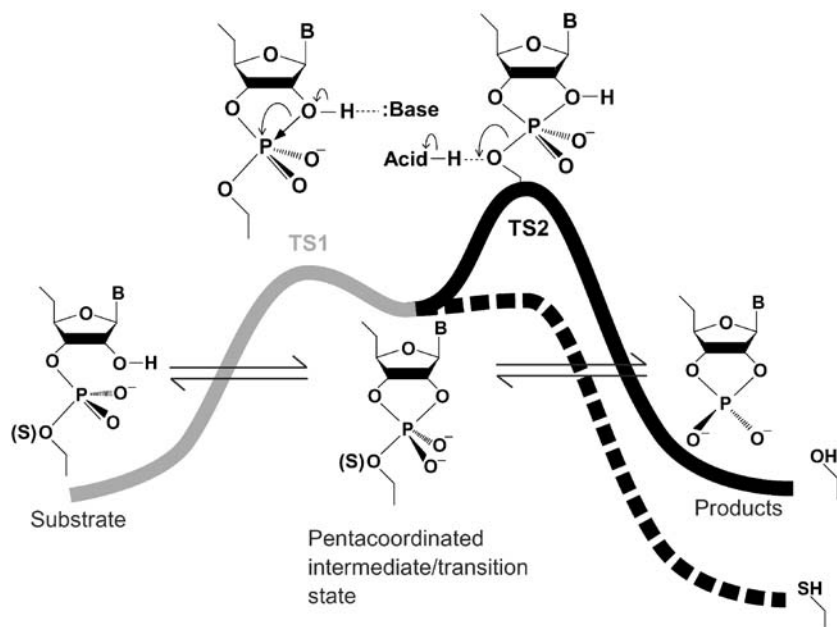
Fig. 2 The two-step reaction scheme for the hydrolysis of a phosphodiester bond in RNA. First, the 2′-oxygen attacks the phosphorus atom, acting as an internal nucleophile, to generate the pentacoordinated intermediate (or transition state), TS1. The 5′-oxygen then departs from the intermediate to complete cleavage at TS2. TS1 can be stabilized by a general base catalyst and TS2 can be stabilized by a general acid catalyst, as illustrated at the summits of the energy diagram. These transition states can also be stabilized by the direct binding of Lewis acids to the 2′-attacking oxygen and the 5′-leaving oxygen

ing step (that is, if TS1 was a higher-energy state than TS2) in the natural RNA, the phosphorothiolate RNA (RNA with a 5′-bridging phosphorothiolate at the scissile linkage) should be hydrolyzed at a rate similar to the rate of the hydrolysis of the natural RNA because the 5′-bridging phosphorothiolate linkage would not be expected to enhance the attack by the 2′-oxygen [41]. In contrast, if the decomposition of the intermediate was the rate-limit-

Fig. 1A–F The two-dimensional structures of various ribozymes. The ribozyme or intron portion is printed in black. The substrate or exon portion is printed in *gray*. *Arrows* indicate sites of cleavage by ribozymes: **A** (*left*) the two-dimensional structure of a hammerhead ribozyme and its substrate. Outlined letters are conserved bases that are involved in catalysis; (*right*) The γ-shaped structure of the hammerhead ribozyme-substrate complex; **B–F** the two-dimensional structures of a hairpin ribozyme, the genomic HDV ribozyme, a group I ribozyme from *Tetrahymena*, a group II ribozyme from *S. cerevisiae* (aiγ5), and the ribozyme of RNase P from *E. coli*

ing step (that is, if TS2 was a higher-energy state than TS1) in the natural RNA, we would expect that the phosphorothiolate RNA would be hydrolyzed much more rapidly than the natural RNA because the pK_a of a thiol is lower than that of the corresponding alcohol by more than 5 units. Several groups have confirmed that the phosphorothiolate RNA is significantly more reactive than the corresponding natural RNA in non-enzymatic hydrolytic reactions [30, 37, 42–44] and, thus, TS2 is, indeed, always a higher-energy state than TS1.

2.2
Possible Catalytic Functions of Metal Ions in the Cleavage of RNA

If ribozymes operate as metalloenzymes in chemical cleavage [29, 30, 36, 37, 45–55], the possible catalytic functions of metal ions can be summarized as follows (Fig. 3):

1. A metal-coordinated hydroxide ion might act as a general base, abstracting the proton from the 2′-OH (Fig. 3b) or, alternatively, a metal ion might act as a Lewis acid to accelerate the deprotonation of 2′-OH by coordinating directly with the 2′-oxygen (Fig. 3d).
2. The developing negative charge on the 5′-oxygen leaving group might be stabilized by a proton that is provided by a solvent water molecule or by a metal-bound water molecule as a general acid catalyst (Fig. 3a) or, alternatively, by direct coordination of a metal ion that acts as a Lewis acid catalyst (Fig. 3c).
3. Direct coordination of a metal ion to the non-bridging oxygen might render the phosphorus center more susceptible to nucleophilic attack (electrophilic catalysis; Fig. 3e) or, alternatively, hydrogen bonding between a metal-
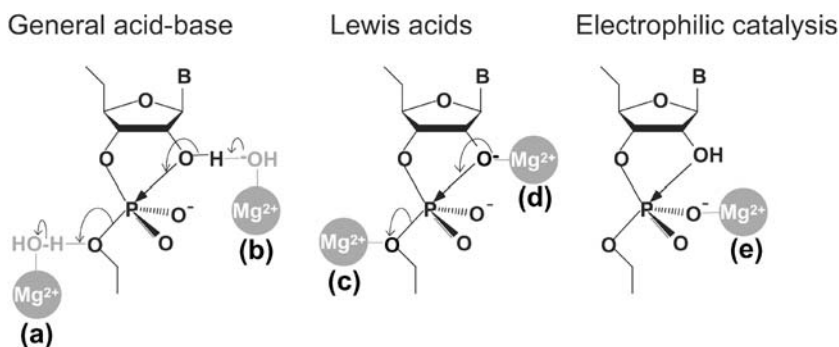
Fig. 3 Possible catalytic functions of metal ions in the cleavage of a phosphodiester bond. Metal ions can act as (**a**) a general acid catalyst, (**b**) a general base catalyst, (**c**) a Lewis acid that stabilizes the leaving group, (**d**) a Lewis acid that enhances the deprotonation of the attacking nucleophile, and (**e**) an electrophilic catalyst that increases the electrophilicity of the phosphorus atom

bound water molecule and the non-bridging oxygen might stabilize the charged trigonal-bipyramidal intermediate (or transition state).

Metal ions can function in several different ways as cofactors in ribozyme-catalyzed reactions, as described above, and proposed mechanisms for the reactions catalyzed by several ribozymes have taken advantage of such functions. Significant aspects of these functions of metal ions might be subsumed by nucleobases if their pK_a values could be adjusted appropriately. The full details of the mechanisms of action of metalloenzymes remain to be elucidated.

3
Ribozymes

3.1
Hammerhead Ribozymes

3.1.1
Catalytic Mechanism

Hammerhead ribozymes are among the smallest catalytic RNAs. The sequence motif, with its three duplex stems and a conserved core consisting of two non-helical segments that are responsible for the self-cleavage action (*cis*-action), was first recognized in the satellite RNAs of certain viruses [56]. Engineered *trans*-acting hammerhead ribozymes, consisting of antisense sections (stem I and stem III) and a catalytic core with a flanking stem-loop II section (Fig. 1a), have been used in mechanistic studies and tested as potential therapeutic agents [57, 58]. Hammerhead ribozymes cleave their target RNAs at specific sites. The chemical cleavage requires two events, which can occur either via a two-step mechanism or via a concerted mechanism. In the first step of the non-enzymatic hydrolysis of RNA, the 2′-OH attacks the adjacent scissile phosphate by acting as an internal nucleophile (transition state 1: TS1 in Fig. 2). In the second step, the 5′-oxygen of the leaving nucleotide is released to produce a 3′-end 2′,3′-cyclic phosphate and a 5′-OH terminus (transition state 2: TS2 in Fig. 2).

To determine the rate-limiting step in reactions catalyzed by hammerhead ribozymes, phosphorothiolate was introduced at the cleavage site. In the case of a 5′-S RNA substrate, the rate of the ribozyme-mediated cleavage of the modified substrate in the presence of Mg^{2+} ions was higher, by almost two orders of magnitude, than that of the natural substrate [44]. If TS1 were a higher energy state than TS2 in the ribozyme reaction with the natural substrate, the cleavage rate for the 5′-S RNA substrate should be similar to that for the natural substrate because the 5′-bridging phosphorothiolate linkage would not be expected to enhance the attack by the 2′-OH [41]. In contrast, if TS2 were a higher energy state than TS1 in the ribozyme reaction with the natural substrate, we would expect that the rate of cleavage of the

5′-S RNA substrate would be much higher than that of the natural RNA substrate because a mercapto group is a better leaving group than a hydroxyl group. On the basis of these considerations, the results indicate that TS2 is a higher energy state than TS1 in the reactions of hammerhead ribozymes with natural substrates, as indicated in Fig. 2.

It is generally accepted that the tertiary structures of RNA molecules are stabilized by metal ions. The roles of metal ions in ribozyme-catalyzed reactions fall into two distinct types: the metal ions can act as catalysts during the chemical cleavage step, as shown in Fig. 3, and they can also stabilize the conformation of the ribozyme-substrate complex.

The generally accepted mechanism of hammerhead ribozyme reactions was a single-metal-ion mechanism [37, 55, 59–63], although recent observations that hammerhead ribozymes are active in the presence of extremely high concentrations of monovalent cations suggest that the hammerhead ribozyme may not be a metalloenzyme [64–66]. In the originally proposed single-metal-ion mechanism as shown in Fig. 4B, the hydroxide ion of a hydrated Mg^{2+} ion acts as a general base to deprotonate the attacking 2′-OH [47]. The Mg^{2+} ion coordinates directly with the pro-Rp oxygen at the scissile phosphate, acting as an electrophilic catalyst in TS1. Instead of a metal ion, a proton acts as a general acid to stabilize TS2.

Double-metal-ion mechanisms, in which two metal ions are involved in the chemical cleavage step, have been proposed [30, 48, 49–51, 54, 67]. We postulated, from the results of molecular orbital calculations and kinetic analyses, that the direct coordination of the Mg^{2+} ions with the attacking or the leaving oxygen might promote the formation or cleavage of the P-O bond, with these ions acting as Lewis acids (Fig. 4C) [30, 49, 50, 67]. Moreover, we excluded the possible coordination of metal ions, as electrophilic catalysts, with the pro-Rp oxygen at the scissile phosphate bond [30, 68–72]. Studies of solvent isotope effects and the kinetic analysis of a modified substrate (phosphorothiolate; 5′-S substrate), with a 5′-mercapto leaving group at the cleavage site, provided support for the double-metal-ion mechanism of catalysis [30, 50, 52].

Figure 5A shows experimentally derived profiles of pH vs rate for reactions in H_2O and D_2O [30, 50, 71]. The magnitude of the apparent isotope effect (ratio of rate constants in H_2O and D_2O) is 4.4 and the profiles appear to support the possibility that a proton is transferred from (Mg^{2+}-bound) water molecules. However, careful analysis led us to conclude that a metal ion binds directly to the 5′-oxygen. Since the concentration of the deprotonated 2′-oxygen in H_2O should be higher than that in D_2O at a fixed pH, we must take into account this difference in pK_a, namely ΔpK_a (=pK_a^{D2O}– pK_a^{H2O}), when we analyze the solvent isotope effect of D_2O [30, 50, 68, 71]. We can estimate the pK_a in D_2O from the pK_a in H_2O using the linear relationship shown in Fig. 5B [30, 68, 73–75]. If the pK_a for a Mg^{2+}-bound water molecule in H_2O is 11.4, the ΔpK_a is calculated to be 0.65 (solid line in Fig. 5B). Then, the pK_a in D_2O should be 12.0. Demonstrating the absence of an intrinsic isotope effect ($k_{H2O}/k_{D2O}=1$), the resultant theoretical curves closely fit the experimental data, with an approximate 4-fold difference in
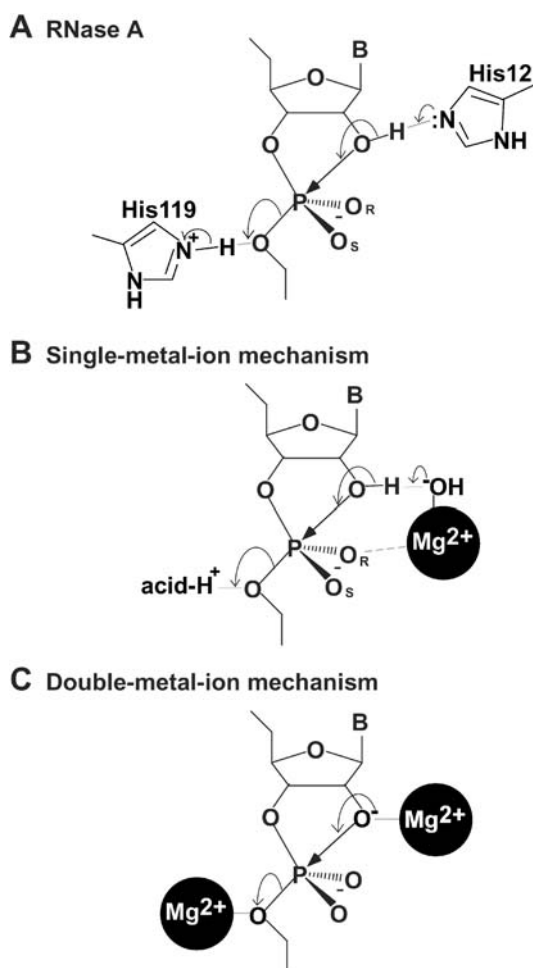
Fig. 4A The mechanism of cleavage by ribonuclease A. Two imidazole residues function as general acid-base catalysts. **B** The single-metal-ion mechanism proposed for cleavage by the hammerhead ribozyme. One metal ion binds directly to the *pro-R*p oxygen and functions as a general base catalyst. **C** The double-metal-ion mechanism proposed for cleavage by the hammerhead ribozyme. Two metal ions bind directly to the 2′-oxygen and the 5′-oxygen

observed rate constants (Fig. 5A). This result indicates that no proton transfer occurs in the hammerhead ribozyme-catalyzed reaction in the transition state and supports the hypothesis that the metal ions function as Lewis acids. In Fig. 5A, the apparent plateau of rate constants above pH 8 reflects the disruption of the active hammerhead complex by the deprotonation of uridine and guanosine residues.

Further evidence was also presented, by von Hippel's group, for a double-metal-ion mechanism. This was based on their analysis of the effects of
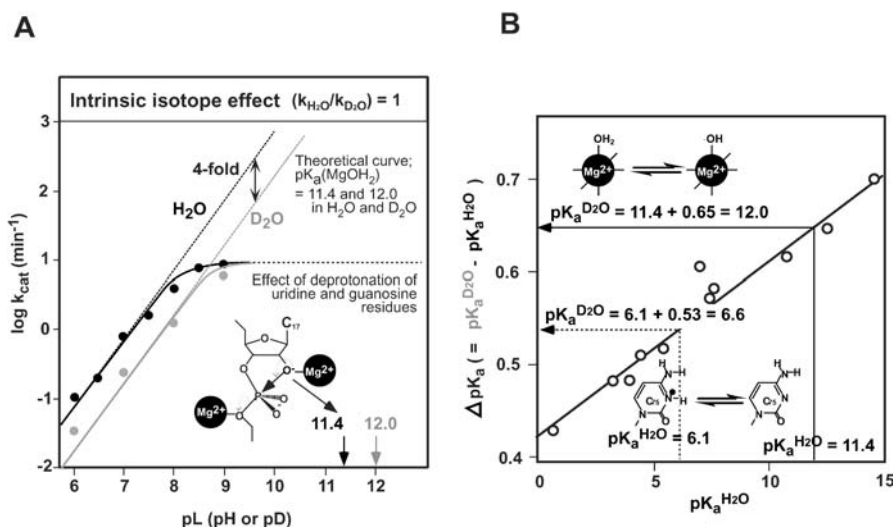
Fig. 5A The dependence on pH of the deuterium isotope effect in the hammerhead ribozyme-catalyzed reaction. *Black circles* show rate constants in H_2O; *gray circles* show rate constants in D_2O. *Solid curves* are experimentally determined curves. The apparent plateau of cleavage rates above pH 8 is due to disruptive effects on the deprotonation of uridine and guanosine residues. *Dotted lines* are theoretical lines calculated from pK_a values of hydrated Mg^{2+} ions of 11.4 in H_2O and 12.0 in D_2O and on the assumption that there is no intrinsic isotope effect ($\alpha = k_{H2O}/k_{D2O}=1$; α is the coefficient of the intrinsic isotope effect). The following equation was used to plot the graph of pL vs log(rate): log $k_{obs}=\log(k_{max})-\log(1+10^{(pKa(base)-pL)})-\log(1+10^{(pL-pKa(acid))})$. In this equation, k_{max} is the rate constant in the case of all acid and base catalysts in active forms: in H_2O, $k_{max}=k_{H2O}$; and in D_2O, $k_{max}=k_{D2O}=k_{H2O}/\alpha$. **B** The isotope effects on the acidities ($pK_a^{D2O}-pK_a^{H2O}$) of phenols and alcohols as a function of their acid strengths (pK_a). The pK_a of hydrated Mg^{2+} ions in H_2O is 11.4, and the *solid arrow* indicates the isotope effect of 0.65 that results in the pK_a of hydrated Mg^{2+} ions in D_2O being 12.0. The pK_a of the N3 of cytosine in H_2O is 6.1 and the *broken arrow* indicates the isotope effect of 0.53 that results in the pK_a of N3 of cytosine in D_2O being 6.6

changes in the concentration of La^{3+} ions in the presence of a fixed concentration of Mg^{2+} ions [54]. Analysis of the effects of adding La^{3+} ions yielded a bell-shaped curve, with the cleavage first being activated and then inhibited (Fig. 6A). Under the experimental conditions, the La^{3+} and Mg^{2+} ions competed to coordinate with restricted sites that are catalytically important to cleavage by the ribozyme. At lower concentrations of La^{3+}, a La^{3+} ion (rather than a Mg^{2+}) ion coordinates with the 5′-leaving oxygen and absorbs the negative charge that accumulates at that position in the transition state [(b) in Fig. 6A]. The fully hydrated La^{3+} ion has a pK_a of 9, which is more than two units lower than that of Mg^{2+}. When the leaving oxygen is directly coordinated with a trivalent La^{3+} ion, it forms a better leaving group than when the oxygen is coordinated with a divalent Mg^{2+} ion. This difference results in a decline in the relative energy of TS2 and the acceleration of the
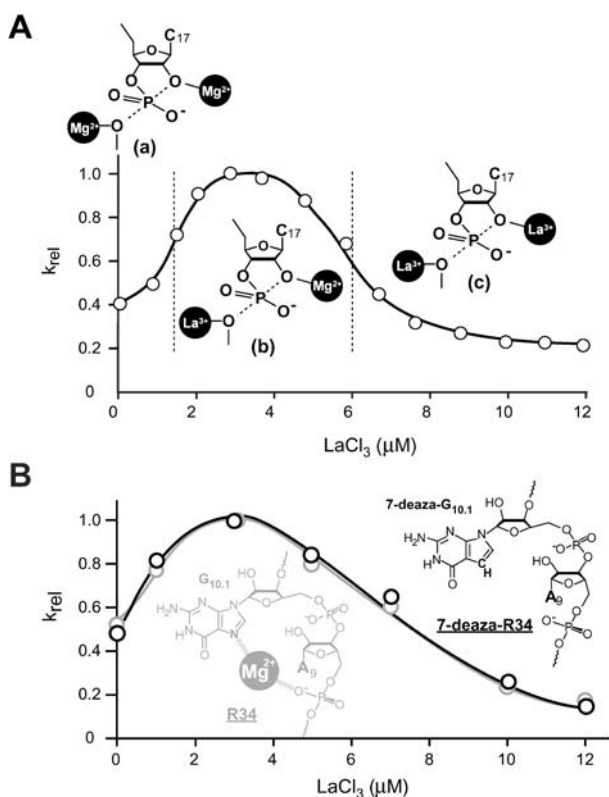
Fig. 6A,B Titration with La^{3+} ions. The hammerhead ribozyme reaction was examined on a background of Mg^{2+} ions: **A** data obtained by Lott et al. [54]. The proposed binding of metal ions is illustrated; **B** data obtained by Nakamatsu et al. [87]. An unmodified ribozyme (R34; *gray curve*) and a modified ribozyme (7-deaza-R34; *black curve*) were used. The rate constants were normalized by reference to the maximum rate constant ([La^{3+}]=3 μmol/l). Reactions were performed under single-turnover conditions in the presence of 80 nmol/l ribozyme and 40 nmol/l substrate at 37 °C

cleavage. At higher concentrations of La^{3+}, however, a La^{3+} ion (instead of a Mg^{2+} ion), coordinates not only with the 5′-leaving oxygen but also directly with the 2′-attacking oxygen ((c) in Fig. 6A). Although the La^{3+} ion, which is more positively charged than the Mg^{2+} ion, might enhance the deprotonation of 2′-OH and, as a result, increase the equilibrium concentration of 2′-O$^-$, it would also reduce the nucleophilicity of 2′-O$^-$ toward the electropositive phosphorus. Because the coordination of a trivalent metal ion at this position reduces the nucleophilicity of the resulting 2′-O$^-$ much more dramatically than would be expected with a series of divalent ions, and since this negative effect is greater than that of an induced higher concentration of 2′-O$^-$, a higher concentration of La^{3+} ions reduces the overall rate of cleavage ((c) in Fig. 6A).

Regarding catalysis in the absence of divalent metal ions, our recent analysis, based on kinetic solvent isotope effects, demonstrated that proton transfer occurs in those reactions that are catalyzed by a hammerhead ribozyme in the presence of high concentrations of monovalent NH_4^+ ions but without metal ions [76], whereas no such proton transfer occurs in reactions catalyzed by the same ribozyme in the presence of divalent metal ions [30, 50, 68]. This conclusion is based on the fact that the value of the intrinsic isotope effect for NH_4^+-mediated ribozyme reactions was 2, whereas the corresponding value for Mg^{2+}-mediated reactions was 1. These results could be explained, for the natural hammerhead ribozyme under physiological conditions, by the double-metal-ion mechanism shown in Fig. 4C. In the case of NH_4^+-mediated reactions in the absence of divalent metal ions, an NH_4^+ ion neutralizes the developing negative charge in the transition state by transferring a proton to the leaving 5′-oxygen, instead of neutralization by a Mg^{2+} ion. It is interesting because these data suggest that hammerhead ribozymes can change a catalyst(s) depending on their surrounding conditions.

We cannot exclude other mechanisms in which a single Lewis acid catalyst of a divalent metal ion are involved. When the cleavage in the ribozyme reaction is in accordance with the concerted mechanism, no intrinsic isotope effect strongly supports the idea of the double-metal-ion mechanism as shown in Fig. 4C. When it is in accordance with the sequential mechanism, no intrinsic isotope effect suggests either the double-metal-ion mechanism or that one Mg^{2+} ion works as a Lewis acid catalyst at the rate-limiting step and the other Mg^{2+} ion or a nucleobase works as a general acid/base catalyst. In this case, when the rate-limiting step is the attacking of a 2′-oxyanion to the phosphorus atom (TS1 in Fig. 2), it supports the idea that the metal ion works as a Lewis acid catalyst to the 2′-OH. When the rate-limiting step is the leaving of 5′-oxyanion from the phosphorus atom, it supports the idea that the metal ion works as a Lewis acid catalyst to the 5′-oxygen. Calculations and experiments with the analog substrate in which the 5′-oxygen was substituted with a sulfur atom as described above suggest the rate-limiting of the leaving step. Taken it into account, we conclude no proton transfer indicates that, at least, one Mg^{2+} ion works as a Lewis acid catalyst at the 5′-oxygen. As mentioned above, the result of La^{3+} experiments also supports this idea and, furthermore, it supports the double-metal ion mechanism. But we have to keep in mind the fact that the ribozyme reaction can proceed only in the presence of $[Co(NH_3)_6]^{3+}$ at a higher pH (data not shown). The complex is known to be exchange-inert which means the coordination group, ammine, is not substituted with a water molecule. It is very unlikely that Co^{2+} in the complex works as a Lewis acid catalyst. We have to solve this contradictory problem which remains unclear.

3.1.2
Folding Pathway and Several Metal Binding Affinities

The folding pathway of the ribozyme-substrate complex upon addition of metal ions is also well studied. Bassi et al. analyzed the global structure of
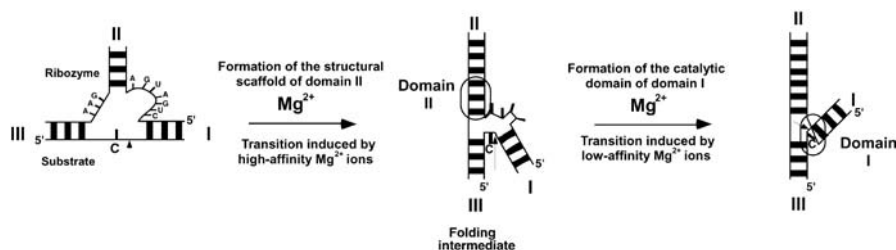
Fig. 7 The two-stage folding scheme for the hammerhead ribozyme, as proposed by Lilley's group [77–80]. The *arrow* indicates the cleavage site. The scheme consists of two steps to generate the Y- or γ-shaped ribozyme/substrate complex. The higher affinity of Mg^{2+} is related to formation of domain II (structural scaffold: non-Watson-Crick pairings between G_{12}-A_9, A_{13}-G_8 and A_{14}-U_7 forming a coaxial stack between helices II and III that runs through $G_{12}A_{13}A_{14}$) and the lower affinity of Mg^{2+} to formation of domain I (catalytic domain: formation by the sequence $C_3U_4G_5A_6$ and the C_{17} with the rotation of helix I around into the same quadrant as helix II) [78]

the hammerhead ribozyme-substrate complex in terms of ion-induced folding transitions by electrophoresis on non-denaturing gels and FRET [77–79]. They detected two sequential ion-dependent transitions (two-phase folding model, Fig. 7). The first transition was the formation of domain II, resulting in coaxial stacking of helices II and III, which was induced by the binding of a higher-affinity Mg^{2+} ion(s) (with a lower, submillimolar dissociation constant, K_d) to the ribozyme·substrate complex. The second transition was the formation of the catalytic domain [the folding of domain I that consists of the sequence $C_3U_4G_5A_6$ ("uridine turn ") and the cleavage site C_{17}] of the ribozyme with resultant movement of stem I toward stem II, which is induced by the binding of a lower-affinity Mg^{2+} ion(s) (with a higher, millimolar K_d). Such ion-induced folding of the ribozyme was also confirmed by recent NMR analysis [80]. It is assumed that the ribozyme reaction proceeds in accordance with this scheme, with completion of the second transition by formation of domain I, and subsequent chemical cleavage of the scissile phosphodiester bond, with or without addition of a further divalent metal ion(s).

Horton et al. analyzed the Mn^{2+}-binding properties of hammerhead ribozyme·substrate complexes by EPR [81]. The results are consistent with the two-phase folding model. They found two classes of metal-binding sites with higher affinity and lower affinity, by monitoring the number of bound Mn^{2+} ions per hammerhead ribozyme-substrate complex at various concentrations of NaCl. They observed, in the presence of a constant concentration of Mn^{2+} ions, a sudden decrease in the number of bound low-affinity Mn^{2+} ions at a lower concentration of NaCl, followed by a slow decrease or a plateau value of the number of bound high-affinity Mn^{2+} ions at a higher concentration of NaCl. For example, in the absence of NaCl and in the presence of either 0.3 mmol/l or 1 mmol/l Mn^{2+} ions, the number of bound Mn^{2+} ions per hammerhead ribozyme-substrate complex was approximately 14. Addition
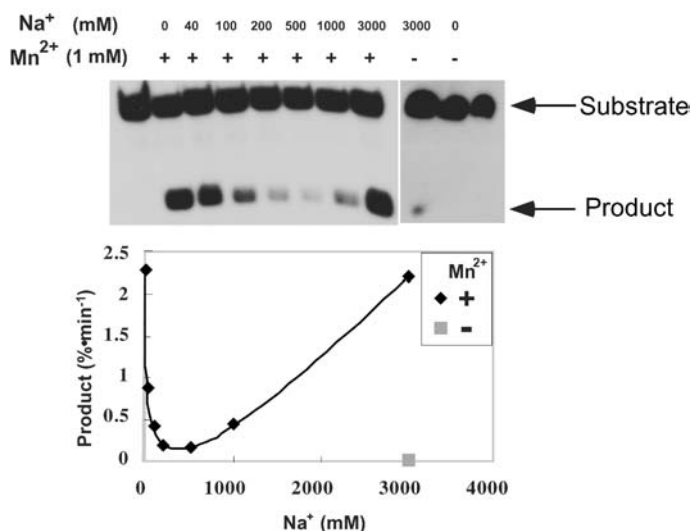
Fig. 8 Effects of the monovalent Na$^+$ cation on the hammerhead ribozyme reaction in the presence of the divalent cation Mn^{2+}. The reactions were performed under single-turnover conditions ([Ribozyme]>>[Substrate]). They were 15 min-reaction in the presence of 1 mmol/l Mn^{2+} ions at various concentrations of Na$^+$ ions from 0 to 3000 mmol/l or no Mn^{2+} ions at 3000 mmol/l Na$^+$ ions

of the NaCl at lower concentrations, 0–60 mmol/l, reduced this number dramatically to approximately seven. As the concentration of NaCl was increased above 60 mmol/l, the number of bound Mn^{2+} ions decreased slowly on a background of 0.3 mmol/l Mn^{2+} ions down to one or remained constant on a background of 1 mmol/l Mn^{2+} ions at seven. These results indicate that there are two types of bound Mn^{2+} ion with different affinity for the ribozyme·substrate complex and that the bound Mn^{2+} ion(s) with lower affinity can easily be removed from the complex by Na$^+$ ions at a lower concentration.

In our recent study of reaction kinetics, we observed an unusual phenomenon when we analyzed the activity of a hammerhead ribozyme as a function of the concentration of Na$^+$ ions on a background of a low concentration of either Mn^{2+} or Mg^{2+} ions [82]. At lower concentrations of Na$^+$ ions, Na$^+$ ions had an inhibitory effect on ribozyme activity, whereas at higher concentrations, Na$^+$ ions had a rescue effect. We propose that these observations can be explained if we accept the existence of two kinds of metal-binding site that have different affinities. Our data also support the "two-phase folding theory" [77–80, Fig. 7], in which divalent metal ions in the ribozyme·substrate complex have lower and higher affinities, as proposed by Lilley and coworkers on the basis of their observations of ribozyme complexes in the ground state.

Our data indicate that ribozyme activity in a low concentration of divalent metal ions decreases dramatically at lower concentrations of NaCl (Fig. 8).

This inhibitory effect of NaCl can be explained on the basis of the data from Horton et al. [81] that is described above. The Na^+ ions remove Mn^{2+} ions from the lower affinity site(s), which is somehow involved in the ribozyme activity, from the ribozyme-substrate complex. When Hammann et al. used Mg^{2+} ions in their NMR analysis, they noticed that the apparent K_d for the lower affinity Mg^{2+} ions depended on the concentration of Na^+ ions [80]. An increase in the background concentration of NaCl from 10 mmol/l to 50 mmol/l weakened the affinity of the Mg^{2+} ions for the complex. Their observations also reconcile with the observed inhibition by Na^+ ions in our study, with the competitive removal of Mg^{2+}/Mn^{2+} ions from the ribozyme-substrate complex.

As the concentration of NaCl is increased after ribozyme activity has reached a minimum, the activity of the ribozyme is restored (Fig. 8). This rescue cannot be explained in terms of the number of bound Mn^{2+} ions since the number does not increase at higher concentrations of NaCl, according to Horton et al., as described above. It is likely that, at higher concentrations, Na^+ ions can work to fold the complex into the active structure and, as a result, more efficient Mn^{2+} ions, even at limited concentrations, can work as a catalyst (see below for details). More efficient Mn^{2+} ions can work as a catalyst even at a limited concentrations. As we would anticipate from the structural role and inefficient catalytic activity of Na^+ ions, several groups have reported that ribozyme-mediated cleavage reactions can occur even in the absence of divalent metal ions provided that the concentration of monovalent ions, such as Na^+ ions, is extremely high [64–66].

We also observed a strange phenomenon of Mg^{2+} titration on the ribozyme activity under single-turnover conditions. The profile has approximately first order dependence on the Mg^{2+} concentration. Importantly, the increasing rate constant at higher Mg^{2+} concentrations did not reach a plateau value even at as high as around 1 mol/l of Mg^{2+} ions [submitted]. The continuous linear increase in rate upon the addition of Mg^{2+} ions suggests the involvement of one Mg^{2+} ion that has a very low affinity to the ribozyme-substrate complex. Values of the estimated K_d turned out to be higher than, at least, 800 mmol/l. Under the condition of such a high concentration of Mg^{2+} ions, the formation of domain II and I would be completed. Taking this structural information into account, it seems reasonable to suggest that the very low affinity Mg^{2+} ion is involved in another step besides the steps in the formation of the domains. The step might be a further conformational change or the binding of a catalytic species into the ribozyme-substrate complex.

3.1.3
A Specific Metal Ion Binding Site, $A_9/G_{10.1}$

The $A_9/G_{10.1}$ site in its conserved core region of the ribozyme has been well identified as a metal binding site by many researchers. This is strongly supported or confirmed by kinetic, NMR and X-ray crystal analyses [83–95]. The important metal-binding site within the hammerhead ribozyme, $A_9/$

$G_{10.1}$, is located around domain II (U_7-A_9 pairs with G_{12}-A_{14}), which forms a continuous stack between stem II ($G_{10.1}$-$C_{10.4}$ pairs with $C_{11.1}$-$G_{11.4}$) and stem III ($A_{15.1}$-$C_{15.5}$ pairs with $U_{16.1}$-$G_{16.5}$) (Fig. 7) and consists of two sheared-type basepairs, G_8-A_{13} and A_9-G_{12}. Many studies of crystal structures of hammerhead ribozymes have identified the metal-binding site between the pro-Rp oxygen of the phosphate of A_9 (P_9 phosphate) and the N7 atom of $G_{10.1}$. Moreover, Uhlenbeck, Herschlag and their coworkers reported that, by the use of ribozymes with a phosphorothioate group instead of the A_9 phosphate, indicated that an Rp-phosphorothioate linkage reduced the cleavage rate by a factor of 10^3, with the rate returning to the control value after the addition of Cd^{2+} ions. Tanaka et al. demonstrated, by NMR analysis, that the motif captures the metal ion without the assistance of other conserved residues of the ribozyme [95] and also showed the direct coordination of the metal ion to the N7 atom of $G_{10.1}$ [submitted by Tanaka et al.]. Nakamatsu et al. checked how this interaction was important in the cleavage reaction, using a minimally modified ribozyme in which N7 of $G_{10.1}$ was merely replaced by a carbon atom. This N7-deazaguanine residue was to prevent the metal ion from binding to this site. Cleavage was retarded with 30-fold reduction in the rate of cleavage by the modified ribozyme [87]. It is likely that this metal ion induces the first transition to form the domain II as mentioned above since A_9/$G_{10.1}$ is located in domain II. Thus, we think that the metal ion captured into the A_9/$G_{10.1}$ site plays, at least, an important structural role in the ribozyme·substrate complex.

It has been proposed that the metal ion also has an interaction with the pro-Rp oxygen atom at the scissile phosphate, $P_{1.1}$. However, the scissile phosphodiester bond, within the crystal structure, is located approximately 20 Å from the A_9/$G_{10.1}$ site [96]. It should be true that a conformational change occurs to rotate the initial structure that is not feasible for the inline attack to in-line structure around the scissile phosphate, but molecular dynamics analysis denies to arrange A_9/$G_{10.1}$ to come close to $P_{1.1}$ via a metal ion. Furthermore, although it has been suggested that there is a weak interaction of a metal ion with the oxygen atom at $P_{1.1}$, our recent experiments observed no interaction of a metal ion with the $P_{1.1}$ phosphate by kinetic and NMR analyses [97, 98].

3.2
HDV Ribozymes

3.2.1
Catalytic Mechanism

HDV ribozymes are derived from the genomic and the antigenomic RNAs of hepatitis delta virus [99–102]. Studies by three groups have revolutionized our understanding of the mechanism of HDV ribozyme-catalyzed reactions [28, 103, 104]. They demonstrated recently that an intramolecular functional group, namely N3 at C_{76} in the antigenomic HDV ribozyme and N3 at C_{75} in the genomic HDV ribozyme, can, in fact, act as a true catalyst. However,

with respect to the roles of these N3s, two different mechanisms, namely general base catalysis and general acid catalysis, were proposed. In the former scenario, it was proposed that the deprotonated N3 of C_{76} might be involved in cleavage as a general base that abstracts a proton from the 2′-OH to promote its nucleophilic attack on the scissile phosphate in the transition state of reactions catalyzed by the antigenomic HDV ribozyme [104]. In the latter case, it was proposed that the protonated N3 of C_{75} in the genomic HDV ribozyme might act as a general acid to stabilize the developing negative charge at the 5′-leaving oxygen and that a metal ion might act as a general base [28]. However, although further investigations are required, there remains the possibility that both ribozymes have the same catalytic mechanism [105].

A novel finding related to the mechanism of catalysis by the genomic HDV ribozyme is that the pK_a of C_{75} is perturbed to neutrality in the ribozyme·substrate complex and, more importantly, that C_{75} acts as a general acid catalyst in combination with a metal hydroxide which acts as a general base catalyst (Fig. 9A) [105]. The discovery of this phenomenon provided the first direct proof that a nucleobase can act as an acid/base catalyst in RNA. As a result, as shown by the solid curve in Fig. 9B, the curve that represents the dependence on the pH of the self-cleavage of the precursor genomic HDV ribozyme has a slope of unity at pH values that are below 7 (the activity increases linearly as the pH increases, with a slope of +1). Then, at higher pH values, the observed rate constant is not affected by the pH.

The slope of unity below pH 7 is consistent with an increase, with pH, in the relative level of the metal hydroxide [B:], which acts as the general base upon deprotonation, and a constant amount of the functional protonated form of C_{75} [AH], which acts as a general acid. The slope of zero from pH 7 to pH 9 indicates that the relative level of the metal hydroxide [B:] increases (Fig. 9A), while the relative level of protonated C_{75} [AH] falls by the same amount (Fig. 9A). Backing up this interpretation, when C_{75} was replaced by uracil, the resulting C75U mutant, which was unable to assist in the transfer of a proton, did indeed lack catalytic activity. However, the activity of the C75U mutant was restored by the addition of imidazole, whose protonated form, the imidazolium ion, is known to act as an excellent proton donor [104, 105]. Another mutant, C75A, in which the ring nitrogen N1 at A_{75} has a slightly lower pK_a than the corresponding ring nitrogen N3 of C_{75}, supported self-cleavage, albeit less efficiently. The observed pK_a of the C75A mutant was slightly lower than that of the wild-type C_{75} ribozyme, supporting the interpretation shown in Fig. 9A.

Participation of a nucleobase as a catalyst in the reaction is supported by the analyses of the kinetic deuterium solvent isotope effects. There was a significant, apparent D_2O solvent isotope effect over the entire range of pH values, confirming that transfer of a proton(s) occurs in the transition state; the ratio of the observed rate constants, $k_{obs(H2O)}/k_{obs(D2O)}$, were as high as around 10 at lower pL as shown in Fig. 9B [28]. Moreover, since the observed pK_a for self-cleavage corresponded to that for the general acid and since the overall rate-limiting step appeared to be the cleavage of the bond

between the phosphorus and the 5′-leaving oxygen (Fig. 2), the transferred proton in the transition state must have been derived from C75. Under the measurement conditions, the pK_a of C_{75} in H_2O was 6.1 and, thus, the estimated ΔpK_a was 0.53, as indicated by the broken arrow in Fig. 5B. Indeed, in the pL profile (pL=pH or pD) in Fig. 9B, the pK_a in D_2O is shifted upward by ~0.4±0.1 pH units, consistent with the estimated value [28]. If we take the pK_a of C_{75} as 6.1 in H_2O and 6.5 in D_2O and the respective pK_a values for Mg^{2+}-bound water to be 11.4 and 12.0 (see the section on hammerhead ribozymes), and if we assume that the value of the intrinsic D_2O solvent isotope effect is two ($k_{H2O}/k_{D2O}=2$), we can generate theoretical curves for HDV-catalyzed reactions in H_2O (black solid curve) and D_2O (gray solid curve), as shown in Fig. 9B. The good agreement of the theoretical curves with the experimentally determined curves (indicated by solid lines in Fig. 9B; [28]) supports a scenario wherein transfer of a proton does indeed occur from protonated C_{75} in the P-O(5′) bond-cleaving transition state (TS2; see Fig. 9C). This conclusion is different from the conclusion in the case of hammerhead ribozymes because, in the case of hammerhead ribozymes, the observed, apparent isotope effect (Fig. 5A) can be fully explained by the difference in relative levels of the active species in H_2O and in D_2O without invoking any intrinsic D_2O solvent isotope effect ($k_{H2O}/k_{D2O}=1$; see section on hammerhead ribozymes and Fig. 5A). Proton inventory analysis of the reaction by Nakano and Bevilacqua indicated the involvement of two protons at the rate-limiting step [106]. One is from the nucleobase proton and the other is from 2′-OH at the cleavage site, suggesting that the cleavage of RNA is in accordance with a concerted mechanism. In our opinion, it is also possible to interpret the result as the second proton may be proton donation to the non-bridging oxygen at the scissile phosphate with a sequential mechanism. Shih and Been also performed a proton inventory analysis on the antigenomic HDV ribozyme, and this resulted in an involve-

◀───

Fig. 9A–C Reactions catalyzed by the genomic HDV ribozyme [28]: **A** fractions of the active species [AH] that acts as an acid catalyst (gray) and the active species [B:] that acts as a base catalyst (black), respectively. The pK_a of the acid catalyst is 6.1 and that of the base catalyst is 11.4 in H_2O. The theoretical curve for H_2O in B was produced by the multiplication of these two curves; **B** dependence on pH of the deuterium isotope effect in the HDV ribozyme-catalyzed reaction [28]. *Black circles*, rate constants in H_2O; *gray circles*, rate constants in D_2O; *solid curves*, experimental data; *dotted curves*, theoretical curves calculated using the equation in Fig. 5 and pK_a values for C_{75} and for hydrated Mg^{2+} ions of 6.1 and 11.4 in H_2O and 6.5 and 12.0 in D_2O, respectively, and assuming an intrinsic isotope effect of 2 ($\alpha=k_{H2O}/k_{D2O}=2$) [68]. The *long-dash curve* is a pH-profile in 1 mol/l NaCl and 1 mmol/l EDTA in the absence of divalent metal ions; **C** energy diagram for cleavage of its substrate by an HDV ribozyme. The rate-limiting step in the reaction with the natural substrate is the cleavage of the P-(5′-O) bond. The structures of transition states TS1 and TS2 are also shown. P(V), the pentacoordinate intermediate/transition state

ment of one proton of the nucleobase, C_{76} [107]. It is confirmed that a cytocine works as an acid/base catalyst in the reactions.

Further convincing evidence for the model by Nakano et al. comes from the observation that, in the absence of divalent metal ions (in the absence of base [B:], see Fig. 5A) and in the presence of a high concentration of monovalent cations (1 mol/l NaCl plus 1 mmol/l EDTA), the logarithm of the observed rate constant decreased with pH with a slope of −1, as shown in Fig. 9B [28]. This observation is consistent with exclusively general acid catalysis, as shown by the curve in Fig. 9A: later, a very small amount of contamination of free Mg^{2+} ions under these conditions was pointed out since the chelation ability of EDTA at acidic conditions was weakened due to protonations of its functional groups [108]. According to the further careful investigation by Nakano et al., two pK_as were observed in a pH profiles under the condition of 1 mol/l NaCl, 100 mmol/l EDTA with Chelex 100 to remove the contaminating divalent metal ions. The higher pK_a in the profile is eventually assigned to be that of C_{75} and the lower pK_a is thought to be caused by some structural element. These additional results have not changed the previous conclusion that C_{75} works as a acid/base catalyst in the genomic HDV ribozyme reaction [109]. This type of profile clearly demonstrates that the observed pK_a (pK_a=6.1) for self-cleavage in the presence of divalent metal ions (the curve in Fig. 9B) reflects the pK_a of a general acid rather than that of a general base. It is worth noting that $[Co(NH_3)_6]^{3+}$ competitively inhibits the Mg^{2+}-catalyzed reaction, a result that suggests that $[Co(NH_3)_6]^{3+}$ might bind to the same site as the functional Mg^{2+} ion with outer-sphere coordination [28]; note that $[Co(NH_3)_6]^{3+}$ does not ionize to yield base catalyst [B:]. The similar rate constants determined in the presence of Ca^{2+} ions and Mg^{2+} ions are also consistent with the action of a hydrated metal ion as a Brønsted base rather than as a Lewis acid in the reaction catalyzed by the HDV ribozyme [28, 51].

As described above, the HDV ribozyme requires a Mg^{2+} ion to ensure efficient catalysis. The possibility of coordinating the Mg^{2+} ion with the non-bridging oxygen during the ribozyme-mediated cleavage was examined with RpS and SpS substrates in which one of the non-bridging oxygens of the scissile bond (pro-Rp and pro-Sp oxygen in Fig. 4) was replaced by sulfur [110]. Determination of the rates of the cleavage steps revealed that the cleavage rates for both substrates were almost the same as that for the natural substrate, irrespective of the presence of Mg^{2+} ions or Mn^{2+} ions. These results indicate the absence of a thio effect in the HDV ribozyme-catalyzed reaction. Similarly, the association constants for Mg^{2+} ions and the ribozyme-substrate complex were almost the same for the two substrates. This result supports the hypothesis that no direct coordination of the Mg^{2+} ion with any non-bridging oxygen atoms occurs at the scissile phosphate during cleavage in HDV ribozyme-catalyzed reactions, and that the base catalysis involves the Mg^{2+} ion with outer-sphere coordination [28, 109, 110].

All the available data supports the HDV ribozyme-catalyzed reaction mechanism shown in Fig. 9C. In this model, the donation of a proton is favored and the model involves an acid with an optimal pK_a of 7 under physi-

ological conditions [28]. In contrast, the self-cleavage of the HDV ribozyme in the absence of divalent cations, but in the presence of high concentrations of monovalent cations, suggests that high concentrations of monovalent cations can replace divalent cations in the tertiary folding of the RNA. Thus, divalent cations are not absolutely essential, as in the case of hammerhead ribozymes, for the folding or cleavage of the HDV ribozyme, even though a functional Mg^{2+} ion participates in the cleavage under physiological conditions. Although the perturbation of C_{75} is still controversial [111], these features appear to be unique among the mechanisms of known ribozymes.

3.3
Hairpin Ribozymes

3.3.1
Catalytic Mechanism

Hairpin ribozymes were originally derived from the minus strand of the satellite RNA of tobacco ringspot virus (sTRSV), chicory yellow mottle virus type 1 (sCYMV1), and arabis mosaic virus (sArMV) [5–7]. Hairpin and hammerhead ribozymes can also catalyze the ligation of cleaved products, with the ligation efficiency being much higher for the hairpin ribozyme than the hammerhead. The ligation reaction is thought to be the reverse of the cleavage reaction since it uses the same termini as those produced upon cleavage. Hairpin ribozymes favor the ligation reaction rather than cleavage: ligation occurs ten times faster than cleavage. In contrast, hammerhead ribozymes favor the cleavage reaction (cleavage occurs $\geq$100 times faster than ligation [112–115]). The ratio of equilibrium constants (=$k_{cleavage}/k_{ligation}$) can be explained by the differences between entropies: the loss of entropy that occurs with ligation is smaller for the hairpin than for the hammerhead ribozyme, indicating that the more rigid hairpin structure undergoes a smaller change in dynamics on ligation than the more flexible hammerhead [116]. Catalysis by hairpin ribozymes in the absence of metal ions has been reported by several groups independently [21–26]. Hairpin ribozymes can be considered to be a distinct class of ribozymes that do not require metal ions as cofactors [117]. Strong experimental evidence for this statement is provided by the observation that the reaction proceeds efficiently in the presence of $[Co(NH_3)_6]^{3+}$, polyamines or aminoglycoside antibiotics, and in the absence of additional metal ions [21–26]. The pK_a of the coordinated NH_3 groups of $[Co(NH_3)_6]^{3+}$ is estimated to be above 14 [118]. Moreover, it is an exchange-inert complex (the ligand exchange rate is 10^{-10} /s [118]), and it can replace a fully hydrated Mg^{2+} ion since both $[Co(NH_3)_6]^{3+}$ and the fully hydrated Mg^{2+} ion have octahedral symmetry and similar radii. Thus, it seems unlikely that $[Co(NH_3)_6]^{3+}$ functions as a general base or a Lewis acid to deprotonate the 2′-OH for nucleophilic attack and it is likely that $[Co(NH_3)_6]^{3+}$ supports the structure of the RNA appropriately in the same way as do the hydrated Mg^{2+} ions.

Other evidence supporting the putative passive (non-catalytic) role of metal ions is that ribozyme-catalyzed cleavage in the presence of Mg^{2+} ions exhibits no preference for the RpS vs the SpS substrate [21]. This result suggests that non-bridging oxygen atoms at the scissile phosphate do not interact with metal ions, at least in any direct manner, during cleavage. Additional evidence for a passive role comes from the observation that the ribozyme reaction can occur in films of partially hydrated RNA in the absence of divalent cations [26]. This result indicates that all elements essential for catalytic function are provided by the folded RNA itself. Taken together, all the results support the hypothesis that a nucleobase(s) functions as a general acid/base catalyst.

Recently, a very attractive catalytic mechanism is proposed in which a nucleobase works as an acid/base catalyst in the hairpin ribozyme reaction on the basis of the result of deuterium isotope effect experiment for the reaction by Pinard and Hampel et al. [119]. They constructed the two-way junction of the hairpin ribozyme in which a cleavage chemistry is a rate-limiting step during the reaction. They noticed a specific nucleotide, G_8, might be a catalyst of the reaction, because the calculated energy-minimized model showed that N1 of G_8 is positioned in the vicinity of the cleavage site while 2′-OH is positioned for an in-line SN_2 attack on the scissile phosphorus. In the crystal structural analysis by Rupert and Ferré-D'Amaré, the proton of N1 of G_8 in the hairpin ribozyme is within hydrogen bonding distance of the 2′-O of A_{-1} at the cleavage site [120]. Thus, they checked pH profiles on the ribozyme activity with variants including different pK_a values of N1. In the case of inosine whose pK_a of N1 is similar to that of guanosine (Inosine: 8.7, Guanosine: 9.6), its pH profile shows a similar pattern to that of the authentic ribozyme in which the activity arises upon increase of pH and reaches a plateau at higher pH (<9). In contrast, in a case of purine analogue such as adenine, 2-aminopurine and 2,6-diaminopurine whose pK_a of N1 is in the range of 3.5 through 5.1, its pH profile shows a drop in the activity at higher pH (Fig. 10A) [119]. The direction of observed pK_a difference is the same as that of pK_a difference between analogues of aminopurines. These results are consistent with the idea that a proton of N1 of a purine analogue at position 8 is involved in cleavage chemistry. They have also pointed out the possibility of involvement of O6 of G_8 because deletion or modification of O6 is inhibitory of cleavage. One potential mechanism is shown in Fig. 10B in which G_8 functions as a general acid/base catalyst involving proton transfers from the attacking hydroxyl to O6, and from N1 to the leaving group at the cleavage site, accompanied with the tautomerization of G_8. The transfer of two protons is supported by the result of proton inventory experiment in which they checked the effects of deuterium solvent isotope on the cleavage rate of the hairpin ribozyme to reveal the number of protons involved in cleavage chemistry [119]. This result also suggests that the reaction proceeds in accordance with the concerted acid/base mechanism as does ribonuclease A. However, as they pointed out, there can be other possible mechanism that explain these data. For example, the experimental data do not rule out one proton inventory. In this case, we can consider the sequential mechanism in-
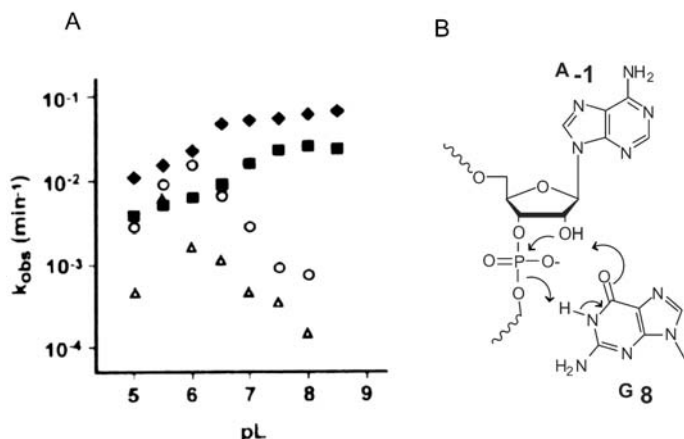
Fig. 10A pL (L=H or D) profiles of hairpin ribozyme of the native sequence of and 2,6-diaminopurine at position 8 [119]. The native sequence in H_2O and in D_2O are represented by *filled diamonds* and *filled squares*, respectively. 2,6-diaminopurine at position 8 in H_2O and in D_2O are represented by *open circles* and *open triangles*, respectively. **B** Proposed catalytic mechanism. RNA cleavage catalyzed by the keto-enol tautomerization of G_8 is achieved by a abstraction of a proton from the N1 to the 5′-O leaving group [119]

stead of the concerted mechanism, in which the attacking or the leaving step is a rate-limiting that cover the other proton transfer effect, if occurred, in the faster step and G_8 works as a general acid or base catalyst and an unidentified catalyst works in the other side. Although further investigation seems to be needed to elucidate the detailed chemistry, it is likely that, at least, G_8 works as a catalyst in cleavage chemistry [121].

3.4
Tetrahymena Group I Intron Ribozyme

3.4.1
Catalytic Mechanism

Group I and II introns are found in bacteria and in the organelles of higher plants, fungi, and algae [3, 122]. The group I introns are spliced out of their primary transcripts by a two-step mechanism (Fig. 11A). In the first step of splicing, the 5′ splice site is attacked by the 3′-OH of the external guanosine. In the second step, the 3′-OH of the 3′-end of the upstream exon attacks the 3′ splice site to produce splicing products.

In studies of the reactions mediated by the ribozyme from the *Tetrahymena* group I intron, detailed kinetic and thermodynamic analysis, combined with modifications at the atomic level, helped to define the reaction mechanism of this ribozyme at the atomic level [27, 48, 123–128]. Modification at the atomic level has generally involved replacement by a sulfur atom of an
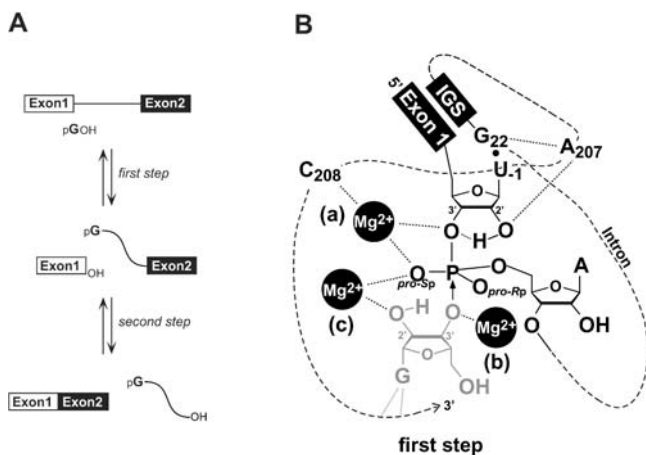
Fig. 11A,B A schematic representation of the group I intron splicing reactions and the structures of transition states at each step: **A** in the first step, the 3′-OH of the exogenous conserved guanosine attacks the phosphorus at the 5′ splice site and generates the guanosine-attached intron-3′-exon 2 intermediate and a free 5′ exon 1. In the second step, the 3′-OH of the 5′ exon 1 attacks the phosphorus at the 3′ splice site to produce ligated exons and the excised guanosine-attached intron; **B** the proposed chemical mechanism of the first step [125, 127]. The 3′-OH of the exogenous guanosine (*gray*) is a nucleophile and the 3′-OH of the uridine numbered −1 is a leaving group (3′-site of Exon 1). One of the Mg^{2+} ions [site (**b**)] coordinates with the 3′-OH of the guanosine to activate the attacking group [124]. The second one [site (**c**)] coordinates with the 2′-OH of the guanosine [135–137], and coordinates with the *pro-S*p oxygen to stabilize the transition state or the intermediate [134]. The third one [site (**a**)] coordinates with the 3′-OH of the uridine to stabilize the leaving group [123, 131], and coordinates with the *pro-S*p oxygen as does the second one [123]. The 2′-OH also protonates the 3′-leaving oxygen of the uridine [127, 139]. IGS represents the internal guide sequence. IGS and intron are represented in *dotted line*

oxygen atom that has the potential to interact with a catalytically important metal ion. The observed reduction in the cleavage rate in the presence of Mg^{2+} ions after such modification [the so-called thio effect] and the observed restoration of a normal cleavage rate in the presence of Mn^{2+} ions [the so-called manganese rescue effect] have been taken as evidence that supports the direct coordination of the atom in question with a metal ion. This phenomenon can be explained by the HSAB [Hard and Soft, Acid and Base] rule [129, 130]. According to this rule, a "hard acid ", such as a Mg^{2+} ion, prefers to bind to a "hard base " oxygen atom rather than to a "soft base " sulfur atom. In contrast, a "soft acid " such as Cd^{2+} and Zn^{2+} ions prefers to bind to a "soft base " sulfur atom. A Mn^{2+} ion is also softer than a Mg^{2+} ion and, thus, the former can bind to a "soft " sulfur atom (as well as to a "hard " oxygen atom). This ability of Mn^{2+} ions is believed to be the origin of the manganese rescue effect.

Analyses of both the thio effect and of "soft acid " rescue effects, such as the rescue effects of Cd^{2+}, Mn^{2+}, and Zn^{2+} ions, have contributed significant-

ly to our understanding of the catalytic mechanism of the first step of the reaction catalyzed by the group I intron. Such analysis has revealed the importance of three independent metal ions, as shown in Fig. 11B [125, 127]. It is strongly proposed that the group I intron is a metalloenzyme that operates via a three-metal-ion mechanism of catalysis, in which the first Mg^{2+} ion at site (b) (see Fig. 11B for locations of (a), (b) and (c)) enhances the deprotonation of the $3'$-OH of the guanosine nucleophile [124], the second Mg^{2+} ion at site (a) stabilizes the leaving $3'$-bridging oxygen of U_{-1} [123] and the third Mg^{2+} ion coordinating to the $2'$-OH of the guanosine at site (c) stabilizes the pentacoordinated transition/intermediate state with the second Mg^{2+} ion at site (a), playing a role of building an active configuration. In this case, the divalent metal ions function as Lewis acids for activation of the nucleophile and stabilization of the leaving group by coordinating directly with them [123]. This mechanism is, strictly speaking, different from the double-metal-ion mechanism (Fig. 4C); however we can easily imagine that both mechanisms make use of divalent metal ions as Lewis acid catalysts for the stabilization of TSs.

These details of coordination at the catalytic site in the ribozyme reaction were derived from the following observations. The substitution of the $3'$-oxygen of the guanosine nucleophile with a sulfur atom reduced the rate of the reverse reaction in the presence of the "hard acid", namely Mg^{2+} ions, and an efficient cleavage was restored by Mn^{2+} ions [124]. This result suggests that a Mg^{2+} ion at site (b) coordinates with the $3'$-oxygen of the guanosine nucleophile to activate the first step. Next, the $3'$-bridging phosphorothiolate substrate ($3'$-S substrate), in which the $3'$-leaving oxygen had been replaced by a sulfur atom, had a dramatically reduced cleavage rate for the forward reaction in the presence of Mg^{2+} ions. An efficient cleavage was restored by Mn^{2+} ions [123, 131]. This result suggests that a Mg^{2+} ion at site (a) in Fig. 11B coordinates with the $3'$-leaving oxygen during cleavage. These observations can be explained by the double-metal-ion model, in which one Mg^{2+} ion coordinates with the nucleophile to activate the attacking group and the other Mg^{2+} ion coordinates with the $3'$-leaving oxygen to stabilize the developing negative charge during RNA cleavage.

The coordination of a Mg^{2+} ion with the *pro-S*p oxygen atom at the scissile phosphate in Fig. 11B was suggested on the basis of the following experimental data. The *R*pS substrate, in which the *pro-R*p oxygen at the scissile phosphate had been replaced by sulfur, was cleaved at a modestly reduced rate [132]. In contrast, the *S*pS substrate, in which the *pro-S*p oxygen at the scissile phosphate had been replaced by sulfur, had a drastically reduced cleavage rate in the presence of Mg^{2+} ions [127, 131, 133]. Furthermore, the *S*pS/$3'$-S substrate, in which not only the *pro-S*p oxygen but also the $3'$-leaving oxygen had been replaced by sulfur atoms at the same scissile phosphate, was cleaved at a lower rate than the $3'$-S substrate in the presence of Mn^{2+} ions on a background of Mg^{2+} ions. An efficient cleavage of the *S*pS/$3'$-S substrate, with the double-thio substitution, was restored by Zn^{2+} or Cd^{2+} ions, which are more thiophilic than Mn^{2+} ions, on a background of Mg^{2+} ions [131]. Thus, a thio effect seemed apparent at the *pro-S*p oxygen, and

rescue both by Cd^{2+} and by Zn^{2+} ions was also evident. These results suggested that a Mg^{2+} ion(s) coordinates with the *pro-S*p oxygen, as well as with the 3'-leaving oxygen. Shan et al. tried to define the identity of the metal ion(s) interacting with the the *pro-S*p oxygen by a similar way as described above [134]. They concluded that the two Mg^{2+} ions coordinating with the 3'-bridging oxygen of U_{-1} and the 2'-OH of the guanosine nucleophile, respectively, interact with the *pro-S*p oxygen of the scissile phosphate in a direct way like a bridge.

Additional coordination has been proposed at the catalytic site. A Mg^{2+} ion at site **(c)** in Fig. 11B might interact directly with the 2'-OH of the guanosine, as suggested by experiments with a 2'-amino-2'-deoxyguanosine substrate and various metal ions in the ribozyme reaction [135–137]. The cleavage rate was reduced by replacement of the 2'-OH with 2'-NH$_2$ on a background of Mg^{2+} ions. An efficient cleavage was restored by addition of "soft " Mn^{2+} or Zn^{2+} ions [135, 136]. This result suggests that a metal ion at site **(c)** coordinates directly with the 2'-OH. Another coordination of the metal ion at site **(a)** has also been proposed. Szewczak et al. prepared several ribozymes having stereospecific single-site phophorothioate in the vicinity of the catalytic core within the intron, evaluated activities with several metal ions in a similar way as described above, and reached a conclusion that the metal ion at site **(a)** may be coordinated to the *pro-S*p phosphate oxygen of the C_{208}, next to A_{207} as shown in Fig. 11B [138]. This coordination can be understood to play a structural role of the complex to position the metal ion at a proper site in the core.

In addition to the coordination of metal ions discussed above, other interesting interactions have been proposed. Linear free-energy analysis of the cleavage of oligonucleotide substrates with a series of 2'-substituents at U_{-1} indicated that the effect on the rate of the 2'-OH group is larger than might be expected from simple inductive effects [139]. The weaker electron-withdrawing 2'-OH enhanced the chemical cleavage step to a greater extent than did the more strongly electron-withdrawing 2'-F atom of the corresponding 2'-deoxy-2'-fluoro derivative. Therefore, the possibility was recently examined of a symmetrical transition state, in which the 2'-OH of U_{-1} might or might not interact with a metal ion (as observed at site **(c)** in Fig. 11B) [127]. Despite the absence of lone-pair electrons at the 2'-NH$_3^+$ group that need to interact with a metal ion, the higher reactivity of the substrate with a 2'-deoxy-2'-NH$_3^+$ group than that of the substrate with a 2'-OH group at U_{-1} suggested that interaction of a metal ion with the 2'-OH of U_{-1} might not be important for catalysis by the group I intron ribozyme. The higher reactivity of the 2'-NH$_3^+$ derivative suggests that donation of a hydrogen bond from the 2'-group to the neighboring 3'-leaving oxygen might allow specific stabilization of the transition state relative to the ground state, thereby facilitating the chemical cleavage step.

The 2'-OH of U_{-1}, the 2'-OH of A_{207} and the exocyclic amino group of G_{22} have been referred to as a catalytic triad [126]. However, the observation that the chemical cleavage step with a 2'-NH$_3^+$ derivative is faster than that with the substrate with a 2'-OH [the natural substrate], despite the absence

of lone-pair electrons at the $2'$-NH_3^+ group that can accept a hydrogen bond from A_{207}-OH, suggests another possibility for the arrangement of active-site groups within this network of interactions [127, 128].

Even though the ribozyme-mediated chemical cleavage step with the $2'$-OH group at U_{-1} (the natural substrate) is significantly (1000-fold) faster than that with $2'$-H, with the metal-binding site (a) in Fig. 11B being occupied by a Mn^{2+} ion, the rate constants for reactions with the $3'$-S substrates are similar, irrespective of whether there is a $2'$-OH or $2'$-H at U_{-1}. Moreover, in the presence of Mg^{2+} ions, with the metal-binding site (a) being unoccupied by a metal ion, the rate constants for reactions with the $3'$-S substrates are similar with a $2'$-OH or with $2'$-H at U_{-1}, indicating that the $2'$-OH at U_{-1} does not contribute significantly to the chemical cleavage of the phosphorus-sulfur bond with the $3'$-mercapto leaving group. Since sulfur is a weaker acceptor of a hydrogen bond than is oxygen, and, furthermore, since sulfur is a significantly better leaving group than oxygen, the $3'$-mercapto leaving group suppresses the catalytic advantage provided by a hydrogen bond from the $2'$-OH in the native transition state [121].

The second step of the splicing reaction is catalyzed within the same catalytic site as the first step [48, 140, 141]. Moreover, in the presence of Mg^{2+} ions, both the reverse reaction of the first step and the forward reaction of the second step were inhibited with the RpS substrate [note that the *pro-R*p oxygen at these steps corresponds to the *pro-S*p oxygen in the forward reaction of the first step]. These observations indicate that the stereochemical requirements are the same in both reactions [123, 132, 142, 143]. Therefore, the mechanism of the second step is considered to be analogous to the mechanism of the first step [48].

It is clear that the analysis of thio effects, rescue experiments and other experiments with derivatives have contributed significantly to our understanding of the mechanism of the action of the large group I intron ribozyme of *Tetrahymena*. All the available data appear to support the Lewis acid catalysis for activation of the attacking nucleophile and enhancement of the leaving group that is shown in Fig. 11B.

3.5
Small Nuclear RNA of Spliceosome

3.5.1
Catalytic Mechanism

The removal of introns from pre-messenger RNAs in eukaryotes is catalyzed by the spliceosome, which is a large ribonucleoprotein consisting of at least 70 proteins and five small nuclear RNAs (snRNA) [144]. This splicing pathway involves two phosphotransfer reactions. In the first step, the $5'$ splice site is attacked by a $2'$ hydroxy group of an adenosine nucleotide within the intron [indicated by "A" in Fig. 12] that corresponds to the 'branch point' in the lariat intermediate (Fig. 12,middle). In the second step, the $3'$-OH group of the free $5'$ exon attacks the phosphodiester bond between the intron and
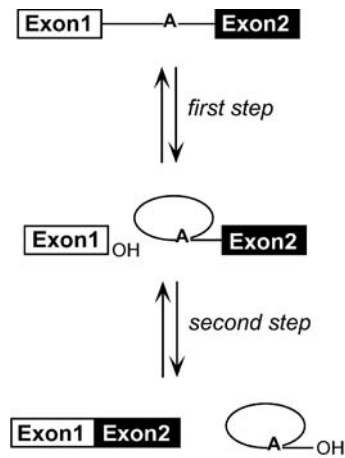
Fig. 12 The spliceosome splicing reaction. In the first step, the 2′-OH of an adenosine residue that is conserved in the intron attacks the phosphorus at the 5′ splice site and generates an intron-3′-exon 2 intermediate and a free 5′ exon 1. In the second step, the free 3′-OH of the 5′ exon attacks the phosphorus at the 3′ splice site to produce ligated exons and an excised intron

the downstream exon (3′ splice site), resulting in the joining of the upstream and downstream exons (Fig. 12, bottom). This pathway is the same as that of the group II intron ribozyme reaction [68 as review]. Since the spliceosome is a ribonucleoprotein, the major question has been "Is the spliceosome a ribozyme? ". Similarities of the snRNA to self-splicing group II introns suggest that the spliceosome might be a ribozyme.
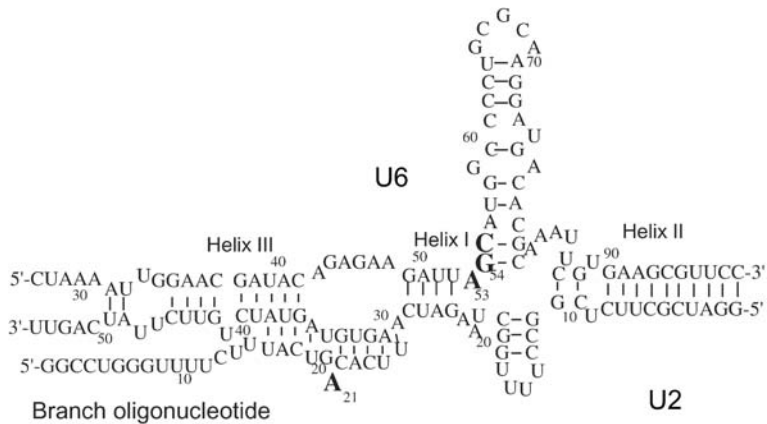
Fig. 13 Base-pairing interactions in the in vitro-assembled complex of U2-U6 and the branch oligonucleotide (Br). The numbers indicate the nucleotide positions relative to the 5′ ends of full-length human U2 and U6. The large, bold letters denote the residues involved in the covalent link between Br and U6 in RNA X [145]
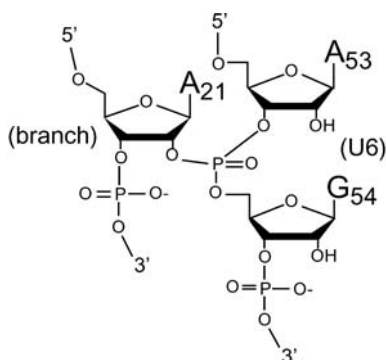
Fig. 14 Model for the covalent bond between U6 and Branch sequence[145]

Of the five snRNAs, U2 and U6 interact with the reaction site (the 5′ splice site and the branch point) in the first chemical step. These two snRNAs are known to anneal together to form a stable-based paired structure in the absence of proteins and in the presence of Mg^{2+} ions as shown in Fig. 13, with U2 acting as an inducer molecule that displaces the U4 (that is an antisense molecule that regulates the catalytic function of U6 RNA) from the initially formed U4-U6 duplex. The secondary (or higher ordered) structure of the U2-U6 complex consists of the active site of the spliceosome. Recent data suggests that these two snRNAs function as the catalytic domain of the spliceosome that catalyzes the first step of the splicing reaction [145].

In a model case, the previously well-characterized U2-U6 snRNA complex was incubated with a short RNA that contained a branch-point sequence that interacts with U2 [145]. In the presence of Mg^{2+} ions, a newly formed RNA species (RNA X) was isolated, which was cross-linked with the catalytic RNA by a covalent bond (Fig. 14). Further analysis indicated that the RNA X resulted from a covalent bond between the bulged adenosine of the branch-point sequence and the AGC triad of U6 (Fig. 13), which is an essential element of the catalytic domain. The unique character involved in the formation of this product is its unusual chemistry. The alkali sensitivity of RNA X as well as the treatment of phosphorothioate-substituted RNA X with iodoethanol confirmed that the RNA X contains a phosphotriester linkage (Fig. 14). This means that, in this reaction, the leaving group is a non-bridging phosphate oxygen instead of the 5′ fragment of U6, which might be considered to be a more favorable leaving group. In this model case, the absence of the 5′ splice site sequence (the junction sequence between the upstream exon and the intron) might have placed this oxygen into the pocket for the leaving group. The low efficiency of this reaction can be reconciled by this hypothesis. Importantly, for this reaction to proceed, only Mg^{2+} ions were required.

Apparently, for promoting this unusual reaction, the attacking 2′ hydroxy group must be activated and the leaving oxygen must also be stabilized. As has been observed in reactions catalyzed by several other ribozymes [30, 48,
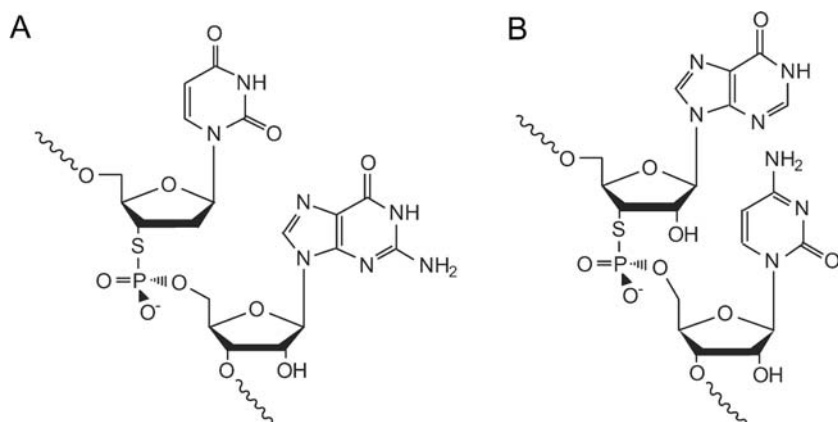
Fig. 15A,B Modified motif of the adenovirus pre-mRNA substrates studied by Sontheimer et al. [151]: **A** in the Ad5-1S, the guanosine at 5′ splice site position was substituted by 2′-deoxy-3′-thiouridine; **B** in the Ad3-1S, the guanosine at 3′ splice site position was substituted by 3′-thioinosine

49–51, 54, 67, 123–125, 128, 131, 134, 135, 146–150], some metal ions and/or the specific tertiary structure of snRNAs with or without a perturbed pK_a are likely to play this role. Sontheimer et al. have uncovered the stabilization by a divalent metal ion in the splicing reaction. They substituted the 3′-oxygen leaving group in the first step of splicing with a sulfur [151]. They synthesized an adenovirus-derived splicing substrate (Ad5-1S) containing a single 2′-deoxy-3′-thiouridine at the 5′ splice site as shown in Fig. 15A. The Ad5-1S substrate failed to undergo splicing even in the presence of 1.5 mmol/l $MgCl_2$, however, when the splicing buffer contained 1.5 mmol/l $MnCl_2$, 5′-splice-site cleavage and lariat formation occurred. This metal specificity switch experiment indicates that a metal ion stabilizes the leaving group in the first step of splicing as shown in Fig. 16A. The developing negative charge on the 3′-oxygen in the transition state could be stabilized by a coordinating metal ion [151].

They also synthesized splicing substrate containing a single 3′-thioinosine at the 3′ splice site, in which the 3′-oxygen leaving group in the second step of splicing was substituted by a sulfur [151, 152] as shown in Fig. 15B. By monitoring the second step of splicing using a bimolecular exon-ligation assay (the 3′ splice site oligonucleotide was supplied in trans [152]), a switch in metal specificity was detected. This indicates that the 3′-oxygen leaving group in the second step of splicing is stabilized by a catalytic metal ion as shown in Fig. 16B. It is likely that the splicesome employs similar strategies for catalyzing both steps of splicing. Yean et al. have also shown that a specific phosphodiester linkage in U6 interacts with a Mg^{2+} ion in the first step of splicing [153]. These results strongly add support to an RNA-based catalytic mechanism of splicing.
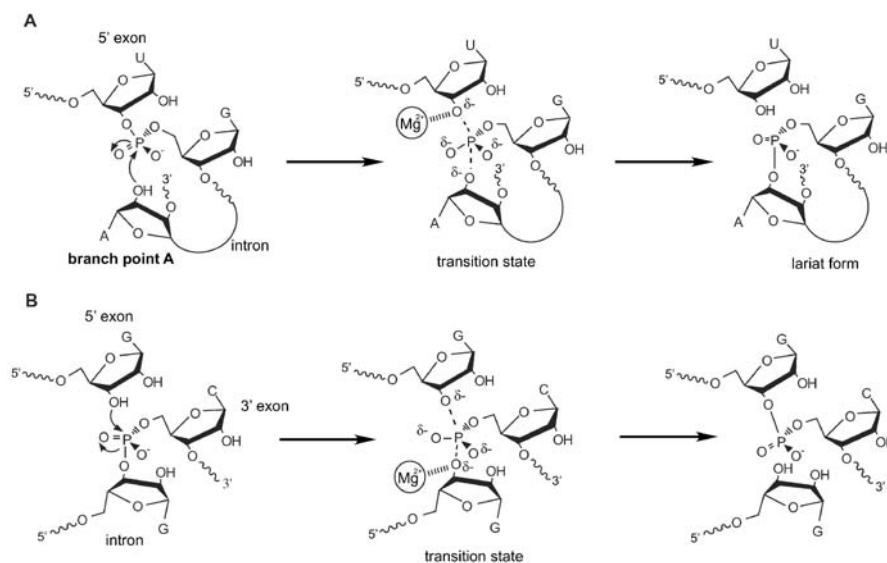
Fig. 16A,B Proposed mechanism of the pre-mRNA splicesomal splicing. A catalytic metal ion is essential for both steps: **A** the first step; **B** the second step. A catalytic magnesium ion is inferred to directly coordinate the $3'$ oxyanion leaving group in the transition state. Catalysts which deprotonate from the nucleophiles have still remained unclear [152]

In the reactions, it is likely that Mg^{2+} ions work as a Lewis acid catalyst to stabilize the leaving oxygens. This stabilization is the same as for group I & II and possibly hammerhead ribozymes. But identification of the activator, encouragement of deprotonation of $2'$-OH of nucleophiles, remains unclear in the reactions catalyzed by this sn RNA and group II intron ribozymes.

3.6
Ribosomal RNA

3.6.1
Catalytic Mechanism

As in the case of the HDV ribozyme, if ribozymes require general acid/base catalysis, the pK_a of some nucleobases within the catalytic pocket is expected to be perturbed so as to have pK_a values of around 7. In a normal setting, however, the nucleobases do not have any pK_a values around 7 (Table 1). If, therefore, they were to be used as acid/base catalysts, it would be necessary to perturb some of their pK_a values toward 7. It is already known that certain RNA structures allow such an alteration [154], as we have pointed out for the HDV ribozyme. In this case, hydrogen bonding between phosphoryl oxygen and the amino group of C_{75} is thought to perturb the acidity of the N3 to that of having a pK_a value of around 7, and, as a result, proton transfer

Table 1 pK$_a$ values of normal nucleotides

	pK$_a$	
	Basic	Acidic
Adenosine	3.5	12.5
Cytidine	4.15	12.5
Guanosine	1.6	9.2–12.4
Uridine	-	9.2–12.5

from the N3 to the leaving oxygen becomes possible, as shown in the boxed diagrams in Fig. 9C.

The origin of the idea that a ribosome might be a ribozyme is derived from the experiment in which peptidyl transferase activity was observed even after digestion of protein components of the ribosome [15]. This was surprising because the most important biological function involved in the synthesis of proteins is catalyzed by RNA. Recently, a large ribosomal subunit from *Haloarcula marismortui* was determined at a resolution of 2.4 Å [16, 155]. Importantly, because of the absence of proteins at the active site, it was concluded that the key peptidyl transferase reaction is accomplished by the ribosomal RNA (rRNA) itself, not by proteins. How does it work?

The crystallization experiment used two substrate analogs. One was a 12-base pair RNA hairpin with an aminoacylated 3′ end with a puromycin, which was expected to bind to the A site of a ribosome. The other was the Yaurus tetrahedral intermediate analog, CCdA-p-Puro, which was expected to bind to the P-site [16]. The resulting crystallographic data indicated that, among approximately 7,000 nucleotides, one specific A_{2486} (A_{2451} in *Escherichia coli*) played a pivotal role in acting as a general base. The unperturbed pK$_a$ of the N1 of adenosine is 3.5 and that of N3 of the nucleobase is lower by two pH units. Therefore, unless perturbation occurs, they are not expected to be good acid/base catalysts.

In the vicinity of the A_{2486}, there is a solvent-inaccessible phosphate group. It was proposed that this buried-phosphate of A_{2485} could electrostatically interact with the amino group of G_{2482} and then affect the pK$_a$ of A_{2486}, specifically via hydrogen bonding interactions between N6 of A_{2486} and O6 of G_{2482} and G_{2102} as shown in Fig. 17. As a result, the rare imino tautomeric form of A_{2486} (Fig. 17,right) might be stabilized [note that G_{2482} is also in the imino tautomeric form] and this would result in a more negative charge on N3 of A_{2486} (in other words, the pK$_a$ value would be shifted toward neutrality). As in the proposal of the HDV ribozyme, the negative electrostatic charge originating from a solvent-inaccessible phosphate was relayed to the nucleobases and perturbed their pK$_a$s. In another experiment based on the pH dependence of dimethylsulfate (DMS) modifications, it was shown that the conserved A_{2486} has a pK$_a$ of around 7.6 [17].

The A_{2486} with a perturbed pK$_a$ can now function as a general base, as described below [16, 17]. At first, N3 of A_{2486} can abstract a proton upon attack
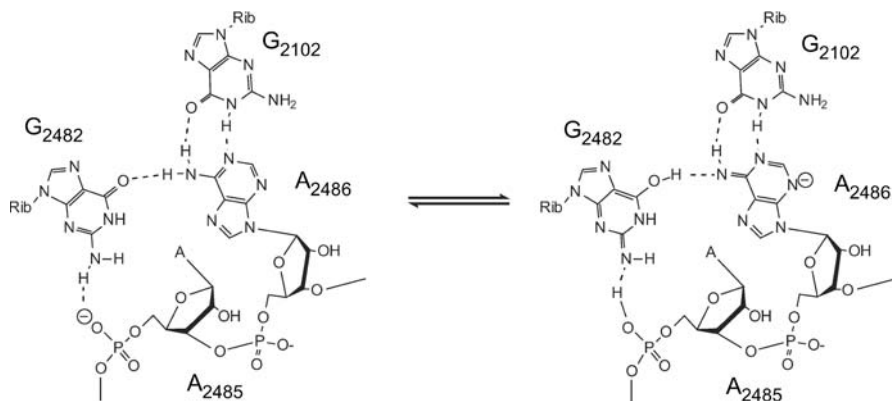
Fig. 17 The mechanism of pK_a value pertubation of N3 of A_{2486} originating on the buried phosphate [16]

of -NH$_2$ of the A site-bound aa-tRNA on C=O (Fig. 18,left). The resulting protonated N3 of A_{2486} is now near the oxyanion of the tetrahedral intermediate and, therefore, it can stabilize the intermediate by means of hydrogen bonding (Fig. 18,center). Finally, this protonated N3 transfers its proton to the leaving 3′-oxygen of the P site-bound tRNA (Fig. 18,right). This process completes the aminoacylation at the A site.

More recently, however, this mechanism was questioned by several researchers [156–158]. In the case of *E. coli* 50S subunits, the pH-dependent modification of A_{2451} by DMS (A_{2486} in *Haloarcula marismortui*) occurred only in its inactive conformation [157]. Under the conditions wherein the ribosomes were fully active, in contrast, the modification of A_{2451} by DMS could not be recognized. These results indicate that A_{2451} becomes shielded from chemical modification by a conformational change upon activation. Thus, it was concluded that the conditional modification of A_{2451} by DMS
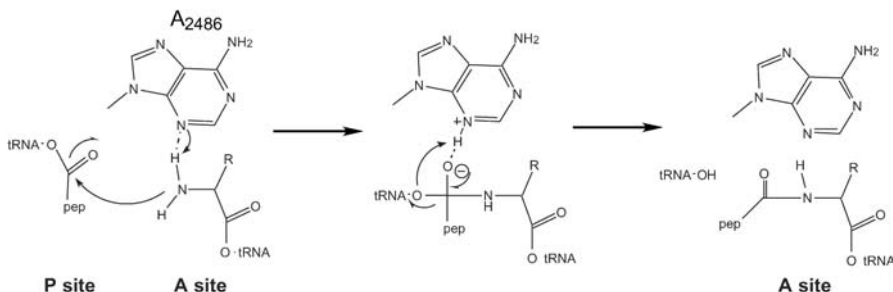
Fig. 18 Proposed mechanism of peptide synthesis catalyzed by the ribosome. The N3 of A_{2486} abstracts a proton from the amino group, and then this protonated N3 stabilized intermediate[16]

was caused by a conformational change relating to the active/inactive transition rather than a perturbed pK_a [157].

The analysis of mutations at residues A_{2451} (A_{2486} in *Haloarcula marismortui*) and G_{2447} (G_{2482} in *Haloarcula marismortui*) of 23S rRNA has also been reported [156, 158]. The A2451U mutant ribosome was engaged in in vivo protein synthesis, although at an apparently reduced rate relative to the wild-type ribosome. In addition, the G2447A mutant ribosome was as active as a wild-type ribosome in terms of the rate of protein synthesis. The peptidyl transferase activities of the 2451 and 2447 mutant ribosomes were also measured in two different single-turnover assays [156]. In assay A in which the reaction was initiated by the addition of the minimal A-site substrate (puromycin), the rate of conversion to a product reflected the altered A-site binding or the alteration in the rate of steps including the chemical step(s) of peptidyl transfer. In assay B, the A-site substrate, puromycin, was added at a saturating level. This high concentration of puromycin overcomes the A-site binding deficiencies of the mutant ribosomes and allows for the monitoring the effects of the mutations on subsequent steps. The similar rate reductions (3- to 14-fold) observed for the 2451 mutant (A2451U) ribosome in these two assays suggest that the A-site substrate binding is not severely compromised in this mutated ribosome, and that these reductions can be explained by the effects on the chemical step(s). In contrast, the 14-fold rate reduction observed for the G2447A ribosome in assay A was overcome by the saturating level of puromycin in assay B, suggesting that the A-site substrate interaction is perturbed by this G2447A mutation [156]. Taking into account the role proposed for these residues based on the X-ray structure, the reductions in the activities of these mutants were surprisingly modest. If the peptidyl transferase assays in this study reflect the chemical step(s) of catalysis, that is, if the chemical step(s) of peptidyl transfer is/are the rate limiting, these modest decreases in activity suggest that A_{2451} and G_{2447} are not critical to the catalytic mechanism.

Although these arguments do not necessarily exclude the involvement of these residues in the peptidyl transfer reaction, other models should be considered [159, 160]. To investigate the significance of the 2′-OH group of the ribose, Dorner et al. synthesized the 2′-deoxy derivative of aminoacylated adenosine (AcLeuAMP) for the P-site substrate [161]. In their fragment reaction assay, this 2′-deoxy substrate (AcLeu-dAMP) was inactive. Considering the results of the fragment reaction assays using some other aminoacylated AMP derivatives, they proposed alternative mechanism as shown in Fig. 19. In their model, the nucleophilic attack of the amino group of A-site-bound tRNA is accompanied by transfer of a proton from the amino group to the 2′-oxygen [161]. They mentioned that their model is supported by the analysis of X-ray structures of the 50 S subunit, which show that the 2′-position of the P-site substrate is within 2.5 Å. Chamberlin et al. also have implied the important role of the hydroxy group for the stabilizing a transition state of the peptidyl transfer reaction [162].

Although the details of the catalytic mechanism are still being debated, the peptidyl transfer reaction is clearly catalyzed by RNAs. One of the disad-
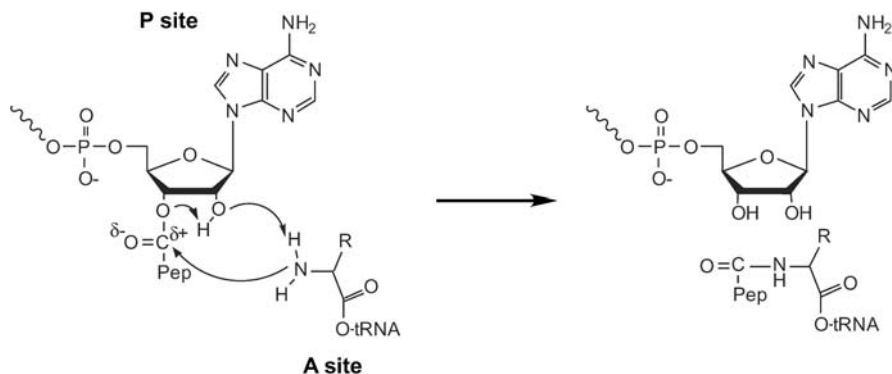
Fig. 19 Another proposed mechanism of peptide synthesis catalyzed by the ribosome. The P-site 2′-OH group abstracts a hydrogen from the amino group [161]

vantages of ribozymes over protein enzymes is the limited number of varieties of functional groups within RNAs that might function at around a neutral pH with pK_a values of around 7. As demonstrated above, however, the flexibility within the RNA scaffold makes it possible to create hydrogen bonding networks that can perturb the acidity of the involved nucleotides. Two examples (ribosomal RNA as well as HDV ribozymes) strongly suggested that perturbations originate from solvent-inaccessible phosphate. This could be a general cause of perturbation.

4
Conclusions

The mechanisms exploited by naturally existing ribozymes appear to be more diverse than originally expected. It is clear, however, that at least two effective catalysts are necessary to facilitate the overall pathway for the efficient hydrolysis of RNA. In the case of the group I intron ribozyme, three metal ions appear to function as Lewis acids by coordinating directly with the nucleophile, the leaving group and non-bridging oxygen at the scissile phosphate (Fig. 11). In the genomic HDV ribozyme, a metal ion functions as a general base catalyst and the internal N3 moiety of a cytosine residue functions as a general acid (Fig. 9C). Hammerhead ribozymes also need two effective catalysts to activate the attack by the 2′-oxygen and to stabilize the departure of the 5′-oxygen. Two divalent metal ions are candidates for these catalysts: one acts as a catalyst to assist in the deprotonation of the nucleophile and/or the other helps in the departure of the leaving oxygen atom from the phosphorus center (stabilization of the product). In hairpin ribozyme reactions, the catalysis apparently does not depend on divalent metal ions so that there must be other catalysts such as a nucleobase that can assist in the attack by the 2′-oxygen and the departure of the 5′-oxygen (Fig. 4C). G_8 is now the strong candidate as the catalyst (Fig. 10B).

   In conclusion, the mechanisms of RNA hydrolysis by ribozymes in nature are becoming clearer, and the diversity of the various candidates that might serve as catalysts is becoming apparent. Catalysts that stabilize the leaving oxygen, as well as those for deprotonation of the nucleophile, are required to ensure effective catalytic reactions. It is worth noting that the architecture of the complex between the substrate and the ribozyme allows the perturbation of the pK_a of the nucleobases which, in addition to metal ions, can act as efficient catalysts. The importance of nucleobases with a perturbed pK_a has been clearly demonstrated in the case of the genomic HDV ribozyme, as well as for ribosomal RNAs. It should be emphasized that biologically important reactions such as splicing and peptide-bond formations are still catalyzed by evolutionarily ancient RNA molecules. And very recently, Joyce's group reported the binary ribozyme [163]. They showed that the binary informational macromolecules composed of only two different nucleotides-2,6-diaminopurine and uracil nucleotides- can act as a ligase. Their binary ribozyme strongly supports the 'two letter genetic system' during the early history of life [164].

References

1. Cech TR, Zaug AJ, Grabowski PJ (1981) Cell 27:487
2. Guerrier-Takada C, Gardiner K, Marsh T, Pace N, Altman S (1983) Cell 35:849
3. Michel F, Umesono K, Ozeki H (1989) Gene 82:5
4. Foster AC, Symons RH (1987) Cell 50:9
5. Buzayan JM, Gerlach WL, Bruening G (1986) Nature 323:349
6. Feldstein PA, Buzayan JM, van Tol H, de Bear J, Gough GR, Gilham PT, Bruening G (1990) Proc Natl Acad Sci USA 87:2623
7. Hampel A, Tritz R, Hicks M, Cruz P (1990) Nucleic Acids Res 18:299
8. Feldstein PA, Bruening G (1993) Nucleic Acids Res 21:1991
9. Sharmeen L, Kuo MYP, Dinter-Gottlieb G, Taylor J (1988) J Virol 62:2674
10. Kuo MYP, Sharmeen L, Dinter-Gottlieb G, Taylor J (1988) J Virol 62:4439
11. Perrotta AT, Been MD (1991) Nature 350:434
12. Lai MM (1995) Annu Rev Biochem 64:259
13. Collins RA, Saville BJ (1990) Nature 345:177
14. Collins CA Guthrie C (2000) Nature Struct Biol 10:850
15. Noller HF, Hoffarth V, Zimniak L (1992) Science 256:1416
16. Nissen P, Hansen J, Ban N, Moor PB, Steitz TA (2000) Science 289:920
17. Muth GW, Ortoleva-Donnelly L, Strobel SA (2000) Science 289:947
18. Cech TR (2000) Science 289:878
19. Lee N, Bessho Y, Wei K, Szostak JW, Suga H (2000) Nature Struct Biol 7:28
20. Johnston WK, Unrau PJ, Lawrence MS, Glasner ME, Bartel DP (2001) Science 292:1319
21. Hampel A, Cowan JA (1997) Chem Biol 4:513
22. Nesbitt S, Hegg LA, Fedor MJ (1997) Chem Biol 4:619
23. Young KJ, Gill F, Grasby JA (1997) Nucleic Acids Res 25:3760
24. Chowrira BM, Berzal-Herranz A, Burke JM (1993) Biochemistry 32:1088
25. Earnshaw DJ, Gait MJ (1998) Nucleic Acids Res 26:5551
26. Seyhan AA, Burke M (2000) RNA 6:189
27. Cech TR, Golden BL (1999) Building a catalytic active site using only RNA. In: Gesteland RF, Cech TR, Atkins JF (eds) The RNA world. Cold Spring Harbor Laboratory Press, Cold Spring Harbor, NY

29. Carola C, Eckstein F (1999) Curr Opin Chem Biol 3:274
30. Zhou DM, Taira K (1998) Chem Rev 98:991
31. Saville BJ, Collins RA (1990) Cell 61:685
32. van Tol H, Buzayan JM, Feldstein PA, Eckstein F, Bruening G (1990) Nucleic Acids Res 18:1971
33. Dahm SC, Uhlenbeck OC (1991) Biochemistry 30:9464
34. Slim G, Gait MJ (1991) Nucleic Acids Res 19:1183
35. Koizumi M, Ohtsuka E (1991) Biochemistry 30:5145
36. Warashina M, Zhou DM, KuwabaraT, Taira K (1999) Ribozyme structure and function. In: Söll D, Nishimura S, Moore PB (eds), Comprehensive natural products chemistry. Elsevier Science, Oxford, vol. 6, p 235
37. Kuimelis RG, McLaughlin LW (1998) Chem Rev 98:1027
38. Kuusela S, Lönnberg H (1997) Curr Topics Solution Chem 2:29
39. Oivanen M, Kuusela S, Lönnberg H (1998) Chem Rev 98:961
40. Komiyama M, Takeda N, Shigekawa H (1999) Chem Commun 16:1443
41. Komiyama M, Bender ML (1980) Bull Chem Soc Jpn 53:1073
42. Liu X, Reese CB (1995) Tetrahedron Lett 36:3413
43. Thomson JB, Patel BK, Jiménez V, Eckart K, Eckstein F (1996) J Org Chem 61:6273
44. Zhou DM, Usman N, Wincott FE, Matulic-Adamic J, Orita M, Zhang LH, Komiyama M, Kumar PKR, Taira K (1996) J Am Chem Soc 118:5862
45. Pyle AM (1993) Science 261:709
46. Yarus M (1993) FASEB J 7:31
47. Dahm SC, Derrick WB, Uhlenbeck OC (1993) Biochemistry 32:13,040
48. Steitz TA, Steitz JA (1993) Proc Natl Acad Sci USA 90:6498
49. Uebayashi M, Uchimaru T, Koguma T, Sawata S, Shimayama T, Taira K (1994) J Org Chem 59:7414
50. Sawata S, Komiyama M, Taira K (1995) J Am Chem Soc 117:2357
51. Pontius BW, Lott WB, von Hippel PH (1997) Proc Natl Acad Sci USA 94:2290
52. Zhou DM, Zhang LH, Taira K (1997) Proc Natl Acad Sci USA 94:14,343
53. Birikh KR, Heaton PA, Eckstein F (1997) Eur J Biochem 245:1
54. Lott WB, Pontius BW, von Hippel PH (1998) Proc Natl Acad Sci USA 95:542
55. Wang S, Karbstein K, Peracchi A, Beigelman L, Herschlag D (1999) Biochemistry 38:14,363
56. Symons RH (1992) Annu Rev Biochem 61:641
57. Haseloff J, Gerlach WL (1988) Nature 334:585
58. Stage-Zimmermann TK, Uhlenbeck OC (1998) RNA 4:875
59. Scott WG, Murray JB, Arnold JRP, Stoddard BL, Klug A (1996) Science 274:2065
60. Kuimelis RG, McLaughlin LW (1996) Biochemistry 35:5308
61. Kuimelis RG, McLaughlin LW (1997) Bioorg Med Chem 5:1051
62. Torres RA, Bruice TC (1998) Proc Natl Acad Sci USA 95:11,077
63. Torres RA, Bruice TC (2000) J Am Chem Soc 122:781
64. Murray JB, Seyhan AA, Walter NG, Burke JM, Scott WG (1998) Chem Biol 5:587
65. O'Rear JL, Wang S, Feig AL, Beigelman L, Uhlenbeck OC, Herschlag D (2001) RNA 7:537
66. Curtis EA, Bartel DP (2001) RNA 7:546
67. Uchimaru T, Uebayasi M, Tanabe K, Taira K (1993) FASEB J 7:137
68. Takagi Y, Warashina M, Stec WJ, Yoshinari K, Taira K (2001) Nucleic Acids Res 29:1815
69. Yoshinari K, Taira K (2000) Nucleic Acids Res 28:1730
70. Zhou DM, Kumar PKR, Zhang LH, Taira K (1996) J Am Chem Soc 118:8969
71. Warashina M, Takagi Y, Sawata S, Zhou DM, Kuwabara T, Taira K (1997) J Org Chem 62:9138
72. Suzumura K, Yoshinari K, Tanaka Y, Takagi Y, Kasai Y, Warashina M, Kuwabara T, Orita M, Taira K (2002) J Am Chem Soc 124:8230
73. Warashina M, Takagi Y, Stec WJ, Taira K (2000) Curr Opin Biotechnol 11:354
74. Bell RP, Kuhn AT (1963) Trans Faraday Soc 59:1789
28. Nakano S, Chadalavada DM, Bevilacqua PC (2000) Science 287:1493

75. Jenckes WP (1969) In: Catalysis in chemistry and enzymology. McGraw-Hill, NY, p 250
76. Takagi Y, Taira K (2002) J Am Chem Soc 124:3850
77. Bassi GS, Møllegaard NE, Murchie AI, von Kitzing E, Lilley DM (1995) Nat Struct Biol 2:45
78. Bassi GS, Murchie AI, Walter F, Clegg RM, Lilley DM (1997) EMBO J 16:7481
79. Bassi GS, Møllegaard NE, Murchie AI, Lilley DM (1999) Biochemistry 38:3345
80. Hammann C, Norman DG, Lilley DM (2001) Proc Natl Acad Sci USA 98:5503
81. Horton TE, Clardy DR, DeRose VJ (1998) Biochemistry 37:18,094
82. Zhou JM, Zhou DM, Takagi Y, Kasai Y, Inoue A, Baba T, Taira K (2002) Nucleic Acids Res 30:2374
83. Peracchi A, Beigelman L, Scott EC, Uhlenbeck OC, Herschlag D (1997) J Biol Chem 272:26,822
84. Knöll R, Bald R, Fürste JP (1997) RNA 3:132
85. Peracchi A, Beigelman L, Usman N, Herschlag D (1996) Proc Natl Acad Sci USA 93:11,522
86. Peracchi A, Karpeisky A, Maloney L, Beigelman L, Herschlag D (1998) Biochemistry 37:14,765
87. Nakamatsu Y, Kuwabara T, Warashina M, Tanaka Y, Yoshinari K, Taira K (2000) Genes Cells 5:603
88. Markley JC, Godde F, Sigurdsson ST (2001) Biochemistry 40:13,849
89. Ruffner DE, Uhlenbeck OC (1990) Nucleic Acids Res 18:6025
90. Ruffner DE, Stormo GD, Uhlenbeck OC (1990) Biochemistry 29:10,695
91. Tuschl T, Eckstein F (1993) Proc Natl Acad Sci USA 90:6991
92. Hansen MR, Simorre JP, Hanson P, Mokler V, Bellon L, Beigelman L, Pardi A (1999) RNA 5:1099
93. Suzumura K, Warashina M, Yoshinari K, Tanaka Y, Kuwabara T, Orita M, Taira K. (2000) FEBS Lett 473:106
94. Maderia M, Hunsicker LM, DeRose VJ (2000) Biochemistry 39:12,113
95. Tanaka Y, Morita EH, Hayashi H, Kasai Y, Tanaka T, Taira K (2000) J Am Chem Soc 122:11,303
96. Murray JB, Scott WG (2000) J Mol Biol 296:33
97. Yoshinari K, Taira K (2000) Nucleic Acids Res 28:1730
98. Suzmura K, Yoshinari K, Tanaka Y, Takagi Y, Kasai Y, Warashina M, Kuwabara T, Orita M, Taira K (2002) J Am Chem Soc 124:8230
99. Sharmeen L, Kuo MYP, Dinter-Gottlieb G, Taylor J (1988) J Virol 62:2674
100. Kuo MYP, Sharmeen L, Dinter-Gottlieb G, Taylor J (1988) J Virol 62:4439
101. Perrotta AT, Been MD (1991) Nature 350:434
102. Lai MM (1995) Annu Rev Biochem 64:259
103. Ferré-D'Amaré AR, Zhou K, Doudna JA (1998) Nature 395:567
104. Perrotta AT, Shih I, Been MD (1999) Science 286:123
105. Shih I, Been MD (2000) Biochemistry 39:9055
106. Nakano S, Bevilacqua PC (2001) J Am Chem Soc 123:11,333
107. Shih I, Been MD (2001) Proc Natl Acad Sci USA 98:1489
108. Wadkins TS, Shih I, Perrotta AT, Been MD (2001) J Mol Biol 305:1045
109. Nakano S, Proctor DJ, Bevilacqua PC (2001) Biochemistry 40:12,022
110. Hamid F, Kawakami J, Nishikawa F, Nishikawa S (1997) Nucleic Acids Res 25:3124
111. Lupták A, Ferré-D'Amaré AR, Zhou K, Zilm KW, Doudna JA (2001) J Am Chem Soc 123:8447
112. Fedor MJ (2000) J Mol Biol 297:269
113. Hertel KJ, Herschlag D, Uhlenbeck OC (1994) Biochemistry 33:3374
114. Hegg LA, Fedor MJ (1995) Biochemistry 34:15,813
115. Shippy R, Lockner R, Farnsworth M, Hampel A (1999) Mol Biotech 12:117
116. Nesbitt SM, Erlacher HA, Fedor MJ (1999) J Mol Biol 286:1009
117. Sargueil B, McKenna J, Burke JM (2000) J Biol Chem 41:32,157
118. Basolo F, Pearson RG (1967) Mechanism of inorganic reactions. A study of metal complexes in solution. Wiley, New York

119. Pinard R, Hampel KJ, Heckman JE, Lambert D, Chan PA, Major F, Burke JM (2001) EMBO J 20:6434
120. Rupert PB, Ferré-D'Amaré AR (2001) Nature 410:780
121. Burke JM (2001) Nat Struct Biol 8:3
122. Cech TR, Herschlag D (1996) Group I ribozyme: substrate recognition, catalytic strategies and comparative mechanistic analysis. In: Eckstein F, Lilley DMJ (eds) Nucleic acids and molecular biology, vol 10, catalytic RNA. Springer, Berlin Heidelberg New York, p 1
123. Piccirilli JA, Vyle JS, Caruthers MH, Cech TR (1993) Nature 361:85
124. Weinstein LB, Jones BC, Cosstick R, Cech TR (1997) Nature 388:805
125. Shan S, Yoshida A, Sun S, Piccirilli JA, Herschlag D (1999) Proc Natl Acad Soc USA 96:12,299
126. Strobel SA, Ortoleva-Donnelly L (1999) Chem Biol 6:153
127. Yoshida A, Shan S, Herschlag D, Piccirilli JA (2000) Chem Biol 7:85
128. Shan S, Herschlag D (2000) RNA 6:795
129. Pearson RG (1968) J Chem Educ 45:581
130. Pearson RG (1968) J Chem Educ 45:643
131. Yoshida A, Sun S, Piccirilli JA (1999) Nature Struct Biol 6:318
132. Herschlag D, Piccirilli JA, Cech TR (1991) Biochemistry 30:4844
133. McConnell TS, Cech TR (1995) Biochemistry 34:4056
134. Shan S, Kravchuk AV, Piccirilli JA, Herschlag D (2001) Biochemistry 40:5161
135. Sjögren AS, Pettersson E, Sjöberg BM, Strömberg R, (1997) Nucleic Acids Res 25:648
136. Shan S, Herschlag D (1999) Biochemistry 38:10,958
137. Shan S, Narlikar GJ, Herschlag D (1999) Biochemistry 38:10,976
138. Szewczak AA, Kosek AB, Piccirilli JA, Strobel SA (2002) Biochemistry 41:2516
139. Herschlag D, Eckstein F, Cech TR (1993) Biochemistry 32:8312
140. Inoue T, Sullivan FX, Cech TR (1986) J Mol Biol 189:143
141. Been MD, Perrotta AT (1991) Science 252:434
142. Rajagopal J, Doudna JA, Szostak JW (1989) Science 244:692
143. Suh E, Waring RB (1992) Nucleic Acids Res 20:6303
144. Valadkhan S, Manley LJ (2002) Nature Struct Biol 9:498
145. Valadkhan S, Manley LJ (2001) Nature 413:701
146. Sontheimer EJ, Gordon PM, Piccirilli JA (1999) Genes Dev 13:1729
147. Gordon PM, Sontheimer EJ, Piccirilli JA (2000) Biochemistry 39:12,939
148. Guerrier-Takada C, Haydock K, Allen L, Altman S (1986) Biochemistry 25:1509
149. Smith D, Pace NR (1993) Biochemistry 32:5273
150. Warnecke JM, Sontheimer EJ, Piccirilli JA, Hartmann RK (2000) Nucleic Acids Res 28:720
151. Sontheimer EJ, Sun S, Piccirilli JA (1997) Nature 388:801
152. Gordon PM, Sontheimer EJ, Piccirilli JA (2000) RNA 6:199
153. Yean SL, Wuenschell G, Termini J, Lin RJ (2000) Nature 408:881
154. Legault P, Pardi A (1997) J Am Chem Soc 119:6621
155. Ban N, Nissen P, Hansen J, Moore PB, Steitz TA (2000) Science 589:905
156. Thompson J, Kim DF, O'Connor M, Lieberman KR, Bayfield MA, Gregory ST, Green R, Noller HF, Dahlberg AE (2001) Proc Natl Acad Sci USA 98:9002
157. Bayfield MA, Dahlberg AE, Schulmeister U, Dorner S, Barta A (2001) Proc Natl Acad Sci USA 98:10,096
158. Polacek N, Gaynor M, Yassin A, Mankin AS (2001) Nature 411:498
159. Barta A, Dorner S, Polacek N (2001) Science 291:203a
160. Berg JM, Lorsch JR (2001) Science 291:203a
161. Dorner S, Polacek N, Schulemeister U, Panuschka C, Barta A (2002) Biochem Soc Trans 30:1131
162. Chamberlin SI, Merino EJ, Weeks MK (2002) Proc Natl Acad Sci USA 99:14,688
163. Reader JS, Joyce GF (2003) Nature 420:841
164. Crick FHC (1968) J Mol Biol 38:367

Author Index Volumes 201–232

Subject Index